

Investigating Human Embryo Implantation –  
Developing Clinical Applications from *in vitro*  
Models

HELEN RACHEL HUNTER

DClinSci 2023

Investigating Human Embryo Implantation –  
Developing Clinical Applications from *in vitro*  
Models

HELEN RACHEL HUNTER

A thesis submitted in partial fulfilment of the  
requirements of Manchester Metropolitan  
University for the degree of Doctorate in  
Clinical Science

Department of Life Sciences  
Manchester Metropolitan University  
2023

## Abstract

**Introduction:** While assisted conception success rates have increased, factors limiting IVF success include inadequacies in identifying viable embryos, and transfer of embryos into uteri with an unknown state of receptivity.

**Aims and experimental approaches:** The aims of this project are to determine the possibility of using non-invasive techniques to reveal differences between preimplantation human embryos which successfully form a pregnancy and those that fail to implant. The experimental approaches are: 1 Sampling of conditioned media and co-culture with a 3D *in vitro* model of mid-secretory phase normal human endometrium, followed by transcriptomic analysis of these endometrial cells; 2 Development of a time lapse annotation system to improve selection of PN stage frozen embryos cultured to blastocyst and replaced in FET cycles.

**Methods:** Endometrial epithelial and stromal cells in an *in vitro* model of mid-secretory phase human endometrium were exposed to conditioned media samples from 10 human embryos cultured singly to the blastocyst stage, with known pregnancy outcomes. These cells were subjected to RNA sequencing and transcriptomic analysis. Time lapse recordings of these embryos were taken through an experimental AI model (eM-Life). Retrospective analysis and annotation of time lapse videos of embryo development of 193 PN stage frozen embryos thawed and cultured to the blastocyst stage for replacement in an FET cycle was performed.

**Results:** Endometrial epithelial cells showed changes in gene expression in response to media from successful embryos, while stromal cells responded to a lesser extent to media from unsuccessful embryos. The deep learning model ranked embryos on morphology but did not correlate with endometrial response in this project. From the analysis of 193 PN stage frozen embryos, statistically significant differences in several morphokinetic parameters between implanting and non-implanting embryos were found and morphological differences not previously studied in frozen thawed embryos relating to embryo viability were identified.

**Conclusions:** Both experimental approaches revealed differences between embryos which implant successfully and those which fail, not detected by standard morphological grading. Further work is needed to identify upstream factors in conditioned media which cause gene expression changes in the *in vitro* endometrial model, and to test the morphokinetic model developed for frozen embryos in culture.

## Acknowledgments

I would like to thank my academic supervisor Dr Michael Carroll for support in constructing this thesis – from my embryology trainee to my DClSci supervisor!

My workplace research supervisors Dr Peter Ruane and Professor Daniel Brison have contributed enormously in helping me complete the research component of HSST, and made me believe I could be a bit of a research scientist after years and years of clinical work.

Thanks to my Laboratory Manager at the Department of Reproductive Medicine, St Mary's Hospital, Manchester, Greg Horne – who also believed I could do it. Sorry I got out before you.

All the amazing Reproductive Scientists at St Mary's who work brilliantly together to create miracles for our patients – often in difficult circumstances. Thank you for supporting me through HSST and putting up with my crazy projects and lectures on leadership.

I also need to mention the patients who continue to inspire me (after almost 30 years) to continue to be a better scientist. Your continuing faith and trust that science will give you the chance to be parents takes my breath away. You are all so brave and strong.

Finally, I want to thank my husband Alex, who has always supported me, and my children James and Naomi. The joy and fulfilment of my family is what drives me to make it happen for others.

*"Far and away the best prize that life has to offer is the chance to work hard at work worth doing."*

-- Theodore Roosevelt

## Declaration

No material contained in this thesis has been used in any other submission for another academic award.

# Contents

	Page
<b>Abstract</b>	<b>1</b>
<b>Acknowledgements</b>	<b>2</b>
<b>Declaration</b>	<b>3</b>
<b>Contents</b>	<b>4</b>
<b>List of figures</b>	<b>7</b>
<b>List of tables</b>	<b>8</b>
<b>List of appendices</b>	<b>9</b>
<b>List of abbreviations</b>	<b>10</b>
<b>Chapter 1: Introduction</b>	
<b>1.0 Background: Infertility, ART and <i>in vitro</i> Embryo Culture and Development</b>	<b>11</b>
<b>1.1 The need to investigate implantation</b>	<b>20</b>
<b>1.2 Implantation – the ‘black box’ in ART</b>	<b>20</b>
<b>1.3 ‘An embryo competent to implant’</b>	<b>22</b>
<b>1.4 ‘A receptive endometrium’</b>	<b>27</b>
<b>1.5 ‘A successful conversation between embryo and endometrium’</b>	<b>30</b>
<b>1.6 Experimental Aims and objectives</b>	<b>35</b>
<b>Chapter 2: Materials and Methods</b>	
<b>2.1 Conditioned media co-culture experiment</b>	<b>37</b>
<b><i>2.1.1 Patient identification and selection</i></b>	<b>34</b>
<b><i>2.1.2 Embryo culture</i></b>	<b>39</b>
<b><i>2.1.3 Collection of conditioned media</i></b>	<b>40</b>
<b><i>2.1.4 Establishment of <i>in vitro</i> model of mid-secretory phase endometrium</i></b>	<b>41</b>
<b><i>2.1.5 Sample preparation for RNA sequencing</i></b>	<b>42</b>
<b><i>2.1.6 RNA sequencing analysis</i></b>	<b>45</b>
<b><i>2.1.7 Machine Learning Video Analysis of embryos</i></b>	<b>45</b>
<b>2.2 Timelapse imaging and annotations of PN stage frozen embryos cultured to blastocyst.</b>	
<b><i>2.2.1 Patient Selection</i></b>	<b>46</b>
<b><i>2.2.2 Video collection and annotation</i></b>	<b>46</b>
<b><i>2.2.3. Analysis of videos</i></b>	<b>49</b>

**Chapter 3: Endometrial transcriptomic responses to embryo-conditioned culture media and associated morphokinetic machine learning analysis**

<b>3.1 Background</b>	<b>50</b>
<b>3.2 Details of samples used for analysis</b>	<b>51</b>
<b>3.3 <i>In vitro</i> endometrial transcriptomic responses to embryo-conditioned culture media</b>	<b>51</b>
<b>3.3.1 <i>Principal component analysis</i></b>	<b>51</b>
<b>3.3.2 <i>Differential gene expression</i></b>	<b>53</b>
<b>3.3.3 <i>Gene ontology analysis of differentially expressed genes</i></b>	<b>56</b>
<b>3.3.4 <i>Upstream regulators of epithelial DEG</i></b>	<b>58</b>
<b>3.4 Results of Machine Learning Video Analysis of embryos</b>	<b>59</b>

**Chapter 4: Timelapse imaging and annotations of PN stage frozen embryos cultured to blastocyst.**

<b>4.1 Introduction and background</b>	<b>62</b>
<b>4.2 Details of patients and embryos selected for analysis</b>	<b>63</b>
<b>4.3 Results of Morphokinetic measurements</b>	<b>63</b>
<b>4.3.1 <i>Timepoint data</i></b>	<b>63</b>
<b>4.3.2 <i>Time between setpoints</i></b>	<b>66</b>
<b>4.4 Summary of results for morphokinetic data</b>	<b>73</b>
<b>4.5 Results of morphological observations</b>	<b>76</b>
<b>4.5.1 <i>Observations of pronuclei</i></b>	<b>76</b>
4.5.1a <i>Pattern of PNMBD</i>	76
4.5.1b <i>Size of PN at last image before PNMBD</i>	76
<b>4.5.2 <i>Observations of blastocysts</i></b>	<b>77</b>
4.5.2a <i>Cytoplasmic strings</i>	77
4.5.2b <i>Blastocyst contraction and collapse</i>	80
4.5.2c <i>Pulsatile expansions</i>	82
<b>4.6 Summary of results of morphological observations</b>	<b>84</b>

**Chapter 5: General Discussion**

<b>5.0: General Introduction</b>	<b>85</b>
<b>5.1: Results of conditioned media co-culture experiment: Transcriptomic data from <i>in vitro</i> model of mid-secretory phase endometrium and machine learning video analysis of embryos</b>	<b>91</b>
<b>5.2: Timelapse imaging and annotations of PN stage frozen embryos</b>	
-aids to embryo selection	92
<b>5.3 Limitations of the study</b>	<b>101</b>
<b>5.4 Concluding remarks</b>	<b>103</b>

<b>References</b>	<b>106</b>
<b>General Appendices</b>	
<b>Appendix 1: Description of the Higher Specialist Scientist Training (HSST) programme sections A and B</b>	<b>122</b>
<b>Appendix 2: Relevant sections from 'Guidance from Manchester Metropolitan University on completion of Section C of HSST'</b>	<b>127</b>
<b>Appendix 3: BGI Sample testing report for endometrial cells submitted for RNA extraction.</b>	<b>128</b>
<b>Appendix 4: Letter Confirming Ethical Approval from MMU for project.</b>	<b>160</b>
<b>Appendix 5: Tables of differentially expressed genes (DEG) from conditioned media co-culture experiments.</b>	<b>161</b>



## List of Figures

Figure 1	Schematic of stages of a standard IVF cycle.	14
Figure 2	Cleavage stage grading scheme for human embryos used at St Mary's Hospital.	16
Figure 3	Schematic of decision making pathway for day of transfer and number of embryos to replace	17
Figure 4	Blastocyst grading scheme used at St Mary's Hospital	18
Figure 5	Schematics of early embryo implantation in the human	21
Figure 6	Progression of development during time after fertilization in mouse, bovine and human embryos	22
Figure 7	Endometrial changes across the menstrual cycle	28
Figure 8	Overview of culture slides for Embryoscope™ time-lapse incubators	37
Figure 9 a,b	Cross section of Embryoslide™ a =used for culture of embryos in this study, b=not used	38
Figure 10	Diagram of organoid co-culture	42
Figure 11	Unsupervised PCA of endometrial organoid epithelial and stromal cell transcriptomes	52
Figure 12	PCA (based on the 500 most variably expressed gene between groups) of organoid epithelial and stromal cell transcriptomes.	53
Figure 13	DEG in epithelial and stromal cells exposed to conditioned media from successful and unsuccessful embryos, and media not exposed to an embryo (control).	55
Figure 14	Heatmaps of DEG for epithelial and stromal cells	56
Figure 15	Gene ontology (biological processes) for DEG in endometrial epithelium exposed to conditioned media from successful embryos	57
Figure 16	Results of ingenuity pathway analysis of 76 DEG in endometrial epithelium.	58
Figure 17	Scatter plots of ML generated scores for embryos in conditioned media co-culture experiment	61
Figure 18	Chart showing size differences between male and female pronuclei just before PNMBD and pregnancy rates	77
Figure 19	Presence and number of cytoplasmic strings, number of collapses and outcome (a=actual numbers, b=percentage of embryos).	79

## List of Tables

Table 1:	Main causes of infertility in couples aged 15-49	11
Table 2:	Main types of fertility treatment in use in UK	12
Table 3	Details of conditioned media samples	40
Table 4	Morphokinetic setpoint stages from time-lapse videos of frozen-thawed embryos	47
Table 5	Morphological observations and measurements from time-lapse videos of frozen-thawed embryos	48
Table 6	ML scores, morphological grade at embryo transfer (ET) and cycle outcome for embryos in conditioned media co-culture experiment	60
Table 7	Sum of ML scores, morphological grade at embryo transfer (ET) and cycle outcome for embryos in conditioned media co-culture experiment	60
Table 8	Time embryos reach morphological setpoints, (taking tPN-f as zero) 167 embryos, time in hours	65
Table 9	Time taken to reach setpoints T2 to TB in quartile ranges	666
Table 10a,b,c,d	Time taken for embryos to progress between setpoints t2-tB	68-70
Table 11 a,b	Time taken for embryos to progress between setpoints t2-tB in quartile ranges	71-72
Table 12	Summary of stages where there are statistically significant differences in mean times between groups of successful and unsuccessful embryos	74
Table 13	Proposed thresholds for morphokinetic selection of embryos from PN freezing and extended culture	75
Table 14	Pronuclear fade pattern and rates of clinical pregnancy	76
Table 15	Presence and number of cytoplasmic strings, number of collapses and outcome	78
Table 16 a,b	$\chi^2$ <i>p</i> values comparing clinical pregnancy rates between cohorts of embryos collated by maximum number of strings observed.	80
Table 17 a,b	$\chi^2$ <i>p</i> values comparing blastocyst collapse rates between cohorts of embryos collated by maximum number of strings observed	80
Table 18	Percentage size of largest observed blastocyst collapse and outcome	81
Table 19	Table 20a: $\chi^2$ <i>p</i> values when comparing clinical pregnancy rates in groups of embryos collated by percentage size of collapse	82
Table 20	Number of pulsatile expansions observed and outcome	83
Table 21	$\chi^2$ <i>p</i> values when comparing clinical pregnancy rates in groups of embryos collated by number of pulsatile expansions	83

## List of Appendices

**Appendix 1:** Description of the Higher Specialist Scientist Training (HSST) programme sections A and B

**Appendix 2:** Relevant sections from 'Guidance from Manchester Metropolitan University on completion of Section C of HSST'

**Appendix 3:** BGI Sample testing report for endometrial cells submitted for RNA extraction.

**Appendix 4:** Letter Confirming Ethical Approval from MMU for project.

**Appendix 5:** Tables of differentially expressed genes (DEG) from conditioned media co-culture experiments.

## List of Abbreviations

ART	Assisted reproductive technology
CAN	Causal Network Analysis
DEG	Differentially expressed gene(s)
DSC	Decidualised stromal cells
EEC	Endometrial epithelial cells
FDR	False discovery rate
FET	Frozen embryo transfer
HA	Hyaluronic acid
HB-EGF	Heparin binding epidermal growth factor-like growth factor
hCG	human chorionic gonadotrophin
HFEA	Human Fertilisation and Embryology Authority
HSST	Higher Specialist Scientist Training (programme)
ICM	Inner cell mass
ICSI	Intra-cytoplasmic sperm injection
IGFBP 1	Insulin like growth factor binding protein 1
IPA	Ingenuity Pathway Analysis
IVF	<i>In vitro</i> fertilisation
KEGG	Kyoto Encyclopaedia of Genes and Genomes
LIF	Leukaemia inhibitory factor
ML	Machine Learning
OHSS	Ovarian hyperstimulation syndrome
PCA	Principal Component analysis
PCOS	Polycystic ovarian disease
PGT-A	Preimplantation genetic testing for aneuploidy
PN	Pronucleus/pronuclei
PNMBD	Pronuclear membrane breakdown
RIF	Recurrent implantation failure
RM	Recurrent miscarriage
RNA	Ribonucleic acid
TE	Trophectoderm
TGF- $\beta$	Transforming growth factor-beta
TL	Time lapse (technology)
URA	Upstream Regulator Analysis

## CHAPTER 1: Introduction

### 1.0 Background: Infertility, ART and *in vitro* Embryo Culture and Development

The published definition of infertility is the inability to conceive after at least 1 year of unprotected sexual intercourse, and using this definition, affects 15-20% of couples worldwide (Boivin *et al.*, 2007). The most common causes of infertility are summarised in Table 1. It is important to note that often couples have combined factors contributing to their inability to conceive (e.g. ovulatory disorders in the female, and a reduced sperm count in the male) making treatment more complex.

**Table 1: Summary of the main causes of infertility in patients aged 15-49** (adapted from Carson and Kallen, 2021). Main causes of infertility are placed into broad categories with examples and their estimated incidence as percentage of diagnoses.

<i>Category</i>	<i>Examples/aetiology</i>	<i>Estimated percentage of diagnoses</i>
Ovulatory dysfunction	Polycystic ovarian disease (PCOS), thyroid disease.	25%
Blockage of oviducts	Following infection (after miscarriage, termination or Sexually transmitted disease)	11-67% depending on population studied
Endometriosis	Can cause tubal blockage, ovarian masses	25-40%
Diminished ovarian reserve	Age related, post chemo/radiotherapy	Depends on population. More significant in women over 36
Male Factor	Abnormal semen parameters Azoospermia (obstructive/non obstructive)	35%
Unexplained (idiopathic)	No cause determined by standard investigations	15-32%

It is estimated that 60,000 people access fertility services in the UK each year (HFEA, 2021). There are a number of different fertility treatments available, and the most suitable depends on the underlying causes of infertility and female age – it may be more appropriate to move quickly to a more intensive form of treatment if female age is above 36 (Carson and Kallen, 2021). The main types of fertility treatment available in the UK and relevant to this thesis are summarised in Table 2.

**Table 2: Main types of fertility treatment in use in UK.** Brief descriptions of the most commonly used treatments for infertility with indications for suitability depending on patient diagnosis, and estimates of success rates. (Information adapted from Carson and Kallen, 2021)

<i>Treatment</i>	<i>Description</i>	<i>Suitability</i>	<i>Success rates</i>
Induction of ovulation	<p>First line treatment for women with ovulatory disorders.</p> <p>Ovarian stimulation with clomiphene citrate, aromatase inhibitors, gonadotropins.</p> <p>Ovarian response needs monitoring with blood tests and ultrasound to avoid multiple ovulation and risk of multiple birth.</p> <p>Non-invasive</p>	<p>Couple should have no male factor issues or use donor sperm</p> <p>No tubal blockages</p>	10-20% (when ovulation occurs)
Intrauterine insemination (IUI)	<p>Can be used with or without induction of ovulation.</p> <p>Sperm is washed, then placed into the uterus 24 to 36 hours after an endogenous LH surge or an exogenous ovulation trigger</p>	<p>Couple should have no male factor issues or use donor sperm.</p> <p>Sometimes recommended for mild male factor infertility</p> <p>No tubal blockages</p>	5-15% per insemination
<i>In vitro</i> fertilisation (IVF)	<p>Gonadotropin stimulation, careful monitoring of ovarian response, followed by surgical aspiration of multiple ovarian follicles. Oocytes can be fertilized <i>in vitro</i> by mixing with spermatozoa (IVF). Resulting embryos are cultured, then selected for transfer into the uterus under ultrasound guidance. Supernumerary embryos can be frozen for future use.</p>	<p>Invasive procedure. Risk of side effects, risk of multiple pregnancy. First line treatment for patients with tubal occlusion. Often recommended as first line when maternal age &gt;36</p>	19-32% per embryo transfer depending on maternal age and stage of embryo at transfer*
Intracytoplasmic sperm injection (ICSI)	<p>As IVF, except oocytes are fertilised <i>in vitro</i> by injection of a single sperm (by micromanipulation) or with intracytoplasmic sperm injection (ICSI). Used when severe male factor infertility is present, or following failed fertilisation with IVF.</p>	<p>As IVF, plus first line treatment for patients with male factor infertility and required when sperm surgically retrieved.</p>	19-32% per embryo transfer depending on maternal age and stage of embryo at transfer*
Frozen embryo transfer	<p>Suitable supernumerary embryos from IVF/ICSI cycles can be frozen (cryopreserved) for use in future treatment cycles.</p>	<p>Availability of frozen embryos from previous IVF/ICSI or donated. Less invasive as ovarian stimulation and oocyte recovery not required.</p>	Similar to fresh cycles.

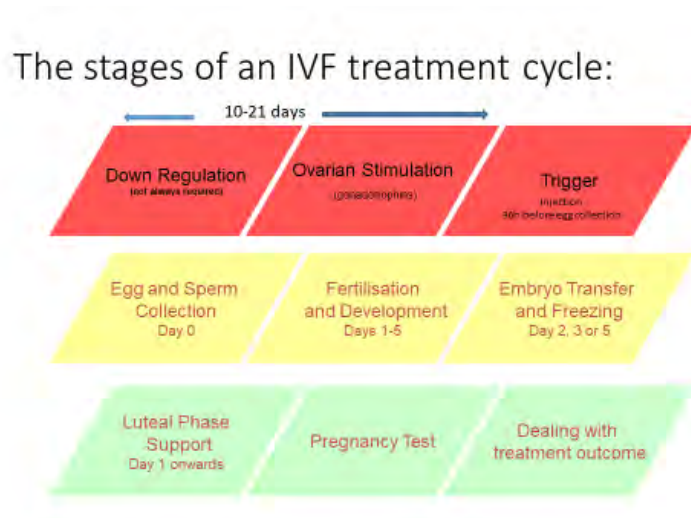
\* Data from HFEA, 2021

Less invasive treatments such as induction of ovulation (OI) and intrauterine insemination (IUI) are often first line treatments for infertility, but induction of ovulation is of no benefit

alone if the female is ovulating regularly without intervention. Intrauterine insemination (IUI) is most commonly used in the UK when donated sperm is required (due to severe male factor infertility, treatment of same sex female couples or treatment of single women). The success rate per insemination is approximately 10% (Carson and Kallen, 2021). The use of IUI with partner's sperm is generally not beneficial in couples having regular sexual intercourse. Induction of ovulation and/or IUI can only be offered when the oviducts are patent, as tubal occlusions prevent sperm and oocyte meeting *in vivo*. For these patients, the more invasive treatments under the banner of *in vitro* fertilisation (IVF) are their treatment options. IVF may also be recommended over OI and IUI depending on female age and ovarian reserve. Raised female age and reduced ovarian reserve result in declining chances of success in all fertility treatments (HFEA, 2021). IVF with Intracytoplasmic sperm injection (ICSI) is at present the only type of fertility treatment recommended for couples with severe male factor infertility (reduced sperm count, motility or sperm morphology, or sperm retrieved surgically from the testes). An advantage of IVF is that sperm and egg interactions and the quantity and quality of embryos generated can be studied. This can sometimes aid diagnosis of idiopathic (unexplained) infertility (Johnson *et al.*, 2013). The ability to generate multiple embryos and use of embryo selection tools (discussed later) to choose the 'best' embryo to replace mean IVF has a higher success rate per cycle than OI/IUI (HFEA, 2021). Supernumerary embryos can also be cryopreserved for use in future treatment cycles, meaning some patients can achieve multiple embryo transfers from a single round of IVF/ICSI (HFEA, 2021).

While OI and IUI have a place in the fertility treatment pathway, it is the more invasive, more expensive, but also more successful per cycle IVF and ICSI treatments that form the background of this thesis.

The stages of an IVF cycle are summarised in Figure 1.



**Fig 1: Schematic of stages of a standard IVF cycle.** The processes in red represent the ovarian stimulation and monitoring phases (which can take 10 to 21 days depending on the regimen). Laboratory processes are indicated by the yellow boxes, while the final stages in blue are post embryo transfer.

An IVF treatment cycle involves:

- Use of gonadotrophin-releasing hormone (GnRH) agonists or antagonists to induce pituitary downregulation- suppressing endogenous gonadotrophin release which prevents premature ovulation and synchronises growth of follicles with the development of the endometrium (Jin *et al.*, 2021),
- stimulating the ovaries with supraphysiological doses of exogenous gonadotrophins to produce multiple oocytes
- retrieving and fertilising those oocytes,
- culturing and selecting resulting embryos,
- returning embryos to the uterus.

There are a range of clinical protocols in use for downregulation and ovarian stimulation. They vary in length, type and dose of medication and the choice of which is used for the patient depends on female ovarian reserve, cause of infertility, ovarian response in any previous cycles and local protocols (Farquar *et al.*, 2017). Ovarian response is monitored by transvaginal ultrasound and once follicular development reaches an optimum size and number (dependent on local protocols), a carefully timed 'trigger' injection of human chorionic gonadotrophin (hCG) or a GnRH agonist is administered to mimic or induce the LH



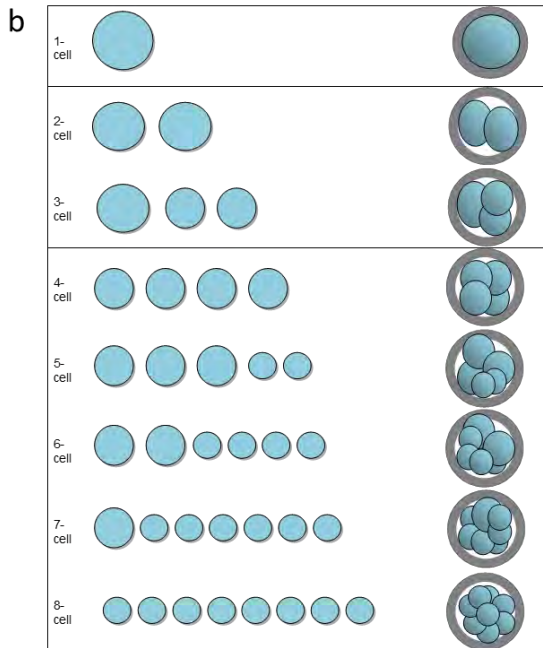
surge. Approximately 36 hours later, egg collection is performed by ultrasound guidance under sedation. Fertilisation is performed by IVF or ICSI on day of egg collection. The processes involved in embryo development and assessment are detailed below. Embryo transfer is performed trans-cervically, usually without the need for sedation. Pregnancy is confirmed initially by detecting human chorionic gonadotrophin (hCG) in urine or blood, 14-16 days after egg collection, then by ultrasound to detect foetal heart activity (clinical pregnancy) at approximately 7 weeks gestation (5 weeks post egg collection) (<https://www.nhs.uk/conditions/ivf/what-happens/>)

Embryo culture, selection and grading at The Department of Reproductive Medicine, Saint Mary's Hospital, Manchester is carried out according to standard operating procedures, which are regularly reviewed, and outcomes audited. Time lapse (TL) incubation is used for the majority of patients. Time-lapse systems combine a high quality, stable, low oxygen incubator with an optical microscope and a software programme, thus providing continual surveillance in uninterrupted optimal culture conditions (Castello *et al.*, 2016). The system used in St Mary's is Embryoscope™ (Vitrolife, Sweden). A more detailed introduction to TL technology is provided later in this chapter.

Immediately after ICSI, injected oocytes are placed into the Embryoscope™, while IVF inseminated oocytes are cultured from the morning of day 1 (pronuclear (PN) stage). Embryos which have been frozen at the PN stage are also cultured in Embryoscope™ after thawing. Embryo grading is performed by initially reviewing TL videos on day 2 and day 3 of development. The grading scheme used is the 'ACE/BFS National Embryo Grading Scheme 2016' (implemented for clinical treatment from January 2017 and for UK NEQAS from April 2017) (Cutting *et al.*, 2009) and is illustrated in Figure 2.

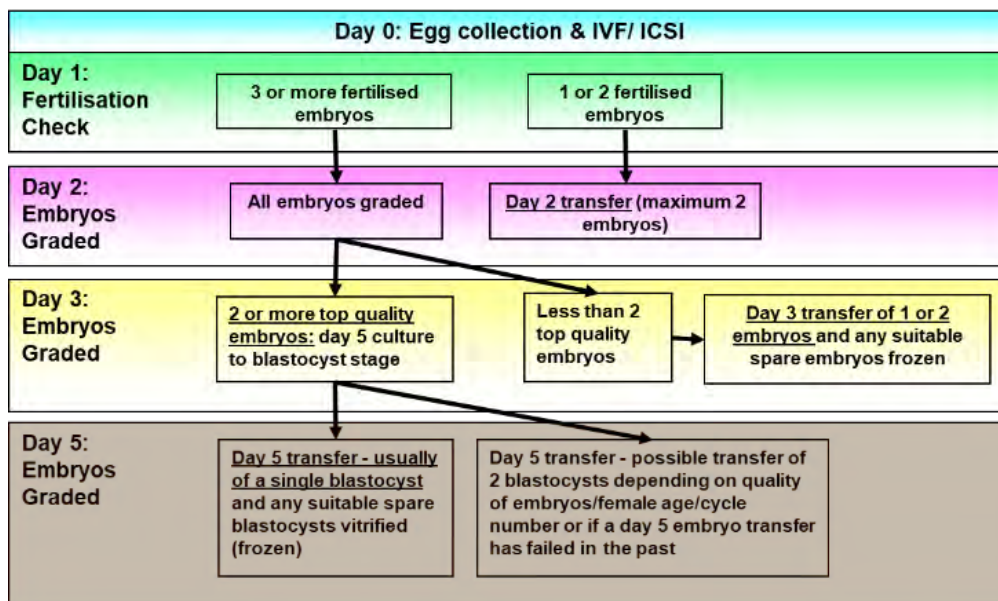
a **Early cleavage stage embryos:** Assess number of blastomeres followed by blastomere size (ideal stage specific) and degree of fragmentation to give a 3-digit code for each embryo based on these parameters. An explanation of stage specific grading for cleavage stage embryos is given below:

Grades	Blastomere size	Fragmentation
4	Same as ideal stage specific embryo (see diagrams)	<10%
3	Stage specific size for majority of blasts(i.e. slightly uneven sizes)	10-20%
2	majority of blasts different sizes	20-50%
1	Not stage specific	>50%



**Fig 2: Cleavage stage (days 2 and 3 of development) grading scheme for human embryos used at St Mary's Hospital.** The scheme captures blastomere number, relative size (stage specific) and degree of fragmentation seen. For blastomere relative size and degree of fragmentation Grade 4 is the highest score, while Grade 1 indicates lowest quality. All 3 parameters are scored independently to give a numeric score, recorded as cell number/blastomere size/fragmentation -for example a high quality 4 cell embryo would be scored 4,4,4 while a poorer quality embryo at the same cell stage might be scored 4,2,2 .

The decision when to proceed to embryo transfer is determined by the number of embryos available and their quality (see Figure 3). Algorithmic scores generated by TL annotations may provide additional information to aid decision making alongside standard morphological grading.



**Fig 3: Schematic of decision making pathway for day of transfer and number of embryos to replace** (taken from St Mary's patient information leaflet). This decision tree is used when the number of embryos to transfer is not pre-determined by the clinician. The initial decision on whether to perform embryo transfer on day 2 is determined by number of embryos available. If more embryos are available than it is planned to transfer, culture beyond day 2 is indicated. Embryos are graded on day 2 and day 3, and if only 1 embryo scores as high quality on day 3, embryo transfer is advised. All other scenarios suggest culture to day 5 improves embryo selection. Number of embryos to replace into the uterus is also determined by availability of good quality embryos.

If there is more than one good quality embryo or embryos in a cohort on day 3 of development, embryo culture is extended to day 5, when embryos should be at the blastocyst stage. Selection of patients who might benefit from extended culture is based on our own data, patient history and patient choice. For example, a young patient with a high number of good quality embryos on day 3, and who can only have a single embryo transferred for health reasons is an obvious candidate. A patient with previous poor development from day 3 to blastocyst may elect to have a day 3 transfer. A minimum of one embryo graded at 8/3/3 on the morning of day 3 (and at least one other 8 cell or good quality 6 or 7 cell embryo) is required for consideration of extended culture.

Embryos are next assessed on day 5 of development. Gardner and Schoolcraft (1999) developed a scoring system for human blastocysts which captured the quality of the two cell types found (trophectoderm (TE) and inner cell mass (ICM)) and the degree of expansion of the blastocoel cavity and related these to chance of implantation. The current blastocyst grading scheme used at St Mary's Hospital is the 'ACE/BFS National Embryo Grading Scheme 2016' (implemented for clinical treatment from January 2017 and for UK NEQAS from April 2017) which is an adaptation of Gardner and Schoolcraft, 1999. It is illustrated in Figure 4.

a

Expansion Score	Expansion status	ICM/ TE score*	Inner Cell Mass (ICM)	Trophectoderm (TE)
6	Hatched blastocyst (the blastocyst has evacuated the ZP)			
5	Hatching blastocyst (trophectoderm has started to herniate through ZP)			
4	Expanded (blastocoel volume larger than the embryo, with thinning of ZP)	<b>A</b>	ICM prominent, easily seen, tightly adhered compacted cells	Continuous layer of small identical cells
3	Full blastocyst (blastocoel completely fills embryo)	<b>B</b>	ICM less prominent (cells appear compacted and larger in size, loosely adhered)	Fewer cells with gaps, not continuous
2	Blastocyst (blastocoel >50% volume of embryo)	<b>C</b>	Very few cells visible (cells similar to TE)	Fewer small cells with large cells, not continuous
1	Early blastocyst (blastocoel <50% volume of embryo)	<b>D</b>	No visible cells or visible cells are degenerate or necrotic	Sparse cells, large/flat/degenerate

Blastocyst Grading Scheme

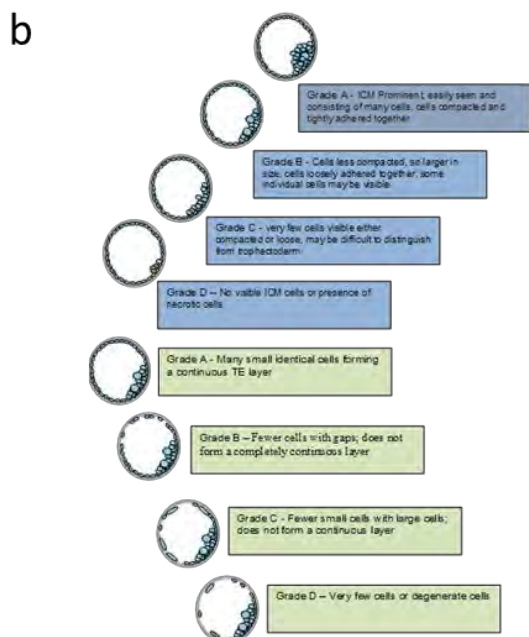


Fig 4: Blastocyst grading scheme used at St Mary's Hospital; a=written schematic, b=visual guide. Blastocysts are graded by degree of expansion/ICM grade/TE grade. For example a 5AA would be a top quality blastocyst beginning to hatch from the zona pellucida.

Embryo cryopreservation is a routine procedure in IVF laboratories, where it is a valuable technique to aid safe and efficient use of all good quality embryos generated from a single egg collection (Veeck *et al.*, 1993, 2004). Freezing can be carried out at all stages from pronucleate stage to day 6 blastocyst. There are two main protocols in routine use – ‘slow

freezing' followed by rapid thawing, and vitrification followed by warming. Both techniques use cryoprotective agents to prevent cell damage due to ice crystal formation. Slow freezing uses lower levels of cryoprotectants and requires a programmable controlled rate freezer which takes the embryos through defined steps and cooling rates to -70°C then plunged to -180°C. Seeding, where ice crystal enucleation at a point away from the sample is induced, takes place around -7°C and is a crucial part of this process. Vitrification uses a shorter exposure to much higher concentrations of cryoprotectants, followed by an immediate submersion in liquid nitrogen, giving ultrarapid cooling rates and a glass-like state is formed without ice crystals (Cascianni *et al.*, 2023). As part of an assisted conception programme, successful embryo cryopreservation helps to prevent multiple pregnancy as single embryo transfer programmes are more widely accepted when supernumerary embryos can be frozen and used at a later date (Gerris *et al.*, 2003; Pandian *et al.*, 2005). Freezing of all embryos generated is a treatment strategy used in IVF clinics where a fresh embryo transfer following IVF or ICSI is not recommended, usually as the female is at risk of developing ovarian hyperstimulation syndrome (OHSS), although there are other indications (reviewed in Bourdon *et al.*, 2021). Creating then storing embryos for use in a subsequent frozen embryo transfer (FET) cycle is an effective strategy for managing this risk. Pregnancy increases the chance that OHSS will develop, as human chorionic gonadotrophin (hCG) is implicated in its development. An ongoing pregnancy increases the severity of the condition as hCG levels rise and reduces options available for treatment (Devroey *et al.*, 2011).

At St Mary's Hospital, patients who had undergone IVF or ICSI and have a 'freeze all' cycle where an embryo transfer was not planned routinely have embryos frozen at the PN stage using a slow-freezing protocol. Freezing at this stage has the benefits of high post thaw survival rates (>95% compared to 60-70% for cleavage stage embryos) and is less labour intensive than culturing and vitrifying large numbers of blastocysts (Hunter *et al.*, 2020). An audit of patients who had freeze all cycles at St Mary's showed around 30% never returned to use their stored embryos. Hence the decision was made to invest time and resources in embryo culture when the patient returned for frozen embryo transfer.

Since a review of results from PN stage freezing in 2019, the recommendation of the clinic has been to thaw at least 6 and up to 12 PN stage embryos (where available), then allow these embryos to develop for up to 5 days in culture, to replicate the conditions of the fresh

treatment cycle, and allow selection of the most viable embryo(s) from the cohort for replacement in the uterus. Supernumerary embryos from this thaw that also reach good quality blastocyst stage can be re-cryopreserved using a vitrification method for use in subsequent cycles. At present, there are no morphokinetic algorithms available for this group of embryos, so although TL is routinely used for their culture, the full benefit of the technology cannot be utilised.

### **1.1 The need to investigate implantation**

There is significant embryo loss during all human reproduction, with estimates that only 30% of conceptions end in live birth (Zinamen *et al.*, 1996; Slama *et al.*, 2002). These odds may define the maximum birth rates that can be reached with IVF, despite advances in embryo culture techniques. Factors limiting IVF success include inadequacies in identifying viable embryos, and the transfer of embryos into uteri with an unknown state of receptivity (Cha *et al.*, 2013).

The financial, physical and psychological costs of repeated IVF cycles place significant burdens on individuals and health systems (Cousineau and Domar., 2007; Nicoloro-SantaBarbara *et al.*, 2017). Low success rates encourage the transfer of several embryos at each attempt, resulting in high numbers of multiple pregnancies, which bring risks to the mother of pregnancy associated complications (gestational diabetes, preeclampsia, anaemia, need for caesarean section) and to the foetus (preterm delivery, growth restriction, birth defects) (Macklon *et al.*, 2002). Failures to address gaps in our knowledge of embryo selection and implantation mean that we are failing our patients. We ought to be to help couples to achieve healthy singleton pregnancies in the shortest time possible, minimising all types of costs for all stakeholders.

### **1.2 Implantation – the ‘black box’ in ART**

There is a ‘diagnostic gap’ for patients who fail to achieve successful pregnancies despite transfers of multiple embryos over multiple treatment cycles. This could be due to recurrent miscarriage (RM) or recurrent implantation failure (RIF). Improved outcomes after management of benign gynaecological diseases such as endometriosis support the hypothesis that failure of endometrial receptivity may contribute to infertility (Cakmak and Taylor, 2011; Lessey, 2011; Sharkey and Macklon 2013).

Implantation is a process, not a single event, and can be defined as the initiation of a stable adhesion between the blastocyst and maternal tissue (endometrium) (Aplin and Ruane, 2017). It can be broadly divided into 3 stages: apposition, attachment and invasion and these are illustrated in Figure 5 (Sharkey and Macklon, 2013; Aplin and Ruane, 2017).

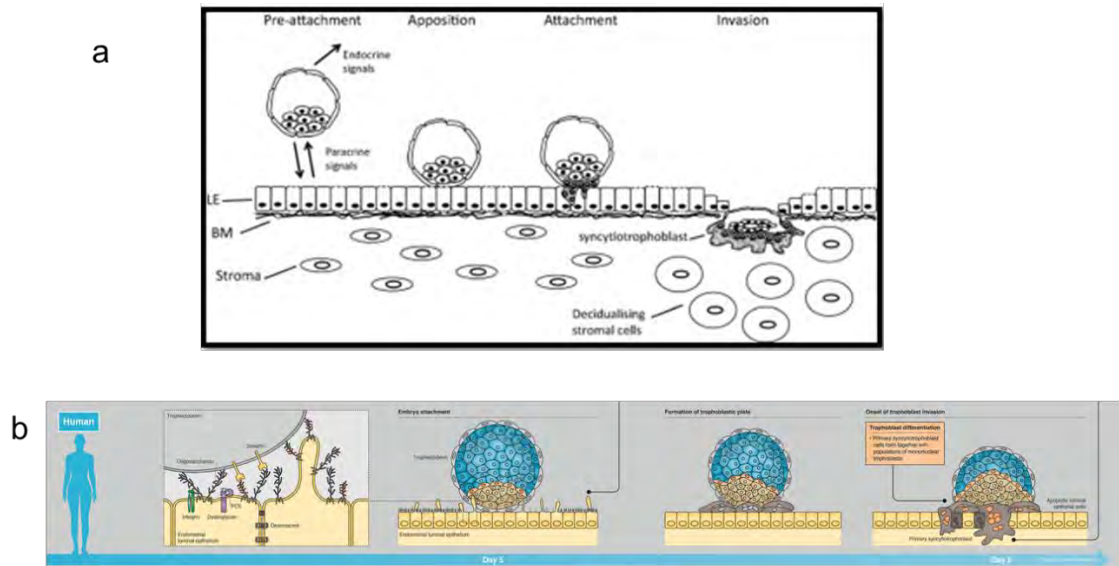
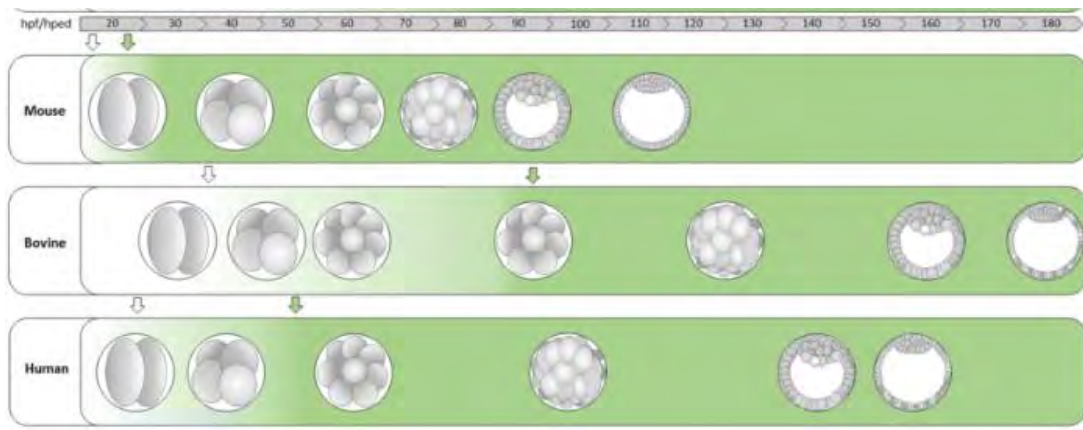


Fig 5: Schematics of early embryo implantation in the human. 5a (Sharkey and Macklon, 2013) is a broad overview: the pre-implantation embryo signals its presence by endocrine mediators, (hCG) and paracrine growth factors. These act locally on the endometrium. As shown, following attachment the embryo penetrates the luminal epithelium (LE), breaches the basement membrane (BM) and invades into the underlying stromal cells. The process of attachment and invasion is shown in more detail in 5b (adapted from Aplin and Ruane, 2017).

For successful implantation, there are 3 key elements: an embryo competent to implant, a receptive endometrium, and a successful 'conversation' between the two. (Sharkey and Macklon, 2013).

### 1.3 'An embryo competent to implant'

The timeline of preimplantation development in human, mouse and bovine embryos is summarised in Figure 6.



**Fig 6: Progression of development during time after fertilization in mouse, bovine and human embryos.** Mammalian embryos divide approximately every 12–24 h and reach the blastocyst stage after 4 days (mouse), 5-6 days (human) 7-9 days (cattle). Embryonic genome activation (EGA) occurs around 8-16 cell stage in cattle, by the 8 cell stage in human and the 2 cell stage in the mouse ( image adapted from Toralová *et al*, 2020)

Human embryos generated during IVF are cultured for up to 6 days, and embryo transfer or cryopreservation is performed normally on day 5 of development (blastocyst stage), but can also be performed on day 2 (2-4 cell stage) or day 3 (8 cell stage). Selection of the embryo with the highest implantation potential is crucial in achieving pregnancy in the shortest time for a patient undergoing IVF (Tran *et al.*, 2018).

Assessment of embryo quality using static morphology remains the most common method for selection (Gardner *et al.*, 2015; Ebner *et al.*, 2020). Assessments routinely take place at 18, 44, 68 and 120 hours after insemination (Ilyin *et al.*, 2019). There are several grading systems which aim to provide consensus as to what is a 'good quality' embryo. (Alpha, 2011; Dokras *et al.*, 1993; Racowsky *et al.*, 2010; Shapiro *et al.*, 2000; Steer *et al.*, 1992; Cutting *et al.*, 2008; Harbottle *et al.*, 2015). While there is a general move towards blastocyst culture and even preimplantation genetic screening such as PGT-A (preimplantation genetic testing for aneuploidy – an invasive procedure involving removing cells from the trophectoderm to determine the chromosomal status of the embryo), to identify embryos with the highest



implantation potential, there may still be value in scoring earlier in development. Culture to the blastocyst stage helps improve morphological selection and synchronisation when returning the embryo to the uterus, but must be balanced against increased cost, risk of cancelled cycles and possible epigenetic effects on the embryo (Miles *et al.*, 2007; Kirkegaard *et al.*, 2012). Concerns have been raised that interventions during assisted conception (ICSI, embryo biopsy) and exposure of embryos to suboptimal culture conditions during development to blastocyst might raise the risk of imprinting disorders (such as Prader-Willi syndrome), and such effects have been seen in animal studies (Gad *et al.*, 2012). Some studies have indicated that the relative risk for some imprinting disorders in children born from assisted conception can be raised by 5 times compared to natural conception (Vermeiden and Bernardus, 2013). Recent studies summarised in Sciorio and El Hajj (2022) suggest that some alterations may be related to parental age (often raised in couples seeking IVF) and cause of infertility rather than assisted conception techniques, but stress further work is needed.

Embryo scoring at the pronucleate (PN) stage (16-18 hours post-insemination) has long been used – especially in regions of the world where extended embryo culture is not permitted (Scott, 2003a, b; Azzarello *et al.*, 2012; Braga *et al.*, 2013). The most well established method is Z-scoring, which assesses PN size, localisation, and number and localisation of nucleoli (Scott and Smith, 1998; Scott, 2003a, b). Some sources report that Z score can predict the formation of blastocysts in humans and mice with 90% accuracy (Yanez *et al.*, 2016), and a number of studies link zygote morphology with embryo quality and chromosomal status (Zamora *et al.*, 2011; Aydin *et al.*, 2011; Braga *et al.*, 2013; Yanez *et al.*, 2016; Gianaroli *et al.*, 2007; Ilyin *et al.*, 2019). An alternative to the full Z-score is postulated (Otsuki *et al.*, 2017). Measuring only pronuclear size in a time-lapse system, just before breakdown of the pronuclear membranes (PNMBD) seems to provide a relatively accurate prediction of live birth. Further work has developed a non-invasive time-lapse evaluation of zygotes with a success rate of >50% and a failure rate of <10% in predicting embryos that would NOT result in healthy pregnancies, based on changes in the relative size of the male and female PN (Otsuki *et al.*, 2019).

Work by Gerris and colleagues retrospectively determined key parameters from images of embryos on day 2 and day 3 which were known to have implanted. These included having 4 or 5 blastomeres on day 2, at least 7 on day 3, <20% fragmentation and no signs of

multinucleation (Gerris *et al.*, 1999; Van Royen *et al.*, 1999). A grading scheme based on these parameters plus blastomere symmetry and cytoplasmic appearance was developed and found to efficiently predict blastocyst formation and implantation (Rienzi *et al.*, 2005). High degrees of chromosomal abnormality have been observed with low (<6) or high (>9) cells on day 3 of development (Magli *et al.*, 1998). A study by Kong and colleagues (2016) found that the main reason for low cell numbers and blastomere loss on day 3 was fragmentation of daughter blastomeres at divisions. Higher than expected cell numbers were usually caused by a blastomere dividing into 3 cells. An embryo of 7-8 cells on day 3 was much less likely to have exhibited any abnormal behaviours in the first two cleavage stages.

While limited static observations protect the embryo from changes to its environment (as embryos needed to be removed from incubators for viewing), they conceal what happens between assessments. (Cruz *et al.*, 2012). The introduction of time-lapse (TL) technology has been a huge advance; embryos benefit from undisturbed culture – there is no need to remove them from the incubator for assessment. Embryologists can also not only analyse embryo morphology but also view dynamic changes between set timepoints, observing transitional events such as vacuolation, reverse cleavage and fragmentation (Almagor *et al.*, 2015; Lui *et al.*, 2014; Rubio *et al.*, 2012; Zhan *et al.*, 2016), allowing the de-selection of embryos that might otherwise appear as good quality (Kirkegaard *et al.*, 2013). Timing of certain stages within preimplantation development can also be recorded (morphokinetics) (Meseguer *et al.*, 2011, 2012). Time to first cleavage is strongly associated with implantation potential (Lundin *et al.*, 2001; Sakkas *et al.*, 2001; Salumets *et al.*, 2003; Van monfoort *et al.*, 2004) with cleavage before and after the window of 26-28 hours post insemination giving a poorer prognosis. In a 2015 study, the authors found significant differences in mean time of pronuclear fading (PNf), time of 1<sup>st</sup> cleavage (t<sub>2</sub>), time to 5 cells (t<sub>5</sub>), t<sub>5</sub>-t<sub>3</sub> and t<sub>5</sub>-t<sub>2</sub> between genetically normal and abnormal embryos (Chawla *et al.*, 2015). While many reports support the use of morphokinetics in embryo selection (Meseguer *et al.*, 2011, 2012; Fishel *et al.*, 2017; Aparicio-Ruiz *et al.*, 2016), there is not yet a strong enough association with embryo ploidy to replace the use of PGT-A (Kaser and Racowsky, 2014; Mumusoglu *et al.*, 2017).

Time-lapse systems have only been in routine clinical use since 2008 (Pribenszky *et al.*, 2010). Morphokinetic algorithms representing optimum implantation vary between clinics, due to differing culture and environmental conditions and patient demographics (Kirkegaard *et al.*,

2014; Basile *et al.*, 2015; Barrie *et al.*, 2017). An algorithm which aims to 'deselect' embryos of low implantation potential may be more generally applicable (Petersen *et al.*, 2016), this type of model also has a much lower risk of rejecting embryos which might still have some potential. Many algorithms currently in use (e.g. KIDScore) have a higher predictive potential for blastocyst formation than implantation, useful in aiding the embryologist in selecting patients for extending culture to day 5, but should not necessarily be relied upon when selecting embryos for replacement. An important future study might be to analyse the inclusion of morphology with morphokinetics to develop more sensitive algorithms (Petersen *et al.*, 2016).

Morphological grading of blastocysts considers degree of blastocoel expansion, as well as a subjective judgement of the number and quality of cells in the trophectoderm (TE) and inner cell mass (ICM). Some studies have determined that TE quality and expansion are most strongly associated with pregnancy and live birth (Ahlstrom *et al.*, 2011; Ebner *et al.*, 2016; Hill *et al.*, 2013; Thompson *et al.*, 2013; Van den Abbeel *et al.*, 2013; Zaninovic *et al.*, 2001) while others indicate that the quality of the ICM is more important (Licciardi *et al.*, 2015; Subira *et al.*, 2016). The dynamic nature of blastocyst development and expansion has been correlated with hatching potential in the mouse and human (Mio, 2006; Mio and Maeda, 2008; Pribenszky *et al.*, 2010). Huang and colleagues (Huang *et al.*, 2016, 2019) aimed to establish a morphokinetic measurement of blastocyst expansion that could relate to embryo ploidy – a non-invasive approach to embryo screening. Successful blastocysts had a comparatively more rapid rate of expansion than unsuccessful embryos. A delay in time to the initiation of blastulation is associated with aneuploidy in human embryos in a study by Campbell *et al.* (2013a), but this finding was not replicated in a retrospective study in a different clinic (Kramer *et al.*, 2014). Relatively slow expansion has been reported in embryos *in vitro* that have impaired zona hatching (Iwata *et al.*, 2012; Pribenszky *et al.*, 2010). The authors identified 2 patterns of pulse-like oscillations during expansion: firstly, a generally positive, relatively uninterrupted expansion (E-type) and a C type, characterised by dramatic collapses of the blastocoel cavity with a loss of up to 50% of volume. The mechanisms involved in both types of oscillation remain to be identified and may be passive responses to building pressure in the expanding blastocoel, and there may be a role for the zona pellucida in modulation (Chinn and Huang, 2015). There may be an active control by TE cells altering

ion transport across the developing epithelium or intercellular leakiness may occur as dividing cells are inserted into the TE layer (Guillot and Lecuit, 2013, Hu *et al.*, 2013). Dramatic C type contractions are related to impaired zona hatching *in vitro* (Niimura, 2003) and differences in extent and frequency of this collapse may account for slower expansion rates in unsuccessful embryos. E type oscillations may reflect a normal response of the embryo to pressure changes during expansion, while C type represent an acute failure to respond (Huang *et al.*, 2016). It would be valuable to link these observations to a larger group of unsuccessful cases, more defined group of patients, or relate to embryos with known aneuploidy.

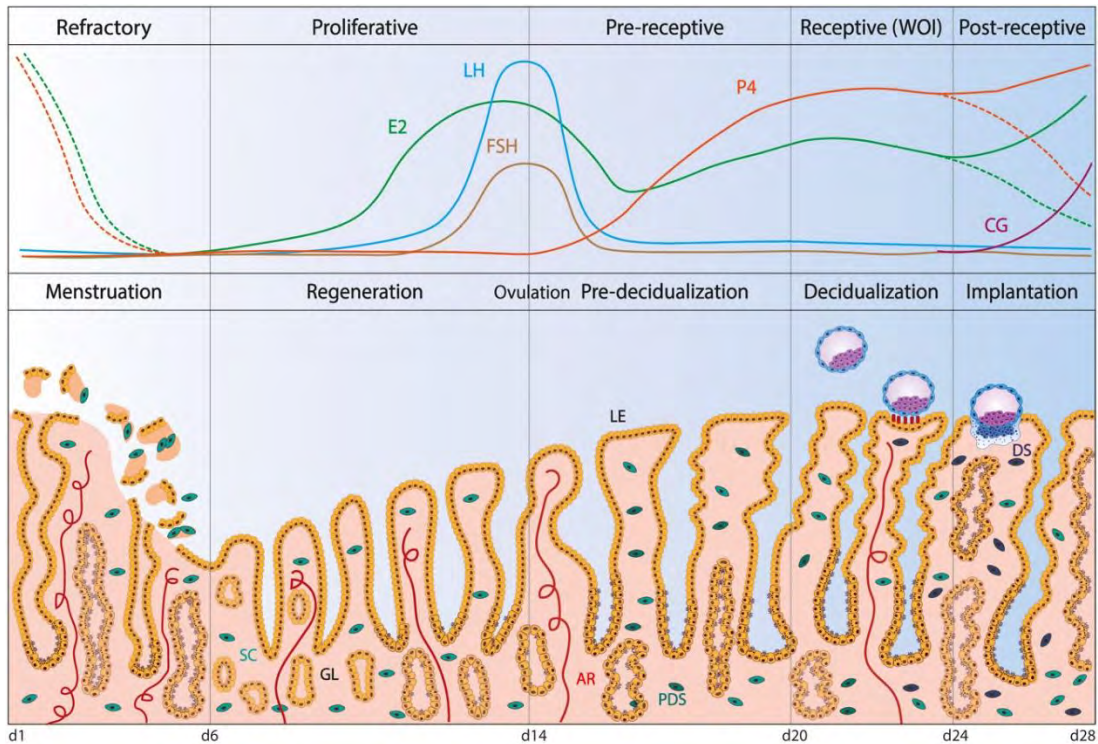
TL has also facilitated closer studies of morphological features which may be markers of viability – for example the presence of thread-like cytoplasmic strings in the expanded blastocyst, observed to bridge the ICM with the TE. Some studies (Scott, 2000; Hardarson *et al.*, 2012 ) claim that persistent cytoplasmic strings are a negative predictor of viability, arising from problems with polarisation or an *in vitro* artefact from poor media conditions, while others state no effect (Alpha, 2011; Ciray *et al.*, 2014). These strings are also observed in mouse embryos *in vitro* and less often *in vivo* (Salas-Vidal and Lomeli, 2004) and there is a small amount of evidence for their presence in *in vivo* human blastocysts (Munne *et al.*, 2018). There is a significant association between blastocyst collapse and the appearance of strings. As already discussed, blastocyst collapse per se is not an independent predictor of pregnancy or live birth, and it is interesting that a series of collapses leading to string formation could be a mechanism for monozygotic twinning (Otsuki *et al.*, 2016). In the mouse these strings are actin-rich and strong evidence shows direct communication between ICM and TE cells possibly via receptors for fibroblast growth factor 2 and human epidermal growth factor 3, found in specialised cell compartments of the strings (Salas-Vidal and Lomeli, 2004). These compartments appear as bulges in the strings in mouse and human embryos, possibly indicating a vesicle transport mechanism (Miller *et al.*, 1995; Ebner *et al.*, 2020). Some authors report a high number of moving vesicles in human blastocysts that gave rise to clinical pregnancies (Eastwick *et al.*, 2019)

The high rate of early pregnancy loss observed in human reproduction is thought to be due to two key features of human embryos – their intrinsic ability to invade the endometrium, and the high prevalence of chromosomal abnormalities (Macklon and Brosens, 2014). In excess of 70% of high-quality cleavage stage human IVF embryos harbour cells with complex,

large scale structural chromosomal imbalances, mostly due to mitotic non-disjunction (Fragouli *et al.*, 2013; Mertzaniidou *et al.*, 2013; Vanneste *et al.*, 2009). Even after PGT-A, the live birth rate per embryo is still only around 50% (Kang *et al.*, 2016; Friedenthal *et al.*, 2018; Rosenwaks *et al.*, 2018). False positive PGT-A results, and mosaicism can also result in viable embryos being discarded unnecessarily (Otsuki *et al.*, 2019). There are some suggestions in the literature that some degree of cytogenetic anomalies in the human embryo may give an implantation advantage, as they resemble those found in cancer cells which have a highly invasive phenotype (Vanneste *et al.*, 2009; Brosens *et al.*, 2014).

#### **1.4 'A receptive endometrium'**

Human embryo implantation occurs approximately seven days after ovulation. Oestrogen and progesterone induce extensive remodelling of the endometrium throughout the menstrual cycle, which lasts for approximately 28 days in the human, and it becomes receptive for just a few days in the mid-secretory phase. The developing embryo moves from the fallopian tube into the uterine cavity around 4 days after ovulation (or following IVF is placed into the cavity via the cervix any time from 2 to 5 days of development). Hatching of the blastocyst from the zona pellucida is thought to occur late on day 5 or day 6. In mice, a discrete 'window of implantation' (WOI) lasts for 24 hours between days 4 and 5 after ovulation (Psychoyos, 1986) and co-ordinated interactions between oestrogen and progesterone are known to be vital in the mouse for opening and closing this window (Ma *et al.*, 2003). In humans, the window is thought to extend from day 5 to day 10 and is less well defined (Navot *et al.*, 1991). The dynamic processes involved in the hypothalamic-pituitary-ovarian axis, ovulation and embryo development and changes in the endometrium are summarised in Figure 7.



**Fig 7: Endometrial changes across the menstrual cycle.** Menstruation is the first phase: spiral arteries (AR) contract, resulting in ischaemia and shedding of the epithelial and stromal cells and repair starts almost simultaneously. In the proliferative phase, regeneration is driven by rising levels of oestrogen (E2) from the ovarian follicle, stimulating proliferation of epithelial, stromal and endothelial cells. At midcycle, follicle-stimulating hormone (FSH) and luteinizing hormone (LH) released from the anterior pituitary induce ovulation. Ovulation marks the beginning of the secretory phase during which the corpus luteum forms from the ruptured ovarian follicle and secretes progesterone (P4), which prepares the uterine environment for pregnancy. The endometrial glands (GL) become cork-screw shaped and twisted. The stromal cells (SC) differentiate into pre-decidualized stromal first (PDS) and then decidualized stromal (DS) cells. Rising levels of E2 in combination with P4 mark the window of implantation (WOI). In the absence of a blastocyst, the WOI spontaneously becomes refractory due to the rapid decrease in P4 levels leading to menstruation, thus resetting the cycle. Conversely, an implanting blastocyst secretes chorionic gonadotropin (CG) to maintain the secretion of P4 from the corpus luteum, thereby supporting pregnancy. (From Nikolakopoulou and Turco, 2021)

Primarily, receptivity is acquired due to maternal sequential exposure to oestrogen then progesterone altering the transcription of hundreds of genes (Ruiz-Alonso *et al.*, 2012). Although many of these have been identified in humans, the correlation with a receptive period is difficult to establish as studies are hampered by relatively small sample sizes, differences in study design, and an inherent variability of endometrial gene expression not only between women, but also from cycle to cycle in any one individual (Lessey *et al.*, 1995; Ruiz-Alonzo *et al.*, 2013; Edgell *et al.*, 2013).

As well as issues with failing to form a pregnancy, there is evidence that IVF pregnancies are associated with altered foetal growth, with long term impacts on the health of the individual

(Ceelan *et al.*, 2008; Hart and Norman, 2013). One putative cause for high rates of implantation failure after human IVF is that supraphysiological levels of oestrogen (arising from the hyperstimulation of the ovaries to collect multiple oocytes) induces uterine non-receptivity too early, and the blastocyst cannot implant no matter its quality. (Evans *et al.*, 2014; Fauser and Devroey, 2003).

The first point of contact for the blastocyst is the luminal endometrial epithelium, and this transforms from a non-adhesive to an adhesive surface by extensive remodelling of the glycocalyx, and changes to epithelial polarity, lateral junction complexes and epithelial-mesenchymal transition (Murphy, 2004). In contrast to other species, human trophoblast cells do not destroy the epithelium to reach the stroma but invade between epithelial cells (Bentin-Ley *et al.*, 2000; Li *et al.*, 2015; Ruane *et al.*, 2022). (Figure 5)

Transcriptomic profiling studies have identified large numbers of genes whose profile of regulation changes at the time of endometrial receptivity, but these data sets vary hugely between studies (reviewed in Evans *et al.*, 2016, and Walker *et al.*, 2023). Some molecular changes have been more thoroughly studied across mouse and human. These include endometrial transcription factors such as HOXA10, STAT3 and p53 (Catalano *et al.*, 2005; Hu *et al.*, 2007; Lynch *et al.*, 2008; Nakamura *et al.*, 2006), cell adhesion molecules and their ligands, for example integrins, osteopontin, L-Selectin (Aoki *et al.*, 2000; Donaghy *et al.*, 2007; Genbacev *et al.*, 2003), growth factors and cytokines such as heparin-binding epidermal growth factor-like growth factor (HB-EGF), and cell surface associated mucins (Dey *et al.*, 2004, reviewed in Davidson *et al.*, 2016). There is strong evidence for the role of leukaemia inhibitory factor (LIF) (a member of the IL-6 family of cytokines) as a mediator of oestrogen action. Expression of the *lif* gene is higher in the endometrium of fertile women than infertile women around the time of implantation (Laird *et al.*, 1997; Piccinni *et al.*, 1998; Hambartsoumian *et al.*, 1998), but whether it is essential for implantation in humans remains unclear (Cha *et al.*, 2012) as most of the evidence is from mouse models. Female mice lacking a functional LIF gene show failure of implantation, although their blastocysts, if transferred to a wild type female implant and develop to term (Stewart *et al.*, 1992), and intraperitoneal injections of anti-LIF antibody (Terakawa *et al.*, 2011) and LIF antagonist (White *et al.*, 2007) both inhibited pregnancy in mouse models.

In the void that remains in our understanding of endometrial receptivity, a number of commercially available tests claiming to analyse an individual's endometrium for receptivity and personalise their 'window of implantation' (WOI) have emerged. Following on from histological biopsies, Endometrial Receptivity Analysis (ERA) uses molecular arrays (or now next generation sequencing) to analyse the transcriptomic profile of a biopsy taken from the patient in a non-treatment cycle, during her predicted WOI (i.e. LH surge +7 days). This profile is then compared to a panel of differentially expressed genes identified as expressed in 'receptive' as well as 'pre'-or 'post'-receptive endometrium, in order to diagnose the status of the biopsy and hence if the patient's WOI is outside the normal range (Diaz-Gimeno et al., 2011). The limitations of this test have been debated, and there are several factors which limit its value and efficacy – the method and timing of biopsy, the lack of clarity around what a 'normal' WOI transcriptome looks like, and normal variation in menstrual cycles to name just a few (Rafael, 2021). Although in wide use across the field, the HFEA have recently given endometrial receptivity testing a red rating on their survey of treatment add-ons, meaning that moderate to high quality evidence suggests the test may reduce treatment effectiveness. Some authors, however, argue that it may be of benefit in some populations and further study is required (Rubin *et al.*, 2023; Mahajan et al., 2018). Additional tests of the endometrial microbiome (endometrial microbiome metagenomics analysis [EMMA] and analysis of infectious chronic endometritis {ALICE}) are increasing in popularity as part of testing (alongside ERA) for recurrent implantation failure, despite a lack of published studies.

### **1.5 'A successful conversation between embryo and endometrium'**

There is a developing body of evidence that signalling between the human embryo and the endometrium modulates endometrial receptivity (Evans *et al.*, 2016).

Once the blastocyst is in close proximity to the endometrium, there is evidence for molecular cross talk via paracrine and juxtacrine activation of membrane receptors. Paracrine signals from the embryo may be necessary to develop a fully receptive endometrium (Wang and Dey, 2006). Some *in vivo* studies have found changes in global endometrial gene expression only when an embryo is present (Duncan *et al.*, 2011; Van Vaerenbergh *et al.*, 2010). Human chorionic gonadotrophin (hCG), secreted by the TE is one mediator of this local dialogue;



infusing hCG into the uterine cavity *in vivo*, and *in vitro* studies show changes in expression of multiple endometrial genes (Horne *et al.*, 2009; Licht *et al.*, 2007)

In the mouse, a dialogue is mediated by ErbB4 activation by soluble and membrane bound HB-EGF, leading to expression of integrin cell adhesion molecules at the surface of both TE and epithelial cells, facilitating blastocyst attachment and invasion (Wang *et al.*, 2000, 2002). In humans the HB-EGF axis may be activated by homophilic binding of trophinin. In both species it appears that the effect is both to trigger proliferation of TE cells to promote invasion, and apoptosis in the epithelial cells, permitting breaching by the blastocyst (Sugihara *et al.*, 2007; Tamura *et al.*, 2011). Recent work by Ruane *et al.* (2017) has demonstrated that physical apposition to endometrial epithelial cells for 24 hours prior to the time of attachment is required for mouse blastocysts to develop the invasive behaviours required. Co-culture where the embryo is separated from the epithelial cell line by a permeable insert showed embryos could stably attach to, but not breach the monolayer. A more recent study (Ruane *et al.*, 2022) modelled the epithelial stage of human implantation using a co-culture of human blastocysts or human trophoblast stem cell spheroids with Ishikawa cells (an endometrial epithelial cell (EEC) line). This study found that interactions with EEC promote the differentiation of trophoblast to the invasive syncytiotrophoblast, which then breaches the endometrial epithelium. This evidence supports earlier studies suggesting a maternal mechanism which promotes TE differentiation to an invasive phenotype, possibly via HB-EGF, trophinin or microRNA I-miR-30d (Wang *et al.*, 2002; Sugihara *et al.*, 2007; Vilella *et al.*, 2015). Addition of HB-EGF to culture media during IVF procedures has been shown in some studies to have a beneficial effect on embryo development and attachment *in vitro* (Martin *et al.*, 1998; Lim and Dey, 2009), although clinical trial data is lacking. Dysregulation of HB-EGF is also linked with pre-eclampsia, a serious complication of pregnancy, which originates from defects during implantation (most notably poor trophoblast invasion) (Leach *et al.*, 2002)

The initial 'physical' contact of the embryo with maternal tissue is via TE cells and the glycocalyx of the apical cells of the endometrial luminal epithelium (Aplin and Ruane, 2017). The glycocalyx is generally anti-adhesive and has been shown to contain the intercalating mucins MUC-1 and MUC 16 in large amounts in mouse and human. (Aplin *et al.*, 2001; Dharmaraj *et al.*, 2014; Diaz-Gimeno *et al.*, 2014; Fukuda and Sugihara, 2008; Fukuda *et al.*, 2008; Gipson *et al.*, 2008). In the mouse, MUC-1 is downregulated by day 3 post ovulation to

reduce this layer in time for the embryo to attach (although this alone does not allow full uterine receptivity) (Fouladi-Nashta *et al.*, 2005). In humans, MUC-1 and MUC-16 are expressed throughout the menstrual cycle, and there is evidence for MUC-1 being locally cleared in the area under and around the attached embryo (Meseguer *et al.*, 2001; Singh *et al.*, 2010), possibly via an embryo derived trypsin-like protease (Brosens *et al.*, 2014). Uterodomes (protrusions on the apical epithelial cells) have a thinner glycocalyx (Gipson *et al.*, 2008; Lopata *et al.*, 2002) which may facilitate interaction with the embryo, but studies have queried their absolute requirement for implantation (Quinn and Casper, 2009).

Another cell surface glycoprotein found on both TE of human and mouse blastocysts and the endometrium (Campbell *et al.*, 1995a; Lu *et al.*, 2002) is the hyaluronic acid (HA) receptor CD44. A ligand for osteopontin, which has been implicated in implantation (Johnson *et al.*, 2014; Berneau *et al.*, 2019), binding to CD44 causes a cascade which activates the Wnt/ $\beta$ -catenin signalling pathway (Zheng *et al.*, 2017), associated with endometrial receptivity in mice (Mohamed *et al.*, 2005). HA is present in uterine fluid, and a commercially available embryo transfer medium (Embryoglu<sup>TM</sup>, Vitrolife) containing high levels of HA has been reported to increase live birth rates after IVF in humans (Bontekoe *et al.*, 2014), although other studies have shown no improvement (Chun *et al.*, 2016). As a result it is considered an 'add-on' by the HFEA and rated amber, due to conflicting high quality evidence as to whether its use improves treatment outcomes. An *in vitro* model suggests HA acts not by bridging CD44 receptors (as a 'glue') but by altering expression of genes important in implantation (Ruane *et al.*, 2020).

The cell adhesion molecules integrins have been long postulated to have a role in mammalian implantation. Human hatched blastocysts express several integrins (Campbell *et al.*, 1995b), and integrins are also found on the endometrial epithelium. There is some evidence that the attachment of an embryo regulates expression of integrins  $\beta$ 3,  $\alpha$ 4 and  $\alpha$ 1 in human endometrial cell lines *in vitro* (Simon *et al.*, 1997). Experiments with function-inhibiting antibodies to  $\alpha$ v $\beta$ 3 or  $\alpha$ v $\beta$ 8 in animal models reduces embryo attachment *in vitro* (Kaneko *et al.*, 2011, 2013) and *in vivo* (Illera *et al.*, 2000, 2003; Kumar *et al.*, 2015). In mouse, integrins appear in TE at different stages of development, suggesting a dynamic role in the implantation process (Sutherland *et al.*, 1988, 1993). Binding of extracellular matrix macromolecules such as fibronectin, vitronectin and osteopontin to the mouse blastocyst also stimulates

movement of integrins to the TE surface and formation of focal-contact-like structures (Chaen *et al.*, 2012; Yelian *et al.*, 1995).

Uterine fluid provides an environment for preimplantation development, containing nutrients essential for blastocyst growth and regulatory molecules (Salamonsen *et al.*, 2016). Maternal micro RNAs (miRNAs) (specifically Has-miR-30d) have been shown to be released into human endometrial fluid during the window of implantation, and taken up by mouse embryos via the TE. This results in an overexpression of genes associated with embryonic adhesion in the mouse, suggesting maternal miRNAs can modify the transcriptome of the embryo before attachment (Vilella *et al.*, 2015). Some miRNAs could act as potential markers for receptivity and cycle phase – profiles are altered in women with infertility, endometriosis, RM and RIF (reviewed in Evans *et al.*, 2016). Human blastocysts can also secrete miRNAs to modify the endometrial response – and could be a biomarker for implantation potential. Culture media from ‘high quality’ blastocysts that did not implant contained miR-661, which blocks the adhesive capacity of endometrial epithelial cells in culture (Cuman *et al.*, 2013, 2015)

*In vitro* models of abnormal implantation – where poor quality embryos were co-cultured with decidualised stromal cells (DSC)– showed downregulation of cytokine secretion (IL-1 $\beta$ , HB-EGF and LIF) in the DSC, suggesting DSC recognise poor embryos and prevent implantation (Tecklenberg *et al.*, 2010). Further support for this hypothesis comes from RM patients, whose DSC fail to respond in the same way, revealing a lack of embryo ‘sensing’ (Weimar *et al.*, 2012). One possible mechanism is that impaired human embryos are metabolically ‘noisy’ (Leese, 2002; Brison *et al.*, 2004; Sturmey *et al.*, 2009), sending signals into their surroundings which induce the DSC to ‘switch off’ genes implicated in implantation. In experiments using conditioned media from poor quality embryos, HSPA8 (a member of the heat shock protein 70 family) was the most downregulated gene in DSC – and this knockdown induced a proteotoxic stress response in decidualising cells (Brosens *et al.*, 2014). Conditioned media from high quality human embryos was found to induce short Ca<sup>2+</sup> oscillations in mouse endometrial epithelial cells (EECs), inducing COX-2 expression (and prostaglandin E2 release) along with 28 other known implantation factors. The authors suggest that high quality embryos actively enhance the uterine environment to make it favourable for implantation.

The question of how human embryos signal to the endometrium their competence requires further study. Finding answers could be not only an enormous advance in our understanding of implantation but have huge clinical benefits in managing infertility.

Information gained using non-invasive methods about implantation potential during routine embryo culture would be an enormous benefit to patients and clinicians alike, improving outcomes for patients, shortening time to pregnancy and increasing our understanding of what makes for a successful implantation.

Ultimately the findings might also help diagnose patients whose IVF continually fails by determining whether the fault is with embryo or endometrium, or the interaction between them.

## 1.6 Experimental Aims and objectives

The overarching hypothesis for the thesis is that it is possible to use non-invasive techniques to determine more fully the process of early implantation in the human, and use these findings in the clinical setting to improve outcomes.

The aims of this project are to determine if two different non-invasive techniques can reveal differences between preimplantation human embryos which successfully form a pregnancy and those that fail.

The experimental approaches are:

1. Sampling of conditioned media and co-culture with a 3D *in vitro* model of mid-secretory phase normal human endometrium, followed by transcriptomic analysis of these endometrial cells
2. Development of a time lapse annotation system to improve selection of PN stage frozen embryos cultured to blastocyst and replaced in FET cycles.

The use of a 3D co-culture system is an exciting development in *in vitro* modelling of human implantation. As the embryos have been selected as high quality according to standard morphological criteria yet some have failed to implant, we would hope to gain some insight into communication between blastocyst and endometrium at this very early stage of implantation and see differences between embryos not identifiable using current methods.

Additionally, we have taken time-lapse videos of this group of embryos and run them through a novel machine learning programme which aims to predict likelihood of an embryo resulting in a live birth. This programme (eM-Life) is being developed by a PhD student in the Faculty of Biology at University of Manchester. We will compare the predictions of the ML programme to the transcriptomic data.

The lack of morphokinetic algorithms for frozen-thawed PN stage embryos cultured to blastocyst means this large patient group may not benefit fully from time lapse incubation. Additionally, other morphological features that may be markers of implantation potential have not been previously evaluated in frozen embryos. Some suggestions from the literature not currently included in routine assessments are – synchronicity of PN fade, PN size differences prior to pronuclear membrane breakdown, blastocoel expansion and collapse

patterns, and the presence of cytoplasmic strings in the expanded blastocyst. Combining all these observations, we may be able to develop a scoring scheme for this group of patients that could not only improve outcomes but also improve our understanding of the effect of cryopreservation on early development.

The need for non-invasive techniques to improve embryo selection has been demonstrated. To embryologists the ability to reliably 'de-select' or rank embryos in order of potential is highly beneficial. Resources are wasted if embryos with lower chance of success are replaced first, or frozen to be used later.

The inadequacy of current *in vitro* models for investigating human implantation is also clear, as implantation happens in a three-dimensional system, specific to our species and with much variation and overlap between success and failure. We need to open up the 'black box' of early human pregnancy loss (Macklon *et al.*, 2002) if we are to improve outcomes from assisted conception.

## Chapter 2: Materials and Methods

### 2.1 Conditioned media co-culture experiment

#### 2.1.1 Patient identification and selection

Between November 2020 and October 2021, conditioned media was collected by the author from embryos cultured to blastocyst and replaced in single embryo transfer (SET) cycles during IVF, ICSI or frozen embryo transfer (FET cycles) carried out in the Department of Reproductive Medicine, St Mary's Hospital, Manchester. Patients were identified during their IVF, ICSI or frozen embryo transfer cycles. All patients were under 40 years of age, non-smokers and had body mass index of <30. Treatment cycle number or previous obstetric history was not collected. To be included in sample collection, embryos must have been cultured from zygote stage to blastocyst in the same well of an Embryoslide™ designed for the Embryoscope™. The slides for this model of time-lapse incubator are individual and there is no communication between wells as in Embryoscope+™ models (see Figures 8, 9a,b).

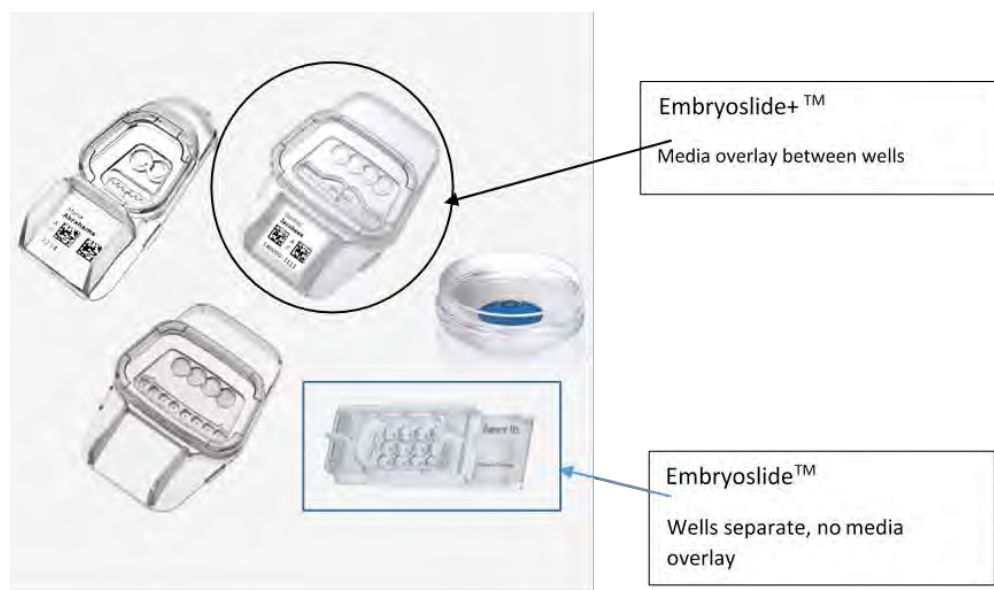
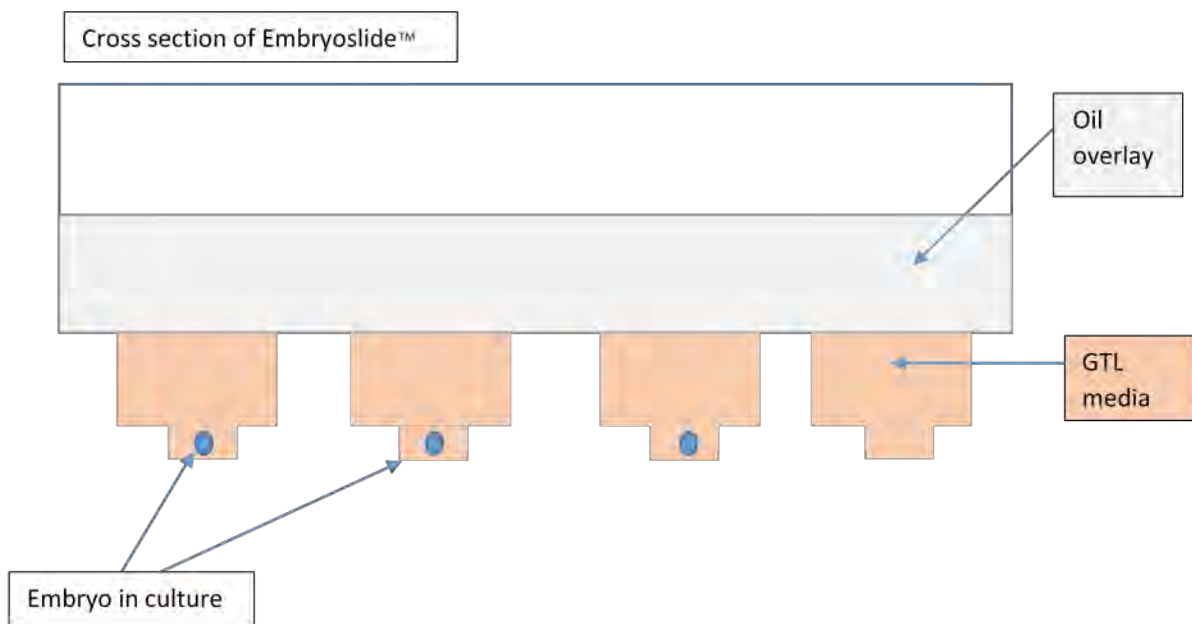
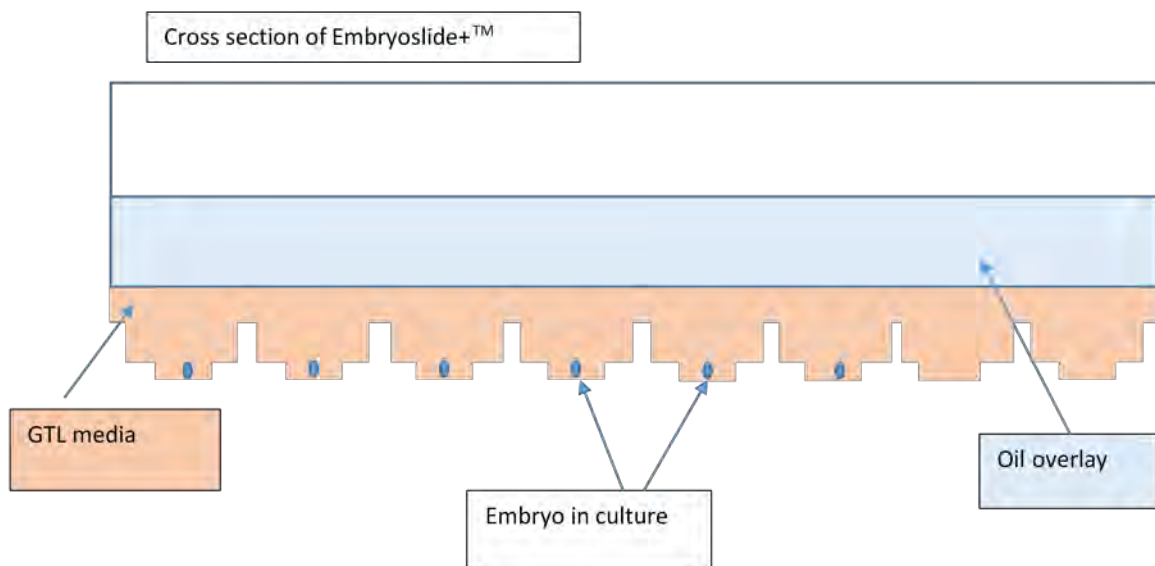


Image from <https://www.vitrolife.com/products/time-lapse-systems/time-lapse-dishes/>

**Fig 8: Overview of culture slides for Embryoscope™ time-lapse incubators.** 5 different types of slide are shown, used in different models of incubators. The two types used at St Mary's Hospital are circled in the figure.



**Fig 9a: Cross section of Embryoslide™ used for culture of embryos in this study.** Note no overlay of media between wells, an oil overlay to prevent evaporation and the 'well on well' cross section of the embryo culture section.



**Fig 9b: Cross section of Embryoslide+™ excluded for culture of embryos in this study.** Note that culture media overlays all the wells shown, allowing possible migration of solutes between wells.



Additionally, it was important that another well in the slide had not been used for embryo culture or washing so unexposed media exposed to the same storage and culture conditions was available as a control. Cycles where more than one embryo was replaced into the uterus were excluded so that the implantation status of the embryo could be accurately determined.

Due to the cost of the experiment and the transcriptomic analysis it was not possible to assess a larger number of samples. Selection for co-culture experiments was based on knowledge of cycle outcome (i.e. live birth or no pregnancy) and sufficient conditioned media available for the co-culture experiment ( at least 17 $\mu$ L of media in storage).

### **2.2.3. Embryo culture**

Standard laboratory operating procedures were followed. Briefly, embryos were cultured singly in Embryoscope™ slides. Each slide holds up to 12 embryos in separate wells. Wells were filled with 25 $\mu$ L of GTL media (Vitrolife, Sweden) and the whole slide overlaid with 1.5mL Ovoil (Vitrolife, Sweden). (Figure 8). Embryos were placed into the slides late on day zero of development (after ICSI), on the morning of day 1 (after fertilisation check) or immediately after thawing of slow frozen pronuclear stage embryos (see Table 3 below). The slide was then placed into the Embryoscope incubator and left in undisturbed culture until the morning of day 5 of development. The selected embryo was then removed for embryo transfer and the well left undisturbed. The slide was immediately returned to the Embryoscope for the remaining embryos to be monitored until day 6 of development for potential cryopreservation. Once the clinical observations had concluded the slide was removed from incubation and the media taken from the relevant wells and snap frozen in liquid nitrogen.

**Table 3: Details of conditioned media samples.** The table outlines some cycle details of the patients selected to have conditioned media stored, and then selected for possible use in the co-culture experiments described. Sample code, date of sample collection and freeze, mode of insemination and outcome of embryo transfer are given.

<i>Sample code</i>	<i>Date of sample freeze</i>	<i>IVF/ICSI/PN thaw</i>	<i>Outcome</i>	<i>Comments</i>
HH01	26/11/2020	IVF	Live birth	Sample lost during thawing
HH02	3/12/2020	ICSI	Not pregnant	
HH03	3/12/2020	IVF	Not pregnant	
HH04	3/12/2020	IVF	Live birth	
HH05	8/12/2020	IVF	Not pregnant	
HH06	8/12/2020	IVF	Miscarriage 12/40	Excluded from analysis due to outcome
HH07	8/12/2020	PN thaw	Not pregnant	
HH08	9/12/2020	ICSI	Not pregnant	
HH09	23/12/2020	PN thaw	Live birth (monozygotic twin)	
HH10	2/2/2021	PN thaw	Live birth	
HH11	10/8/2021	IVF	Live birth	
HH12	26/10/21	PN thaw	Not pregnant	

#### **2.2.4. Collection of conditioned media.**

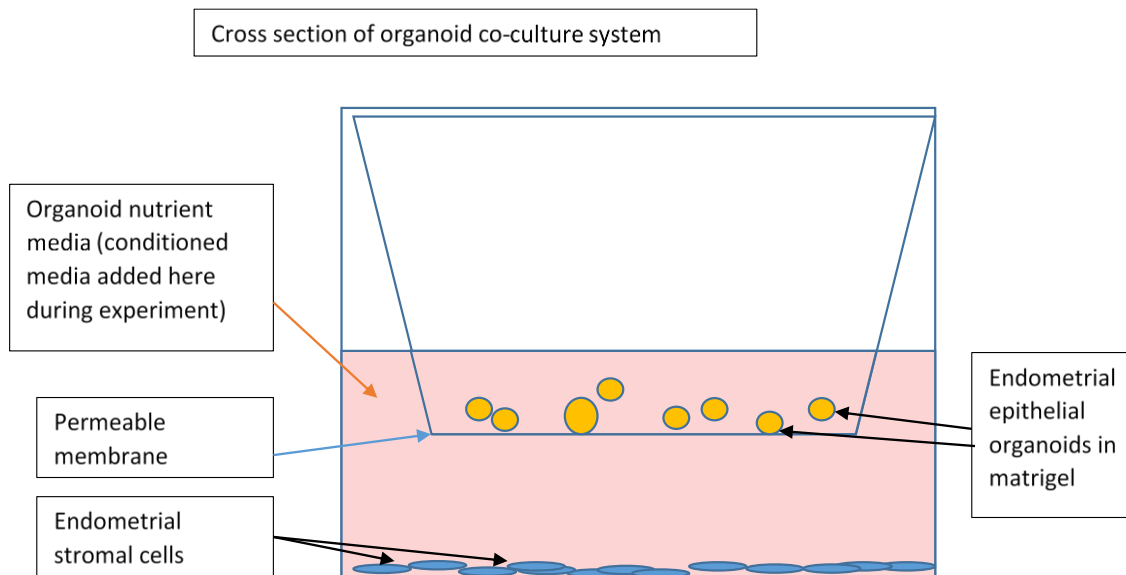
Media collection and storage was carried out solely by the author. Media was taken from the well which had contained the transferred embryo initially using a sterile 145µm Flexipet™ tip (CooperSurgical) (to ensure the liquid from the very bottom of the well was sampled) then a sterile Gilson pipette tip to remove the remaining media while taking care to ensure none of the oil overlay was taken up. The same procedure was used to sample media from another well in the same slide which had not been exposed to an embryo. Approximately 20µL was able to be taken from each well. A fresh Flexipet and Gilson tip were used for each sampled well.

Media was placed in a labelled PCR tube (MicroAmp<sup>R</sup> Fast Reaction Tube, Life Technologies, UK) and immediately plunged into a small dewar of liquid nitrogen. The tubes were then stored under liquid nitrogen in an embryo storage vessel.

#### **2.1.4 Establishment of *in vitro* model of mid-secretory phase endometrium .**

Matched endometrial organoids and stromal cells were derived from a single patient; proven fertile with successful obstetric history attending colposcopy clinic at St Mary's Hospital, Manchester (Preston Research Ethics Committee 21/NW/0195). Samples were taken by a Clinical collaborator for a separate project but ethically approved for use in this project.

Organoids and stromal cells were established and maintained according to published protocols. (Barros *et al.*, 2016; Turco *et al.*, 2017). Organoids were seeded in Matrigel (Corning) in a 24-well transwell insert and stromal cells were seeded in 24 well plates, initially both were cultured separately in their respective growth media. This initial culture work was carried out by Dr Peter Ruane, Research Supervisor. Once healthy cells were established in culture, media changes for experimental purposes were carried out by the author. After three days culture, organoids were treated with 10nM estrogen (Sigma-Aldrich) for 48h before treatment with 10nM estrogen (Sigma-Aldrich), 1 $\mu$ M progesterone (Sigma-Aldrich) and 1 $\mu$ M 8-bromoadenosine-3-5-cyclicmonophosphate (cAMP) (Sigma-Aldrich) for 48h to model mid-secretory menstrual cycle phenotype. In parallel, stromal cells were grown to confluence before treatment with 1 $\mu$ M methoxy-progesterone (Sigma-Aldrich) and 500 $\mu$ M cAMP for 96h to induce decidualisation. Mid-secretory organoid cultures in transwells were then combined with stromal cell cultures in plates to produce model mid-secretory endometrium (Figure 10). This model endometrium was established in a basal media (DMEM:F12 1:1, Sigma-Aldrich) containing 1 $\mu$ M progesterone and embryo-conditioned media/controls was then added, minimally diluted for this culture setup at 1:30, for 24h culture period. Figure 10 below is a schematic of the co-culture system

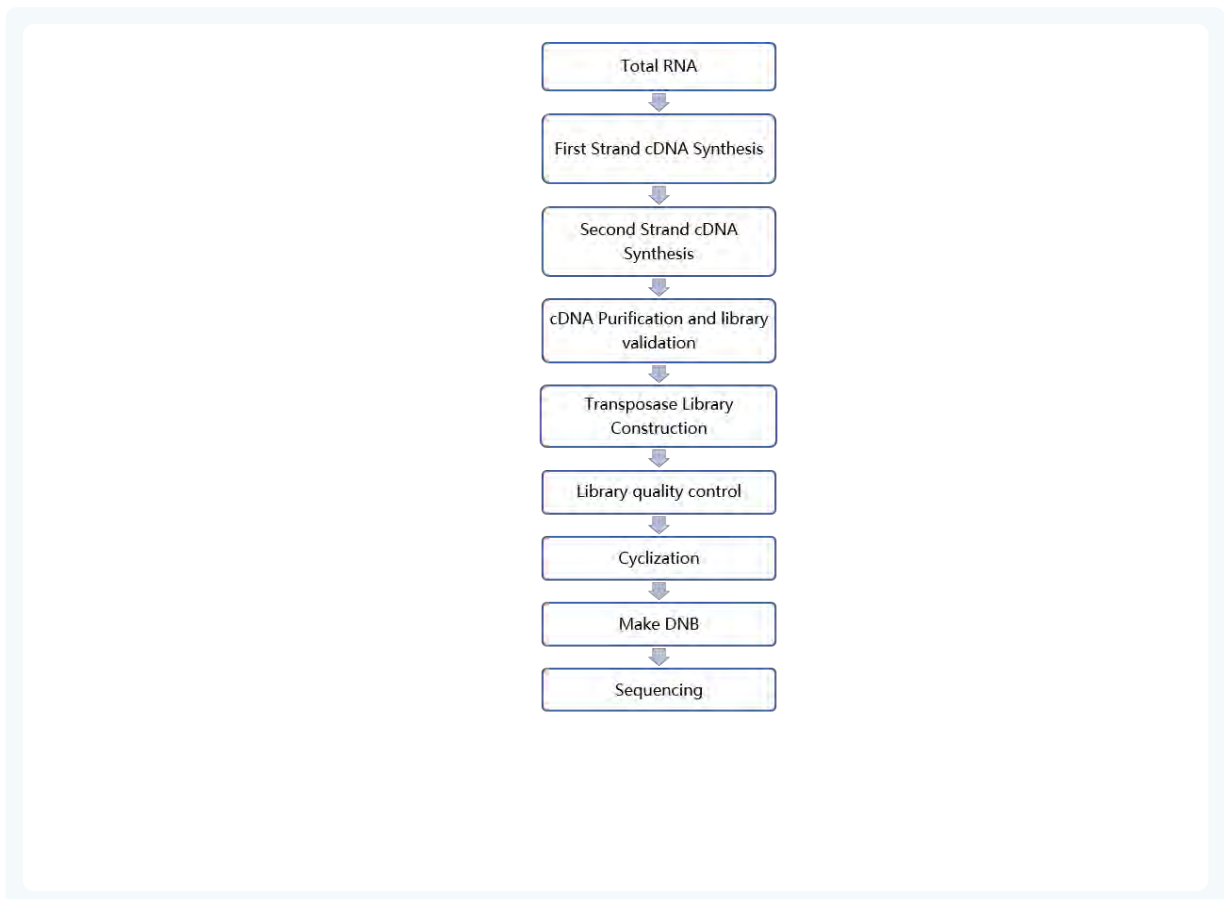


**Fig 10: Diagram of organoid co-culture system.** Figure shows endometrial epithelial organoids in transwell insert, sited over endometrial stromal cells on the base of a 24-well plate. Organoid nutrient media covers both cell types demonstrating communication between epithelial and stromal cell compartments without mixing of cell types.

### 2.2.5. *Sample preparation for RNA sequencing*

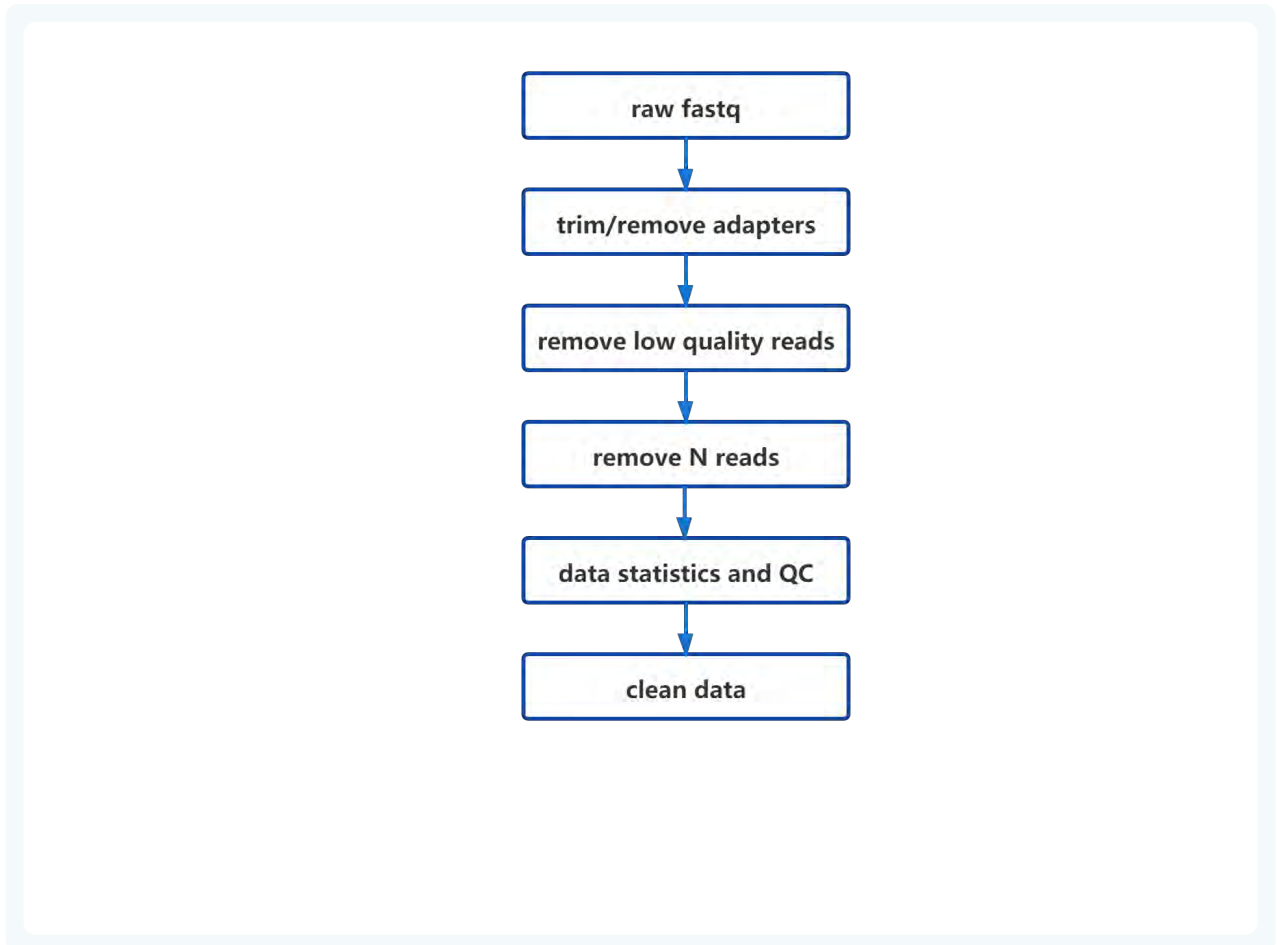
Organoids from the mid-secretory endometrium model were harvested from Matrigel culture using Cell Recovery Solution (Corning), according to manufacturer's instructions and pelleted by centrifugation at 2400xg and then snap frozen in liquid nitrogen. Stromal cells were recovered from wells using trypsin treatment, similarly pelleted and snap frozen. (Cell recovery and freezing carried out by research supervisor). Samples were then shipped to for RNA extraction and RNA sequencing (DNBSEQ platform) by Beijing Genomics Institute (BGI), Hong Kong. Further detail is in appendix 3 but briefly their method is described below:

The library construction method and sequencing process are carried out according to the following steps (taken from Appendix 3):



1. Take appropriate amount of total RNA samples, and add oligo-dT reverse transcription primer and denature the total RNA sample by heat;
2. Add the reverse mix reagent, and reverse transcribed to first-strand cDNA by SMART amplification technology;
3. Synthesize the second-strand cDNA, and use magnetic beads to purify the cDNA, and validate the cDNA;
4. The qualified double stranded cDNA, were used to construct the library with transposase;
5. The library was qualified by the Agilent Technologies 2100 bioanalyzer;
6. The library was circularized;
7. Sequencing: The library was amplified to make DNA nanoball (DNB) and sequenced on DNBSEQ platform.

## Bioinformatic analysis workflow



### Parameters for data filtering

Raw data with adapter sequences or low-quality sequences was filtered. BGI first went through a series of data processing to remove contamination and obtain valid data. This step was completed by SOAPnuke software developed by BGI.

SOAPnuke software filter parameters: “ -n 0.001 -l 20 -q 0.4 -adaMR 0.25 -ada\_trim -minReadLen 100”, steps of filtering:

1. Filter adapter: if the sequencing read matches 25.0% or more of the adapter sequence (maximum 2 base mismatches are allowed), cut the adapter;
2. Filter read length: if the length of the sequencing read is less than 100 bp, discard the entire read;
3. Remove N: if the N content in the sequencing read accounts for 0.1% or more of the entire read, discard the entire read;
4. Filter low-quality data: if the bases with a quality value of less than 20 in the sequencing read account for 40.0% or more of the entire read, discard the entire read;
5. Obtain Clean reads: the output read quality value system is set to Phred+33.

### **2.2.6. RNA sequencing analysis**

RNA sequencing outputs were validated by BGI, and samples were deemed comparable (Appendix 3). This data was then returned to us and further assessment carried out by research supervisor. All samples passed BGI QC. Although 7 samples had a RNA integrity number (RIN) of <7.0, only 1 was lower than 6. The decision was made to include all in the analysis as the RIN was deemed to still be of a high enough value, and as the experiment was small, interpretation of results is already limited. Sample sequencing was processed through EdgeR (Rstudio) to determine normalised expression levels for each transcript (counts per million) and differential expression levels using adjusted p-value cut-off of 0.05. Log<sub>2</sub> fold change in gene expression levels and log<sub>2</sub> counts per million(CPM) were also outputted, giving indications of levels of gene expression. This data was used to construct heatmaps using Clustvis (Metsalu and Vilo, 2015) and gene ontology was interrogated using Webgestalt (Zhang *et al.*, 2005) and Ingenuity Pathway Analysis (Qiagen).

### **2.2.7. Machine Learning Video Analysis of embryos**

To enable comparison of the predictions of a ML programme to the transcriptomic data, timelapse videos of the embryos used in this experiment were extracted by the author and taken through a deep learning computer model (eM-Life) which is in development as part of a PhD project in the Faculty of Biology at University of Manchester. The PhD student applied the model to the timelapse videos and assessment of the output was made by the author. This model aims to improve assessment of embryo quality, aiding selection by embryologists of good quality blastocysts within a cohort. Embryos can be ranked according to the predicted chance of live birth given by the computer model (the closer to 1 the better). A single frame from each video was taken at one hour before nuclear envelope breakdown (PN fade), first appearance of 2 cells, first appearance of 4 cells, morula stage and last frame before embryo was removed for transfer (blastocyst stage).

### **2.3. Timelapse imaging and annotations of PN stage frozen embryos cultured to blastocyst.**

As described in the introduction, at St Mary's Hospital, patients who had undergone IVF or ICSI and have a 'freeze all' cycle where an embryo transfer was not planned routinely have embryos frozen at the PN stage using a slow-freezing protocol.

#### ***2.3.3. Patient Selection***

For this section of the study, patients were identified (by the author) from the ACUBase™ electronic patient record who had returned to use their PN stage frozen embryos in an FET cycle and embryo transfer had taken place at the blastocyst stage. As the study relied on annotation and measurements from the Embryoscope™ system, patients were excluded when time-lapse was not used, or the videos were compromised or corrupted.

#### ***2.3.4. Video collection and annotation***

Embryoscope videos of the blastocyst(s) replaced in the original thaw cycle, and also any re-frozen embryos which had been used within the study period were assessed by the author. Videos were only studied where the outcome of each transferred embryo could be determined-i.e. double embryo transfers (DET) resulting in singleton births or miscarriages were excluded as it could not be determined which embryo had implanted. Twin pregnancies from DETs were only included where the outcome was the delivery of a male and a female child.

The data collected from each video is described in Tables 4 and 5 below (images from embryos used in this study):



**Table 4: Morphokinetic setpoint stages from time-lapse videos of frozen-thawed embryos.** Table shows images of human embryos in time-lapse culture at morphokinetic setpoints (time of PN fade, 2-, 3-,4-,5-,8-cell stages, time at start of compaction, time at morula, time at start of cavitation and time at blastocyst stage) and descriptions/definitions of those setpoints (all images from embryos used in this study).

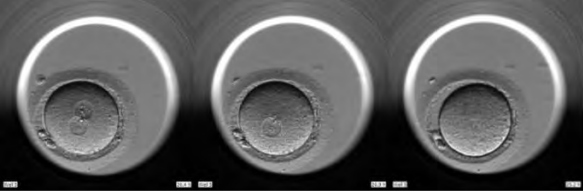

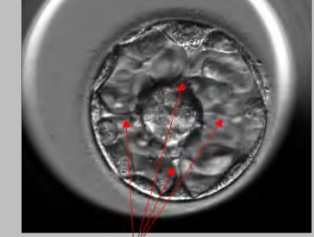
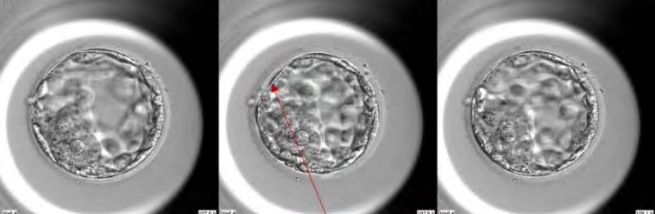

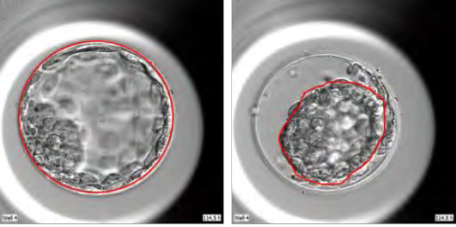
*Table 4a: Setpoint stages from pn fade to 8 cell stage*

Annotation	Time of PN fade (t-PNf)	2 cell (t-2)	3 cell (t-3)	4 cell (t-4)	5 cell (t-5)	8 cell (t-8)
Description	Taken as time zero for this study	Time when 2 distinct cells can be identified	3 distinct cells can be identified	4 distinct cells can be identified	5 distinct cells can be identified	8 distinct cells can be identified
Example image from Embryoscope™						

*Table 4b: Setpoint stages from start of compaction to blastocyst*

Annotation	Time at start of compaction (t-SC)	Time at morula (t-M)	Time at start of cavitation (t-SC)	Time at blastocyst (t-B)
Description	First time that membranes between 2 adjacent blastomeres become indistinct	First timepoint when embryo is fully compacted (ignoring any excluded cells which never compact)	Initial stage of blastulation – cavitation begins as a very small gap between cells.	Blastocyst is expanding, timepoint at which zona starts to thin.
Example image from Embryoscope™				

**Table 5: Morphological observations and measurements from time-lapse videos of frozen-thawed embryos.** Table shows images of human embryos in time-lapse culture illustrating morphological observations discussed in this thesis (asynchronous PN fade, size difference between PN, cytoplasmic strings, pulsatile blastocyst expansions and blastocyst collapses) and descriptions/definitions of those observations (all images from embryos used in this study).

Observation	Description	Example image from Embryoscope™
Asynchronous PN fade	Y/N – do PNs disappear within 2 frames or does one persist longer than 2 images?	 <p>2pn visible      1<sup>st</sup> pn fade 20.9h      2<sup>nd</sup> pn fade 25.2h</p>
Size difference between PN	Measured at clearest image just before PN fade. Diameter measured using Embryoscope tool	 <p>pronucleus outlined with drawing tool and area of shape calculated by Embryoscope™ software</p>
Number of strings	The maximum number of cytoplasmic strings observed at any time between ICM and TE	 <p>Cytoplasmic strings between ICM and TE bridging blastocoel cavity</p>
Number of pulsatile expansions	Number of small (<20%) size changes in expansion of blastocyst after t-B.	 <p>Full blastocyst at 107.6h      small change in size at 107.9h      Return to full blastocyst by 109.1h</p>
Number of collapses	Number of larger contractions (>20%) of blastocyst after t-B	
Largest collapse as %	Difference between diameter of blastocyst just before collapse and diameter of blastocyst at smallest point of collapse expressed as percentage of diameter of blast just before collapse	 <p>Full and collapsed blastocyst outlined with drawing tool and area of shapes calculated by Embryoscope™ software</p>

Time of PN fade was taken as time zero for this study. Time lapse annotation of fresh embryos begins at time of insemination after IVF or injection of sperm after ICSI (Barrie *et al*, 2017). As the embryos in this study were cryopreserved at the PN stage and the time of freeze thaw is variable (within a 2-6 hour window usually), time of insemination/injection was not thought to be a useful or valid parameter. Cryopreservation may also affect time of PN fade compared to fresh embryos.

Embryoscope™ software takes images approximately every 6 minutes (depending on model of incubator and local settings) and runs these as a video. Hours are converted into a metric system so each hour is divided into tenths (hence notations at 2.9 hours etc.)

### **2.3.5. Analysis of videos**

Embryos were grouped into 'clinical pregnancy' or 'no clinical pregnancy' based on the presence of a foetal heartbeat observed on a transvaginal ultrasound scan at 7-8 weeks of pregnancy. The mean timepoints for each annotation stage from t-2 to blastocyst were determined for each group. The times between setpoints were also determined. To aid in determining threshold values (where the time between morphological stages became useful to separate successful from unsuccessful embryos), and following the statistical methods used by Meseguer *et al.*, (2011), the data was divided into quartiles.

Other observations (asynchronous PN fade, size difference between PN, number of cytoplasmic strings, number of contractions and number and size of collapses at blastocyst stage were also compared. Statistical significance was determined using. Independent two sample t-tests and  $X^2$  tests as appropriate for the type of data.

## Chapter 3: Endometrial transcriptomic responses to embryo-conditioned culture media and associated morphokinetic machine learning analysis

### 3.1 Background

The use of *in vitro* models to study human implantation is not novel, but previous studies have used epithelial models which are less representative of the endometrial epithelium *in vivo*, for example the Ishikawa endometrial carcinoma cell line (Singh *et al.*, 2010; Kaneko *et al.*, 2011; Kang *et al.*, 2016). Endometrial organoid cultures more closely resemble the whole endometrial epithelium as a 3D structure and functionally respond to oestrogen and progesterone (Turco *et al.*, 2017).

Exposing these endometrial epithelial organoids and stromal cells to conditioned media from individual human blastocysts with known implantation outcomes is an advance on previous studies. Other groups have used pooled media from cleavage stage embryos, grouped by morphological quality and not clinical outcomes, and assessed responses mostly in stromal cells and in one instance on the Ishikawa carcinoma-derived endometrial epithelial cell line (Tecklenberg *et al.*, 2010; Weimar *et al.*, 2012; Berkhout *et al.*, 2018, 2020; Brosens *et al.*, 2014). Transcriptomic profiling studies have identified large numbers of genes whose profile of regulation changes at the time of endometrial receptivity, but these data sets vary (Evans *et al.*, 2016, Walker *et al.*, 2023). Endometrial transcriptomic responses to embryo media has only been reported in stromal cells, not epithelial (Brosens *et al.*, 2014).

All blastocysts giving rise to the conditioned media in this experiment were graded as high quality and selected for embryo transfer using current morphological criteria and standard time lapse algorithmic scores where appropriate (i.e. for fresh embryos where more than one blastocyst shared the same morphological grade). Conditioned media was grouped based on clinical outcome and not embryological quality. An additional experimental approach was attempted where a machine learning programme was applied to time lapse videos of these embryos. The results of this analysis are described in section 3.4.

### **3.2 Details of samples used for analysis**

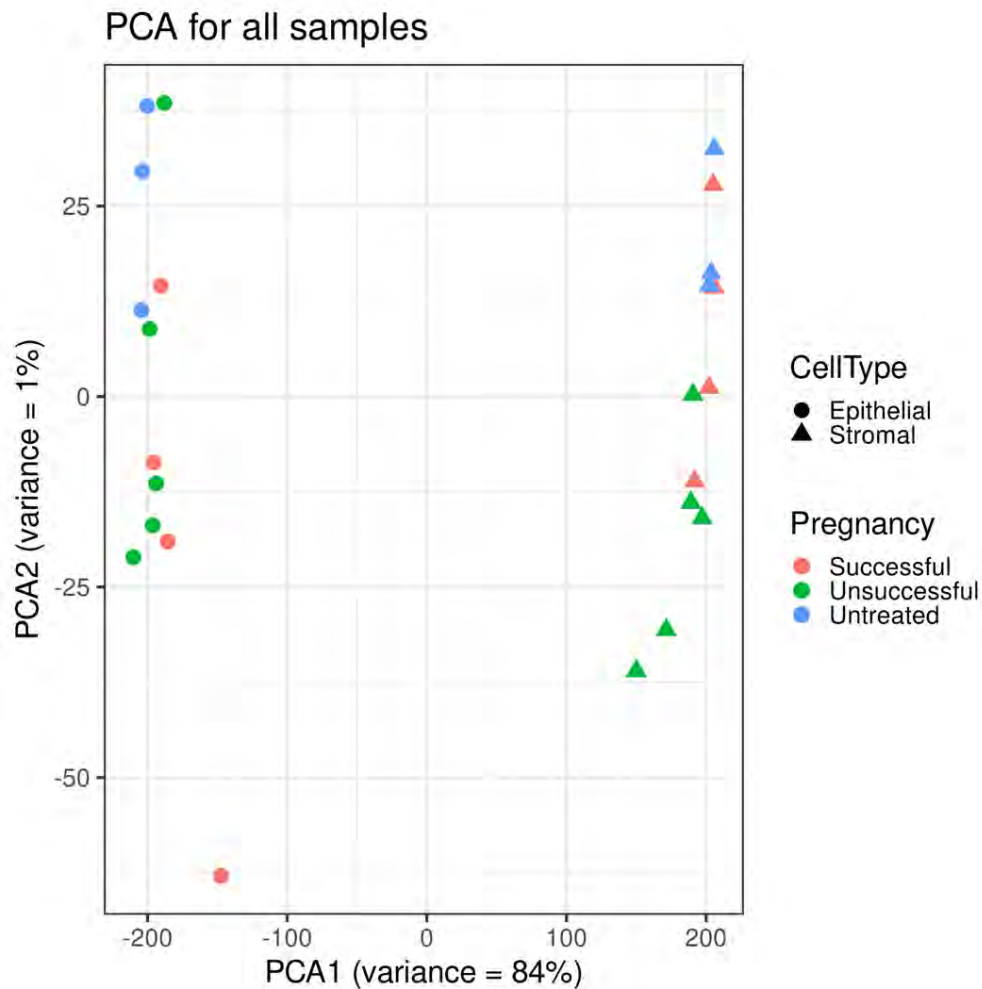
Conditioned media samples were collected and stored at -180°C as described in 2.1.3. Samples chosen for incubation with the 3D implantation model are detailed in Table 3. There were limitations on the number of samples that could be sent for transcriptomic analysis due to cost, as each co-culture well gave rise to two cell populations for transcriptomics (organoid epithelial and stromal). Embryo transfers resulting in early pregnancy loss were excluded from this study, to give a clear separation between embryos which implanted successfully (and resulted in a healthy pregnancy beyond 1<sup>st</sup> trimester) ('successful', n=4) and those which gave no detectable signs of implantation (negative pregnancy test 14-16 days after embryo transfer) ('unsuccessful', n=5). Three aliquots of unexposed media were selected as controls ('untreated').

Each media sample was incubated in a separate co-culture well as described. Epithelial organoids and stromal cells were recovered from the wells and analysed separately as described in section 2.1.5. To minimise variability, organoid and stromal cell cultures from the same biopsy sampled from one fertile donor were used. Thus there were 24 separate samples sent for RNA sequencing analysis (epithelial and stromal cells exposed to the 9 aliquots from embryo-conditioned media [18 samples] and epithelial and stromal cells exposed to the aliquots of unexposed media [6 samples]).

### **3.3 *In vitro* endometrial transcriptomic responses to embryo-conditioned culture media**

#### **3.3.1 *Principal component analysis***

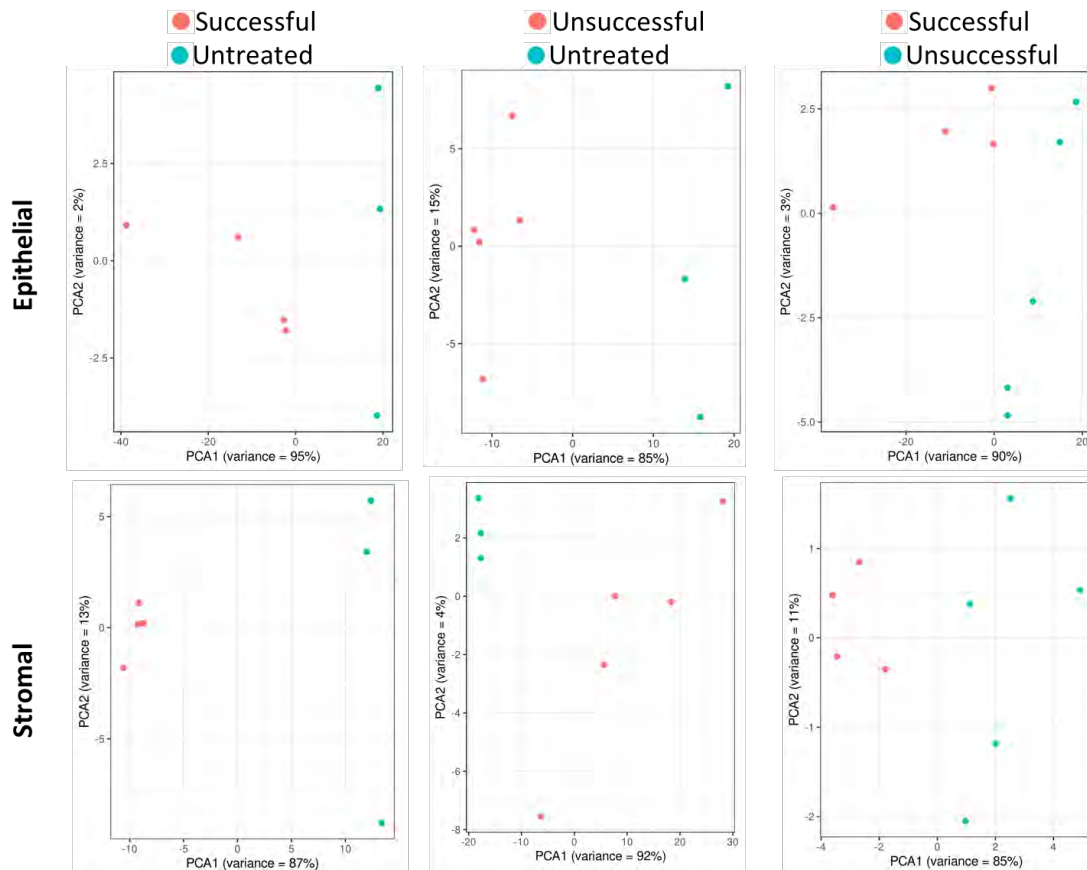
RNA sequencing analysis of organoid and stromal cells co-cultures (see sections 2.1.5 and 2.1.6) returned data on tens of thousands of transcripts expressed by the two cell types. Principal component analysis (PCA) is a dimensional reduction technique used to explore differences between large data sets. By finding the biggest differences in a data set (PC1 and PC2) and plotting them against each other, it allows for a visual exploration of the data to understand key differences and identify any outliers. The most similar samples are clustered together, and the most different are further apart (summarised in Lever *et al.*, 2017). The PCA for the most variable transcripts (unsupervised variability; not based on comparison between groups) among all samples is shown in Figure 11.



**Fig 11: Unsupervised PCA of endometrial organoid epithelial and stromal cell transcriptomes** treated in co-culture for 24h with blank embryos culture media, and successful and unsuccessful embryo-conditioned culture media. Each datapoint represents a sample. The amount of variance among the samples that is explained by each component is stated on the axes.

A total of 84% of the difference between data points is explained by the difference between epithelial and stromal cells (circles v triangles), with the samples very well segregated by this component. This verifies the transcriptomic differences between the cell types and the tight clustering along this axis, without any outliers, is suggestive of no cross contamination of cell types when sampled from the co-culture.

The variance on the y-axis is much less, at 1%, however some separation between non-conditioned and conditioned media exposure can be seen (blue v red/green). To better determine discrimination of successful and unsuccessful embryos by epithelial and stromal cells, PCA based on the 500 most variable genes within the cell types is shown in Figure 12.



**Fig 12:** PCA (based on the 500 most variably expressed gene between groups) of organoid epithelial and stromal cell transcriptomes treated for 24h with successful and unsuccessful embryo culture media. Each datapoint represents a sample. The amount of variance among the samples that is explained by each component is stated on the axes.

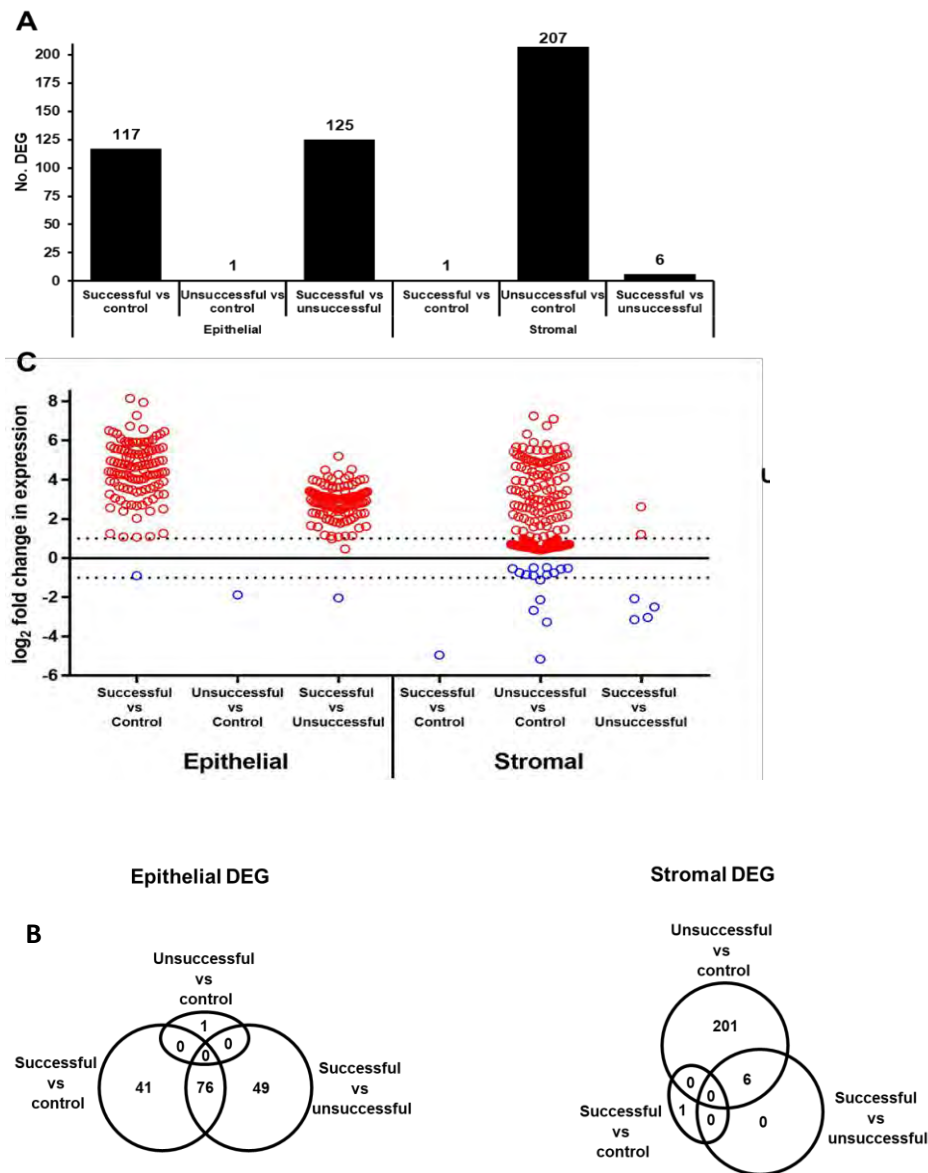
The separation of data points shows discrimination along the PC1, but not PC2, by epithelial cells between media conditioned by ‘untreated’ embryo culture media, successful embryo-conditioned culture media and unsuccessful embryo culture media (Figure 10). Discrimination between samples is highest in successful versus ‘untreated’ treatment, as indicated by segregation of approximately one quarter of the PC1 axis. Discrimination of treatments by stromal cells in general is similarly effective, however, in contrast to the epithelial cells, segregation of samples is best in the unsuccessful vs ‘untreated’ comparison. This indicates that there are differences between responses of epithelial and stromal cells to successful and unsuccessful embryos media.

### 3.3.2 Differential gene expression

Differentially expressed genes (DEG) in direct comparisons of the embryo culture media treatments were determined for each cell type. One hundred and twenty-six DEG were found in epithelial cells when successful embryo-conditioned media treatment was compared to

unsuccessful embryo-conditioned media or to unconditioned media, with 76 DEG (45.8%) matching between these comparisons (Figure 13a, b). Two hundred and eight DEG were found when unsuccessful embryo-conditioned media treatment of stromal cells was compared to unconditioned media, however only six DEG were detected in successful embryo-conditioned media treatment compared to unsuccessful embryo-conditioned media (Figure 13a, b). The majority of epithelial DEG were upregulated in response to successful embryo-conditioned media while the majority of stromal DEG were upregulated in response to unsuccessful embryo-conditioned media (Figure 13c). This reflects the segregation of successful and unsuccessful embryo-conditioned media treatment away from controls seen in the PCA for epithelial and stromal samples, respectively. Furthermore, a higher magnitude of upregulation was seen in the epithelial response compared to the stromal response ( $p < 0.0001$ ). Indeed, 91 (44%) stromal DEG were differentially regulated at  $< 1 \log_2$  fold change whereas all but one epithelial DEG were altered at  $> 1 \log_2$  fold change.

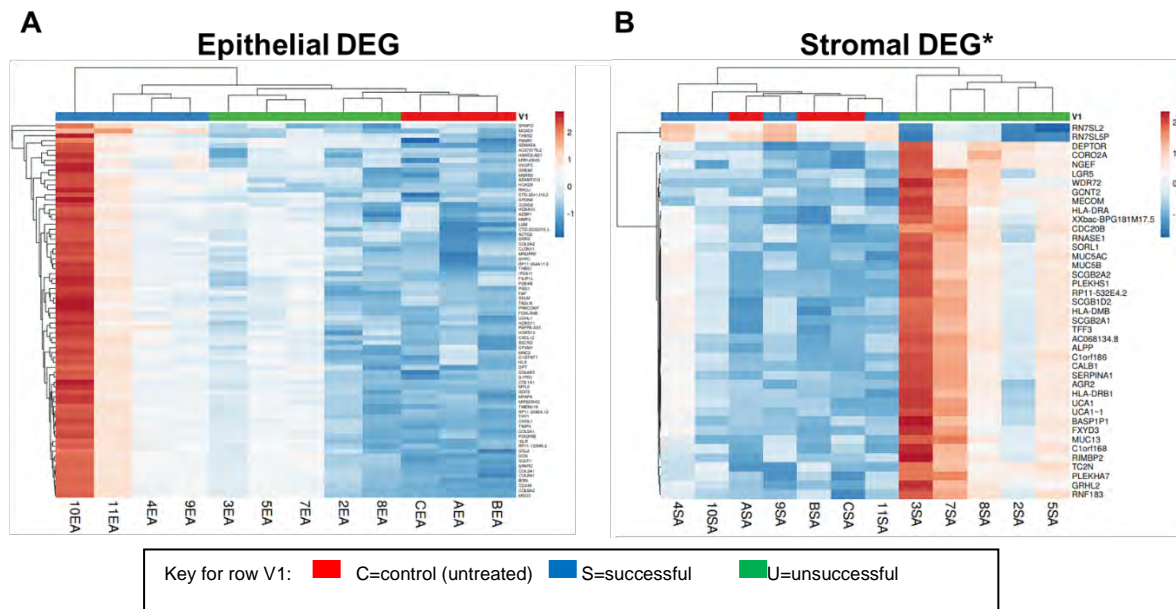




**Fig 13: DEG in epithelial and stromal cells exposed to conditioned media from successful and unsuccessful embryos, and media not exposed to an embryo (control).** 3a= number of DEG (FDR <0.05) plotted by comparison of media exposure and cell type. 3b= data from 3a expressed as Venn diagram to show matching DEG. 3c=scatter graph of DEG in 3a (red circles show upregulated expression, blue show downregulated expression, and dotted lines equate to 1 log<sub>2</sub> fold change)

Epithelial and stromal DEG (n=76 and n=41, respectively) were clustered in heatmaps, where the colours in each row are normalised and represent relative expression. Samples are clustered by the gene expression similarity based on Euclidean distance. Epithelial DEG matched between both comparisons with successful embryo-conditioned media were chosen

for this analysis (Figure 14a), and for stromal DEG the threshold was raised to FDR <0.1 to provide enough matched DEG between both unsuccessful embryo-conditioned media comparisons for clustering (Figure 14b).



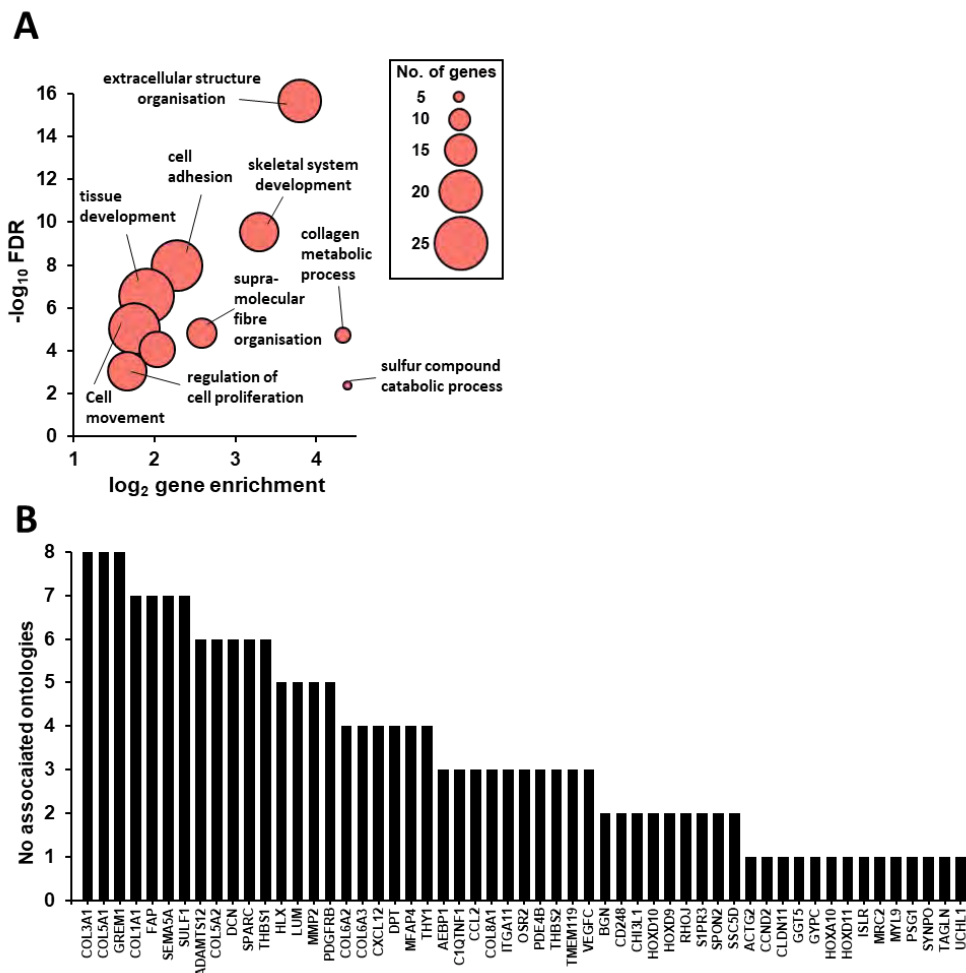
**Fig 14: Heatmaps of DEG for epithelial and stromal cells.** Legend: Top row (V1) colour coding of media sample source (see key). 4a shows response of epithelial cells to media and clustering of samples by gene expression similarity matches source of media sample. 4b shows stromal cell response, with good clustering of samples from unsuccessful embryos only. Colour coding in each row show relative expression of gene in question.

As expected, successful embryo-conditioned media and unsuccessful embryo-conditioned media treatments clustered away from the other groups for epithelial and stromal DEG, respectively. This analysis also demonstrates that different embryos elicit different response magnitudes, with successful embryo #10 inducing an especially strong response in epithelial cells and unsuccessful embryo #3 inducing a particularly strong response in stromal cells

### 3.3.3 Gene ontology analysis of differentially expressed genes

To interpret biological functions associated with the endometrium, transcriptional response to embryo-conditioned media gene ontology analysis was carried out on the matched DEG identified in the epithelial response to successful embryos (n=76) and the total DEG identified in the stromal response to unsuccessful embryos (n=207, FDR<0.05). Moreover, only 1 significantly enriched biological process ontology was identified among the stromal DEG (FDR<0.05); MHC protein complex assembly, which overlapped with just three DEG (HLA-

DMB, HLA-DRA, HLA-DRB1). In sharp contrast, 10 highly enriched biological process ontologies were associated with epithelial DEG (FDR<0.005) (Figure 13a). Fifty five DEG were mapped to these ontologies (Figure 15b), with the most frequently associated genes ( $\geq 6$  ontologies) all being extracellular proteins. The enriched ontologies include those associated with extracellular matrix, developmental processes, and cell adhesion and movement, all of which are important processes of epithelial remodelling during implantation (Aplin and Ruane, 2017). Also of note, four HOX genes are present among the DEG and associated with the developmental process ontologies. HOXA10 is among these and is known to be especially important as a transcriptional regulator of endometrial receptivity (Xu *et al.*, 2014).



**Fig 15: Gene ontology (biological processes) for DEG in endometrial epithelium exposed to conditioned media from successful embryos.** Legend: 5a shows ten enriched biological processes associated with epithelial DEG. Size of circle represents the number of genes in each pathway found amongst DEG. One circle missing a label due to size= 'negative regulation of multicellular organismal process'. 5b The 55 DEG from epithelial cells mapped onto the processes in 5a are detailed here, showing the number of ontologies each gene maps on to. Most frequently associated genes (associated with >6 ontologies) are extracellular proteins.

### 3.3.4 Upstream regulators of epithelial DEG

Ingenuity pathway analysis (IPA) allowed prediction of upstream regulators likely to induce the DEG observed (Qiagen, 2023). Two components of IPA were used for this analysis: Upstream regulator analysis (URA) and causal network analysis (CNA). CNA is an expansion of URA, and includes regulators not directly connected to targets in the dataset, giving a broader view. The 76 matched DEG in the epithelial response to successful embryo-conditioned media were analysed. Among regulators identified in both URA and CAN, 8 components of the TGF- $\beta$  signalling pathway were predicted as activated in the lead up to this transcriptional response (Figure 16). Sortilin related receptor 1 (SORL1) is also a top hit. This is a transmembrane protein, and belongs to both the low-density lipoprotein receptor (LDLR) family and the vacuolar protein sorting 10 (VPS10) domain receptor family (Yin *et al.*, 2015). Together, this analysis suggests that successful embryo-conditioned media could have stimulated these pathways to upregulate epithelial remodelling genes, perhaps enhancing epithelial receptivity to implantation.

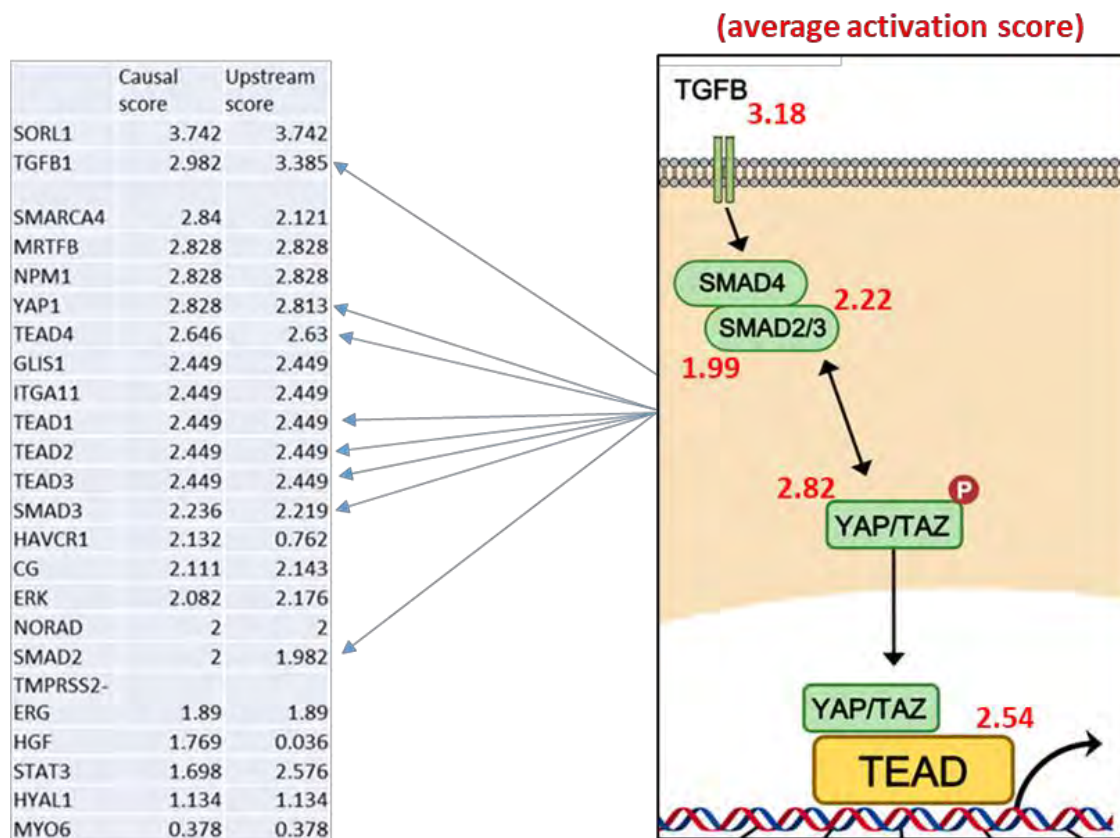


Fig 16: Results of ingenuity pathway analysis of 76 DEG in endometrial epithelium.

IPA analysis indicates 8 components of TGF- $\beta$  signalling pathways (indicated by blue arrows) are predicted as being activated upstream of the DEG seen in epithelial cells. Their location within the signalling pathway is shown (figure adapted from Huh *et al.* Cells 2019, 8(6), 600)

### 3.4 Machine Learning Video Analysis of embryos

As described in the Methods chapter, an experiment was performed to compare the predictions of a novel ML programme to the transcriptomic data extracted above, to measure the ability of another non-invasive method to determine embryo potential. Embryoscope™ time lapse videos of embryos whose conditioned media was used in the co-culture experiment described above were taken through a deep learning computer model (eM-Life) in development at the University of Manchester (see section 2.1.7). A single frame from each video was taken at the following time points:

1. one hour before nuclear envelope breakdown (PN fade),
2. first appearance of 2 cells,
3. first appearance of 4 cells,
4. morula stage
5. last frame before embryo was removed for transfer (blastocyst stage).

The eM-Life software gave a score to each embryo at each time point (the closer to the value of 1 the higher the predicted chance of a live birth). The ML model has been trained on approximately 200 fresh embryos grown to the blastocyst stage, with known outcomes, from St Mary's Hospital. The overall aim is to help the embryologist rank embryos within a cohort, so the highest scoring is selected for clinical use first.

All embryos scored as good or excellent quality by morphological grade at the time of embryo transfer and were the best available from the patient cohort at the time of selection. The ML scores for each embryo in this section of the study, along with morphological grade, are displayed in Table 6. This table shows the embryos ranked by embryo transfer. Machine learning scores at each stage are given as generated by the programme at each stage of assessment. This data is also represented as scatter plots in Figure 17 a-e.

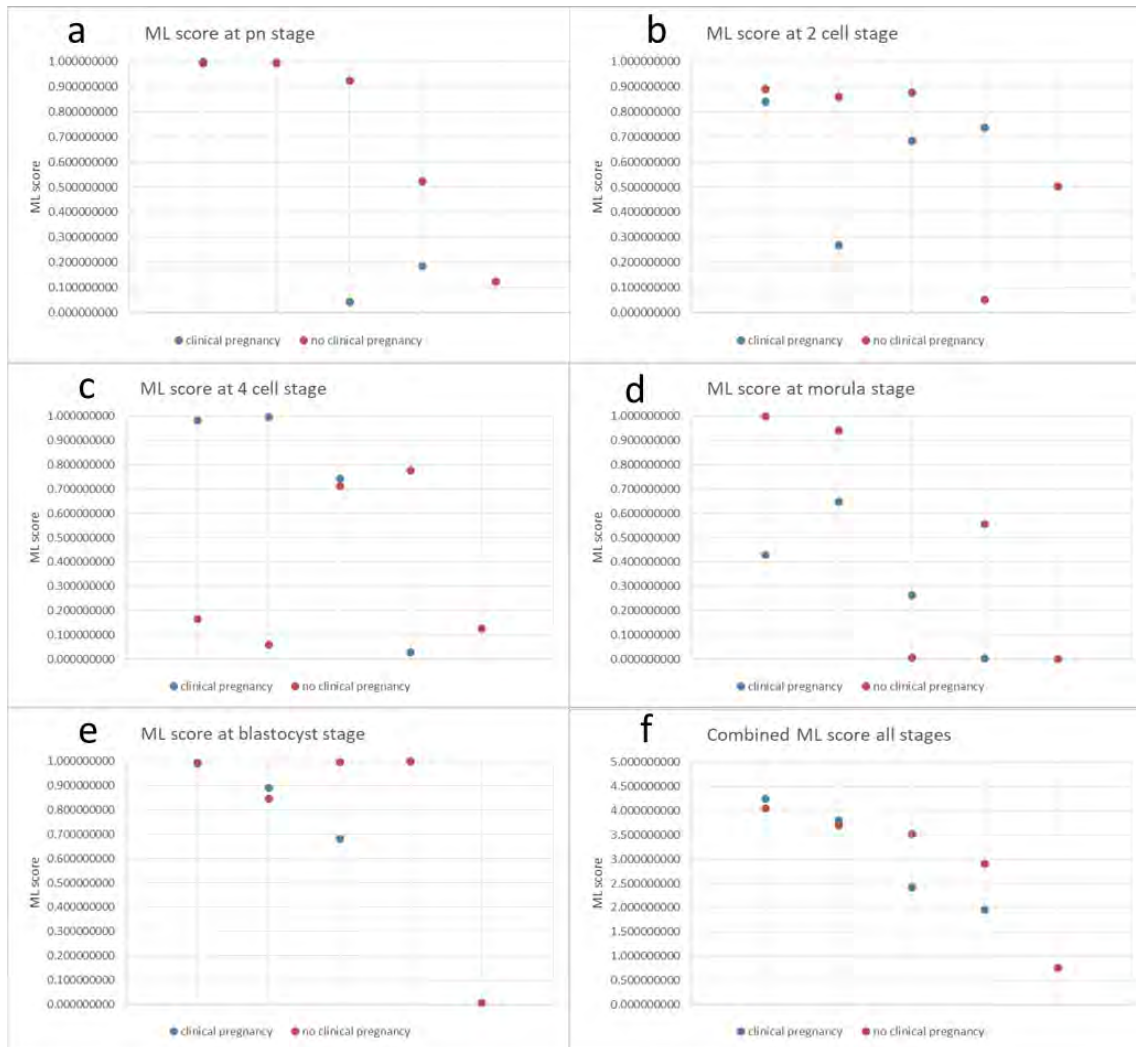
**Table 6: ML scores, morphological grade at embryo transfer (ET) and cycle outcome for embryos in conditioned media co-culture experiment, ranked by outcome of embryo transfer.** ML scores at each developmental stage are given as generated by eM-Life programme.

<i>Code</i>	<i>ML score at pn stage</i>	<i>ML score at 2 cell stage</i>	<i>ML score at 4 cell stage</i>	<i>ML score at morula</i>	<i>ML score at blastocyst</i>	<i>Cycle outcome</i>	<i>morphological grade at ET</i>
HH02	0.123614005	0.503556111	0.125164084	0.000117118	0.005802896	not pregnant	3BB
HH03	0.522485884	0.051658123	0.775479637	0.554285043	0.999167125	not pregnant	4AB
HH05	0.992620919	0.859073747	0.060374173	0.939262409	0.844881884	not pregnant	4BA
HH07	0.924429728	0.877431322	0.710427657	0.007416446	0.996911261	not pregnant	4AB
HH08	0.994200484	0.890975564	0.164297557	0.999934803	0.994671633	not pregnant	5AB
HH04	0.995332493	0.268020694	0.996885391	0.647206273	0.891583246	LIVE BIRTH M	4AA
HH09	0.042287004	0.682790231	0.742420025	0.264196927	0.682170960	twin live birth (monozygotic) MM	3BB
HH10	0.184702166	0.736095408	0.029146169	0.004533790	0.998736427	LIVE BIRTH F	4BB
HH11	0.999999840	0.839019202	0.981706054	0.430043618	0.991081927	ongoing singleton	5AA

By summing the score at each developmental stage, the eM-Life model gives an overall score for an embryo developing to blastocyst. Table 7 shows embryos ranked by this total score and is shown as a scatter plot in Figure 17f

**Table 7: ML total scores, morphological grade at embryo transfer (ET) and cycle outcome for embryos in conditioned media co-culture experiment, ranked by total ML score generated by eM-Life programme.**

<i>Embryo code</i>	<i>total score</i>	<i>rank by total score</i>	<i>outcome</i>	<i>morphological grade at ET</i>
HH11	4.241850641	1	ongoing singleton	5AA
HH08	4.044080041	2	not pregnant	5AB
HH04	3.799028097	3	LIVE BIRTH M	4AA
HH05	3.696213132	4	not pregnant	4BA
HH07	3.516616141	5	not pregnant	4AB
HH03	2.903075181	6	not pregnant	4AB
HH09	2.413865147	7	twin live birth (monozygotic) MM	3BB
HH10	1.953213960	8	LIVE BIRTH F	4BB
HH02	0.758254214	9	not pregnant	3BB



**Fig 17: Scatter plots of ML generated scores for embryos in conditioned media co-culture experiment.** a=score at pn stage, b=score at 2 cell stage, c=score at 4 cell stage, d=score at morula, e=stage at blastocyst, f=combined scores. Each data point represents a single embryo, blue signifies an embryo which gave rise to a clinical pregnancy, red represents an embryo which failed to implant. No clear visual separation of successful vs non-successful embryos can be determined.

No discernible pattern can be seen between successful and unsuccessful embryos from scatter plots. Ranking embryos by the sum of the scores from ML assessment is broadly related to morphological quality and does not appear to be related to cycle outcome in this small cohort of embryos, all from different patients. Embryo 10 was a successful transfer and gave the strongest transcriptional response in epithelial cells but ranked number 8, while embryo 3 was an unsuccessful transfer and gave the strongest stromal response but ranked higher at number 6. Both have similar morphology.

## Chapter 4: Time-lapse imaging and annotations of PN stage frozen embryos cultured to blastocyst.

### 4.1 Introduction and background

As described in the general introduction, embryo freezing at the pronucleate (PN) stage is a treatment strategy used at St Mary's Hospital where a fresh embryo transfer following IVF or ICSI is not recommended, usually due to the risk of OHSS. PN freezing is performed using a slow freezing protocol (Hunter *et al.*, 2020) and FreezeKit Cleave™ media (Vitrolife, Sweden).

Until 2019, the Unit's standard protocol for FET after a PN freeze was to thaw only a small number of PN stage embryos (2-4), and replace 1 or 2 embryos into the uterus on day 2 of their development (2-4 cell stage). While the cumulative pregnancy rate was acceptable, pregnancy rate per transfer was low, and several thaw cycles were often needed to achieve a successful outcome. As frozen cycles were included in patients' NHS funding, conservative thawing was generally acceptable to patients.

NHS funding changes applied in 2015 meant frozen cycles after a live birth became self-funded. This change, alongside scrutiny from the HFEA on the Clinic's below average live birth rate per FET prompted a review of these standard protocols in 2019. Following this review, the recommendation of the clinic to patients has been to thaw at least 6 and up to 12 PN stage embryos (where available), and allow these embryos to develop for up to 5 days in culture, to replicate the conditions of the fresh treatment cycle. This allows faster selection of the most viable embryo(s) from the cohort for replacement in the uterus. Supernumerary embryos from this thaw that also reach good quality blastocyst stage can be re-cryopreserved using a vitrification method for use in subsequent cycles, as for fresh embryo culture.

Although these embryos are routinely cultured in Embryoscope™ time lapse incubators, embryologists are unable to use morphokinetics as aids to decision making as published algorithms are based on embryos which have not undergone PN stage freezing. In fresh treatment cycles, time zero is taken as time of insemination (IVF) or sperm injection (ICSI). PN freezing is performed between fertilisation check and PN fade on the morning of day 1 of pre-implantation development. Embryo thawing and return to culture can be any time on day 1 of a frozen embryo transfer cycle therefore there is an unquantified and non-



standardised offset between insemination time and other morphokinetic measurements. The time taken to recover from cryopreservation and resume cell cycle kinetics is also ill-defined. Overall the standard zero set point for all current morphokinetics is not valid for this group.

To meet the standards required for the Higher Specialist Scientist Training programme (HSST), the DClSci project must include an innovation element which is directly related to clinical care (see appendix 2) This section of the project was developed to meet this criteria with the aim of identifying morphological and morphokinetic markers from time lapse video data for frozen embryo development to aid embryo selection.

In order to make a usable model to aid embryo selection for transfer and re-cryopreservation, the decision was made to look at other morphological observations not used in standard grading schemes (PN size difference, number of blastocyst contractions, blastocyst collapse size and presence of cytoplasmic strings between ICM and TE). These observations were related to outcomes post-transfer and some recommendations for their use in selecting, de-selecting or ranking embryos within a cohort made.

## **4.2 Details of patients and embryos selected for analysis**

A total of 152 PN thaw cycles were identified from the ACUBase™ electronic patient database as meeting the criteria set out in the Methods section. From these cycles, 141 patients underwent a total of 167 embryo transfer procedures, and 193 embryos with known outcomes were identified.

For this cohort of patients and embryos the clinical pregnancy rate (CPR) per embryo transfer procedure was 47.9% (Clinical pregnancy was defined as the presence of at least one foetal heart (FH) seen on ultrasound scan at 7-8 weeks gestation). CPR per embryo was 41.5%, and FH per embryo transferred was  $86/193=44.6\%$  (7 sets of monozygotic twins were created).

## **4.3 Results of Morphokinetic measurements**

### **4.3.1 Timepoint data**

As a standardised point for starting morphokinetic timings, the timepoint of pronuclear membrane breakdown (PNMBD, recorded as t-PNf) was used. 167 embryos had this timepoint clearly identifiable on time lapse video (87%). Embryos which had already

undergone PNMBD by the start of recording were excluded from timepoint data and PN morphology measurements but included in the 'time between setpoints' and later morphology assessments.

Timepoint data is detailed in Table 8. For each time-point the mean, full range and mean +/- 1 standard deviation is reported. The data was shown to be normally distributed using the online tool <https://www.ai-therapy.com/psychology-statistics/distributions/normal> . Equality of variance was similar (SD ratio <2) except for T3 timepoint so an independent two sample t-test assuming equal variance was performed (t-test assuming unequal variance for T3 timepoint was performed). Embryos which resulted in a clinical pregnancy took significantly longer to reach 3-cell and 4 cell stages, but began to compact and formed morulae significantly faster than embryos which did not implant. To aid in determining threshold values (where the time to reach morphological stage became useful to separate successful from unsuccessful embryos), and following the statistical methods used by Meseguer *et al.*, (2011), the data was divided into quartiles (Table 9). This method of evaluation aids in the practical use of the data – by dividing the set into 4 groups it is easier to see where the results for successful and unsuccessful embryos lie, and upper or lower threshold values of times to morphological setpoints can be suggested. This data also indicates that time to 3 and 4 cells, start of compaction and time when morula formation is complete are possible set

**Table 8: Time embryos reach morphological setpoints, (taking tPN-f as zero) 167 embryos, time in hours.**

Table shows measurements taken from time-lapse videos of embryos which had been frozen at the pronucleate stage, thawed, and cultured for up to 120 hours before transfer or cryopreservation. Time in hours from time of PN fade for setpoints 2-, 3-,4-,5-,8-cell stages, time at start of compaction, time at morula, time at start of cavitation and time at blastocyst stage are shown for all embryos, and separated into embryos which formed a clinical pregnancy and those which gave no clinical pregnancy. Mean times, standard deviations and range of time +/- 1 standard deviation are shown for all setpoints and all groups. Statistical significance between times in cohorts of embryos giving a clinical pregnancy vs those which did not (determined by t-test) are also given. [\* p <.05, \*\*P<.01 != t-test assuming unequal variance used. ^ = data excludes 1 embryo which did not compact; #= data excludes 6 embryos which did not cavitate; £= data excludes 12 embryos which did not reach full blastocyst; \$= excludes 1 embryo which did not reach full blastocyst; &= excludes 11 embryos which did not reach full blastocyst]

		t-2	t-3	t-4	t-5	t-8	t-SC	t-M	t-SB	t-B
<b>All Embryos</b>	Mean time (h)	2.8	14.1	15.1	27.8	33.1	56.0	64.5 <sup>^</sup>	72.1 <sup>#</sup>	80.9 <sup>£</sup>
	Range	1.7-14.6	7.3-25.1	11.7-26.4	15.0-39.1	25.4-53.3	33.0-82.5	37.0-98.0	57.1-93.5	65.2-101.6
	Standard Deviation	1.4	1.5	2.2	3.2	5.0	7.5	8.2	6.4	6.2
	Range +/- 1SD	1.4-4.2	12.6-15.6	12.9-17.3	24.6-31.0	28.1-38.1	48.5-63.5	56.3-72.7	65.7-78.5	74.7-87.1
<b>Clinical Pregnancy (n=69)</b>	Mean time (h)	3.0	14.5	15.6	28.4	33.7	54.1	62.6	71.0	80.5 <sup>£</sup>
	Range	1.8-14.6	7.3-25.1	11.7-26.4	16.5-39.1	26.1-49.3	37.9-73.1	44.5-78.8	57.1-84.8	65.2-96.5
	Standard Deviation	1.8	2.4	2.9	3.7	5.3	6.9	6.8	5.8	5.9
	Range +/- 1SD	1.2-4.8	12.1-16.9	12.7-18.5	24.7-32.1	28.4-39.0	47.2-61.0	55.8-69.4	65.2-76.8	74.6-86.4
<b>No Clinical Pregnancy (n=98)</b>	Mean time (h)	2.6	13.8	14.7	27.4	32.8	57.3	65.9 <sup>£</sup>	72.9 <sup>#</sup>	81.3 <sup>&amp;</sup>
	Range	1.7-11.8	11.7-17.0	12.7-22.5	15.0-33.2	25.4-53.3	33.0-82.5	37.0-98.0	58.0-93.5	66.6-101.6
	Standard Deviation	1.1	1.0	1.6	2.8	4.9	7.6	8.9	6.6	6.4
	Range +/- 1SD	1.5-3.7	12.8-14.8	13.1-16.3	24.6-30.2	27.9-37.7	49.7-64.9	57.0-74.8	66.3-79.5	74.9-87.7
<b>Clinical pregnancy v No clinical pregnancy</b>	p-values	0.136	0.025! <sup>*</sup>	0.009 <sup>**</sup>	0.053	0.270	0.006 <sup>**</sup>	0.011 <sup>*</sup>	0.052	0.426

**Table 9: Time taken to reach setpoints T2 to TB in quartile ranges.** Table shows measurements taken from time-lapse videos of embryos which had been frozen at the pronucleate stage, thawed, and cultured for up to 120 hours before transfer or cryopreservation. Time in hours divided into quartile ranges from time of PN fade for setpoints 2-, 3-, 4-, 5-, 8-cell stages, time at start of compaction, time at morula, time at start of cavitation and time at blastocyst stage are shown. Statistical significance between implantation rates within each quartile at each setpoint (determined by t-test) are also given.

	Q1 Limit (h)	Implantation %	Q2 Limit (h)	Implantation %	Q3 Limit (h)	Implantati on %	Q4 Limit (h)	Implantation %	X2 p values
<b>T2</b>	<=2.2	17/47 36%	2.3- 2.5	21/49 43%	2.6-2.8	16/34 47%	>=2.8	15/37 41%	ns
<b>T3</b>	<=13.1	18/43 42%	13.2- 13.8	13/42 31%	13.9- 14.9	14/41 34%	>=14.9	24/40 60%	Q2 v Q4 p=0.008 Q3 v Q4 P=0.021
<b>T4</b>	<=13.7	16/45 36%	13.8- 14.5	18/46 39%	14.6- 15.9	10/34 29%	>=16.0	25/42 60%	Q1vQ4 p=0.032 Q3 v Q4 p=0.005
<b>T5</b>	<=26.0	16/44 36%	26.1- 27.7	16/43 37%	27.8- 29.6	15/40 38%	>=29.7	22/40 55%	ns
<b>T8</b>	<=29.6	15/42 36%	29.7- 32.0	18/43 42%	32.1- 35.6	15/40 38%	>=35.7	21/42 50%	ns
<b>TSC</b>	<=51.7	25/43 58%	51.8- 55.1	15/41 37%	55.2- 60.8	16/42 38%	>=60.9	13/42 31%	Q1vQ2 p=0.038 Q1 vQ4 p=0.009
<b>TM</b>	<=59.4	22/42 52%	59.5- 63.5	15/41 37%	63.6- 68.9	19/41 46%	>=69.0	13/42 31%	Q1vQ4 p=0.046
<b>TSB</b>	<=67.8	22/41 54%	67.9- 71.4	19/41 46%	71.5- 75.5	14/39 36%	>=75.6	14/40 35%	ns
<b>TB</b>	<=77.0	16/40 40%	77.1- 80.1	22/40 55%	80.2- 84.3	16/37 43%	>=84.4	14/38 37%	ns

#### 4.3.2 Time between setpoints

As well as analysing the time that developmental setpoints occurred, the time taken for embryos to reach these points was also collated. This could be a more useful parameter for embryologists as it is unrelated to the time embryos were put into culture and does not require the start point of PNF to be available. For this section of analysis, the whole dataset of 193 embryos could be included as t-PNF was not included.

Time between setpoints data is detailed in Table 10 a-d. For each value the mean, full range and mean +/- 1 standard deviation is reported. The data was shown to be normally distributed using the online tool <https://www.ai-therapy.com/psychology-statistics/distributions/normal>. Equality of variance was similar (SD ratio <2) so an independent two sample t-test assuming equal variance was performed. To aid in determining threshold values (where the time between morphological stages became useful

to separate successful from unsuccessful embryos), and following the statistical methods used by Meseguer *et al.*, (2011), the data was divided into quartiles (Table R11 a, b).

In concordance with the data already shown, successful embryos are slightly slower in their development in cell divisions from 2 cell to 5 cell (although this only reaches statistical significance when comparing t2-t4. Developmental rates of successful embryos speed up after the 8 cell stage, and from all cleavage stages (2,3,5 and 8 cells), successful embryos are significantly quicker to reach start of compaction, formation of the morula, and start of blastulation, than their unsuccessful counterparts.

**Table 10a,b,c,d: Time taken for embryos to progress between setpoints t2-Blastocyst.** Table 10 a-d show measurements taken from time-lapse videos of embryos which had been frozen at the pronucleate stage, thawed, and cultured for up to 120 hours before transfer or cryopreservation. Time in hours to progress from and between all setpoints 2-, 3-,4-,5-,8-cell stages, time at start of compaction, time at morula, time at start of cavitation and time at blastocyst stage are shown for all embryos, and separated into embryos which formed a clinical pregnancy and those which gave no clinical pregnancy. Mean times, standard deviations and range of time +/- 1 standard deviation are shown for all setpoints and all groups. Statistical significance between times in cohorts of embryos giving a clinical pregnancy vs those with did not (determined by t-test) are also given.

**Table 10a:** Time taken for embryos to progress between setpoints t2-t8 (193 embryos, time in hours)

		<i>Time 2c - 3c</i>	<i>Time 2c-4c</i>	<i>Time 2c - 5c</i>	<i>Time 3c-4c</i>	<i>Time 3c - 5c</i>	<i>Time 4c - 5c</i>	<i>Time 2c-8c</i>	<i>Time 3c-8c</i>	<i>Time 4c-8c</i>	<i>Time 5c-8c</i>
All embryos	Mean	11.3	12.3	24.9	1.0	13.6	12.6	30.0	19.0	18.0	5.5
	Range	0.5- 16.5	9.1- 24.1	12.0- 34.3	0-13.9	0.9- 20.0	0.2- 18.0	23.2- 55.4	12.2- 44.7	11.9- 40.9	0.3- 34.5
	Standard Deviation	1.5	1.8	3.1	1.7	2.2	2.8	5.2	5.0	4.5	5.0
	Range +/- 1SD	9.8- 12.8	10.5- 14.1	21.8- 28.0	0-2.7	11.4- 15.8	9.8- 15.4	24.8- 35.2	14.0- 24.0	13.5- 22.5	0.5- 10.5
Clinical Pregnancy (n=80)	Mean	11.5	12.6	25.1	1.2	13.7	12.5	30.3	18.8	17.7	5.2
	Range	4.3- 16.5	9.1- 24.1	13.5- 34.3	0-13.9	8.5- 20.0	0.2- 17.2	23.6- 46.7	12.5- 34.6	12.2- 33.6	0.3- 20.8
	Standard Deviation	1.6	2.3	3.2	2.1	1.8	2.7	5.0	4.6	3.8	4.3
	Range +/- 1SD	9.9- 13.1	10.3- 14.9	21.9- 28.3	0-3.3	11.9- 15.5	9.8- 15.2	25.3- 35.3	14.2- 23.4	13.9- 21.5	0.9-9.5
No Clinical Pregnancy (n=113)	Mean	11.2	12.1	24.7	0.9	13.5	12.6	30.4	19.1	18.3	5.7
	Range	0.5- 14.2	9.3- 16.2	12.0- 31.0	0-10.2	0.9- 20.0	0.2- 18.0	23.2- 55.4	12.2- 44.7	11.9- 40.9	0.7- 34.5
	Standard Deviation	1.4	1.3	3.1	1.4	2.5	2.9	5.3	5.3	5.0	5.4
	Range +/- 1SD	9.8- 12.6	10.8- 13.4	21.6- 27.8	0-2.3	11.0- 16.0	9.7- 15.5	25.1- 35.7	13.8- 24.4	13.3- 23.3	0.3- 11.1
Clinical Pregnancy v No Clinical Pregnancy	<i>p</i> -values	0.311	0.039*	0.376	0.192	0.582	0.723	0.921	0.685	0.346	0.513

**Table 10b:** Time taken for embryos to progress between setpoints t2-tM (192 embryos for 2c-tSC, 191 embryos for 2c-tM), time in hours)

		<i>Time 2c-SC</i>	<i>Time 3c-SC</i>	<i>Time 4c- SC</i>	<i>Time 4c- SC</i>	<i>Time 8c-SC</i>	<i>Time 2c-M</i>	<i>Time 3c-M</i>	<i>Time 4c-M</i>	<i>Time 5c-M</i>	<i>Time 8c-M</i>	<i>Time SC-M</i>
<b>All Embryos</b>	Mean	53.2	41.9	40.9	28.3	22.8	62.0	50.6	49.6	37.0	31.6	8.8
	Range	31.2-80.0	19.7-67.8	15.2-63.8	4.0-55.0	1.0-44.8	35.2-95.5	23.7-83.0	19.2-82.7	8.0-68.2	5.0-67.0	1.3-30.2
	Standard Deviation	7.2	7.2	7.2	7.5	8.0	8.0	8.0	8.1	8.3	8.6	5.1
	Range +/- 1SD	46.0-60.4	34.7-49.1	33.7-48.1	20.8-35.8	14.8-30.8	54.0-70.0	42.6-58.6	41.5-57.7	28.7-45.3	23.0-40.2	3.7-13.9
<b>Clinical Pregnancy (n=80)</b>	Mean	51.2	39.8	38.6	26.1	20.9	59.8	48.3	47.2	34.7	29.5	8.6
	Range	34.0-70.9	20.6-59.1	20.5-58.4	5.0-43.2	2.5-40.8	42.5-76.6	30.7-64.8	29.5-64.3	16.0-48.9	8.2-46.5	1.3-20.6
	Standard Deviation	6.7	6.7	6.8	6.7	7.4	6.4	6.5	6.6	6.7	7.4	4.8
	Range +/- 1SD	44.5-57.9	33.1-46.5	31.8-45.4	19.4-32.8	13.5-28.3	53.4-66.2	41.8-54.8	40.6-53.8	28.0-41.4	22.1-36.9	3.8-13.4
<b>No Clinical Pregnancy (n=112)</b>	Mean	54.6	43.3	42.5	29.8	24.2	63.5	52.3	51.4	38.7	33.1	9.0
	Range	31.2-80.0	19.7-67.8	12.5-63.8	4.0-55.0	1.0-44.8	35.2-95.5	23.7-83.0	19.2-82.7	8.0-68.2	5.0-67.0	1.6-30.2
	Standard Deviation	7.2	7.2	7.1	7.7	8.2	8.7	8.6	8.6	9.0	9.1	5.3
	Range +/- 1SD	47.4-61.8	36.1-50.5	35.4-49.6	22.1-37.5	16.0-32.4	54.8-72.2	43.7-60.9	42.8-60.0	29.7-47.7	24.0-42.2	3.7-14.3
<b>Clinical Pregnancy v No Clinical Pregnancy</b>	<i>p</i> -values	0.001*	0.0006**	0.0001**	0.0007**	0.005*	0.001*	0.0007**	0.0003**	0.0008**	0.004*	0.593

**Table 10c:** Time taken for embryos to progress between setpoints t2-t start of blastulation (SB) (186 embryos, time in hours)

		<i>Time 2c-SB</i>	<i>Time 3c-SB</i>	<i>Time 4c-SB</i>	<i>Time 5c-SB</i>	<i>Time 8c-SB</i>	<i>tSC-TSB</i>	<i>TM-tSB</i>
<b>All embryos</b>	Mean	69.6	58.3	57.3	44.7	39.4	16.9	8.2
	range	54.8-91.0	44.4-79.5	39.8-79.2	30.0-68.6	13.5-63.3	3.7-41.3	0.5-37.3
	Standard Deviation	6.5	6.3	6.5	6.7	7.6	5.9	4.6
	Range +/- 1SD	63.1-76.1	52.0-64.6	50.8-63.8	38.0-51.4	31.8-47.0	11.0-22.8	3.6-12.8
<b>Clinical pregnancy (n=80)</b>	Mean	68.1	56.6	55.4	42.9	37.8	16.8	8.3
	range	54.8-81.9	44.4-70.2	39.8-70.0	30.0-56.3	18.7-51.8	7.3-33.1	1.0-22.2
	Standard Deviation	5.4	5.2	5.5	5.5	6.6	5.6	4.2
	Range +/- 1SD	62.7-73.5	51.4-61.8	49.9-60.9	37.4-48.4	31.2-44.4	11.2-22.4	4.1-12.5
<b>No Clinical Pregnancy N=(106)</b>	Mean	70.8	59.6	58.8	46.0	40.6	16.9	8.2
	Range	55.8-91.0	45.5-79.5	43.6-79.2	31.0-68.6	13.5-63.3	3.7-41.3	0.5-37.3
	Standard Deviation	7.0	6.8	6.8	7.2	8.2	6.1	4.9
	Range +/- 1SD	63.8-77.8	52.8-66.4	52.0-65.6	38.8-53.2	32.4-48.8	10.8-23.0	3.3-13.1
<b>Clinical Pregnancy v No Clinical Pregnancy</b>	p-values	0.004**	0.001**	0.0004**	0.002**	0.011*	0.972	0.907

**Table 10d:** Time taken for embryos to progress between setpoints t2-t full blastocyst (B) (176 embryos, time in hours)

		<i>Time 2c-B</i>	<i>Time 3c-B</i>	<i>Time 4c-B</i>	<i>Time 5c-B</i>	<i>Time 8c-B</i>	<i>Time SC-B</i>	<i>Time M-B</i>	<i>Time SB-B</i>
<b>All Embryos</b>	Mean	78.2	66.8	65.9	53.2	47.9	25.8	17.4	9.2
	range	62.9-99.1	52.3-87.6	47.8-87.3	37.1-75.4	23.5-71.4	12.0-58.6	8.0-43.0	2.7-33.3
	Standard Deviation	6.1	5.9	6.1	6.2	7.1	6.2	5.3	3.7
	Range +/- 1SD	72.1-84.3	60.9-72.7	59.8-72.0	47.0-59.4	40.8-55.0	19.6-32.0	12.1-22.7	5.5-12.9
<b>Clinical pregnancy (n=79)</b>	Mean	77.4	65.9	64.8	52.3	47.1	26.3	17.8	9.4
	range	62.9-93.7	52.5-79.2	47.8-79.1	40.4-64.7	27.1-61.9	12.0-58.6	8.8-37.1	2.7-33.3
	Standard Deviation	5.6	5.2	5.5	5.4	6.8	6.9	5.5	4.4
	Range +/- 1SD	71.8-83.0	60.7-71.1	59.3-70.3	46.9-57.7	40.3-53.9	19.4-33.2	12.3-23.3	5.0-13.8
<b>No Clinical Pregnancy N=(97)</b>	Mean	78.8	67.5	66.8	53.9	48.5	25.4	17.1	9.0
	Range	63.6-99.1	52.3-87.6	52.1-87.3	37.1-75.4	23.5-71.4	16.0-47.0	8.0-43.0	3.2-16.8
	Standard Deviation	6.5	6.4	6.4	6.8	7.3	5.5	5.2	3.2
	Range +/- 1SD	72.3-85.3	61.1-73.9	62.4-73.2	47.1-60.7	41.2-55.8	19.9-30.9	11.9-22.3	5.8-12.2
<b>Clinical Pregnancy v No Clinical Pregnancy</b>	p-values	0.137	0.077	0.029*	0.088	0.200	0.360	0.385	0.393



**Table 11a: Time taken for embryos to progress between setpoints t2-t8 (193 embryos, time in hours) in quartile ranges.** Table shows measurements taken from time-lapse videos of embryos which had been frozen at the pronucleate stage, thawed, and cultured for up to 120 hours before transfer or cryopreservation. Time in hours divided into quartile ranges from and between all for setpoints 2-, 3-,4-,5-,8-cell stages are shown. Statistical significance between implantation rates within each quartile at each setpoint (determined by t-test) are also given.

	Q1		Q2		Q3		Q4		X2 p values
	Limit (h)	Implantation %	Limit (h)	Implantation %	Limit (h)	Implantation %	Limit (h)	Implantation %	
2c-3c	<=10.7	24/54 44%	10.8-11.2	18/45 40%	11.3-12.0	15/47 32%	>=12.1	23/47 49%	ns
2c-4c	<=11.2	22/54 41%	11.3-11.8	17/44 39%	11.9-13.0	18/52 35%	>=13.1	23/43 53%	ns
2c-5c	<=23.3	21/53 40%	23.4-24.8	20/46 43%	24.9-26.8	19/50 38%	>=26.9	20/44 45%	ns
3c-4c	<=0.2	20/54 37%	0.3-0.5	23/63 37%	0.6-1.0	17/34 50%	>=1.1	20/42 48%	ns
3c-5c	<=12.5	22/53 42%	12.6-13.6	19/49 39%	13.7-14.7	21/43 49%	>=14.8	18/48 38%	ns
4c-5c	<=11.8	22/52 42%	11.9-12.8	21/47 45%	12.9-14.2	23/49 47%	>=14.3	14/45 31%	ns
2c-8c	<=26.8	22/51 43%	26.9-29.2	19/46 41%	29.3-33.0	19/48 40%	>=33.1	20/48 42%	ns
3c-8c	<=15.6	20/49 41%	15.7-17.6	20/49 41%	17.7-21.4	22/48 46%	>=21.5	18/47 38%	ns
4c-8c	<=15.0	21/51 41%	15.1-17.0	22/49 45%	17.1-19.9	20/45 44%	>=20.0	17/48 35%	ns
5c-8c	<=2.3	18/49 37%	2.4-3.7	22/49 45%	3.8-7.0	22/47 47%	>=7.1	18/48 38%	ns

**Table 11b: Time taken for embryos to progress between morphological timepoints 2 cell to blastocyst in quartile ranges.** Table shows measurements taken from time-lapse videos of embryos which had been frozen at the pronucleate stage, thawed, and cultured for up to 120 hours before transfer or cryopreservation. Time in hours divided into quartile ranges from setpoints 2-, 3-,4-,5-,8-cell stages to (and between) time at start of compaction, time at morula, time at start of cavitation and time at blastocyst stage are shown. Statistical significance between implantation rates within each quartile at each setpoint (determined by t-test) are also given.

	<b>Q1 Limit (h)</b>	<b>Implantation %</b>	<b>Q2 Limit (h)</b>	<b>Implantation %</b>	<b>Q3 Limit (h)</b>	<b>Implantation %</b>	<b>Q4 Limit (h)</b>	<b>Implantation %</b>	<b>X2 p values</b>
<b>2c- SC</b>	<=49.1	27/49 55%	49.2- 52.4	21/47 45%	52.5- 57.5	17/48 35%	>=57 .6	15/48 31%	Q1 v Q4 p=0.014 Q1vQ3 p=0.037
<b>3c- SC</b>	<=38.1	26/49 53%	38.2- 41.0	21/47 45%	41.1- 45.8	19/48 40%	>=45 .9	14/48 29%	Q1vQ4 p=0.013
<b>4c- SC</b>	<=37.1	29/48 60%	37.2- 40.1	21/49 43%	40.2- 45.3	15/46 33%	>=45 .4	15/49 31%	Q1vQ3 p=0.004 Q1 v Q4 p=0.003
<b>5c- SC</b>	<=23.8	25/48 52%	23.9- 27.9	23/48 48%	28.0- 33.0	20/50 40%	>=33 .1	12/46 26%	Q1vQ4 p=0.011 Q2 v Q4 p=0.033
<b>8c- SC</b>	<=18.0	25/48 52%	18.1- 23.2	23/48 48%	23.3- 27.3	20/49 41%	>=27 .4	12/47 26%	Q1vQ4 p=0.012 Q2 v Q4 p=0.033
<b>2c- M</b>	<=56.9	25/48 52%	57.0- 61.1	21/50 42%	61.2- 66.5	21/45 47%	>=66 .6	13/48 27%	Q1vQ4 p=0.012 Q3vQ4 p=0.039
<b>3c- M</b>	<=45.2	27/49 55%	45.3- 49.9	18/46 39%	50.0- 55.1	23/47 49%	>=55 .2	12/48 25%	Q1vQ4 p=0.004 Q3vQ4 p=0.011
<b>4c- M</b>	<=44.7	29/51 57%	44.8- 49.0	18/45 40%	49.1- 53.6	23/47 49%	>=53 .7	10/48 21%	Q1vQ4 p=0.000 Q3vQ4 p=0.003
<b>5c- M</b>	<=31.4	26/49 53%	31.5- 36.4	22/48 46%	36.5- 41.8	20/49 41%	>=41 .9	12/45 27%	Q1vQ4 p=0.116
<b>8c- M</b>	<=26.8	23/49 47%	26.9- 30.7	22/47 47%	30.8- 35.5	21/47 45%	>=35 .6	14/48 29%	ns
<b>SC- M</b>	<=5.0	25/53 47%	5.1- 7.7	17/44 39%	7.8- 11.7	18/50 36%	>=11 .8	20/44 45%	ns
<b>2c- SB</b>	<=65.0	27/47 57%	65.1- 68.9	22/46 48%	69.0- 73.0	16/47 34%	>=73 .1	15/46 33%	Q1vQ3 p=0.013 Q1vQ4 p=0.012
<b>3c- SB</b>	<=53.8	28/47 60%	53.9- 58.0	21/48 44%	58.1- 61.4	17/44 39%	>=61 .5	14/47 30%	Q1vQ3 p=0.036 Q1vQ4 p=0.004
<b>4c- SB</b>	<=53.1	27/48 56%	53.2- 57.0	24/46 52%	57.1- 60.6	15/47 32%	>=60 .7	14/46 30%	Q1vQ3 p=0.013 Q1vQ4 p=0.013 Q2vQ3 p=0.036 Q2vQ4 p=0.034
<b>5c- SB</b>	<=40.2	27/47 57%	40.3- 44.3	24/46 52%	44.4- 48.5	14/46 30%	>=48 .6	15/47 32%	Q1vQ3 p=0.012 Q1vQ4 p=0.012 Q2vQ3 p=0.034 Q2vQ4 p=0.036
<b>8c- SB</b>	<=35.1	22/47 47%	35.2- 39.0	27/48 56%	39.1- 43.4	16/44 36%	>=43 .5	15/47 32%	Q2vQ3 p=0.036 Q2vQ4 p=0.013
<b>SC- SB</b>	<=13.0	23/47 49%	13.1- 16.0	19/46 41%	16.1- 20.4	16/49 33%	>=20 .5	22/44 50%	ns
<b>M- SB</b>	<=4.8	18/47 38%	4.9- 7.9	22/47 47%	8.0- 10.3	22/46 48%	>=10 .4	18/46 39%	ns
<b>2c- B</b>	<=74.4	20/44 45%	74.5- 77.3	23/44 52%	77.4- 81.5	20/44 45%	>=81 .6	16/44 36%	ns
<b>3c- B</b>	<=62.8	22/44 50%	62.9- 66.3	23/46 50%	66.4- 70.4	18/42 43%	>=70 .5	16/44 36%	ns
<b>4c- B</b>	<=62.2	24/45 53%	62.3- 65.3	22/45 49%	65.4- 69.0	20/42 48%	>=69 .1	13/44 30%	Q1vQ4 p=0.03
<b>5c- B</b>	<=49.0	22/44 50%	49.1- 52.9	22/44 50%	53.0- 56.8	20/44 45%	>=56 .9	15/44 34%	ns
<b>8c- B</b>	<=43.8	21/44 48%	43.9- 48.1	20/44 45%	48.2- 52.0	22/44 50%	>=52 .1	16/44 36%	ns
<b>SC- B</b>	<=21.7	19/44 43%	21.7- 25.3	17/45 38%	25.4- 29.2	21/45 47%	>=29 .3	22/42 52%	ns
<b>M- B</b>	<=13.5	21/45 47%	13.6- 16.9	16/44 36%	17.0- 20.5	22/45 49%	>=20 .6	20/42 48%	ns
<b>SB- B</b>	<=6.7	20/47 43%	6.8- 8.7	20/42 48%	8.8- 11.0	18/43 42%	>=11 .1	21/44 48%	ns

#### **4.4 Summary of results for morphokinetic data**

Stages and times between stages that show statistically significant difference between successful and unsuccessful embryos are summarised in Table 12. All other timepoints or time between morphological set points did not show statistically significant differences between successful and unsuccessful embryos.

There is overlap between individual successful and unsuccessful embryos even where statistically significant difference in mean times has been established, these data should give some additional information to embryologists to aid in ranking morphologically similar embryos within a patient's cohort. Proposed thresholds for morphokinetic selection of embryos from PN freezing and extended culture are summarised in Table 13.

**Table 12: Summary of stages where there are statistically significant differences in mean times between groups of successful and unsuccessful embryos.** Data extracted from tables 8,9, 10 and 11 for clarity. Broad suggestions of speed of development at each stage recorded could aid in selection of embryos from a cohort, or give more information about the overall potential of embryos within a cohort.

Stage	Significance (clinical pregnancy vs no clinical pregnancy)	Comment
Time at 3 cell stage (t3)	P=0.025	Unsuccessful embryos faster at this stage
Time at 4 cell stage (t4)	P=0.009	Unsuccessful embryos faster at this stage
Time when compaction begins (t-SC)	P=0.006	Successful embryos faster at this stage
Time when morula formed (tM)	P=0.011	Successful embryos faster at this stage
Cleavage from 2c to 4c	P=0.039	Unsuccessful embryos have shorter 2c-4c time
All cleavage stages to t-SC	Various but all P<0.01	Successful embryos have shorter time to start of compaction
All cleavage stages to tM	Various but all P<0.01	Successful embryos have shorter time to morula stage
All cleavage stages to start of blastulation	P<0.01 for all except 8c-tSB p=0.011	Successful embryos have shorter time to start of blastulation
Time from 4 cell stage to blastocyst	P=0.029	Successful embryos have shorter time from 4 cell to blastocyst.

**Table 13: Proposed thresholds for morphokinetic selection of embryos from PN freezing and extended culture.** Data extracted from tables 9 and 11 for clarity. Quartile threshold values where there were statistically significant differences in implantation rates between successful and unsuccessful embryos have been extracted and are displayed as giving 'highest prognosis' where the evidence is that embryos within this limit have a higher implantation rate compared to the rest of the studied cohort, and 'lowest prognosis' where embryos within this time limit have the lowest rate of implantation.

<i>Time from pn fade to embryo</i>	<i>Limit (h) with highest prognosis</i>	<i>Limit (h) with lowest prognosis</i>
T3	≥14.9	13.2-14.9
T4	≥16.0	≤15.9
T-SC	≤51.7	≥60.9
TM	≤59.4	≥69.0
<i>Time between embryo stages</i>		
2c-SC	≤49.1	≥52.5
3c-SC	≤38.1	≥45.9
4c-SC	≤37.1	≥40.2
5c-SC	≤27.9	≥33.1
8c-SC	≤23.2	≥27.4
2c-M	≤56.9	≥66.6
3c-M	≤45.2	≥55.2
4c-M	≤44.7	≥53.7
5c-M	≤31.4	≥41.9
2c-SB	≤65.0	≥69.0
3c-SB	≤53.8	≥58.1
4c-SB	≤57.0	≥57.1
5c-SB	≤44.3	≥44.4
8c-SB	≤39.0	≥39.1
4c-B	≤62.2	≥69.1

## 4.5 Results of morphological observations

### 4.5.1 Observations of pronuclei

#### 4.5.1a Pattern of PNMBD

While scoring embryos as part of this project, it was noted that in 28% of embryos PNMBD is asynchronous – i.e. one PN fades at least 2 frames earlier than its sibling.

To assess whether this was a parameter related to embryo viability and could therefore be a very early aid to embryo selection, videos were re-examined and the results for 153 embryos where this parameter was able to be measured are in Table 14 below.  $\chi^2$  testing was performed on the data but there was insufficient evidence to reject the null hypothesis ( $\chi^2$   $P$  value =0.78). The percentage of ICSI cycles was not significantly different between the two groups which suggests that there is no effect on the type of insemination procedure and synchronicity of PN fade.

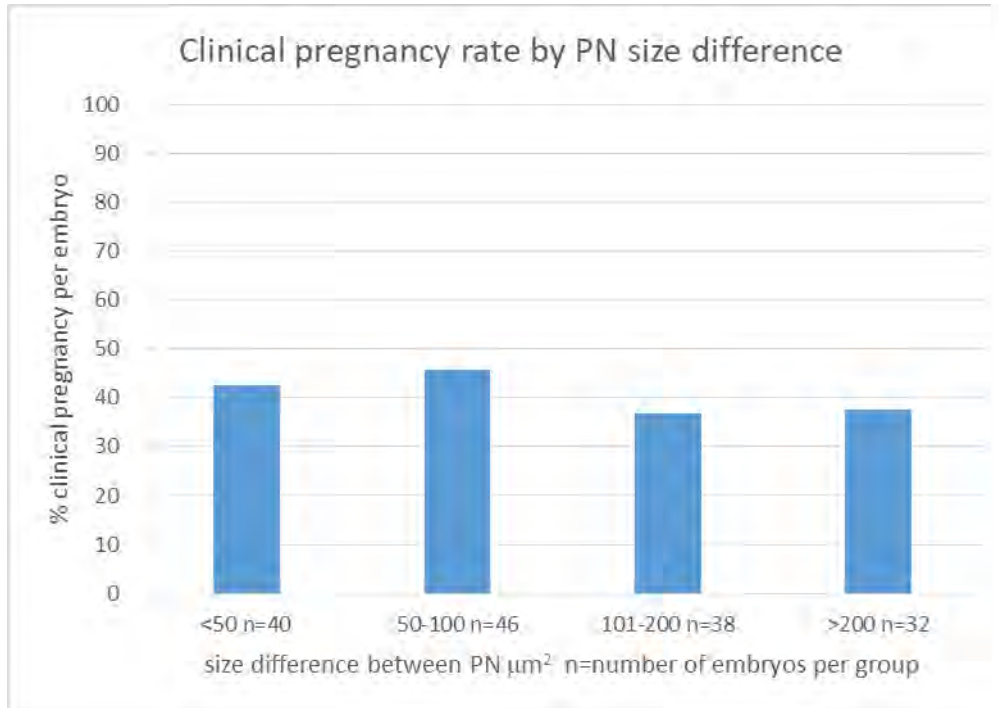
**Table 14: Pronuclear fade pattern and rates of clinical pregnancy.** Table shows observations taken from time-lapse videos of 153 embryos which had been frozen at the pronucleate stage, thawed, and cultured for up to 120 hours before transfer or cryopreservation. Only embryos where one or both PN were visible at time of first observation were included. The number of embryos exhibiting asynchronous PN fade, proportion of ICSI cycles in each group and clinical pregnancy rates are given. Pattern of PN fade does not correlate with outcome in this study.

	N	%ICSI cycles	Clinical Pregnancy per embryo
<b>Asynchronous PN fade Y</b>	43	39.5%	19 (44%)
<b>Asynchronous PN fade N</b>	110	42%	46 (42%)

#### 4.5.1b Size of PN at last image before PNMBD

It has been reported that measuring PN size in a time-lapse system, just before breakdown of the pronuclear membranes (PNMBD) provided a relatively accurate prediction of live birth. Published results indicated a success rate of >50% and a failure rate of <10% in predicting embryos that would NOT result in healthy pregnancies, based on changes in the relative size of the male and female PN, in fresh embryos (Otsuki *et al.*, 2019). The results of these measurements in this population of frozen thawed embryos are given in Figure 18 below. Pronuclei were measured in  $\mu\text{m}^2$  and grouped according to size differences between the pronuclei of <50  $\mu\text{m}^2$ , 51-100  $\mu\text{m}^2$ , 101-200  $\mu\text{m}^2$  and >200  $\mu\text{m}^2$ . Although results do not

reach statistical significance in this study, there is a slight downward trend in CPR as size difference increases.



**Fig 18:** Chart showing size differences between male and female pronuclei just before PNMBD and pregnancy rates. Chart shows measurements taken from time-lapse videos of embryos which had been frozen at the pronucleate stage, thawed, and cultured for up to 120 hours before transfer or cryopreservation. Data from 156 embryos where both PN were visible at time of first observation were included. Embryos were grouped according to size difference between the male and female pronuclei, and clinical pregnancy rate within each group calculated.

## 4.5.2 Observations of blastocysts

### 4.5.2a Cytoplasmic strings

The presence of thread-like cytoplasmic strings in the expanded blastocyst, observed to bridge the ICM with the TE, have been described as negative predictors of viability (Scott, 2000; Hardarson *et al.*, 2012 ) while others report that their presence or absence has no prognostic value (Alpha, 2011; Ciray *et al.*, 2014). Their appearance in frozen-thawed embryos cultured to blastocyst has not, to our knowledge, previously been assessed.

The number of strings seen in the cohort of embryos in this study was determined by observation in the Embryoscope™ incubators; the maximum number of strings seen at any one time from full blastocyst to time of removal for transfer or cryopreservation was

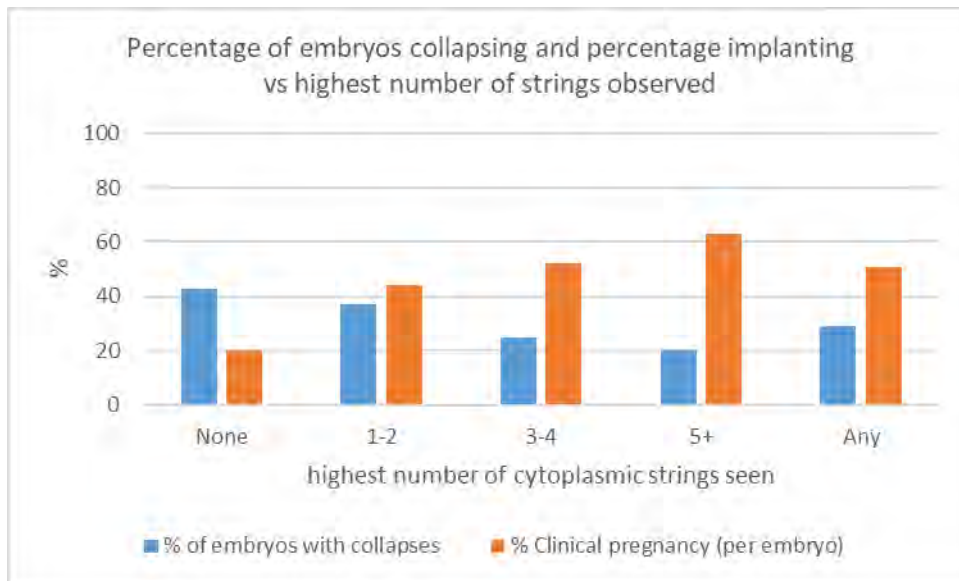
recorded. The number of strings seen was grouped as follows: None (no strings seen at any stage), 1-2 strings, 3-4 strings, 5 and above, all strings (all embryos with any number of strings seen). The mean number of strings per embryo was 2.5, range 0-9, mode =1. The mode of insemination (IVF/ICSI) did not contribute to the number of strings.

As previous studies have linked the appearance of cytoplasmic strings to blastocyst collapse, this data was also analysed. The results are displayed in Table 15 and Figure 19 below.

**Table 15: Presence and number of cytoplasmic strings, number of collapses and outcome.** Table shows observations taken from time-lapse videos of 176 embryos which had been frozen at the pronucleate stage, thawed, and cultured for up to 120 hours before transfer or cryopreservation. Only embryos reaching the blastocyst stage were included in this analysis. Embryos were grouped according to the highest number of cytoplasmic strings seen at any one time during development. The number of embryos within each group that also had a collapse, and the clinical pregnancy rate for each group was also determined and is shown below.

<i>Highest number of cytoplasmic strings seen</i>	<i>Number of embryos</i>	<i>of embryos with collapses</i>	<i>% ICSI cycles</i>	<i>Clinical pregnancy per embryo</i>
None	40	17 (43%)	50%	8 (20%)
1-2	54	20 (37%)	43%	24 (44%)
3-4	52	13 (25%)	44%	27 (52%)
5 and above	30	6 (20%)	47%	19 (63%)
All strings	136	39 (29%)	45%	70 (51%)





**Fig 19: Blastocysts grouped by the highest number of cytoplasmic strings observed during timelapse culture.** The percentage of embryos in each group showing a collapse of at least 20% size change is shown in blue. Orange bars indicate the percentage clinical pregnancy rate per embryo in each group. High numbers of cytoplasmic strings are associated with the lowest proportion of collapsing embryos and the highest clinical pregnancy rate.

For statistical analysis,  $X^2$  tests were performed comparing clinical pregnancy rates and rates of blastocyst collapse depending on the highest number of cytoplasmic strings seen, and the resulting  $p$  values are detailed in Tables 16 (clinical pregnancy rates) and 17 (blastocyst collapse rate) below.

Statistical analysis supports the hypothesis that the presence of **any** cytoplasmic strings (compared to no sign of cytoplasmic string formation) is positively related to the chance of clinical pregnancy. There was no significant difference between clinical pregnancy rates in the groups where strings were observed, but statistically higher pregnancy rates compared to no strings were seen for all groups.

Previous authors have suggested that string formation is linked to blastocyst collapse. In this study we found a statistically significantly **lower** number of embryos collapsed where more than 5 strings were seen compared to no strings seen, but no other parameters reached statistical significance.

**Table 16:  $\chi^2$  p values comparing clinical pregnancy rates between cohorts of embryos collated by maximum number of strings observed (groups compared against each other).** Table shows statistical analysis of data shown in table 17 and figure 19. Embryos with cytoplasmic strings are statistically significantly more likely to implant than embryos where no strings are seen, but the number of strings does not appear to influence chance of pregnancy.

Number of strings	0	1-2	3-4
0			
1-2	0.014*		
3-4	0.002**	0.437	
5+	0.0002**	0.101	0.313

\* $p < .05$ , \*\* $p < .01$

**Table 17:  $\chi^2$  p values comparing blastocyst collapse rates between cohorts of embryos collated by maximum number of strings observed (groups compared against each other).** Table shows statistical analysis of data shown in table 17 and figure 19. Embryos with a large number of cytoplasmic strings (>5) are significantly less likely to collapse than embryos with no strings seen.

Number of strings	0	1-2	3-4
0			
1-2	0.579		
3-4	0.072	0.179	
5+	0.044*	0.104	0.590

\* $p < .05$

#### 4.5.2b Blastocyst contraction and collapse

Impaired zona hatching impedes implantation and may be an explanation for the failure of some blastocysts which have good morphology *in vitro* to implant. Studies of expansion patterns and rates in embryos *in vitro* that have impaired zona hatching describe 2 patterns of pulse-like oscillations during expansion: a generally positive short episode of expansion (E-type, named in this study as ‘*pulsatile expansions*’) and C type characterised by dramatic collapses of the blastocoel cavity with a loss of up to 50% of volume (named in this study as ‘*collapse*’) (Iwata *et al.*, 2012; Pribenszky *et al.*, 2010, Niimura, 2003). The occurrence and clinical relevance of these two types of blastocyst size change has not, to our knowledge, previously been studied in frozen thawed embryos.

Numbers of pulsatile expansions and/or number and size of collapses were recorded for all embryos reaching full blastocyst, by observation in the Embryoscope™ incubators, from full

blastocyst stage to time of removal for transfer or cryopreservation. The mean percentage size of blastocyst collapse was 34.5%, range 0=73.9%. The mean number of pulsatile expansions was 1.5, range 0-8. Blastocyst collapse (C type oscillation) was observed in 31% of embryos (53/171). Of these, 47/53 (87%) had only one collapse event, 4 embryos had 2 collapses, 1 embryo had 3, and one had 7. Where more than one collapse was seen the largest change was used. 33 embryos had both pulsatile expansions and collapse events.

The size of blastocyst collapse was measured using the Embryoscope™ measuring tool. The diameter of the blastocyst at its central plane of focus was measured at the frame just before the start of collapse and at the smallest size of the contracted blastocyst in that collapse event. As collapse could occur at any stage from full blastocyst, the percentage change in blastocyst size was calculated and used for analysis, rather than absolute size changes. Blastocysts were grouped according to the percentage size of the largest collapse (no collapse (0), <30% change in size, 30-50% size change and >50% size change). Any collapse was also compared to no collapse. Results are presented below in Table 18. The percentage of ICSI cycles was not significantly different between the groups, suggesting that mode of insemination (IVF/ICSI) did not contribute to chance of collapse event or size.

**Table 18: Percentage size of largest observed blastocyst collapse and outcome.** Table shows observations taken from time-lapse videos of 171 embryos which had been frozen at the pronucleate stage, thawed, and cultured for up to 120 hours before transfer or cryopreservation. Only embryos reaching the blastocyst stage were included in this analysis. Embryos were grouped according to the size of the largest collapse seen at any one time during development. The clinical pregnancy rate for each group was determined and is shown below.

<i>% Size of Collapse</i>	<i>Number embryos</i>	<i>of % ICSI cycles</i>	<i>Clinical pregnancy per embryo</i>
0	118	52%	56 (47%)
<30%	20	20%	8 (40%)
(9.9-29.9)			
30-50%	24	42%	10 (42%)
(30.3-46.9)			
>50%	9	33%	1 (11%)
(51.4-73.9)			
Any collapse	53	31%	19 (35%)

For statistical analysis,  $X^2$  tests were performed comparing clinical pregnancy rates and size of blastocyst collapse, and the resulting  $p$  values are detailed in Table 19 below. Blastocyst collapse is negatively related to clinical pregnancy only when collapse is >50% (and only compared to no collapse observed).

**Table 19:  $X^2 p$  values comparing clinical pregnancy rates in groups of embryos collated by % size of collapse (all groups compared against each other).** A blastocyst which has a large collapse (more than 50% change in embryo volume) is significantly less likely to implant than an embryo which has no collapse of any size, but smaller collapses do not seem to predict embryo potential.

<i>% size of 0 collapse/Clinical pregnancy</i>	<i>0</i>	<i>&lt;30</i>	<i>30-50</i>
0			
<30%	0.528		
30-50	0.592	0.901	
>50	0.036*	0.120	0.097

\* $p < .05$

#### 4.5.2c Pulsatile expansions

The number of pulsatile expansions was counted as described above, and blastocysts grouped into no pulsatile expansions, 1 episode of pulsatile expansion, 2-3 episodes and 4 or more episodes. The total of all embryos showing any pulsatile expansion was also calculated. These results are shown in Table 20. The mode of insemination (IVF/ICSI) did not contribute to chance of collapse event or size.

**Table 20: Number of pulsatile expansions observed and outcome.** Table shows observations taken from time-lapse videos of 175 embryos which had been frozen at the pronucleate stage, thawed, and cultured for up to 120 hours before transfer or cryopreservation. Only embryos reaching the blastocyst stage were included in this analysis. Embryos were grouped according to the number of pulsatile expansions observed during development. The clinical pregnancy rate for each group was determined and is shown below.

<i>Number of pulsatile expansions</i>	<i>Number of embryos</i>	<i>% ICSI cycles</i>	<i>Clinical pregnancy per embryo</i>
0	66	36%	25 (38%)
1	39	54%	18 (46%)
2-3	44	47%	22 (50%)
4+	26	58%	14 (54%)
any	109	53%	54 (49.5%)

For statistical analysis,  $\chi^2$  tests were performed comparing clinical pregnancy rates and number of pulsatile expansions, and the resulting  $p$  values are detailed in Table 21 below. Although clinical pregnancy rate seems to increase with the number of pulsatile contractions seen, there is no statistically significant difference between the groups.

**Table 21:  $\chi^2$   $p$  values comparing clinical pregnancy rates in groups of embryos collated by number of pulsatile expansions (all groups compared against each other).** No statistically significant differences in pregnancy rates between groups was demonstrated, suggesting the number of pulsatile expansions is not a prognostic indicator of embryo implantation potential.

<i>Number of pulsatile expansions/Clinical pregnancy</i>	<i>0</i>	<i>1</i>	<i>2-3</i>
0			
1	0.411		
2-3	0.219	0.725	
4+	0.160	0.543	0.766

#### **4.6 Summary of results of morphological observations**

While some of the morphological observations collated have shown not to distinguish between successful and unsuccessful embryos in this study (asynchronous PN fade, PN size differences and pulsatile expansion number), there are several that demonstrate a positive trend towards embryo selection and/or ranking.

The presence of cytoplasmic strings seems strongly related to viability, and the presence of any visible strings is positively related to the chance of a clinical pregnancy, compared to no strings being seen. A high number of observed strings is also correlated with a lower chance of the blastocyst collapsing *in vitro*. Blastocyst collapse only seems to be important if the size change is more than 50% of the area of the embryo.

## Chapter 5: General Discussion

### 5.0: General Introduction

Two different non-invasive methods for assessing embryo implantation potential *in vitro* have been investigated. The project aims were to extend our understanding of the early stages of implantation; and shorten time to pregnancy by developing non-invasive methods of selecting (or deselecting) embryos in culture, especially frozen-thawed PN stage embryos.

The experimental approaches used were:

1. Sampling of conditioned media and co-culture with a 3D *in vitro* model of mid-secretory phase normal human endometrium, followed by transcriptomic analysis of these endometrial cells
2. Development of a time lapse annotation system to improve selection of PN stage frozen embryos cultured to blastocyst and replaced in FET cycles.

Both approaches have revealed differences between blastocysts which implant successfully and those which fail, not detected by standard morphological grading.

### 5.1: Results of conditioned media co-culture experiment: Transcriptomic data from *in vitro* model of mid-secretory phase endometrium and machine learning video analysis of embryos

This study uses more advanced endometrial epithelial organoid cultures to model endometrium *in vitro* than previous studies that used epithelial models from carcinoma cell lines (Singh *et al.*, 2010; Kaneko *et al.*, 2011; Kang *et al.*, 2016). Furthermore, endometrial organoids were derived from normal fertile donors. In addition, these cell lines have been grown as monolayers, while the endometrial organoid cultures used here enable cells to form a 3D structure, which more closely models cellular behaviour and functionality *in vivo* (Turco *et al.*, 2017). The addition of stromal cells from the same donor biopsy to the co-culture model also more closely models the human endometrium at the peri-implantation stage.

Morphologically high-grade blastocysts were compared based on clinical outcome by machine learning analysis of morphogenetic data and the effects of culture media conditioned by the embryos on gene expression in an *in vitro* model of endometrium. The use

of conditioned media from individual good quality human blastocysts with known implantation outcomes is also an advance on previous studies, for example the use of pooled media from cleavage stage embryos, grouped by morphological quality and not clinical outcomes (Brosens *et al.*, 2014)

Additional data on embryo quality was also investigated, using the EM-Life deep learning pipeline to review TL videos of the embryos generating the conditioned media samples.

The results of the PCA shown in Figure 9 indicates no cross contamination of cell types when sampled from the co-culture and that some separation between non-conditioned and conditioned media exposure is demonstrated. The separation of data points in Figure 10 shows discrimination between samples in epithelial cells is highest in successful vs untreated media. Discrimination of treatments by stromal cells is best in the unsuccessful vs untreated media comparison.

This initial analysis of the transcriptomic data indicates that there are differences between responses of epithelial and stromal cells to conditioned media from successful and unsuccessful embryos.

More than one hundred DEG were found in epithelial cells when comparing media from successful embryos to media from 'untreated' media. In contrast, in the stromal cell analysis, when unsuccessful embryo-conditioned media treatment was compared to 'untreated' media, more than two hundred DEG were found. A higher magnitude of upregulation was seen in the epithelial response compared to the stromal response. Variation in response magnitudes was also seen between individual embryos, with successful embryo #10 inducing an especially strong response in epithelial cells and unsuccessful embryo #3 inducing a particularly strong response in stromal cells. Only 1 significantly enriched biological process ontology was identified among the 207 stromal DEG, while 55 epithelial DEG (Figure 5A) were mapped to ten highly enriched biological process ontologies including those associated with important processes of epithelial remodelling during implantation (Aplin and Ruane, 2017). Eight components of the TGF $\beta$  signalling pathway were predicted as activated in the lead up to the transcriptional response seen in endometrial epithelial cells co-cultured with media conditioned by successful embryos.



In conclusion, conditioned media from successful embryos induced a strong, biologically coherent transcriptional response in endometrial epithelial cells that could be driven by TGF $\beta$  signalling (see below), whereas conditioned media from unsuccessful embryos induced a weaker, less coherent response in stromal cells.

These findings contradict some elements of previous studies, where decidualised endometrial stromal cells (ESC) *in vitro* are proposed as sensors of embryo quality as they show a markedly different response to 'normal' and 'abnormal' embryos *in vitro*. Teklenburg *et al.* (2010) performed co-culture experiments with human blastocysts seeded onto decidualising ESC monolayers and reported that blastocysts which arrested over the 3 day incubation period caused a profound inhibition of cytokine secretion (compared to normally developing embryos). A further study by the same group (Brosens *et al.*, 2014) used pooled conditioned media from embryos too poor for embryo transfer and compared this to pooled media from embryos known to have implanted, and untreated media, in with respect to effects on decidualising ESC monolayers. Gene expression profiling was used, and again, poor quality embryos induced a downregulation in a large number of genes, half of which were associated with transport, translation and cell cycle regulation. While these studies agree with data presented in the present study, this data that healthy embryos induce very little response in ESC, the degree of change in stromal cell transcription is not replicated; this study showed only upregulation and almost no downregulation. As well as being pooled media, embryos were only grown to day 3 of development – the conditioned media used in the present study is from 5 days of culture, as well as being from single embryos.

Non-invasive studies of pre-implantation development have shown that abnormal or unhealthy embryos are metabolically noisy (Leese, 2002; Brison *et al.*, 2004; Sturmey *et al.*, 2009), and Macklon and Brosens (2014) hypothesise that this 'noise' induces a proteotoxic stress response in decidualising ESC. Embryos used in the current study were all graded as good or excellent morphology and selected as the best of their cohort for embryo transfer. Media was also not pooled, so it may be that negative factors in the conditioned media may have been too dilute to induce the reaction seen in previous experiments, and the difference between embryos was too subtle. Nonetheless, endometrial cells **could** differentiate between successful and unsuccessful embryos in this experiment.

Stromal cell response to the implanting blastocyst has been further investigated with observations by various groups on stromal cell migration in response to varying quality embryos or conditioned media. Weimar *et al.* (2012) demonstrated that decidualising ESC from normal women seem to be able to discriminate between high and low quality embryos, only migrating towards implantation competent blastocysts *in vitro*. Berkhout *et al.* (2018) found a similar response, while Macklon and Brosens (2014) describe inhibition of migration by low quality embryos. No transcriptomic evidence for stromal cell migration was found in the present study.

Brosens *et al.* (2014) also studied the effect of their pooled conditioned media from good and poor embryos on Ishikawa EECs *in vitro*, finding that media from competent embryos induced very short  $\text{Ca}^{2+}$  oscillations in EECs compared to the prolonged and disorganised oscillations seen when poor quality embryo media was used (inducing a stress response).  $\text{Ca}^{2+}$  signals are well known to regulate gene expression, however, in the present study conditioned media from embryos which failed to implant did not induce a response in epithelial cells *in vitro*. In the same experiment, the authors also flushed mouse uteri with conditioned media and found media from competent embryos induced multiple metabolic genes and known implantation factors (COX-2, cytochrome p450 26a1 and osteopontin). The authors suggest a dual phase response of recognition by luminal epithelium of high-quality embryos followed by modulation of decidual ESC encountered once epithelium is breached. The data presented here support this hypothesis to some degree – a response from epithelial cells to good quality embryos potentially allowing attachment and early invasion, followed by a null response by stromal cells allowing further invasion. In human, embryo signalling to initiate decidualisation of the stroma is not required (as in some other species e.g. mouse (Aplin and Ruane, 2017)).

Studies in mouse models have revealed a programme of epithelial gene expression that controls implantation (Cha and Dey, 2014; Wang and Dey, 2006). Changes to epithelial apical-basal polarity may allow the TE to progress from attachment to epithelial cells to invasion between them (Denker, 1993); in mouse, E-cadherin expression is reduced in luminal epithelium at embryo attachment sites (Wallingford *et al.*, 2013). Mouse models where E-cadherin is not relocated or other defects in epithelial polarity are induced show a phenotype of implantation failure (Daikoku *et al.*, 2011; Sun *et al.*, 2016). In the present study, gene ontology analysis of the transcriptomic data from epithelial cells exposed to media from

successful embryos strongly indicates the upregulation of genes involved in epithelial remodelling during implantation. This is evidence for a similar programme in the human, where endometrial epithelial organoids respond to a factor (or factors) secreted by viable embryos into their environment and begin to change. The same response is not seen when organoids are exposed to media from unsuccessful embryos or untreated media, suggesting a role for these cells as sensors of embryo quality at this early stage of implantation.

Among the 76 DEG consistently identified in EEC organoids exposed to media from successful embryos, four homeobox (*HOX*) genes were identified. *HOX* genes are known to code for transcription factors essential for embryonic morphogenesis and differentiation (Carroll, 1995) and in mammals are arranged into chromosomal clusters *Hoxa*, *Hoxb*, *Hoxc* and *Hoxd* which have similar functions and overlapping embryonic expression patterns (Krumlauf, 1994; Taylor *et al.*, 1997). Of interest to the present study, *HOXA10* is known to be especially important as a transcriptional regulator of endometrial receptivity (Xu *et al.*, 2014). Targeted deletion of the *Hoxa10* gene in mice resulted in implantation failure (Sakota *et al.*, 1995), and also in the mouse, repression using an anti-sense expression vector reduced litter size (Bagot *et al.*, 2000). *HOXA10* regulates expression of multiple downstream target genes necessary for implantation in mammals (summarised in Xu *et al.*, 2014). Of note in humans is its role in regulating expression of IGFBP I which is expressed by decidualised endometrial stromal cells, where it is thought to negatively affect implantation (Guidice and Irwin, 1999; Irwin *et al.*, 2001). *HOXA10* activity in endometrial epithelial cells has been shown to be important in modulating implantation. Degradation of *HOXA10* in the endometrium of women with endometriosis and Ishikawa cells *in vitro* by over-expression of a binding protein (Calpain 7) is thought to be an explanation for impaired embryo implantation in these women (Yan *et al.*, 2018). Other studies have also demonstrated that repression of *HOXA10* in endometrial epithelium induces responses that reduce or prevent implantation (Zhu *et al.*, 2013; Xue *et al.*, 2021).

Having established that media from successful embryos causes changes that map to cellular processes known to be important in implantation, the final step was to look for factors that could stimulate this transcriptional response in endometrial epithelial cells. Eight components of the TGF- $\beta$  signalling pathway were identified among the most likely candidates, suggesting

'substance X' present in conditioned media from successful embryos could be a TGF- $\beta$  family member, or something that modulates this pathway.

The TGF- $\beta$  family is a large group of cytokines, detected in many species and with roles in inflammation, immune response/regulation, tissue remodelling, cell proliferation, cell differentiation and apoptosis (Heldin *et al.*, 2009; Garcia-Sainz *et al.*, 2003; Brunner *et al.*, 1988; Derynck *et al.*, 1988; Purchio *et al.*, 1988). Its role in reproduction has been studied: TGF- $\beta$  m-RNA, protein and receptor expression have been found in the uteri of other mammals (mouse, pig) during embryo implantation (Das *et al.*, 1992; Gupta *et al.*, 1998; Tamada *et al.*, 1990). Secretion of active TGF- $\beta$  during mouse implantation has been determined (Maurya *et al.*, 2013), and mouse models where TGF- $\beta$  secretion or activity was impaired show reduction in the number of implantations (Das *et al.*, 1997; Zhang *et al.*, 2010). TGF- $\beta$  is involved in both apoptosis and proliferation of cells, and as both these events occur during implantation, it is possible that family members may be key factors in implantation success or failure (Latifi *et al.*, 2019).

The TGF- $\beta$  family is involved in many biological events during embryogenesis; after binding to its specific receptor, signalling to the cell nucleus is via Smad (Massague, 2012). The Hippo pathway is also fundamentally important in mammalian embryological development (Wu and Guan, 2021), including both promoting and inhibiting TGF- $\beta$  activity - TAZ binds SMAD, promoting its nuclear translocation (Varelas *et al.*, 2008), while YAP/TAZ mediated SMAD cytoplasmic sequestration inhibits TGF- $\beta$  signalling (Varelas *et al.*, 2010). The Hippo pathway does not work via specific ligands and receptors, but instead responds to physical and architectural cues from the cell environment (Wu and Guan, 2021).

The Hippo pathway seems to be important in development and differentiation of the preimplantation mouse embryo as lack of maternal YAP/TAZ causes demise before the blastocyst stage (Nishioka *et al.*, 2009). In human embryonic stem cells, YAP, TAZ and TEAD all have important roles in maintaining pluripotency (Ogushi *et al.*, 2015)

Other authors have also suggested a prominent role for TGF- $\beta$  signalling in the earliest cell fate decisions of embryogenesis in the mouse (Goumans *et al.*, 2000). In human undifferentiated embryonic stem cells (hESC) *in vitro*, TGF- $\beta$  activity is mediated via the activin/nodal branch of its signalling pathway through the signal transducer SMAD2/3; a study

by James *et al.* (2005) shows this pathway is associated with pluripotency and required for maintenance of the undifferentiated state in hESCs and ex-vivo mouse blast outgrowths. In ex-vivo mouse blastocysts cultures, SMAD2/3 signalling was also shown to be required to maintain the ICM. Mice with null mutations for SMAD 2 and 3 show loss of pluripotent epiblast by E7.5 (Dunn *et al.*, 2004) supporting the hypothesis that proper maintenance of the ICM and the overlying epiblast needs an intact SMAD2/3 signalling pathway, at least in the mouse.

Most of the discussion in the literature on the role of TGF- $\beta$  in early development suggests an endometrial source of the cytokine, however there is evidence that mouse embryos can produce TGF- $\beta$  (Roelen *et al.*, 1994). There seems to be a well-defined role for TGF- $\beta$  signalling in the development of healthy mouse embryos (Nishioka *et al.*, 2009) and in maintenance of pluripotency in human embryonic stem cells. It is possible, therefore, that markers of good embryo health are components of these pathways, and are secreted into the media by implantation-competent blastocysts, and this is 'substance X' that affects the transcriptome of endometrial epithelial cells.

It is also important to remember that only conditioned media was used in this co-culture experiment, so no influence of the endometrial cells on the embryo could be studied, only one half of the 'cross-talk' conversation between embryo and endometrium is available to study.

Further work is required to identify the factors in the conditioned media from successful embryos that change gene expression in endometrial epithelial cells. One possible experimental approach would be to expose the 3D endometrial model used in the present study to individual cytokines postulated here as upstream regulators (for example TGF $\beta$ ), comparing the transcriptomic results with those from conditioned media. Effects were seen without the need to pool media from different embryos, which is important as embryos responded with different magnitudes of change and this information would have been lost if media from several embryos were combined.

The consequences for defects in the ability of a woman's endometrium to reliably recognise signals from embryos able to implant could result in recurrent implantation failure. The converse, where endometrium is unable to distinguish signals from an impaired embryo could

result in the repeated implantation of embryos without the potential to develop to a full-term baby, and recurrent miscarriage (Macklon and Brosens, 2014). There is, therefore, a potential early detection method for these two extremes of reproductive pathology. If the identity of a reliable marker of embryo viability can be isolated from conditioned media, a test where endometrial biopsy-derived cultures are challenged with this marker could return useful results to aid diagnosis before repeated cycles of assisted conception.

The embryologists at St Mary's have been providing TL videos of fresh embryos in culture to a research project developing a Machine Learning software programme (with the working title eM-Life) which aims to improve embryo selection based on static images of embryos in culture. The 9 embryos giving rise to the conditioned media used in this experiment were selected for transfer based on standard morphological grading as described in the introduction. To test these embryos against another model of embryo selection, TL videos were taken through the trained model.

The ML software programme eM-Life gave a score to each embryo at each time point (the closer to the value of 1 the higher the predicted chance of a live birth). Using a deep learning algorithm, the software aims to predict chance of live birth based on static images of embryos, and work is ongoing to determine the most predictive stage of development. Embryos are placed in 'buckets' numbered 1 to 10, and chance of pregnancy increases as the bucket number increases. In this study the ranking given by eM-Life did not agree with outcome or response of the endometrial cells in culture, but its ranking was more closely correlated with morphological grading. EM-life aims to be most valuable when ranking a cohort of embryos from one patient, so inter-patient variability, combined with the overall high morphological grade of the test cohort reduced its power.

## **5.2: Timelapse imaging and annotations of PN stage frozen embryos – aids to embryo selection**

The time of several morphological set points was found to be significantly different between embryos which fully implanted and those which did not. Time to the 3 cell and 4 cell stage from pronuclear fade was significantly slower in successful embryos. In later stages of development, the reverse was seen. Time to start of compaction and time to morula stage from PN fade were significantly shorter in successful embryos.

Time between setpoints was also calculated, and a similar pattern of initial slower development changing to faster (after the 8-cell stage) in successful compared to unsuccessful embryos was observed. In early stages of development, it was only the mean time taken for embryos to cleave from 2 cell to 4 cell that was significantly longer in successful embryos. While the quartile data in Table 9 shows an increase in implantation rates when this phase was longer than 13.1h, no statistical significance was demonstrated.

When times from cleavage stages to compaction and early blastulation were shorter, generally higher implantation rates were seen (Table 12). For the full developmental timeline of 2 cell to blastocyst, only the time between 4-cell to blastocyst showed a significant difference between mean times and fastest and slowest quartiles.

Suggested thresholds for quantitative morphokinetic selection (or deselection) criteria based on all morphokinetic results were collated (Table 13)

In one of the earliest studies of morphokinetics and embryo implantation (Meseguer *et al.*, 2011), embryo development from the time of ICSI to day 3 (6-8 cells) was observed in the same time lapse system as used in this study (Embryoscope™). This study is valuable as the endpoint was successful or unsuccessful implantation, not quality of *in vitro* development alone, although embryo transfer was performed at an earlier stage so developmental stages to blastocyst are not available. The authors found that median values of time to 2c, 3c, 4c and 5c were not significantly different for implanting v non implanting embryos, but implanting embryos had a tighter distribution (smaller variance). A study by Dal Canto *et al.* (2012) found that successful embryos reached the 8-cell stage earlier than those which did not implant, but found no difference for other cleavage stages, while other authors have also reported finding no significant difference in times to development for any cleavage stage, in agreement with Meseguer and colleagues. (Freour *et al.*, 2013, Chamayou *et al.*, 2013, Kirkegaard *et al.*, 2013)

The data in the present study, however, does show a significantly slower time to 3 cells and 4 cells, and a larger variance at all cleavage stages for mean values in implanting embryos. This finding is in contrast to a previous study on fresh embryos, where delays on the first two cleavage divisions and prolonged transition from 2 to 4 cells was associated with complex aneuploidy (Davies *et al.*, 2012).

This may be due to a different starting timepoint (time of PN fade compared to time of ICSI for previous published studies on fresh embryos). Another contributing factor could be that the embryos have undergone cryopreservation. Wong *et al.* (2010) studied morphokinetics in PN stage frozen embryos to the 4-cell stage to determine if this predicted blastocyst development. Their data was limited and the focus was on predicting embryos which would arrest before reaching blastocyst, but they compared rates of development to the 4 cell stage to a small group of fresh embryos in the same culture conditions and found no difference.

Association between implantation and the time between developmental stages from 2c to 8c has been evaluated in six published studies, and time t2-t3 and t3-t4 are most closely associated with outcome. Three studies (Meseguer *et al.*, 2011, Rubio *et al.*, 2012, Chen *et al.*, 2013) reported that embryos cleaving at intermediate time points (quartiles 2-3) for t2-t3 and/or t3-t4 had the highest chance of implantation, compared with embryos developing faster or slower at these early developmental stages. Three other studies (Hlinka *et al.*, 2012, Chamayou *et al.*, 2013, Kirkegaard *et al.*, 2013) found no difference. In the present study, although the mean time difference from t2-t4 in total was significantly longer for successful embryos, the variance was large and outcomes across all time quartiles were not significantly different.

Rubio *et al.* (2012) also analysed the effect of 'direct cleavage' from 2-3 cells and found these had an implantation rate of only 1.2%. As this is now widely known to be a strong negative indicator of viability, any embryo in the present study showing this behaviour would have been de-selected at a very early stage and never chosen for transfer or freezing.

Comparison of data on time between cleavage stages is difficult due to inconsistency of nomenclature and modes of measurement throughout the literature (Kaser and Racowsky, 2014). Some authors (Kirkegaard *et al.*, 2013) use the abbreviation 'cc' to mean the time required for cell numbers to double (cc1 gives 2 cells, cc2 results in a 4 cell embryo cc3 = 4 cell to 8 cell stage), while Meseguer *et al.* (2012) takes cc2 to mean the duration of the 2 cell stage and cc3 duration of the 4 cell stage. To complicate things even further, Chamayou *et al.* (2013) defines the third round of cleavage as cc3, i.e. time from 3cell to 5 cell. Hence in this thesis the use of simpler t2-t3 (time from 2 cells to 3 cells), t2-tM (time from 2c to morula) etc. have been used for clarity.



Kirkegaard and colleagues (2013) found no difference in duration of t3-t4 or t4-t8 between implanting and non-implanting embryos, as also found in this study. Chamayou *et al.* (2013) however found a significantly longer median duration of t3-t5 in implanting embryos, a result not mirrored here. A shorter time from 4 cell to 8 cell was shown to be significantly positively predictive of pregnancy by Freour *et al.* (2013), but this was not replicated by Chamayou *et al.* (2013), Kirkegaard *et al.* (2013) or in the present study.

Moving forward from cleavage stage embryos, four studies have looked at timings of post cleavage events and chances of implantation in fresh embryos. Two studies (Kirkegaard *et al.*, 2013 and Chamayou *et al.*, 2013) found no differences between successful and unsuccessful embryos when comparing median times to compaction or morula development. Studies by Campbell *et al.* (2013a and b) have found that times to start of blastulation and full blastocyst are predictive of implantation and risk of aneuploidy, with times from ICSI to blastulation of <96.2h and full blastocyst <122.9h predictive of high implantation and low aneuploidy risk. The numbers of embryos in this second study were small, however, and the finding was not replicated in a retrospective study in a different clinic (Kramer *et al.*, 2014). In the present study, time to start of compaction, time to morula stage and time to start of blastulation was significantly shorter from all cleavage stages in successful embryos. Time to full blastocyst was only significantly shorter from the 4-cell stage.

Lack of evidence for significant differences in timings of post-cleavage stage development between successful and unsuccessful embryos is probably in part because later stages are harder to track manually and through image analysis (Meseguer *et al.*, 2011). Variability between annotators, and difficulties in seeing all planes of an embryo mean that some relatively subjective time points (start of compaction, start of blastulation) may not be accurately recorded (Castello *et al.*, 2016). This may weaken the value of many of the suggested 'time between stages' thresholds proposed in Table 13 when different embryologists are annotating embryos, but with careful training and internal quality assurance this could be overcome. The 'time between setpoints' of 4 cell to blastocyst could be used as an initial pilot variable as this is easier to determine on time lapse images, and much less susceptible to inter-operator interpretation.

It should also be noted that embryos which failed to fully compact, or form blastocysts (yet were still the best of the cohort and selected for transfer) are excluded from the data sets

where time to these parameters are measured. It was only possible to measure time to start of blastulation and time to full blastocyst when these set points were reached before removal for embryo transfer. This may account for the lack of statistically significant differences between successful and unsuccessful embryos (apart from 4 cell to blastocyst). As there are many factors which can impact on embryo implantation, it should not be unexpected to find non-implanting embryos with same morphokinetics as implanting embryos (Meseguer *et al.*, 2011).

One of the main criticisms of time-lapse algorithms is that varying culture conditions (type of media used, Co<sub>2</sub> and O<sub>2</sub> gas concentrations) affect the morphokinetic profile of an embryo (Ciran *et al.*, 2012, Barrie *et al.*, 2015) making translation from one clinic to another difficult (Barrie *et al.*, 2017). Other confounding factors from different patient groups can also affect morphokinetics (severe male factor infertility, maternal age over 39yrs, polycystic ovarian disease) and embryos from patients with these backgrounds are often excluded from published data (Barrie *et al.*, 2017). There have been calls in the literature for clinics to develop their own 'in house' algorithms based on their own culture systems and patient demographics (Barrie *et al.*, 2017, Castello *et al.*, 2016, Kaser and Racowsky, 2014, Racowsky *et al.*, 2015). This is especially important for the group of patients at St Mary's having pronucleate stage embryos thawed, cultured and replaced, as there is little published evidence of the effect of PN stage freezing on morphokinetics.

The other factor that prevents the use of morphokinetic algorithms developed on fresh embryos for this patient group is the loss of the 'time of insemination or ICSI' as a set start point. Pronuclear fade (pn-f) has been suggested as an improved start point for timing measurements for all embryos (Barrie *et al.*, 2017) as 'time of ICSI' can be taken as time of procedure start, midpoint or end, or time of injection of each oocyte. 'Time of insemination' for IVF cases is even less specific as the time of entry of sperm to each oocyte cannot be determined. As seen in this study, this could also be used for the majority of frozen/thawed zygotes, but not all. An alternative suggestion by Kaser and Racowsky (2014) is that time of appearance of first cleavage furrow (t-2) should be the first time point for all morphokinetics as an even more standardised start point, and this would be easily recognisable and recordable for all embryos in time lapse culture systems.

Based on a review of the literature, four morphological observations thought to help predict embryo viability and not previously studied in frozen-thawed PN stage embryos were identified. These were: asynchronous PNMBD (asynchronous PN fade) (Ezoe *et al.*, 2021, Rosario *et al.*, 2015, Davies *et al.*, 2012); pronuclear size differential immediately before PNMBD (Otsuki *et al.*, 2019); the presence of thread-like cytoplasmic strings in the expanded blastocyst (Scott, 2000; Hardarson *et al.*, 2012; Alpha, 2011; Ciray *et al.*, 2014; Salas-Vidal and Lomeli, 2004; Munne *et al.*, 2018) and patterns of expansion and/or collapse (Iwata *et al.*, 2012; Pribenszky *et al.*, 2010).

Statistically significant differences between embryos which implanted successfully and those which failed to implant were only seen for large blastocyst collapses and the presence of cytoplasmic strings.

Of 152 embryos where PN were clearly visible from the start of TL incubation, asynchronous PN fade was observed in 43 (28%). This proportion is higher than reported in fresh embryos (1% of fertilised oocytes in Ezoe *et al.*, 2022 and 13% in Rosario *et al.*, 2015), and may be an artefact of slow freezing. The hypothesis that this is artefactual and not related to viability is supported by the observation that no significant difference was seen in outcomes of embryos with and without asynchronous PN fading.

While Ezoe and colleagues (2022) also found no impact of synchronicity of PN fade and chance of implantation, the numbers of embryos exhibiting asynchronous fading were very small. Two studies in fresh embryos have suggested that zygotes exhibiting asynchronous PN fading are more likely to show developmental abnormalities (direct cleavage 1c-3c, irregular blastomere size) (Rosario *et al.*, 2015) and complex aneuploidies (Davies *et al.*, 2012), although these embryos were assessed at 8c and not allowed to develop to blastocyst.

Despite published data suggesting size differences in PN just before PNMBD can be an early predictor of implantation success (Otsuki *et al.*, 2019), the present study found no difference in clinical pregnancy rates even when the size difference between the male and female pronucleus was more than  $200\mu\text{m}^2$ . Otsuki and colleagues (2019) found statistically significantly higher birth rates when the difference in areas between PN was relatively small ( $<39.3\mu\text{m}^2$  and  $<40.0\mu\text{m}^2$  for IVF and ICSI embryos respectively).

A study by a Swiss group (Senn *et al.*, 2006) where embryo selection was prohibited by law, found that pronuclear scoring techniques used on fresh zygotes could be used after freezing and thawing, but some structures were altered, resulting in significantly lower scores for embryos that then implanted. Cooling is known to induce depolymerisation of microtubules (Mandelbaum *et al.*, 2004) which play key roles in PN migration and apposition (Simerly *et al.*, 1995), and organelle movement within the oocyte (Bavister and Squirrell, 2000, Ebner *et al.*, 2003); thus, freezing may alter this microtubule network displacing PN and organelles and altering observations used when scoring fresh embryos. PN scoring techniques used alone are therefore less useful for frozen-thawed zygotes, as shown by the current study.

The presence of cytoplasmic strings bridging the ICM and TE, visible on TL videos in human embryos has been noted since 2000 (Scott, 2000), but there is a scarcity of information on their relevance to embryo viability. Mouse data suggests they are an *in vitro* artefact (Salas-Vidal and Lomeli, 2004), but this is difficult to determine in the human, although small numbers of *in-vivo* derived human blastocysts have shown cytoplasmic strings (Munne *et al.*, 2018). Some studies claim that cytoplasmic strings are a negative predictor of viability, a result of poor media conditions or polarisation problems (Hardarson *et al.*, 2012, Scott, 2000); others, however, maintain that they have no effect on blastocyst viability (Alpha, 2011, Ciray *et al.*, 2014).

In the present study, the maximum number of strings seen at any one time from full blastocyst to removal from culture was recorded. Blastocysts were examined in the Embryoscope™ and through all planes of focus. It was found that the presence of even 1-2 cytoplasmic strings was significantly positively associated with successful implantation, which contradicts the studies mentioned above, but agrees with a recent study from Ebner *et al.* (2020), although data presented in that study did not reach statistical significance. In the present study, the actual number of strings counted did not affect the chance of implantation, but this may reflect the difficulty in accurately counting strings in the Embryoscope™. Although visualising their presence or absence is easy, accurate counts are difficult due to the optical sectioning of the TL videos. The physiological role of cytoplasmic strings is yet to be firmly established, but in the mouse are involved in the polarised flow of cells from the polar to the mural TE (Gardner, 2000), are actin-rich and may be part of a vesicle transport mechanism providing direct communication between the ICM and mural TE cells (Salas-Vidal

and Lomeli, 2004). A higher number of these vesicles on cytoplasmic strings are found in human blastocysts leading to clinical pregnancy (Eastwick *et al.*, 2019).

Ebner *et al.* (2020) also found a significant association of cytoplasmic strings with blastocyst collapse, with 61% of embryos with strings having at least one collapse, compared to 19% of blastocysts without visible strings. The data in this study provides a slightly more complex picture – blastocysts with a high number of strings were significantly less likely to collapse than when no strings were observed. However, Ebner does not define what change in blastocyst volume is recorded as a collapse and may have counted even small changes in volume.

Blastocyst expansion is a functional property of the TE; formation and maintenance of the blastocoel requires a competent epithelium (Huang *et al.*, 2016). The embryo also needs metabolic competency to create an ionic gradient (facilitated by Na/K ATPases in the basolateral membranes of TE cells) which allows fluid to accumulate and form the blastocoel (Gardner and Balaban, 2016). Previous authors have identified 2 patterns of pulse-like oscillations during blastocyst expansion: firstly, a generally positive, relatively uninterrupted expansion (E-type) and a C type, characterised by dramatic collapses of the blastocoel cavity with a loss of up to 50% of volume (Iwata *et al.*, 2012; Pribenszky *et al.*, 2010).

Both types of oscillation were observed in embryos in this study. E-type oscillations were renamed pulsatile expansions, and were generally positive, small but sudden changes in blastocyst size, once full blastocyst stage had been reached (negative change of more than 9.9% was recorded as a collapse). The mean number of pulsatile expansions per blastocyst was 1.5, range 0-8. Although a slightly lower pregnancy rate was observed when no pulsatile expansions were seen, this did not reach statistical significance. Mode of insemination (IVF v ICSI) was also not a contributing variable.

Blastocyst collapse (C type oscillation) was observed in 31% of embryos (53/171). The clinical pregnancy rate for embryos showing any collapse was lower than those which did not collapse but did not reach statistical significance. When size of collapse was taken into consideration, embryos experiencing changes in blastocyst diameter of more than 50% were significantly less likely to implant than embryos which did not collapse.

Published data suggest that dramatic collapses are related to impaired zona hatching in mouse embryos *in vitro* (Niimura, 2003), but it remains unclear whether this translates to issues with implantation of human embryos *in vivo* (Huang *et al.*, 2016). A previous study recommended not to transfer blastocysts which collapse *in vitro* if other embryos are available (Marcos *et al.*, 2015), but other authors have not found collapse to be a predictor of pregnancy or live birth (Bodri *et al.*, 2016; Ebner *et al.*, 2020).

The mechanisms involved in pulsatile expansion and collapse remain to be identified. Some authors suggest they are passive responses to building pressure in the expanding blastocoel, and the zona pellucida may play a role in their modulation (Chinn and Huang, 2015). Pulsatile expansions may be a normal response to increasing pressure of the blastocoel during expansion (Huang *et al.*, 2016), active control by TE cells altering ion transport across the developing epithelium or due to intercellular leakiness as dividing cells are inserted into the TE layer (Guillot and Lecuit, 2013, Hu *et al.*, 2013). Large collapses (defined here as >50% change in blastocyst diameter) may represent an acute failure of this normal response (Huang *et al.*, 2016). Ebner and colleagues postulated that a subtype of cytoplasmic string may be associated with blastocoelic collapse, (Ebner *et al.*, 2020).

Embryos frozen at the PN stage, thawed and cultured to blastocyst cannot be assessed using morphokinetic data developed on fresh embryos. A framework for differentiating between embryos with highest and lowest chances of forming viable pregnancies by their morphokinetics and other time-lapse observations has been developed. Further work is required to apply these findings prospectively to embryos in culture, and also to increase the data pool so variables such as mode of insemination, maternal age and sperm source can be accounted for, to improve the predictive power of the algorithm.

As there are many factors which can impact on embryo implantation, it should not be unexpected to find non-implanting embryos with same time lapse observations as implanting embryos (Meseguer *et al.*, 2011). It has been suggested that the maximum accuracy of prediction of clinical pregnancy based on embryo quality is around 80%; the other 20% being dependent on patient-related factors (e.g. poor endometrial receptivity), or process errors (poor handling techniques) (Annan *et al.*, 2013; VerMilyea *et al.*, 2020).

It has proven difficult in this data set to find parameters which separate successful from unsuccessful embryos with statistical significance at cleavage stages. The majority of the measurements and observations that appear to be of value are in post cleavage developmental stages. The reasons for this are unclear, but should be taken as evidence that thawing multiple PN stage embryos for culture to the blastocyst stage is the best method for embryo selection and reduced time to pregnancy when a 'PN freeze all' strategy has been used.

### **5.3 Limitations of the study**

#### *Limitations of the study*

Research involving human embryos and implantation is always limited by availability of suitable experimental models and material. As implantation varies widely in placental mammals (McGowen *et al.*, 2014), animal models are of limited value, and data is often extrapolated from a mixture of *in vitro* cell lines and *in vivo* mouse models.

The use of a 3D model of human endometrium has overcome some of these issues, but there are still limitations. Epithelial organoids mean these cells are in a more physiological state, but stromal cells are separated so not in direct contact. The endometrial stroma *in vivo* is heterogeneous, containing (amongst others) haematological cell types such as macrophages and natural killer cells, which contribute to cellular responses to an invading embryo (Macklon and Brosens, 2014). There can also be experimental artefacts induced by cell culture – repeated passaging of cells can cause phenotypic changes, where they lose tissue specific functions *in vitro*. Endometrial organoids have been shown to be genetically stable in long term culture by comparison of transcriptomic data with the cells of origin (Turco *et al.*, 2017). Characterisation of the endometrial epithelial phenotype in organoids can also be confirmed by immunohistochemical methods, for example staining for the oestrogen receptor  $\alpha$  and detection of mucus in the lumen, correlating with expression of MUC-1 (Boretto *et al.*, 2017)

Access to experimental material is also limited, and this study benefited from donation of normal endometrium collected as a control for another study within the same research group. Initial proposals for the project included the use of endometrium from patients with recurrent

miscarriage and recurrent implantation failure. Regrettably, one impact of the Covid-19 pandemic was a hiatus in non-urgent gynaecological care, meaning no procedures where samples could be collected were performed for approximately 18 months. Having demonstrated a response to conditioned media in normal endometrium, it is certainly scope for a future project to evaluate responses to endometrial samples from patients with suspected pathologies using the same methodologies. Collection of conditioned media was limited by restrictions on type of Embryoscope™ slide could be used and future work may be more limited as Embryoscope+™ use increases and the isolated wells of the older style slide are less common. Once samples were collected, there was then a delay while the outcome of the cycle was established, and some samples were unusable in this study as the transfer ended in early miscarriage. As the co-culture and transcriptomic analysis is expensive to perform, financial limitations significantly impacted this section of the study.

The format and funding of the HSST programme adds a further limitation on the DClSci programme. Time for the research component of DClSci is limited and the impact of the Covid-19 pandemic (discussed below) exacerbated this. As a workplace-based training scheme there are many conflicting demands on time, and a project had to be planned that did not demand large periods of time in a research laboratory. Other restrictions were the need for elements of the project to be applicable directly to the clinical service, and funding. Some funding is paid to each Trust as part of the HSST programme (£13,000 per annum), but this is not solely for research, is paid quarterly, and at my Trust was not ring-fenced, so any reserves could not be carried over into a new financial year. This budget restricted the number of samples that could be sent for transcriptomics and therefore also limited the scope of the co-culture study.

This project has been impacted by the Covid-19 pandemic. Some parts of the initial preparation (Literature review, extended project proposal) were deferred from Spring 2020 to Autumn 2020 and the C1 lay presentation delayed until March 2021 (from Spring 2020) hence C1 was not assessed until 9/4/2021. The delays in approvals, and in submitting and



passing section C1 meant I could not fully move forward with my C2 research project (presented here) until spring of 2021. I required access to the University of Manchester Laboratories in our Hospital campus. The decision was made by UoM to close these labs completely in between March 2020, followed by a phased reopening where new projects were given the lowest priority.

Supply chain issues for laboratory consumables and worldwide lack of a vital tissue culture component meant that the organoid co-culture experiments had to be pushed back from February 2022 to July 2022.

Clinical pressures within the NHS have also impacted on sample collection. The Department of Reproductive Medicine closed completely to all patients having routine treatments from March 2020 to July 2020. To enable safe working, patient numbers on re-opening were cut initially to 30% of normal levels then to 50%. At time of submission (Early 2023) patient numbers are still not back to pre-pandemic levels, primarily due to backlogs in referral pathways. I have therefore not been able to collect as much data for the timelapse on frozen embryos element of the project as less than 50% of expected patients have presented for treatment.

#### **5.4 Concluding remarks**

Data presented here has raised interesting findings about the response of human endometrial cells in a 3D implantation model to media conditioned by human blastocysts *in vitro*. It is an improvement on previous studies in several ways – a more physiological model of mid-secretory phase normal human endometrium was exposed to media from individual embryos with known clinical outcomes. Despite the embryos being of high morphological grades, endometrial cells in the co-culture model responded differently to media from implanting and non-implanting embryos, demonstrated by changes in their transcriptomic profiles. Further assessment of the transcriptomic data showed that endometrial epithelial cells respond to successful embryos in a co-ordinated fashion, possibly allowing cellular changes that facilitate implantation. Endometrial stromal cells, however, respond to unsuccessful embryos in a

much less organised manner. This 'sensing' of embryo quality appears independent of other measures of embryo quality (morphological grade and computer assisted embryo selection) and has exciting implications for future research and diagnostic options for patients with repeated IVF failures.

On a practical level, co-culture experiments could be enhanced by integrating stromal cells into the 3D organoid structure. Further work is needed to extend the data pool by repeating these experiments.

Future research would involve identification of the upstream regulators of the transcriptomic response seen, to determine what successful embryos are secreting into their media. If a specific extracellular factor can be found that is a non-invasive marker of embryo potential, this raises exciting possibilities for embryo selection and could give answers to patients with repeated cycle failures. Lack of secretion of this marker in media from morphologically high-grade embryos would indicate an embryo with a very low chance of implantation. A pre-treatment diagnostic test where patient's endometrial cells are exposed to this factor and their response studied could diagnose RIF *in vivo*.

The lack of morphokinetic algorithms for frozen-thawed PN stage embryos cultured to blastocyst has meant this large patient group has not benefitted from advances in embryo selection available to patients having fresh embryo transfer. St Mary's continues to have a strong approach to OHSS management preferring to err on the side of 'freeze all' for patients at even moderate risk. This means a relatively high number of PN freezes as well as a large historical bank of PN frozen embryos. Although the number of patients using their frozen embryos during the study period was lower than hoped, it has still been possible to develop TL parameters that should improve embryo selection.

Other morphological features that may be markers of implantation potential that had not been previously evaluated in frozen embryos proved to be not predictive of success (synchronicity of PN fade, PN size differences prior to PNMBD) while others showed some power (blastocoel expansion and collapse patterns, and the presence of cytoplasmic strings in the expanded blastocyst).

Further work now needs to take place to test the morphokinetic and morphological parameters identified as predictive prospectively, alongside standard grading. The finding of

this study will not only improve outcomes but also improve our understanding of the effect of cryopreservation on early development.

Two methods of assessing the potential of embryos *in vitro* for successful implantation have been studied. The Information that has been gained using these non-invasive methods to investigate implantation potential during routine embryo culture has significant potential to be an enormous benefit to patients and clinicians alike, improving outcomes for patients, shortening time to pregnancy and increasing our understanding of what makes for a successful implantation.

## References

- 1 Ahlstrom, A., Westin, C., Reismer, E, Wikland, M. and Hardarson, T. (2011) 'Trophectoderm morphology: an important parameter for predicting live birth after single blastocyst transfer'. *Human Reproduction*, 26 pp 3289-3296.
- 2 Almagor, M., Or, Y., Fieldust, S. and Shoham, Z. (2015) 'Irregular cleavage of early preimplantation human embryos: characteristics of patients and pregnancy outcomes'. *Journal of Assisted Reproduction and Genetics*, 32 pp .1811-1815.
- 3 Alpha Scientists in Reproductive Medicine and ESHRE Special Interest Group of Embryology. (2011) 'The Istanbul consensus workshop on embryo assessment: proceedings of an expert meeting'. *Human Reproduction*, 26 pp. 1270–1283.
- 4 Aoki, R and Fukada, M.N (2000) 'Recent molecular approaches to elucidate the mechanism of embryo implantation: trophinin, bystin and tastin as molecules involved in the initial attachment of blastocysts to the uterus in humans'. *Seminars in Reproductive Medicine*, 18 pp 265-271.
- 5 Aparicio-Ruiz, B., Basile, n., Perez Albala, s., Bronet, F., Remohi, J. and Meseguer, M. (2016) 'Automatic time-lapse instrument is superior to single-point morphology observation for selecting viable embryos: retrospective study in oocyte donation'. *Fertility and Sterility*, 106 pp. 1379-1385.
- 6 Aplin, J.D., Meseguer, M., Simon, C., Ortiz, M.E., Croxatto, H. and Jones, C.J.P. (2001) 'MUC1, glycans and the cell surface barrier to embryo implantation. *Biochemical Society Transactions*, 29 pp. 153-156
- 7 Aplin, J.D. and Ruane, P.T. (2017) 'Embryo-epithelium interactions during implantation at a glance'. *Journal of Cell Science*, 130 pp. 15-22.
- 8 Aydin, S., Cinar, O., Demir, B., Korkmaz, C., Ozdegirmenci, O., Dilbaz, S. and Goktolga, U. (2011) 'Is pronuclear scoring a really good predictor for ICSI cycles? *Gynecological Endocrinology*, 27(10) pp.742-747.
- 9 Azzarello, A., Hoest, T. and Mikkelsen, A. L. (2012) 'The impact of pronuclei morphology and dynamicity on live birth outcome after time-lapse culture'. *Human Reproduction*, 27(9) pp. 2649-2657
- 10 Bagot, C.N., Troy, P.J. and Taylor, H.S. (2000) 'Alteration of maternal Hoxa10 expression by *in vivo* gene transfection affects implantation'. *Gene Therapy*, 7 pp1378-1384
- 11 Barrie, A., Homburg, R., McDowell, G., Brown, J., Kingsland, C. and Troup, S. (2017) 'Examining the efficacy of six published time-lapse imaging embryo selection algorithms to predict implantation to demonstrate the need for the development of specific, in-house morphokinetic selection algorithms'. *Fertility and Sterility*, 107(3) pp 613-621.
- 12 Barros, F., Brosens, J.J. and Brighton, P.J. (2016) 'Isolation and Primary Culture of Various Cell Types from Whole Human Endometrial Biopsies'. *Bio-Protocol*, 6(22) DOI:10.21769/BioProtoc.2028
- 13 Basile, N., Vime, P., Florensa, M., Aparicio Ruiz, B., Garcia Velasco, J.A., Remohi, J. and Meseguer, M. (2015) 'The use of morphokinetics as a predictor of implantation: a multicentric study to define and validate an algorithm for embryo selection'. *Human Reproduction*, 30 pp. 276-283.
- 14 Bentin-Ley, U., Horn, T., Sjogren, A., Sorensen, S., Falck Larsen, J. and Hamberger, L. (2000) 'Ultrastructure of human blastocyst-endometrial interactions *in vitro*'. *Journal of Reproduction and Fertility*, 120(2) pp 337-350
- 15 Berkhout, R.P., Lambalk, C.B., Huirne, J., Mijatovic, V., Repping, S., Hamer, G. and Mastenbroek, S. (2018) 'High quality human preimplantation embryos actively influence endometrial stromal cell migration'. *Journal of Assisted Reproduction and Genetics*, 35 pp659-667

- 16 Berkhout, R.P., Keijser, R., Repping, S., Lambalk, C.B., Afink, G.B., Mastenbroek, S. and Hamer, G. (2020) 'High-quality human preimplantation embryos stimulate endometrial stromal cell migration via secretion of microRNA hsa-miR-320a'. *Human Reproduction*, 35(8) pp1797-1807
- 17 Berneau, S.C., Ruane, P.T., Brison, D.R., Kimber, S.J., Westwood, M. and Aplin, J.D. (2019) 'Investigating the role of CD44 and hyaluronate in embryo-epithelial interaction using an in-vitro model'. *Molecular Human Reproduction*, 25 (5) pp 265-273
- 18 Beyer, T.A. Weiss, A., Khomchuk, Y., Huang, K., Ogunjimi, A.A, Varelas, X. *et al* (2013) ' Switch enhancers interpret TGF-beta and Hippo signalling to control cell fate in human embryonic stem cells'. *Cell Reports*, 5(6) pp1611-1624
- 19 Boivin, J., Bunting, L., Collins, J.A. and Nygren, K.G. (2007) 'International estimates of infertility prevalence and treatment -seeking: potential need and demand for infertility medical care'. *Human Reproduction*, 22 pp1506-1512
- 20 Bontekoe, S., Heineman, M.J., Johnson, N. and Blake, D. (2014) 'Adherence compounds in embryo transfer media for assisted reproductive technologies'. *Cochrane Database of Systemic Reviews*, 2:CD007421.
- 21 Boretto, M., Cox, B., Noben, M., Hendriks, N., Fassbender, A., Roose, H., Amant, F., Timmerman, D., Tomassetti, C., Vanhie, A., Meulman, C., Ferrante, M. and Vankelecom, H. (2017) ' Development of organoids from mouse and human endometrium showing endometrial epithelium physiology and long-term expandability'. *Development*, 144(10) pp1775-1786
- 22 Braga, D.P., Setti, A.S., Figueira, R., Iaconelli, A. and Borges, E. (2013) 'The combination of pronuclear and blastocyst morphology: a strong prognostic tool for implantation potential'. *Journal of Assisted Reproduction and Genetics*, 30(10) pp. 1327-1332.
- 23 Brison, D.R., Houghton, F.D., Falconer, D., Roberts, S.A., Hawkhead, J., Humpherson, P.G., Lieberman, B.A. and Leese, H.J. (2004) 'Identification of viable embryos in IVF by non-invasive measurement of amino acid turnover'. *Human Reproduction*, 19 pp2319-2324.
- 24 Brosens, J.J., Salker, M.S., Teklenburg, G., Nautiyal, J., Salter, S., Lucas, E.S., Steel, J.H., Christian, M., Chan, Y-W., Boomsma, C.M. (2014) 'Uterine selection of human embryos at implantation'. *Scientific Reports*, 4 p3894.
- 25 Brunner, A., Gentry, L., Cooper, J. and Purchio, A. (1988) 'Recombinant type 1 transforming growth factor beta precursor produced in Chinese hamster ovary cells is glycosylated and phosphorylated'. *Molecular and Cellular Biology*, 8 pp2229-2232
- 26 Cakmak, H. and Taylor, H.S (2011) 'Implantation failure: molecular mechanisms and clinical treatment'. *Human Reproduction Update*, 17 pp.242-253
- 27 Campbell, A., Fishel, S., Bowman, N., Duffy, S., Sedler, M. and Hickman, C.F.L. (2013a) 'Modelling a risk classification of aneuploidy in human embryos using non-invasive morphokinetics'. *Reproductive Biomedicine Online*, 26 pp. 477-485.
- 28 Campbell, A., Fishel, S., Bowman, N., Duffy, S., Sedler, M. and Thornton, S. (2013b) 'Retrospective analysis of outcomes after IVF using an aneuploidy risk model derived from time-lapse imaging without PGS'. *Reproductive Biomedicine Online*, 27 pp140-146
- 29 Campbell, S., Swann, H.R., Aplin, J.D., Seif, M.W., Kimber, S.J. and Elstein, M. (1995a) 'CD44 is expressed throughout pre-implantation human embryo development', *Human Reproduction*, 10 pp 425-430.
- 30 Campbell, S., Swann, H.R., Seif, M.W., Kimber, S.J. and Aplin, J.D. (1995b) 'Cell adhesion molecules on the oocyte and preimplantation human embryo'. *Human Reproduction*, 10 pp1571-1578.
- 31 Carroll, S.B. (1995) 'Homeotic genes and the evolution of arthropods and chordates'. *Nature*, 376 pp 479-485
- 32 Carsen, S.A. and Kallen, A.N., (2021) 'Diagnosis and management of infertility: a review'. *Journal of the American Medical Association*, 326(1) pp65-76.

- 33 Casciani, V., Monseur, B., Cimadomo, D., Alvero, R. and Rienzi, L. (2023) 'Oocyte and embryo cryopreservation in assisted reproductive technology: past achievements and current challenges'. *Fertility and Sterility*, 120(3), pp 506-520.
- 34 Catalano, R.D., Johnson, M.H., Campbell, E.A., Charnock-Jones, D.S., Smith, S.K. (2005) 'Inhibition of Stat3 activation in the endometrium prevents implantation: a nonsteroidal approach to contraception'. *Proceedings of the National Academy of Science (USA)*, 102 pp 8585-8590.
- 35 Ceelan, m., van Weissenbruch, M.M., Vermeiden, J.P., van Leeuwen, F.E. and Delemarre-van de Waal, H.A. (2008) 'Cardiometabolic differences in children born after *in vitro* fertilization: follow-up study'. *Journal of Clinical Endocrinology and Metabolism*, 93 pp 1682-1688.
- 36 Cha, j. and Dey, S.K. (2014) 'Cadence of procreation: orchestrating embryo-uterine interactions'. *Seminars in Cell and Developmental Biology*, 34 pp 56-64
- 37 Cha, J., Sun, X. and Dey, S.K. (2013) 'Mechanisms of implantation: strategies for successful pregnancy'. *Nature Medicine*, 18(12) pp. 1754-1767.
- 38 Chaen, T., Konno, T., Egashira, M., Bai, R., Nomura, N., Nomura, S., Hirota, Y., Sakurai, T. and Imakawa, K. (2012) 'Estrogen-dependent uterine secretion of osteopontin activates blastocyst adhesion competence'. *PLoS One*, 7 e48933
- 39 Chamayou, S., Patrizio, P., Storaci, G., Tomaselli, V., Alecci, C., Ragolia, C., Crescenzo, C. and Guglielmino, A. (2013) 'The use of morphokinetic parameters to select all embryos with full capacity to implant'. *Journal of Assisted Reproduction and Genetics*, 30 pp703-710
- 40 Chawla, M., Fakhri, M., Shunnar, A., Bayram, A., Hellani, A., Perumal, V., Divakaran, J. and Budak, E. (2015) 'Morphokinetic analysis of cleavage stage embryos and its relationship to aneuploidy in a retrospective time-lapse imaging study'. *Journal of Assisted Reproduction and Genetics*, 32 pp. 69-75
- 41 Chen, A.A., Tan, L., Suraj, V., Reijo Pera, R. and Shen, S. (2013) 'Biomarkers identified with time-lapse imaging: discovery, validation, and practical application'. *Fertility and Sterility*, 99 pp1035-1043
- 42 Chinn, K and Huang, T. (2015) 'Morphokinetics of blastocyst expansion in the mouse is similar to human embryos: an Embryoscope study'. *Fertility and Sterility*, 103 (2 Suppl).
- 43 Chun.S., Seo, J., Rim, Y., Joo, J., Lee, Y. and Koo, Y. (2016) 'Efficacy of hyaluronan-rich transfer medium on implantation and pregnancy rates in fresh and frozen-thawed blastocyst transfers in Korean women with previous implantation failure'. *Obstetrics and Gynecology Science*, 59 p201.
- 44 Ciray, H.N., Campbell, A., Agerholm, I.E, Aguilar, J., Chamayou, S., Esbert, M. and Sayed, S. (2014) 'Time-lapse user group. Proposed guidelines on the nomenclature and annotation of dynamic human embryo monitoring by a time-lapse user group'. *Human Reproduction*, 29 pp. 2650-2660.
- 45 Cousineau, T.M. and Domar, A.D (2007) 'Psychological impact of infertility'. *Best Practice and Research Clinical Obstetrics and Gynaecology*, 21(2) pp. 293-308
- 46 Cruz, M., Garrido, N., Herrero, J., Perez-Cano, I., Munoz, M. and Meseguer, M. (2012) 'Timing of cell division in human cleavage stage embryos is linked with blastocyst formation and quality'. *Reproductive Biomedicine Online*, 25 pp 371-381.
- 47 Cuman, C., Menkhorst, E.M., Rombauts, L.J., Holden, S., Webster, D., Bilandzic, M., Osianlis, T. and Dimitriadis, E. (2013) 'Preimplantation human blastocysts release factors that differentially alter human endometrial epithelial cell adhesion and gene expression relative to IVF success'. *Human Reproduction*, 28 pp.1161-1171.
- 48 Cuman, C., Van Sinderen, M., Gantier, M.P., Rainczuk, K., Sorby, K., Rombauts, L., Osianlis, T. and Dimitriadis, E. (2015) 'Human blastocyst secreted microRNA regulate endometrial epithelial cell adhesion'. *Ebiomedicine*, 2 pp.1528-1535.

- 49 Cutting, R., Morroll, D., Roberts, S.A., Pickering, S., Rutherford, A. And on behalf of the BFS and ACE (2008) 'Elective Single Embryo Transfer: Guidelines for Practice British Fertility Society and Association of Clinical Embryologists'. *Human Fertility*, 11:3 pp.131-146.
- 50 Daikoku, T., Cha, J., Sun, X., Tranguch, S., Xie, H., Fujita, T., Hirota, T., Lydon, J., DeMayo, F., Maxon, R. (2011) 'Conditional deletion of Msx homeobox genes in the uterus inhibits blastocyst implantation by altering uterine receptivity'. *Developmental Cell*, 21 pp1014-1025
- 51 Dal Canto, M., Coticchio, G., Renzini, M.M., DePonti, E., Novara, P.V., Brambillasca, F., Comi, R. and Fadini, R. (2012) 'Cleavage kinetics analysis of human embryos predicts development to blastocyst and implantation' *Reproductive Biomedicine Online*, 25 pp474-480
- 52 Das, S., Lim, H., Wang, J., Paria, B., Bazdresch, M. and Dey, S. (1997) 'Inappropriate expression of human transforming growth factor (TGF) alpha in the uterus of transgenic mouse causes downregulation of TGF-beta receptors and delays the blastocyst-attachment reaction'. *Journal of Molecular Endocrinology*, 18 pp 243-257
- 53 Das, S.K., Flanders, K.C., Andrews, G.K. and Dey, S.K. (1992) 'Expression of transforming growth factor-beta isoforms (beta- 2 and beta 3) in the mouse uterus: analysis of the periimplantation period and effects of ovarian steroids', *Endocrinology*, 130 pp3459-3466
- 54 Davidson, L.M. and Coward, K. (2016) 'Molecular mechanisms of membrane interaction at implantation'. *Birth Defects Research Part C: embryo today*, 108 pp. 19-32
- 55 Denker, H.W. (1993) 'Implantation: a cell biological paradox'. *Journal of Experimental Zoology*, 266 pp541-558
- 56 Derynk, R., Lindquist, P., Lee, A., Wen, D., Tamm, J., Graycar, J., Rhee, L., Mason, A., Miller, D. and Coffey, R. (1988) 'A new type of transforming growth factor-beta, TGF-beta 3'. *The EMBO Journal*, 7 pp3737-3743
- 57 Devroey, P., Polyzos, N.P. and Blockeel, C (2011) 'An OHSSFree Clinic by segmentation of IVF treatment'. *Human Reproduction* 26: pp2593–2597. doi:10.1093/humrep/der251
- 58 Dey, S.K., Lim, H., Das, S.K., Reese, J. (2004) 'Molecular cues to implantation'. *Endocrinology Review*, 25 pp. 341-373.
- 59 Dharmaraj, N., Chapela, P.J., Morgado, M., Hawkins, S.M., Lessey, B.A., Young, S.L. and Carson, D.D. (2014) 'Expression of the transmembrane mucins, MUC1, MUC4 and MUC16, in normal endometrium and in endometriosis'. *Human Reproduction*, 29 pp.1730-1738.
- 60 Diaz-Gimeno, P., Horcajadas, J.A., Martinez-Conejero, J.A., Esteban, F.J., Alama, P., Pellicer, A. And Simon, C. (2011) 'A genomic diagnostic tool for human endometrial receptivity based on the transcriptomic signature'. *Fertility and Sterility*, 95, pp50-60
- 61 Diaz-Gimeno, P., Ruiz-Alonso, M., Blesa, D. and Simon, C. (2014) 'Transcriptomics of the human endometrium'. *International Journal of Developmental Biology*, 58 pp.127-137.
- 62 Dokras, A., Sargent, I.L. and Barlow, D.H. (1993) 'Human blastocyst grading: an indicator of developmental potential?'. *Human Reproduction*, 8 pp. 2119-2127.
- 63 Donaghy, M. and Lessey, B.A. (2007) 'Uterine receptivity: alterations associated with benign gynecological disease'. *Seminars in Reproductive Medicine*, 25 pp. 461-475
- 64 Duncan, W.C., Shaw, J.L., Burgess, S., McDonald, S.E., Critchley, H.O. and Horne, A.W. (2011) 'Ectopic pregnancy as a model to identify endometrial genes and signalling pathways important in decidualization and regulated by local trophoblast'. *PLOS ONE* 6(8): e23595
- 65 Dunn, N.R., Vincent, S., Oxburgh, L., Robertson, E. and Bikkof, E. (2004) 'Combinatorial activities of Smad2 and Smad 3 regulate mesoderm formation and patterning in the mouse embryo'. *Development*, 131 pp1717-1728
- 66 Eastwick, J., Cooke, S., Venetis, C. and Chapman, M. (2019) 'The presence of filopodia in human blastocysts is associated with the probability of clinical pregnancy with fetal heart'. *Human Reproduction*, 34, pp. i2-i3.

- 67 Ebner, T., Tritscher, K., Mayer, R.B., Oppelt, P., Duba, H.C., Maurer, M., Schappacher-Tilp, G., Petek, E. and Shebl, O. (2016) 'Quantitative and qualitative trophoctoderm grading allows for prediction of live birth and gender'. *Journal of Assisted Reproduction and Genetics*, 33 pp.49-57.
- 68 Ebner, T., Sesli, O., Kresic, S., Enengl, S., Stiober, B., Reiter, E., Oppelt, P., Mayer, B. and Shebl, O. (2020) 'Time-lapse imaging of cytoplasmic strings at the blastocyst stage suggests their association with spontaneous blastocoel collapse'. *Reproductive Biomedicine Online*, 40(2) pp. 191-199.
- 69 Edgell, T.A., Rombauts, L.J.F. and Salamonsen, L.A. (2003) 'Assessing receptivity in the endometrium: the need for a rapid, non-invasive test'. *Reproductive Biomedicine Online*, 27 pp. 486-496.
- 70 Escrich, L., Grau, N., Meseguer, M., Pellicer, A. and Escriba, M.J. (2010) 'Morphologic indicators predict the stage of chromatin condensation of human germinal vesicle oocytes recovered from stimulated cycles'. *Fertility and Sterility*, 93 pp2557-2564
- 71 Evans, J., Hannan, N.J., Edgell, T.A., Vollenhoven, B.J., Lutjen, P.J., Osianlis, T., Salamonsen, L.A. and Rombauts, L. (2014) 'Fresh versus frozen embryo transfer: backing clinical decisions with scientific and clinical evidence'. *Human Reproduction Update*, 20 pp. 808-821.
- 72 Evans, J., Salamonsen, L.A., Winship, A., Menkhorst, E., Nie, G., Gargett, C.E. and Dimitriadis, E. (2016) 'Fertile ground: human endometrial programming and lessons in health and disease'. *Nature Reviews Endocrinology*, 12 pp. 654-667.
- 73 Farquhar, C., Marjoribanks, J., Brown, J., Fauser, B.C.J.M., Lethaby, A., Mourad, S., Rebar, R., Showell, M. and van der Poel, S. (2017) 'Management of ovarian stimulation for IVF: narrative review of evidence provided for World Health Organization guidance' *Reproductive Biomedicine Online*, 35(1) pp3-16
- 74 Fauser, B.C. and Devroey, P. (2003) 'Reproductive biology and IVF: ovarian stimulation and luteal phase consequences'. *Trends in Endocrinology and Metabolism*, 14 pp. 236-242.
- 75 Fishel, S., Campbell, A., Montgomery, S., Smith, R., Nice, L., Duffy, S., Jenner, L., Berrisford, K., Kellam, L., Smith, R., D'Cruz, I. and Beccles, A. (2017) 'Live births after embryo selection using morphokinetics versus conventional morphology: a retrospective analysis'. *Reproductive Biomedicine Online*, 35 pp. 407-416.
- 76 Fouladi-Nashta, A.A., Jones, C.J.P., Nijjar, N., Mohamet, L., Smith, A., Chambers, I. and Kimber, S.J. (2005) 'Characterisation of the uterine phenotype during the peri-implantation period for LIF-null, MF1 strain mice'. *Developmental Biology* 281 pp. 1-21.
- 77 Fragouli, E., Alfarawati, S., Spath, K., Jaroudi, S., Sarasa, J., Enciso, M. and Wells, D. (2013) 'The origin and impact of embryonic aneuploidy'. *Human Genetics*, 132 pp. 1001-1013.
- 78 Freour, T., Desolle, L., Lammer, J., Lattes, S. and Barriere, P. (2013) 'Comparison of embryo morphokinetics after *in vitro* fertilisation-intracytoplasmic sperm injection in smoking and non-smoking women'. *Fertility and Sterility*, 99 pp1944-1950
- 79 Friedenthal, J., Maxwell, S.M., Munne, S., Kramer, Y., McCulloh, D.H, McCaffrey, C. (2018) 'Next generation sequencing for preimplantation genetic screening improves pregnancy outcomes compared with array comparative genomic hybridisation in single thawed euploid embryo transfer cycles'. *Fertility and Sterility*, 109 pp. 627-632.
- 80 Fukuda, M.N. and Sugihara, K. (2008) 'An integrated view of L-selectin and trophinin function in human embryo implantation'. *Journal of Obstetrics and Gynaecology Research*, 34 pp.129-136.
- 81 Fukuda, M.N., Sugihara, K. and Nakayama, J. (2008) 'Trophinin: what embryo implantation teaches us about human cancer'. *Cancer Biology and Therapy*, 7 p1165.
- 82 Gad, A., Schellander, K., Hoelker, M. and Tesfaye, D. (2012) 'Transcriptome profile of early mammalian embryos in response to culture environment'. , 134 pp76-83



- 83 Garcia-Sainz, J., Vilchis-Landeros, M., Juarez, P., Lopez-Casillas, F., Hernandez-Pando, R. and Massague, J. (2003) 'Receptors and functions of TGF-beta, a crucial cytokine in wound healing'. *Gaceta Medica de Mexico*, 139 p126
- 84 Gardner, D.K. and Schoolcraft, W.B. (1999) 'In vitro culture of human blastocyst' R Jansen, D Mortimer (Eds.), Towards reproductive certainty: infertility and genetics beyond 1999, Parthenon Press, Carnforth pp. 378-388
- 85 Gardner, D.K., Meseguer, M., Rubio, C. and Treff, N.R. (2015) 'Diagnosis of human preimplantation embryo viability'. *Human Reproduction Update*, 21 pp.727-747.
- 86 Genbacev, O.D., Prakobphol, A., Foulk, R.A., Krtolica, A.R., Ilic, D. (2003) 'Trophoblast L-Selectin mediated adhesion at the maternal-fetal interface'. *Science*, 299 pp. 405-408.
- 87 Gerris, J., De Neubourg, D., Mangelschots, K., Van Royen, E., Van de Meerssche, M. and Valkenburg, M. (1999) 'Prevention of twin pregnancy after in-vitro fertilization or intracytoplasmic sperm injection based on strict embryo criteria: a prospective randomised clinical trial'. *Human Reproduction*, 14 pp. 2581-2587.
- 88 Gerris, J., de Neuborg, D., de Sutter, P., van Royen, E. and Mangelschots, K. (2003) 'Cryopreservation as a tool to reduce multiple birth'. *Reproductive Biomedicine Online*, 7 pp286-294
- 89 Gianaroli, L., Magli, M.C., Ferraretti, A.P., Lappi, M., Borghi, E. and Ermini, B. (2007) 'Oocyte euploidy, pronuclear zygote morphology and embryo chromosomal complement'. *Human Reproduction*, 22 (1) pp. 241-249.
- 90 Gipson, I.K., Blalock, T., Tisdale, A., Spurr-Michaud, S., Allcorn, S., Stavreus-Evers, A. and Gemzell, K. (2008) 'MUC16 is lost from the uterodome (pinopode) surface of the receptive human endometrium: *in vitro* evidence that MUC16 is a barrier to trophoblast adherence'. *Biology of Reproduction*, 78 pp.134-142.
- 91 Goumans, M.J. and Mummery, C. (2000) 'Functional analysis of the TGFbeta receptor/Smad pathway through gene ablation in mice'. *The International Journal of Developmental Biology*, 44 pp 253-265
- 92 Graham, C.H., Lysiak, J.J., McCrae, K.R. and Lala, P.K. (1992) 'Localization of transforming growth factor-beta at the human fetal-maternal interface: role in trophoblast growth and differentiation'. *Biology of Reproduction*, 46 pp 561-572
- 93 Guidice, L.C. and Irwin, J.C. (1999) 'Roles of the insulinlike growth factor family in nonpregnant human endometrium and at the decidual:trophoblast interface'. *Seminars in Reproductive Endocrinology*, 17 pp13-21
- 94 Guillot, C. and Lecuit, T. (2013) 'Mechanisms of epithelial tissue homeostasis and morphogenesis'. *Science*, 340 pp. 1185-1189
- 95 Gupta, A., Dekaney, C.M., Bazer, F.W., Madrigal, M.M. and Jaeger, L.A. (1998) 'Beta transforming growth factors (TGF-beta) at the porcine conceptus-maternal interface. Part II: Uterine TGF-beta bioactivity and expression of immunoreactive TGF-betas (TGF-beta1, TGF-beta2 and TGF-beta3) and their receptors (type I and type II)'. *Biology of Reproduction*, 59 pp911-917
- 96 Hambartsoumian, E. (1998) 'Endometrial leukemia inhibitory factor (LIF) as a possible cause of unexplained infertility and multiple failures of implantation'. *American Journal of Reproductive Immunology*, 39 pp.137-143.
- 97 Harbottle, S., Hughes, C., Cutting, R., Roberts, S., Brison, D. and On Behalf Of The Association Of Clinical Embryologists (ACE) & The British Fertility Society (BFS) (2015) 'Elective Single Embryo Transfer: an update to UK Best Practice Guidelines'. *Human Fertility*, 18:3 pp. 165-183.
- 98 Hardarson, T., Van Landuyt, L. and Jones, G. (2012) 'The blastocyst'. *Human Reproduction*, 27 pp. i72-i91.

- 99 Hart, R. and Norman, R.J. (2013) 'The longer term health outcomes for children born as a result of IVF treatment: Part 1 – general health outcomes'. *Human Reproduction Update*, 19 pp 232-243.
- 100 Heldin, C-H., Landstrom, M. and Moustakas, A. (2009) 'Mechanism of TGF-beta signalling to growth arrest, apoptosis and epithelial-mesenchymal transition'. *Current Opinions in Cell Biology*, 21 pp 166-176
- 101 Hill, M.J., Richter, K.S., Heitmann, R.J., Graham, J.R., Tucker, M.J., DeCherney, A.H., Browne, P.E. and Levens, E.D. (2013) 'Trophectoderm grade predicts outcomes of single-blastocyst transfers'. *Fertility and Sterility*, 99 pp. 1283-1289.
- 102 Hlinka, D., Kalatova, B., Uhrinova, I., Dolinska, S., Rutarova, J., Rezacova, J., Lazarovska, S. and Dudas, M. (2012) 'Time-lapse cleavage rating predicts human embryo viability'. *Physiological Research*, 61 pp513-525
- 103 Horne, A.W., Duncan, W.C., King, A.E., Burgess, S., Lourenco, P.C., Cornes, P., Ghazal, P., Williams, A.R., Udby, L. and Critchley, H.O. (2009) 'Endometrial cysteine-rich secretory protein 3 is inhibited by human chorionic gonadotrophin and is increased in the decidua of tubal ectopic pregnancy'. *Molecular Human Reproduction*, 15 pp. 287-294.
- 104 Hu, W., Feng, A., Teresky, A.K. and Levine, A.J. (2007) 'p53 regulates maternal reproduction through LIF'. *Nature*, 450 pp.712-724.
- 105 Hu, Y-J., Wand, Y-D., Tan, F-Q. and Yang, W-X. (2013) 'Regulation of paracellular permeability: factors and mechanisms'. *Molecular Biology Reports*, 40 pp. 6123-6142.
- 106 Huang, T.T.F., Chinn, K., Kosasa, T., Ahn, H.J. and Kessel, B. (2016) 'Morphokinetics of human blastocyst expansion *in vitro*'. *Reproductive Biomedicine Online*, 33 pp. 659-667.
- 107 Huang, T.T.F., Huang, D.H., Ahn, H.J., Arnett, C. and Huang, C.T.F (2019) 'Early blastocyst expansion in euploid and aneuploidy human embryos: evidence for a non-invasive and quantitative marker for embryo selection'. *Reproductive Biomedicine Online*, 39(1), pp.27-39.
- 108 Huh, H.D., Kim, D.H., Jeong, H-S. and Park, H.W. (2019) 'Regulation of TEAD transcription factors in cancer'. *Cells*, 8(6) p600
- 109 HFEA (Human Fertilisation and Embryology Authority) (2021) 'Fertility treatment 2019: trends and figures'. <https://www.hfea.gov.uk/about-us/publications/research-and-data/fertility-treatment-2019-trends-and-figures/> accessed 23/3/2023
- 110 Hunter, H., Getreu, N., Wood, M., Fuller, B. (2020). 'Cryopreservation of Human Embryos: Basic Principles and Current Considerations'. In: Allahbadia, G.N., Ata, B., Lindheim, S.R., Woodward, B.J., Bhagavath, B. (eds) Textbook of Assisted Reproduction. Springer, Singapore. [https://doi.org/10.1007/978-981-15-2377-9\\_57](https://doi.org/10.1007/978-981-15-2377-9_57)
- 111 Illera, M.J., Cullinan, E., Gui, Y., Yuan, L., Beyler, S.A. and Lessey, B.A. (2000) 'Blockade of the alpha(v)beta(3) integrin adversely affects implantation in the mouse'. *Biology of Reproduction*, 62 pp.1285-1290.
- 112 Illera, M.J., Lorenzo, P.L., Gui, Y., Beyler, S.A., Apparao, K.B and Lessey, B.A. (2003) 'A role for alphavbeta3 integrin during implantation in the rabbit model'. *Biology of Reproduction*, 68 pp.766-771.
- 113 Ilyin, I.E., Nikitin, O.D., Gontar, J.V., Buderatska, N.O. and Verlinsky, O.Y. (2019) 'Application of the pronuclear scoring system for predicting the morphology and ploidy of early human embryos'. *Cytology and Genetics*, 53(3) pp. 227-232.
- 114 Irwin, J.C., Suen, L.F., Faessen, G.H., Popovici, R.M. and Guidice, L.C. (2001) 'Insulin-like growth factor (IGF)-II inhibition of endometrial stromal cell tissue inhibitor of metalloproteinase-3 and IGF-binding protein-I suggests paracrine interactions at the decidua:trophoblast interface during human implantation'. *The Journal of Clinical Endocrinology and Metabolism*, 86 pp2060-2064

- 115 Iwata, K., Yumoto, K., Mizoguchi, C., Sargent, H., Kai, Y., Ueda, M., Tsuchie, Y., Imajo, A., Iba, Y. and Mio, Y. (2012) 'Dynamic analyses of embryonic morphology during human blastocyst stage using time-lapse cinematography'. *Human Reproduction*, 27 (suppl 2) Abstract P-194.
- 116 James, D., Levine, A.J., Besser, D. and Hemmati-Brivanlou, A. (2005) 'TGF-B/activating/nodal signalling is necessary for the maintenance of pluripotency in human embryonic stem cells'. *Development*, 132 pp1273-1282
- 117 Jin, L., Ai, J., Zheng, Y., Chen, B., Wang, L and Dong, X. (2021) 'The Impact of Down-Regulation on Obstetrics and Perinatal Outcomes in Singleton Pregnancies After In Vitro Fertilization'. *Front Endocrinol* Mar 10;12:622081.
- 118 Johnson, G.A., Burghardt, R.C. and Baser, F.W. (2014) 'Osteopontin: a leading candidate adhesion molecule for implantation in pigs and sheep'. *Journal of Animal Science and Biotechnology*, 5 p56
- 119 Johnson, L.N.C., Sasson, I.E., Sammel, M.D. and Dokras, A. (2013) 'Does intracytoplasmic sperm injection improve the fertilization rate and decrease the total fertilization failure rate in couples with well-defined unexplained infertility? A systematic review and meta-analysis'. *Fertility and Sterility*, 100 (3) pp704-711
- 120 Kaneko, Y., Day, M.L. and Murphy, C.R. (2011) 'Integrin beta3 in rat blastocysts and epithelial cells is essential for implantation *in vitro*: studies with ishikawa cells and small interfering RNA transfection'. *Human Reproduction*, 26 pp. 1665-1674.
- 121 Kaneko, Y., Murphy, C.R. and Day, M.L. (2013) 'Extracellular matrix proteins secreted from both the endometrium and the embryo are required for attachment: a study using a co-culture model of rat blastocysts and ishikawa cells'. *Journal of Morphology*, 274 pp.63-72.
- 122 Kang, H.J., Melnick, A.P., Stewart, J.D., Xu, K. and Rosenwaks, Z. (2016) 'Pre-implantation genetic screening: who benefits?'. *Fertility and Sterility*, 106 pp. 597-602.
- 123 Kaser, D.J. and Racowsky, C. (2014) 'Clinical outcomes following selection of human preimplantation embryos with time-lapse monitoring: a systematic review'. *Human Reproduction Update*, 20 pp. 617-631.
- 124 Kirkegaard, K., Agerholm, I.E. and Ingerslev, H.J. (2012) 'Time-lapse monitoring as a tool for clinical embryo assessment'. *Human Reproduction*, 27 pp. 1277-1285.
- 125 Kirkegaard, K., Kesmodel, U.S., Hindkjaer, J.J. and Ingerslev, H.J. (2013) 'Time-lapse parameters as predictors of blastocyst development and pregnancy outcome in embryos from good prognosis patients: a prospective cohort study'. *Human Reproduction*, 28 pp. 2643-2651.
- 126 Kirkegaard, K., Campbell, A., Agerholm, I., Bentin-Ley, U., Gabrielsen, A., Kirk, J., Sayed, S. and Ingerslev, H.J. (2014) 'Limitations of a time-lapse blastocyst prediction model: a large multicentre outcome analysis'. *Reproductive Medicine Online*, 29 pp. 156-158.
- 127 Kong, X., Yang, S., Gong, F., Lu, C., Zhang, S., Lu, G. and Lin, G. (2016) 'The relationship between cell number, division behaviour and developmental potential of cleavage stage human embryos: a time-lapse study'. *PLoS ONE*, 11(4).
- 128 Kramer, Y.G., Kofinas, J.D., Melzer, K., Noyes, N., McCaffrey, C., Buldo-Liccardi, J., McCulloh, D.H. and Grifo, J.A. (2014) 'Assessing morphokinetic parameters via time-lapse microscopy (TLM) to predict euploidy: are aneuploidy risk classification models universal?'. *Journal of Assisted Reproduction and Genetics*, 31 pp.1231-1242.
- 129 Krumlauf, R. (2004) 'Hox genes in vertebrate development'. *Cell* 78 pp191-201
- 130 Kumar, V., Maurya, V.K., Joshi, A., Meeran, S.M. and Jha, R.K. (2015) 'Integrin beta 8(ITGB8) regulates embryo implantation potentially via controlling the activity of TGF-B1 in mice'. *Biology of Reproduction*, 92 p109.
- 131 Laird, S.M. *et al* (1997) 'The production of leukaemia inhibitory factor by human endometrium: presence in uterine flushings and production by cells in culture'. *Human Reproduction*, 12 pp. 569-574.

- 132 Latifi, Z., Nejabati, H.R., Abroon, S., Mihanfar, A., Farzadi, L., Hakimi, P., Hajipour, H., Nouri, M. and Fattahi, A. (2019) 'Dual role of TGF-beta in early pregnancy: clues from tumor progression'. *Biology of Reproduction*, 100(6) pp1417-1430
- 133 Leach, R.E. *et al* (2002) 'Pre-eclampsia and expression of heparin-binding EGF-like growth factor'. *The Lancet*, 360 pp.1215-1219.
- 134 Lechniak, D., Pers-Kamczyc, E. and Pawlak, P. (2008) 'Timing of the first zygotic cleavage as a marker of developmental potential of mammalian embryos'. *Reproductive Biology*, 8 pp23-42
- 135 Leese, H.J. (2002) 'Quiet please, do not disturb: a hypothesis of embryo development and viability'. *Bioessays*, 24 pp.845-849.
- 136 Lessey, B.A. (2011) 'Assessment of endometrial receptivity'. *Fertility and Sterility*, 96 pp. 522-529
- 137 Lessey, B.A., Castelbaum, A.J., Sawin, S.W. and Sun, J. (1995) 'Integrins as markers of uterine receptivity in women with primary unexplained infertility'. *Fertility and Sterility*, 63 pp535-542.
- 138 Lever, J., Krzywinski, M. and Altman, N. (2017) 'Principal component analysis'. *Nature Methods*, 14 pp. 641-642
- 139 Li, Y., Sun, X. and Dey, S.K. (2015) 'Entosis allows timely elimination of the luminal epithelial barrier for embryo implantation'. *Cell Reports*, 11 pp.358-365.
- 140 Licciardi, F., McCaffrey, C., Oh, C., Schmidt-Sarosi, C. and McCulloh, D.H. (2015) 'Birth weight is associated with inner cell mass grade of blastocysts'. *Fertility and Sterility*, 103 pp382-387.
- 141 Licht, P., Fluhr, H., Neuwinger, J., Wallwiener, D. and Wildt, L. (2007) 'Is human chorionic gonadotrophin directly involved in the regulation of human implantation?' *Molecular and Cellular Endocrinology*, 269 pp.85-92.
- 142 Lim, H.J. and Dey, S.K. (2009) 'HB-EGF: a unique mediator of embryo-uterine interactions'. *Experimental Cell Research*, 315 pp. 619-626.
- 143 Lopata, A., Bentin-Ley, U. and Enders, A. (2002) ' "Pinopodes" and implantation'. Reviews in *Endocrine and Metabolic Disorders*, 3 pp. 77-86.
- 144 Lu, D.P., Tian, L., O'Neill, C. and King, N.J. (2002) 'Regulation of cellular adhesion molecule expression in murine oocytes, peri-implantation and post-implantation embryos' *Cell Research*, 12 pp.373-383.
- 145 Lui, Y., Chapple, V., Roberts, P. and Matson, P. (2014). 'Prevalence, consequence, and significance of reverse cleavage by human embryos viewed with the use of the embryoscope time-lapse video system'. *Fertility and Sterility*, 102 (5) pp.1295-1300.
- 146 Lundin, K., Bergh, C. and Hardarson, T. (2001) 'Early embryo cleavage is a strong indicator of embryo quality in human IVF'. *Human Reproduction*, 16 pp 2652-2657.
- 147 Lynch, V.J., Tanzer, A., Wang, Y., Leung, F.C., Gellersen, B. (2008) 'Adaptive changes in the transcription factor HoxA-11 are essential for the evolution of pregnancy in mammals'. *Proceedings of the National Academy of Sciences of the United States of America*, 195 pp. 14928-14933.
- 148 Ma, W.G., Song, H., Das, S.k., Paria, B.C. and Dey, S.K. (2003) 'Estrogen is a critical determinant that specifies the duration of the window of uterine receptivity for implantation'. *Proceedings of the National Academy of Sciences of the United States of America* 100 pp. 2963-2968.
- 149 Macklon, N.S. and Brosens, J.J. (2014) 'The human endometrium as a sensor of embryo quality'. *Biology of Reproduction*, 91(4) pp. 1-8.
- 150 Macklon, N.S., Geraedts, J.P.M., Fauser, B.C.J.M (2002) 'Conception to ongoing pregnancy: the 'black box' of early pregnancy loss'. *Human Reproduction Update*, 8(4) pp. 333-343.
- 151 Magli, M.C., Gianaroli, L., Munne, S. and Ferraretti, A.P. (1998) 'Incidence of chromosomal abnormalities from a morphologically normal cohort of embryos in poor-prognosis patients'. *Journal of Assisted Reproduction and Genetics*, 15(5) pp. 297-301

- 152 Mahajan, N., Kaur, S. and Alonso, M.R. (2018) 'Window of Implantation is Significantly Displaced in Patients with Adenomyosis with Previous Implantation Failure as Determined by Endometrial Receptivity Assay'. *Journal of Human Reproductive Sciences*, 11(4):353-358.
- 153 Martin, K.L., Barlow, D.H. and Sargent, I.L. (1998) 'Heparin-binding epidermal growth factor significantly improves human blastocyst development and hatching in serum-free medium'. *Human Reproduction*, 13 pp. 1645-1652.
- 154 Massague, J. (2012) 'TGF-beta signalling in context'. *Nature Reviews Molecular Cell Biology*, 13(20) pp161-630
- 155 Maurya, V.K., Jha, R.K., Kumar, V., Joshi, A., Chadchan, S., Mohan, J.J. and Laloraya, M. (2013) 'Transforming growth factor-beta 1 liberation from its latent complex during embryo implantation and its regulation by estradiol in mouse'. *Biology of Reproduction*, 89 (84) p81
- 156 McGowen, M.R., Erez, O., Romero, R. and Wildman, D.E. (2014) 'The evolution of embryo implantation'. *International Journal of Developmental Biology*, 58(2-4) pp155-61
- 157 Mertzaniidou, A., Wilton, L., Cheng, J., Spits, C., Vanneste, E., Moreau, Y., Vermeesch, J.R. and Sermon, K. (2013) 'Microarray analysis reveals abnormal chromosomal complements in over 70% of 14 normally developing human embryos'. *Human Reproduction*, 28 pp. 256-264.
- 158 Metsalu, T. and Vilo, J. (2015) 'ClustVis: a web tool for visualizing clustering of multivariate data using Principal Component Analysis and heatmap'. *Nucleic Acids Research*. 2015 Jul 1;43(W1):W566-70.
- 159 Meseguer, M., Aplin, J.D., Caballero-Campo, P., O'Connor, J.E., Martin, J.C., Remohi, J., Pellicer, A. and Simon, C. (2000) 'Human endometrial mucin MUC1 is up-regulated by progesterone and down-regulated *in vitro* by the human blastocyst'. *Biology of Reproduction*, 64 pp590-601
- 160 Meseguer, M., Herrero, J., Tejera, A., Hilligsoe, K.M., Ramsing, N.B. and Remohi, J. (2011) 'The use of morphokinetics as a predictor of embryo implantation'. *Human Reproduction*, 26(10) pp2658-2671
- 161 Meseguer, M., Rubio, I., Cruz, M., Basile, N., Marcos, J. and Requena, A. (2012) 'Embryo incubation and selection in a time-lapse monitoring system improves pregnancy outcome compared with a standard incubator: a retrospective cohort study'. *Fertility and Sterility*, 98(6) pp.1481-1489.
- 162 Miller, J., Fraser, S.E. and McClay, D. (1995) 'Dynamics of thin filopodia during sea urchin gastrulation'. *Development*, 121 pp. 2501-2511
- 163 Miles, H.L., Hofman, P.L., Peek, J., Harris, M., Wilson, D., Robinson, E.M., Gluckman, P.D. and Cutfield, W.S. (2007) 'In vitro fertilization improves childhood growth and metabolism'. *Journal of Clinical Endocrinology and Metabolism*, 92 pp. 3441-3445.
- 164 Mio, Y. (2006) 'Morphological analysis of human embryonic development using time-lapse cinematography'. *Journal of Mammalian Ova Research*, 23 pp. 27-36.
- 165 Mio, Y. and Maeda, K. (2008) 'Time-lapse cinematography of dynamic changes occurring during *in vitro* development of human embryos'. *American Journal of Obstetrics and Gynecology*, 199 p 660.
- 166 Mohamed, O.A., Jonnaert, M., Labelle-Dumas, C., Kuroda, K., Clarke, H.J. and Dufort, D. (2005) 'Wnt/beta-catenin signalling is required for implantation'. *Proceedings of the National Academy of Sciences of the United States of America*, 102 pp. 8579-8584.
- 167 Mumusoglu, S., Yarali, I., Bozdog, G., Ozdemir, P., Polat, M., Sokmensuer, L.K. and Yarali, H. (2017) 'Timelapse morphokinetic assessment has low to moderate ability to predict euploidy when patient-and ovarian stimulation-related factors are taken into account with the use of clustered data analysis'. *Fertility and Sterility*, 107 pp. 413-421.
- 168 Munne, S., Najmabadi, S., Nakajima, S., Sauer, M.V., Escudero, T. and Buster, J.E. (2018) 'Pre-implantation genetic screening (PGS) of *in vivo* conceived and developed blastocysts recovered by lavage: preliminary experience'. *Human Reproduction*, 33, i119.

- 169 Murphy, C.R. (2004) 'Uterine receptivity and the plasma membrane transformation'. *Cell Research*, 14 pp. 259-267.
- 170 Nakamura, H., Kimura, T., Koyama, S., Ogita, K., Tsutsui, T. (2006) 'Mouse model of human infertility: transient and local inhibition of endometrial STAT-3 activation results in implantation failure'. *FEBS letters*, 580 pp. 2717-2722.
- 171 Navot, D., Bergh, P.A., Williams, M., Garrisi, G.J., Guzman, I., Sandler, B., Fox, J., Schreiner-Engel, P., Hoffman, G.E. and Grunfeld, L. (1991) 'An insight into early reproductive processes through the *in vivo* model of ovum donation'. *Journal of Clinical Endocrinology and Metabolism*, 72 pp. 408-414.
- 172 Nicoloro-SantaBarbara, J.M., Lobel, M., Bocca, S., Stelling, J.R. and Pastore, L.M. (2017) 'Psychological and emotional concomitants of infertility diagnosis in women with diminished ovarian reserve or anatomical cause of infertility'. *Fertility and Sterility*, 108(1) pp.161-167.
- 173 Niimura, s. (2003). 'Time-lapse videomicrographic analysis of contractions in mouse blastocysts'. *Journal of Reproduction and Development*, 49 pp. 413-423.
- 174 Nikolakopoulou, K. and Turco, M. Y. (2021) 'Investigation of infertility using endometrial organoids'. *Reproduction*, 161(5), R113-R127.
- 175 Nishioka, N., Inoue, K., Adachi, K., Kiyonari, H., Ota, m., Ralston, A. (2009) ' The Hippo signalling pathway components Lats and Yap pattern Tead4 activity to distinguish mouse trophectoderm from inner cell mass'. *Developmental Cell*, 16(3) pp398-410
- 176 Ohgushi, M., Minaguchi, M. and Sasai, Y. (2015) ' Rho-signalling-directed YAP/TAZ activity underlies the long-term survival and expansion of human embryonic stem cells'. *Cell Stem Cell*, 17(4) pp448-461
- 177 Otsuki, J., Iwasaki, T., Katada, Y., Sato, H., Furuhashi, K., Tsuji, Y., Matsumoto, Y. and Shiotani, M. (2016) 'Grade and looseness of the inner cell mass may lead to the development of monozygotic diamniotic twins'. *Fertility and Sterility*, 106 pp. 640-644.
- 178 Otsuki, J., Iwasaki, T., Tsuji, Y., Katada, Y., Sato, H., Tsutsumi, Y. (2017) 'Potential of zygotes to produce live births can be identified by the size of the male and female pronuclei just before their membranes break down'. *Reproductive Medicine and Biology*, 16 pp. 200-205.
- 179 Otsuki, J., Iwasaki, T., Enatsu, N., Katada, Y., Furuhashi, K. and Shiotani, M. (2019) 'Non-invasive embryo selection: kinetic analysis of female and male pronuclear development to predict embryo quality and potential to produce live birth'. *Fertility and Sterility*, 112(5) pp. 874-881.
- 180 Pandian, Z., Templeton, A., Serour, G. and Bhattacharya, S. (2005) 'Number of embryos for transfer after IVF and ICSI: a Cochrane review'. *Human Reproduction*, 20 pp2681-2687
- 181 Petersen, B.M., Boel, M., Montag, M. and Gardner, D.K. (2016) 'Development of a generally applicable morphokinetic algorithm capable of predicting the implantation potential of embryos transferred on day 3'. *Human Reproduction*, 31(10) pp. 2231-2244.
- 182 Piccinni, M.P. *et al* (1998) 'Defective production of leukemia inhibitory factor and type 2 T-helper cytokines by decidual T cells in unexplained recurrent abortions'. *Nature Medicine*, 4 pp. 1020-1024
- 183 Pribenszky, C., Matyas, S., Kovacs, P., Losonczi, E., Zadori, J. and Vatja, G. (2010) 'Pregnancy achieved by transfer of a single blastocyst selected by time-lapse monitoring'. *Reproductive Biomedicine Online*, 21 pp 533-536.
- 184 Psychoyos, A. (1986) 'Uterine receptivity for nidation'. *Annals of the New York Academy of Sciences*, 476 pp. 36-42.
- 185 Purchio, A., Cooper, J., Brunner, A., Lioubin, M., Gentry, L., Kovacina, K.S., Roth, R.A. and Marquardt, H. (1988) 'Identification of mannose 6-phosphate in two asparagine-linked sugar chains of recombinant transforming growth factor-beta 1 precursor'. *Journal of Biological Chemistry*, 263 pp14211-14215

- 186 Qiagen (2023) 'Qiagen ingenuity pathway analysis'. Available at: <https://digitalinsights.qiagen.com/products-overview/discovery-insights-portfolio/analysis-and-visualization/qiagen-ipa/> Accessed 11 March 2023
- 187 Quinn, C.E. and Casper, R.F. (2009) 'Pinopodes: a questionable role in endometrial receptivity'. *Human Reproduction Update*, 15 pp.229-236.
- 188 Racowsky, C., Vernon, M., Mayer, J., Ball, G.D., Behr, B., Pomeroy, K.O., Winger, D., Gibbons, W., Conaghan, J. and Stern, J.E. (2010) 'Standardisation of grading embryo morphology'. *Fertility and Sterility*, 94 pp.1152-1153.
- 189 Rafael, Z.B. (2021) 'Endometrial Receptivity Analysis (ERA) Test: an unproven technology'. *Human Reproduction Open*, Volume 2021, issue 2 hoab010
- 190 Rienzi, L., Ubaldi, F., Iacobelli, M., Romano, S., Minasi, M.G., Ferrero, S., Sapienza, F., Baroni, E. and Greco, E. (2005) 'Significance of morphological attributes of the early embryo'. *Reproductive Biomedicine Online*, 10 pp. 669-681.
- 191 Roelen, B.A., Lin, H., Knezevic, V., Freund, E. and Mummery, C. (1994) 'Expression of TGF-beta s and their receptors during implantation and organogenesis of the mouse embryo'. *Developmental Biology*, 166 pp716-728
- 192 Rosenwaks, Z., Handyside, A.H., Fiorentino, F., Gleicher, N., Paulson, R.J., Schattman, G.L. (2018) 'The pros and cons of preimplantation genetic testing for aneuploidy: clinical and laboratory perspectives'. *Fertility and Sterility*, 110 pp.353-361.
- 193 Ruane, P.T., Berneau, S.C., Koeck, R., Watts, J., Kimber, S.J., Brison, D.R., Westwood, M. and Aplin, J.D. (2017) 'Apposition to endometrial epithelial cells activates mouse blastocysts for implantation'. *Molecular Human Reproduction*, 23(9) pp. 617-627.
- 194 Ruane, P.T., Buck, C.J., Babbington, P.A., Aboussahoud, W., Berneau, S.C., Westwood, M., Kimber, S.J., Aplin, J.D. and Brison, D.R. (2020) 'The effects of hyaluronate-containing medium on human embryo attachment to endometrial epithelial cells *in vitro*'. *Human Reproduction Open*, 2020(2) hoz033
- 195 Ruane, P.T., Garner, T., Parsons, L., Babbington, P.A., Wangsaputra, I., Kimber, S.J., Stevens, A., Westwood, M., Brison, D.R. and Aplin, J.D. (2022) 'Trophectoderm differentiation to invasive syncytiotrophoblast is promoted by endometrial epithelial cells during human embryo implantation'. *Human Reproduction* pp777-792
- 196 Rubin, S.C., Abdulkadir, M., Lewis, J., Harutyunyan, A., Hirani, R. and Grimes, C.L.(2023) 'Review of Endometrial Receptivity Array: A Personalized Approach to Embryo Transfer and Its Clinical Applications'. *Journal of Personalized Medicine*, 13(5):749.
- 197 Rubio, I., Kuhlmann, R., Agerholm, I., Kirk, J., Herrero, j., Escriba, M.J., Bellver, J. and Meseguer, M. (2012) 'Limited implantation success of direct-cleaved human zygotes: a time-lapse study'. *Fertility and Sterility*, 98 pp. 1458-1463.
- 198 Ruiz-Alonso, M., Blesa, D. and Simon, C. (2012) 'The genomics of the human endometrium'. *Biochimica et Biophysica Acta*, 1822 pp.1931-1942.
- 199 Ruiz-Alonso, M., Blesa, D., Diaz-Gimeno, P., Gomez, E., Fernandez-Sanchez, M., Carranza, F., Carrera, J., Vilella, F., Pellicer, A and Simon, C. (2013) 'The endometrial receptivity array for diagnosis and personalised embryo transfer as a treatment for patients with repeated implantation failure'. *Fertility and Sterility*, 100(3) pp.818-824.
- 200 Sakkas, D., Percival, G., D'Arcy, Y., Sharif, K. and Afnan, M. (2001) 'Assessment of early cleaving *in vitro* fertilized human embryos at the 2-cell stage before transfer improves embryo selection'. *Fertility and Sterility*, 76 pp. 1150-1156.
- 201 Sakota, I., Benson, G. and Maas, R. (1995) 'Sexually dimorphic sterility phenotypes in Hoxa10-deficient mice'. *Nature*, 374 pp460-463

- 202 Salas-Vidal, E. and Lomeli, H. (2004) 'Imaging filopodia dynamics in the mouse blastocyst'. *Developmental Biology*, 265 pp. 75-89.
- 203 Salamonsen, L.A., Evans, J., Nguyen, H.P. and Edgell, T.A. (2016) 'The microenvironment of human implantation: determinant of reproductive success'. *American Journal of Reproductive Immunology*, 75 pp.218-225.
- 204 Salumets, A., Hyden, Granskog, C., Makinen, S., Suikkari, A.M., Tiitinen, A. and Tuuri, T. (2003) 'Early cleavage predicts the viability of human embryos in elective single embryo transfer procedures'. *Human Reproduction*, 18 pp. 821-825.
- 205 Sciorio, R. and El Hajj, N. (2022) 'Epigenetic risks of medically assisted reproduction'. *Journal of Clinical Medicine*, 11(8) p2151
- 206 Scott, L.A. (2000) 'Oocyte and embryo polarity'. *Seminars in Reproductive Medicine*, 18 pp. 171-183
- 207 Scott, L. (2003a) 'Pronuclear scoring as a predictor of embryo development'. *Reproductive Biomedicine Online*, 6 pp.201-214.
- 208 Scott, L. (2003b) 'The biological basis of non-invasive strategies for selection of human oocytes and embryos'. *Human Reproduction Update*, 9(3) pp. 237-249.
- 209 Scott, L. and Smith, S. (1998) 'The successful use of pronuclear embryo transfers the day after oocyte retrieval'. *Human Reproduction*, 13(1) pp. 1003-1013.
- 210 Selick, C.E., Horowitz, G.M., Gratch, M., Scott Jr, R.T., Navot, D. and Hofmann, G.E. (1994) 'Immunohistochemical localization of transforming growth factor beta in human implantation sites'. *The Journal of Clinical Endocrinology and Metabolism*, 78 pp592-596
- 211 Shapiro, B.S., Harris, D.C. and Richter, K.S. (2000) 'Predictive value of 72-hour blastomere cell number on blastocyst development and success of subsequent transfer based on the degree of blastocyst development'. *Fertility and Sterility*, 73 pp. 582-586.
- 212 Sharkey, A.M. and Macklon N.S. (2013) 'The science of implantation emerges blinking into the light'. *Reproductive Biomedicine Online*, 27 pp. 453-460.
- 213 Simon, C., Gimeno, M.J., Mercarder, A., O'Connor, J.E., Remohi, J., Polan, M.L. and Petticer, A. (1997) 'Embryonic regulation of integrins beta 3, alpha 4 and alpha 1 in human endometrial epithelial cells *in vitro*'. *Journal of Clinical Endocrinology and Metabolism*, 82 pp. 2607-2616.
- 214 Singh, H., Nardo, L., Kimber, S.J. and Aplin, J.D (2010). 'Early stages of implantation as revealed by an *in vitro* model'. *Reproduction*, 139 pp. 905-914.
- 215 Slama, R., Eustache, F., Ducot, B., Jensen, T.K., Jorgensen, N., Horte, A., Irvine, S., Suominen, J., Anderson, A.G., Auger, J. (2002) 'Time to pregnancy and semen parameters: a cross sectional study among fertile couples from four European cities'. *Human Reproduction*, 16 pp.503-515.
- 216 Steer, C.V., Mills, C.L., Tan, S.L., Campbell, S. and Edwards, R.G. (1992) 'The cumulative embryo score: a predictive embryo scoring technique to select the optimal number of embryos to transfer in an *in vitro* fertilisation and embryo transfer programme'. *Human Reproduction*, 7 pp. 117-119.
- 217 Stewart, C.L., Kaspar, P., Brunet, L.J., Bhatt, H., Gadi, I., Köntgen, F. and Abbondanzo, S.J. (1992) 'Blastocyst implantation depends on maternal expression of leukaemia inhibitory factor'. *Nature*, Sep 3;359(6390):76-9.
- 218 Storr, A., Bilir, E., Cooke, S., Garrett, D. and Venetis, C.A. (2019) 'Fine-tuning blastocyst selection based on morphology: a multicentre analysis of 2461 single blastocyst transfers'. *Reproductive Biomedicine Online*, 39(4) pp. 588-598.
- 219 Sturmey, R.G., Hawkhead, J.A., Barker, E.A. and Leese, H.J. (2009) 'DNA damage and metabolic activity in the preimplantation embryo'. *Human Reproduction*, 24 pp.81-91.
- 220 Subira, J., Craig, J., Turner, K., Bevan, A., Ohuma, E., McVeigh, E., Child, T. and Fatum, M. (2016) 'Grade of the inner cell mass, but not trophoctoderm, predicts live birth in fresh blastocyst single transfers'. *Human Fertility*, 19 pp. 254-261.



- 221 Sugihara, K., Sugiyama, D., Byrne, J., Wolf, D.P., Lowitz, K.P., Kobayashi, Y. *et al* (2007) 'Trophoblast cell activation by trophinin ligation is implicated in human embryo implantation'. *Proceedings of the National Academy of Science (USA)*, 104 pp. 3799-3804.
- 222 Sun, X., Park, C.B., Deng, W., Potter, S.S. and Dey, S.K. (2015) 'Uterine inactivation of muscle segment homeobox (Msx) genes alters epithelial cell junction proteins during embryo implantation'. *The FASEB Journal*, 30 pp1425-1435
- 223 Sutherland, A.E., Calarco, P.G. and Damsky, C.H. (1988) 'Expression and function of cell surface extracellular matrix receptors in mouse blastocyst attachment and outgrowth'. *Journal of Cell Biology*, 106 pp.1331-1348.
- 224 Sutherland, A.E., Calarco, P.G. and Damsky, C.H. (1993) 'Developmental regulation of integrin expression at the time of implantation in the mouse embryo'. *Development*, 119 pp.1175-1186.
- 225 Tamada, H., McMaster, M.T., Flanders, K.C., Andrews, G.K. and Dey, S.K. (1990) 'Cell type-specific expression of transforming growth factor-beta 1 in the mouse uterus during the periimplantation period'. *Journal of Molecular Endocrinology*, 4 pp965-972
- 226 Tamura, N., Sugihara, K., Akama, T.O. and Fukuda, M.N. (2011) 'Trophinin mediated cell adhesion induces apoptosis of human endometrial epithelial cells through PKC-delta'. *Cell Cycle*, 10 pp. 135-143.
- 227 Tang, M., Taylor, H.S. and Tabibzadeh, S. (2005) '*In vivo* gene transfer of lefty leads to implantation failure in mice'. *Human Reproduction*, 20 pp1772-1778
- 228 Taylor, H.S., Vanden Heuvel, G.B. and Igarashi, P. (1997) 'A conserved Hox axis in the mouse and human reproductive system: late establishment and persistent expression of the Hoxa cluster genes' *Biology of Reproduction*, 57 pp1338-1345
- 229 Teklenburg, G., Salker, M., Molokhia, M., Lavery, S., Trew, G., Aojanpong, T., Mardon, H.J., Lokugamage, A.U., Rai, R., Landles, C., Roelen, B.A.J., Quenby, S., Kuijk, E.W., Kavelaars, A., Heijnen, C.J., Regan, L., Brosens, J.J. and Macklon N.S. (2010) 'Natural selection of human embryos: decidualising endometrial stromal cells serve as sensors of embryo quality upon implantation'. *PLoS ONE*, 5(4) e10258.
- 230 Terakawa, J., Wakitani, S., Sugiyama, M., Inoue, N., Ohmori, Y., Kiso, Y., Hosaka, Y.Z. and Hondo, E. (2011) 'Embryo implantation is blocked by intraperitoneal injection with anti-LIF antibody in mice'. *Journal of Reproduction and Development*, Dec;57(6):700-7.
- 231 Thompson, S.M., Onwubalili, N., Brown, K., Jindal, S.K. and McGovern, P.G. (2013) 'Blastocyst expansion score and trophoctoderm morphology strongly predict successful clinical pregnancy and live birth following elective single embryo blastocyst transfer (eSET): a national study'. *Journal of Assisted Reproduction and Genetics*, 30 pp.1577-1581.
- 232 Toralová, T., Kinterova, V., Chmelíková, E. and Kanka, J. (2020). 'The neglected part of early embryonic development: maternal protein degradation'. *Cellular and Molecular Life Sciences*. 77. 10.1007/s00018-020-03482-2.
- 233 Tran, D., Cooke, S., Illingworth, P.J and Gardner, D.K. (2018) 'Deep learning as a predictive tool for fetal heart pregnancy following time-lapse incubation and blastocyst transfer'. *Human Reproduction*, 34(6) pp. 1011-1018
- 234 Turco, M.Y., Gardner, L., Hughe, J., Cindrova-Davies, T., Gomez, M.J., Farrell, L., Hollinshead, M., Marsh, S.G.E., Brosens, J.J., Critchley, H.O., Simons, B.D., Hemberger, M., Koo, B-K., Moffett, A. and Burton, G.J. (2017) 'Long-term, hormone-responsive organoid cultures of human endometrium in a chemically defined medium'. *Nature Cell Biology*, 19(5) pp.568-577.
- 235 Van den Abbeel, E., Balaban, B., Ziebe, S., Lundin, K., Cuesta, M.J., Klein, B.M., Helmggaard, L. and Arce, J.C. (2013) 'Association between blastocyst morphology and outcome of single-blastocyst transfer'. *Reproductive Biomedicine Online*, 27 pp.353-361.

- 236 Van Montfoort, A.P., Dumoulin, J.C., Kester, A.D. and Evers, J.L. (2004) 'Early cleavage is a valuable addition to existing embryo selection parameters: a study using single embryo transfers'. *Human Reproduction*, 19 pp. 2103-2108.
- 237 Van Royen, E., Mangelschots, K., De Neubourg, D., Valkenburg, M., Van de Meerssche, M., Ryckaert, G., Eestermans, W. and Gerris, J. (1999) 'Characterization of a top quality embryo, a step towards single embryo transfer'. *Human Reproduction*, 14, pp. 2345-2349.
- 238 Van Vaerenberg, I., McIntire, R., Van Lommel, L., Devroey, P., Giudice, L. and Bourgain, C. (2010) 'Gene expression during successful implantation in a natural cycle'. *Fertility and Sterility*, 93 p268
- 239 Vanneste, E., Voet, T., Le Caignec, C., Ampe, M., Konings, P., Melotte, C., Debrock, S., Amyere, M., Vikkula, M., (2009) 'Chromosome instability is common in human cleavage-stage embryos'. *Nature Medicine*, 15 pp. 577-583.
- 240 Varelas, X., Sakuma, R., Samavarchi-Tehrani, P., Peerani, R., Rao, B.M. *et al* (2008) 'TAZ controls Smad nucleocytoplasmic shuttling and regulates human embryonic stem-cell self-renewal'. *Nature Cell Biology*, 10(7) pp837-848
- 241 Varelas, X., Samavarchi-Tehrani, P., Narimatsu, M., Weiss, A, Cockburn, K. *et al* (2010) 'The Crumbs complex couples cell density sensing to Hippo-dependent control of the TGF-beta-SMAD pathway'. *Developmental Cell*, 19(6) pp831-844
- 242 Veeck, L.L., Amundson, C.H., Brothman, L.J., DeScisciolo, C., Maloney, M.K. *et al* (1993) 'Significantly enhanced pregnancy rates per cycle through cryopreservation and thaw of pronuclear stage oocytes'. *Fertility and Sterility*, 59 pp 1202-1207
- 243 Veeck, L.L., Bodine, R., Clarke, R.N., Berrios, R., Libraro, J., Moschini, R.M. *et al* (2004) 'High pregnancy rates can be achieved after freezing and thawing human blastocysts'. *Fertility and Sterility*, 82, 1418-1427
- 244 Vermeiden, J.P. and Bernardus, R.E. (2013) 'Are imprinting disorders more prevalent after human in vitro fertilization or intra-cytoplasmic sperm injection?' *Fertility and Sterility*, 99, pp642-651
- 245 Vilella, F., Moreno-Moya, J.M., Balaguer, N., Grasso, A., Herrero, M., Martinez, S., Marcilla, A. and Simon, C. (2015) 'Has-miR-30d, secreted by the human endometrium, is taken up by the pre-implantation embryo and might modify its transcriptome'. *Development*, 142 pp. 3210-3221.
- 246 Walker, E.R., McGrane, M., Aplin, J.D., Brison, D.R. and Ruane, P.T. (2023) 'A systematic review of transcriptomic studies of the endometrium reveals inconsistently reported differentially expressed genes'. *Reproduction and Fertility*, In press
- 247 Wallingford, M.C., Angelo, J.R. and Mager, J. (2013) 'Morphogenetic analysis of peri-implantation development'. *Developmental Dynamics*, 242 pp1110-1120
- 248 Wang, H. and Dey, S.K. (2006) 'Roadmap to embryo implantation: clues from mouse models'. *Nature Reviews Genetics*, 7 pp. 185-199.
- 249 Wang, J., Mayernik, L. and Armant, D.R. (2002) 'Integrin signalling regulates blastocyst adhesion to fibronectin at implantation: intracellular calcium transients and vesicle tracking in primary trophoblast cells'. *Developmental Biology*, 245 pp. 270-279.
- 250 Wang, J., Mayernik, L., Schultz, J.F. and Armant, D.R. (2000) 'Acceleration of trophoblast differentiation by heparin-binding EGF-like growth factor is dependent on the stage-specific activation of calcium influx by ErbB receptors in developing mouse blastocysts'. *Development*, 127 pp.33-44.
- 251 Weimar, C.H., Kavelaars, A., Brosens, J.J., Gellersen, B., de Vreeden-Elbertse J.M., Heijnen, C.J. and Macklon, N.S. (2012) 'Endometrial stromal cells of women with recurrent miscarriage fail to discriminated between high and low quality human embryos'. *PLoS One*, 7 e41424.
- 252 White, C.A., Zhang, J.G., Salamonsen, L.A., Baca, M., Fairlie, W.D., Metcalf, D., Nicola, N.A., Robb, L. and Dimitriadis, E. (2007) 'Blocking LIF action in the uterus by using a PEGylated antagonist

- prevents implantation: a nonhormonal contraceptive strategy'. *Proc Natl Acad Sci U S A*. 2007 Dec 4;104(49):19357-62
- 253 Wong, C.C., Loewke, K.E., Bossert, N.L., Behr, B., De Jonge, C.J., Baer, T.M. and Reijo Pera, R.A. (2010) 'Non-invasive imaging of human embryos before embryonic genome activation predicts development to the blastocyst stage'. *Nature Biotechnology* 28(10) doi:10.1038/nbt.1686
- 254 Wu, Z. and Guan, K-L. (2021) 'Hippo signalling in embryogenesis and development'. *Trends in Biochemical Sciences*, 46(1) pp 51-63
- 255 Xu, B., Geerts, D., Bu, Z., Ai, J., Jin, L., Li, Y., Zhang, H. and Zhu, G. (2014) 'Regulation of endometrial receptivity by the highly expressed HOXA9, HOXA11 and HOXD10 HOX-class homeobox genes'. *Human Reproduction*, 29(4) pp781-90
- 256 Xue, P., Zhou, W., Fan, W., Jiang, J., Kong, C., Zhou, W., *et al.* (2021) 'Increased METTL3-mediated m(6)A methylation inhibits embryo implantation by repressing HOXA10 expression in recurrent implantation failure'. *Reproductive Biology and Endocrinology*, 19 pp187
- 257 Yan, Q., Huang, C., Jiang, Y., Shan, H., Jiang, R., Wang, J. *et al.* (2018) 'Calpain7 impairs embryo implantation by downregulating  $\beta$ 3-integrin expression via degradation of HOXA10'. *Cell Death and Disease*, 9 (3) pp291.
- 258 Yanez, L.Z., Han, J., Behr, B.B., Reijo, Pera R.A. and Camarillo, D.B. (2016) Human oocyte developmental potential is predicted by mechanical properties within hours after fertilization. *Nature Communications*, 7, No 10809
- 259 Yelian, F.D., Yang, Y., Hirata, J.D., Schultz, J.F. and Armant, D.R. (1995) 'Molecular interactions between fibronectin and integrins during mouse blastocyst outgrowth'. *Molecular Reproduction and Development*, 41 pp.435-448.
- 260 Yin, R-H., Yu, J-T. and Tan, L. (2015) 'The role of SORL1 in Alzheimer's Disease' *Molecular Neurobiology*. 51(3):909-18. doi: 10.1007/s12035-014-8742-5
- 261 Zamora, R.B., Sanchez, R.V., Perez, J.G., Diaz, R.R., Quintana, D.B and Bethencours, J.C. (2011) Human zygote morphological indicators of higher rate of arrest at the first cleavage stage. *Zygote*, 19(4) pp.339-344.
- 262 Zaninovic, N., Berrios, R., Clarke, R.N., Bodine, R., Ye, Z. and Veeck, L.L. (2001) 'Blastocyst expansion, inner cell mass (ICM) formation and trophectoderm (TM) quality: is one more important for implantation?'. *Fertility and Sterility*, 76 S8.
- 263 Zhan, Q., Ye, Z., Clarke, R., Rosenwaks, Z. and Zaninovic, N. (2016) 'Direct unequal cleavages: embryo developmental competence, genetic constitution and clinical outcome'. *PLoS One*, 11(12): e0166398
- 264 Zhang, B., Kirov, S. and Snoddy, J. (2005) 'WebGestalt: an integrated system for exploring gene sets in various biological contexts'. *Nucleic Acids Research*;33:W741-W748
- 265 Zhang, Y., Xiong, G and Peng, J. (2010) 'Effects of TGF beta-1 on mouse embryo implantation and expression of H2-D1 and H2-DM'. *Frontiers in Bioscience (Elite Edition)*, 2 pp351-360
- 266 Zheng, Q., Zhang, D., Yang, Y.U., Ciu, X., Sun, J., Liang, C., Qin, H., Yang, X., Lui, S. and Yan, Q. (2017). 'MicroRNA-200c impairs uterine receptivity formation by targeting FUT4 and alpha 1, 3-fucosylation'. *Cell Death and Differentiation*, 24 pp.2161-2172.
- 267 Zhu, L.H., Sun, L.H., Hu, Y.L., Jiang, Y., Liu, H.Y., Shen, X.Y., *et al.* (2013) 'PCAF impairs endometrial receptivity and embryo implantation by down-regulating  $\beta$ 3-integrin expression via HOXA10 acetylation'. *Journal of Clinical Endocrinology and Metabolism*, 98 pp4417-28.
- 268 Zinamen, M.J., Clegg, E.D., Brown, C.C., O'Connor, J. and Selevan, S.G. (1996) 'Estimates of human fertility and pregnancy loss'. *Fertility and Sterility*, 65 pp.503-509.

## Appendix 1

### **Description of the Higher Specialist Scientist Training (HSST) programme sections A and B**

#### Background

The Higher Specialist Scientist Training (HSST) programme is a five-year work-place based training programme which allows Clinical Scientists to train and gain qualifications which enable them to apply for Consultant Clinical Scientist roles. The programme is overseen by the National School of Healthcare Science (NSHCS), funded by Health Education England and delivery is supported by the Manchester Academy for Healthcare Science Education (MAHSE). It is described as a bespoke training programme as it requires significant input from the trainee and their employer to develop job plans and balance academic and workplace learning to meet the standards required to complete the programme. The expectation is that the candidate is supported to have one day per week to focus on their HSST programme, although the workplace-based competencies are expected to be met during delivery of clinical services. For Life Sciences (including Reproductive Science) HSST is divided into 4 sections, detailed below. Sections A and C together make up the academic component which is awarded as a Doctorate of Clinical Sciences (DClinSci):

Section A: Postgraduate Diploma in Leadership and Management in the Healthcare Sciences (delivered by Alliance Manchester Business School -University of Manchester)

Section B: Specialist module – for Reproductive Science this requires successful completion of Fellowship of the Royal College of Pathologists. [The written component of the Part 2 examination is satisfied by a pass in the Section C2 of Doctorate of Clinical Science]

Section C: Doctoral Research and Innovation in Clinical Science. Section C is split into 2 components and C1 must be passed before progression to C2.

Workplace-based evidence demonstrating the appropriate application of specialty knowledge and skills in an e-portfolio, appropriately mapped to the domains of the AHCS

Standards of Proficiency for Higher Specialist Scientists and to the learning outcomes of the specialist curriculum.

Details of Sections A, B, C and workplace-based evidence

Section A PgDip Leadership and Management in the Healthcare Sciences (120 credits)

This aspect of the programme was completed in September 2021. The diploma consists of 5 Units, with assessments on each Unit (written assignments or assessed presentations).

Unit A1: Professionalism and Professional Development in the Healthcare Environment

Assignment 1: Construct a personal model of professionalism underpinned by one or more recognised models of professionalism and using a range of tools of critical reflective practice.

Assignment 2: A call to action: Preserving Future Fertility for Young Women With Cancer –Time To Make It Better.

Assessed group presentation to mock NHSE panel ‘CCG position on decision to decommission provision of hearing aids for mild to moderate hearing loss in North Staffs’

Unit A2: Theoretical Foundations of Leadership

Assignment 1: Critically evaluate two models of leadership and how these relate to your specialism

Assignment 2: Critically analyse your wider work environment through the lens of collective leadership approaches providing examples of opportunities or barriers to promoting your organisation’s values and mission. Using the pledge that you have given at Day 3, write an action plan that outlines what you need to do to implement your pledge.

Unit A3: Personal and Professional Development to Enhance Performance

Assignment 1: Consider and reflect on 3 key areas: Key learning from your working life; Learning associated with the Programme; Personal learning from outside of work

Assignment 2: Who am I? Knowing and reflecting on self

#### Unit A4: Leadership and Quality Improvement in the Clinical and Scientific Environment

The written assessments for this Unit required me to identify an area or process requiring improvement within the department. The first assignment was to undertake work to understand the process and the problems (e.g. using process mapping, questionnaires for staff and service users) and identify metrics to measure improvements made. I chose the flow of patients through the Clinic having embryo transfer as this was poorly managed, unpredictable and resulted in long waits for patients which might increase stress and result in poorer outcomes and more difficult procedures. The brief was then to run a series of QI cycles making small changes each time over a period of 3 months, and assignment 2 was then to report on the findings (an experimental write-up effectively).

Unit A4 began in early March 2020. As the UK entered lockdown at the end of the month Fertility clinics were required to close (by the HFEA) and had to provide extensive documentation and risk assessments to re-open. As part of a large NHS Trust most of our clinical team were redeployed so the Clinic did not fully reopen for some months. I therefore chose to defer Unit A4 until March 2021.

#### Unit A5: Research and Innovation in Health and Social Care

Assignment 1: Assessed group presentation: *You are a university research team invited by the NIHR to develop an outline proposal to conduct a research study into Hospital Trust Board Effectiveness – you must present an outline proposal to your client online as a 15 minute presentation*

Assignment 2: A Case Study of One Innovation in Assisted Reproduction: Time-lapse Imaging of Early Human Embryos

## Section B: Specialist Module

The Royal College of Pathologists (RCPATH) opened a route for Reproductive Scientists to gain Fellowship in 2008. Those already working in the field with sufficient experience could apply to the College to be recognised at an appropriate level under a grandparenting clause. Following submission of a portfolio of evidence and a short viva I was awarded Diplomate status of the RCPATH in October 2008 (a pass at Part I of Fellowship examinations).

I sat and passed the oral and practical elements of the Part II examinations in September 2022. The accompanying thesis forms the written component of the Part II examinations.

## Section C: Doctoral Research and Innovation in Clinical Science.

Section C1 is 'Preparing the Proposal' and comprises:

- A literature review (approximately 4000 words)
- Extended project Proposal (5 pages of A4 maximum)
- A Lay Presentation (explain the basics of your project to a lay audience. C1 is normally assessed in Year 3. Delays due to the Covid -19 pandemic meant my assessments took place in year 4.

Section C2 is the research project, and the assessment is this thesis and *viva voce* examination.

### Workplace based assessments:

Throughout the 5 year programme I was gaining experience and collating evidence of working at the level of a Consultant Clinical Scientist. Evidence needed to be appropriately mapped to the domains of the AHCS Standards of Proficiency for Higher Specialist Scientists and to the learning outcomes of the specialist curriculum.

Some examples:

I collated and presented complex data to an external advisor and liaised extensively with her during a trouble-shooting programme to improve our frozen embryo transfer results.

I became a Careers Ambassador for the Trust and presented at schools and careers fairs across the region on Healthcare Science and NHS careers.

I became Lead Station Writer (Lead Examiner) for the Scientist Training Programme (STP) in Embryology. I have responsibility for overseeing the provision of assessment materials for the final assessments (OSFAs and IACCs) and recruiting suitable persons to undertake these assessments.



## Appendix 2

Relevant sections from 'Guidance from Manchester Metropolitan University on completion of Section C of HSST'

*Cohort 3 onwards – Section C guidance*

*Background and Context*

*Students in Cohort 3 moving forwards and who are not undertaking the full DClSci will commence work on unit 6ACP8024, C1: Doctoral Research and Innovation in Clinical Science – Preparing the Proposal in their third year of study. For students not completing the full DClSci, the focus of the unit will be on an Innovation Project Proposal. For those not completing the full DClSci, you are advised to consult with the National School of Healthcare Science regarding the requirements for completion of Higher Specialist Scientific Training.*

*Student from Cohort 3 onwards who are completing the full DClSci will now commence work on the Research Project in their third year. This allows more time to undertake the research required. Students completing the full award will still need to complete 2 units:*

- *6ACP8024: C1: Doctoral Research and Innovation in Clinical Science – Preparing the Proposal*
- *6ACP8025: C2: Research Project Units C1 and C2 will be continuous and on the topic of the final thesis. Students must pass C1 to enable progression to C2.*

*Assessment 6ACP8024: C1- Doctoral Research and Innovation in Clinical Science – Preparing the Proposal*

- *A Literature Review (approximately 4000-words +/- 10%)*
- *Proposal (5 pages of A4 maximum)*
- *A Lay Presentation (explain the basics of your project to a lay audience).*

*6ACP8025: C2: Research Project The assessment for the Research Project unit is:*

- *Thesis (30000 – 40000 words)*
- *Viva-voce examination (approximately 6-8 weeks following submission of the thesis)*

*Innovation Proposal*

*Completion of HSST, requires you to conceive an innovation within your healthcare science discipline that has potential to make a positive contribution to service delivery or patient experience or patient outcomes or health economics, or any other aspect of healthcare. The innovation must be carried out at doctoral level and so must be original, must demonstrate that the student is able to think critically about problems to produce innovative solutions and must include the potential to create new knowledge. In the new Section C format, students undertaking the full DClSci are required to incorporate the innovation in the thesis.*

# Appendix 3

BGI Sample testing report for endometrial cells submitted for RNA extraction.



File Code/Version Number: R-SMD-022/Ad

## BGI Sample Testing Report

### 1. Project Information

Report No.: THK22081005

<b>Project Name</b>	University of Manchester-Peter Ruane-24 humanRNAseq(extraction, lrv-4upit, PE100, 50M)HDD 20220727		<b>Project No.</b>	F22FTSELJHT1184	
<b>Customer Name</b>	Peter Ruane		<b>Customer Unit</b>	The University of Manchester	
<b>Lab Sample Collector</b>	Isangkamleang		<b>Lab Sample Receiving Date</b>	20220808	
<b>Lab Sample Tester</b>	wongngating, shihaiyuan		<b>Lab Sample Testing Date</b>	20220810	
<b>Lab Name</b>	BGI Hongkong Tech Solution NGS Lab		<b>Lab Address</b>	16 Dai Fu Street, Tai Po Industrial Estate, Tai Po, New Territories, Hong Kong.	
<b>Reported by</b>	wongngating	<b>Inspected by</b>	Shuje ZOU	<b>Approved by</b>	Shuje ZOU
				<b>Report Date</b>	20220810

### 2. Sample Test Method

- ①Method of concentration determination:  Agilent 2100,  Fragment Analyzer,  Microplate Reader
- ②Method of 28S/18S & 23S/16S test:  Agilent 2100,  Fragment Analyzer,  Qsep-400
- ③Method of RIN or RQN test:  Agilent 2100,  Fragment Analyzer,  Qsep-400

### 3. Sample Test Result

No.	Sample Name	Sample Number	Tissue Name	Tissue Number	Tissue Residual	Concentration (ng/μL)	Volume (μL)	Total Mass (pg)	RIN/RQN	28S/18S	Library Type	Test Result	Remark
1	AEA	HCYR22080654_A	AE	T85220800195	0	94	20	1.88	7	2.1	DNBSEQ Transcriptome	Level B	Baseline is not smooth
2	ASA	HCYR22080655_A	AS	T85220800196	0	26	20	0.52	6.7	4.1	DNBSEQ Transcriptome	Level B	RIN<7.0
3	BEA	HCYR22080656_A	BE	T85220800197	0	158	20	3.16	8.5	2.2	DNBSEQ Transcriptome	Level A	
4	BSA	HCYR22080657_A	BS	T85220800198	0	29	20	0.58	6.8	3.6	DNBSEQ Transcriptome	Level B	RIN<7.0
5	CEA	HCYR22080658_A	CE	T85220800199	0	115	20	2.3	5.5	2.2	DNBSEQ Transcriptome	Level C	RIN<7.0
6	CSA	HCYR22080659_A	CS	T85220800200	0	23	20	0.46	6.5	2.5	DNBSEQ Transcriptome	Level B	RIN<7.0
7	DEA	HCYR22080660_A	DE	T85220800201	0	204	20	4.08	8.1	2.3	DNBSEQ Transcriptome	Level A	
8	2SA	HCYR22080661_A	2S	T85220800202	0	35	20	0.7	8.9	2.5	DNBSEQ Transcriptome	Level A	
9	3EA	HCYR22080662_A	3E	T85220800203	0	177	20	3.54	6.6	1.7	DNBSEQ Transcriptome	Level B	RIN<7.0
10	3SA	HCYR22080663_A	3S	T85220800204	0	36	20	0.72	8.7	3.0	DNBSEQ Transcriptome	Level A	
11	4EA	HCYR22080664_A	4E	T85220800205	0	151	20	3.02	6	1.7	DNBSEQ Transcriptome	Level B	RIN<7.0
12	4SA	HCYR22080665_A	4S	T85220800206	0	33	20	0.66	8.4	3.0	DNBSEQ Transcriptome	Level A	
13	5EA	HCYR22080666_A	5E	T85220800207	0	182	20	3.64	6.1	2.6	DNBSEQ Transcriptome	Level B	RIN<7.0
14	5SA	HCYR22080667_A	5S	T85220800208	0	30	20	0.6	8.3	3.4	DNBSEQ Transcriptome	Level A	
15	7EA	HCYR22080668_A	7E	T85220800209	0	203	20	4.06	7.7	2.1	DNBSEQ Transcriptome	Level A	
16	7SA	HCYR22080669_A	7S	T85220800210	0	30	20	0.6	7.9	3.4	DNBSEQ Transcriptome	Level A	
17	8EA	HCYR22080670_A	8E	T85220800211	0	174	20	3.48	8.6	2.2	DNBSEQ Transcriptome	Level A	
18	8SA	HCYR22080671_A	8S	T85220800212	0	39	20	0.78	8.5	3.8	DNBSEQ Transcriptome	Level A	
19	9EA	HCYR22080672_A	9E	T85220800213	0	143	20	2.86	8	1.9	DNBSEQ Transcriptome	Level A	
20	9SA	HCYR22080673_A	9S	T85220800214	0	33	20	0.66	8.7	3.7	DNBSEQ Transcriptome	Level A	
21	10EA	HCYR22080674_A	10E	T85220800215	0	102	20	2.04	8.5	2.2	DNBSEQ Transcriptome	Level A	
22	10SA	HCYR22080675_A	10S	T85220800216	0	34	20	0.68	8.6	4.3	DNBSEQ Transcriptome	Level A	
23	11EA	HCYR22080676_A	11E	T85220800217	0	178	20	3.56	7.8	2.5	DNBSEQ Transcriptome	Level A	
24	11SA	HCYR22080677_A	11S	T85220800218	0	36	20	0.72	8.5	4.9	DNBSEQ Transcriptome	Level A	

Note\*: The test conclusion is a comprehensive evaluation based on BGI's sample quality requirements for sequencing.

1. The test result notes:

a) Level A means the sample meets the requirements of library construction and sequencing. The current success rate is around 92.12%.

b) Level B means the sample does not totally meet the requirements of library construction and sequencing. BGI can try to construct the library but the quality of the sequence

**Note\*:** The test conclusion is a comprehensive evaluation based on BGI's sample quality requirements for sequencing.

1. The test result notes:

a) Level A means the sample meets the requirements of library construction and sequencing. The current success rate is around 92.12%.

b) Level B means the sample does not totally meet the requirements of library construction and sequencing. BGI can try to construct the library but the quality of the sequence

is not guaranteed. The current success rate is around 87.54%.

c) Level C means the sample does not meet the requirements of library construction and sequencing. The current success rate is around 70.88%.

d) Samples with "N/A" results are not evaluated according to sample quality standards due to their specific conditions. Such samples will be executed with customized plans according to their specific situation.

2. The success rate is calculated based on the statistics of samples executed in BGI during recent period of time. Many factors contribute to the success rate of a sample. This data is for reference only, it does not guarantee success rate for individual sample.

3. For Level B or Level C samples, transcriptome library construction has the following risk at least, based on historical statistics in BGI:

a) Low RNA concentration or mass may lead to library construction failure, unsuccessful sequence due to low library production or insufficient sequencing data quantity, affected data randomness and bias introduction.

b) Degradation of sample may lead to a library construction failure, high duplication rate, poor randomness of sequencing data, inaccurate gene expression quantitation.

c) High concentration of RNA may lead to library construction failure caused by inaccurate sampling.

d) A high 5S peak may lead to inaccurate RNA quantification which can lead to poor data quality due to inaccurate sampling.

e) For plant, fungi and bacteria, OD260/280<1.8 and OD260/230<1.8 may indicate presence of impurities that can reduce efficiency of enzyme reaction, affecting the success rate of library construction and quality of sequencing data. These samples have 90% successful rate in library construction.

4. If COs insist on constructing library with Level B or Level C samples, COs shall take the responsibility and risk involved in this matter.

5. The following conditions carry moderate risk, and we can try to construct libraries with them:

a) The RIN or RQN value is slightly under standard, but baseline is smooth.

b) The RIN or RQN value reaches standard, but baseline is rises slightly.

c) The baseline is smooth and RIN value reaches standard, but 5S peak is slightly high.

d) 28S/18S or 23S/16S value is slightly under standard, but the baseline is smooth.

e) Sample generally meets Level A requirements, but total amount is below Level A.

6. Other notes:

a) Meta Strand-Specific Transcriptome library construction is not applicable to complex meta samples such as soil bacterial and ocean microorganism samples.

## Result

### 1 Project information

The basic information of the project is shown below:

- Project ID: F22FTSEUHT1184\_HUMgwhaT
- Product name: filter
- Sample size: 24
- Library type: DNBSEQ Low Input Smart-Seq Eukaryotic mRNA library
- Sequencing Platform: DNBseq
- Sequencing read Length: PE100
- Clean fastq phred quality score encoding:Phred+33

### 2 Data production

After sequencing, the raw reads were filtered. Data filtering includes removing adaptor sequences, contamination and low-quality reads from raw reads.

Table 1 Statistics of clean data

Sample Name	Clean Reads	Clean Base	Read Length	Q20(%)	GC(%)
10EA	60,133,954	12,026,790,800	PE100	96.53	48.38
10SA	55,682,307	11,136,461,400	PE100	97.23	50.48
11EA	60,070,445	12,014,089,000	PE100	96.75	48.61
11SA	60,119,562	12,023,912,400	PE100	97.16	50.80
2EA	60,122,588	12,024,517,600	PE100	96.41	48.30
2SA	56,424,294	11,284,858,800	PE100	96.74	49.57
3EA	50,747,984	10,149,596,800	PE100	96.40	48.51
3SA	60,104,820	12,020,964,000	PE100	97.14	50.17
4EA	60,071,095	12,014,219,000	PE100	97.25	48.84
4SA	54,888,821	10,977,764,200	PE100	96.42	50.11
5EA	60,065,687	12,013,137,400	PE100	96.78	48.88
5SA	58,008,141	11,601,628,200	PE100	97.48	50.82
7EA	60,086,595	12,017,319,000	PE100	97.39	48.28
7SA	60,204,317	12,040,863,400	PE100	97.13	50.23
8EA	60,045,541	12,009,108,200	PE100	97.22	48.32
8SA	60,107,302	12,021,460,400	PE100	96.79	49.95
9EA	60,117,024	12,023,404,800	PE100	96.74	48.24
9SA	60,176,979	12,035,395,800	PE100	96.94	51.15
AEA	56,786,622	11,357,324,400	PE100	96.34	48.47
ASA	60,166,219	12,033,243,800	PE100	97.04	51.23
BEA	60,236,760	12,047,352,000	PE100	96.52	48.50
BSA	60,150,382	12,030,076,400	PE100	96.80	50.39
CEA	60,041,962	12,008,392,400	PE100	96.07	48.90
CSA	52,431,380	10,486,276,000	PE100	96.34	50.73

- Sample Name : Sample Name
- Clean Reads : Clean reads
- Clean Base : Clean bases
- Read Length : Read length
- Q20(%) : Proportion of Q20
- GC(%) : Proportion of GC

### 3 Quality control

The quality of data was examined after filtering.

#### 3.1 The distribution of base percentage and qualities along reads after datafiltering

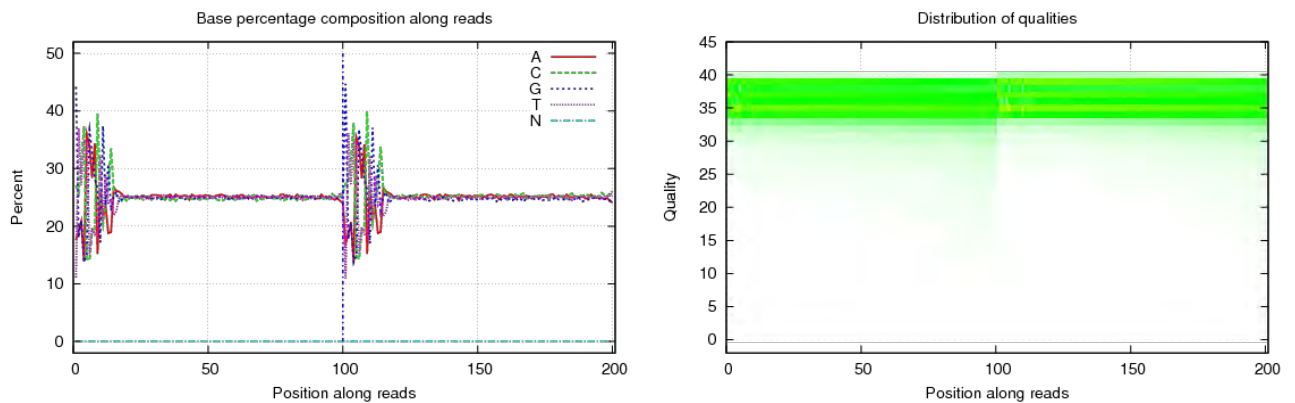


Figure 1 3SA

In the left figure, x-axis represents base position along reads, y-axis represents base percentage at the position; each color represents a type of nucleotide. Under normal conditions, the sample does not have AT/GC separation. It is normal to see fluctuations in the first several bp positions, which is caused by random primer and the instability of enzyme-substrate binding at the beginning of the sequencing reaction. In the right figure, x-axis represents base position along reads, y-axis represents base quality; each dot represents the base quality of the corresponding position along reads, color intensity reflects the number of nucleotides, a more intense color along a quality value indicates a higher proportion of this quality in the sequencing data.

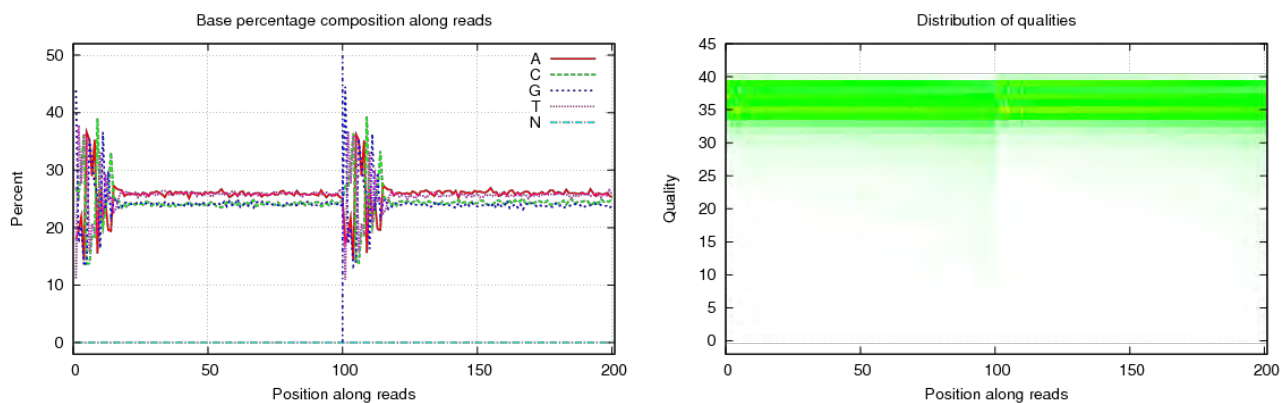


Figure 2 11EA

In the left figure, x-axis represents base position along reads, y-axis represents base percentage at the position; each color represents a type of nucleotide. Under normal conditions, the sample does not have AT/GC separation. It is normal to see fluctuations in the first several bp positions, which is caused by random primer and the instability of enzyme-substrate binding at the beginning of the sequencing reaction. In the right figure, x-axis represents base position along reads, y-axis represents base quality; each dot represents the base quality of the corresponding position along reads, color intensity reflects the number of nucleotides, a more intense color along a quality value indicates a higher proportion of this quality in the sequencing data.

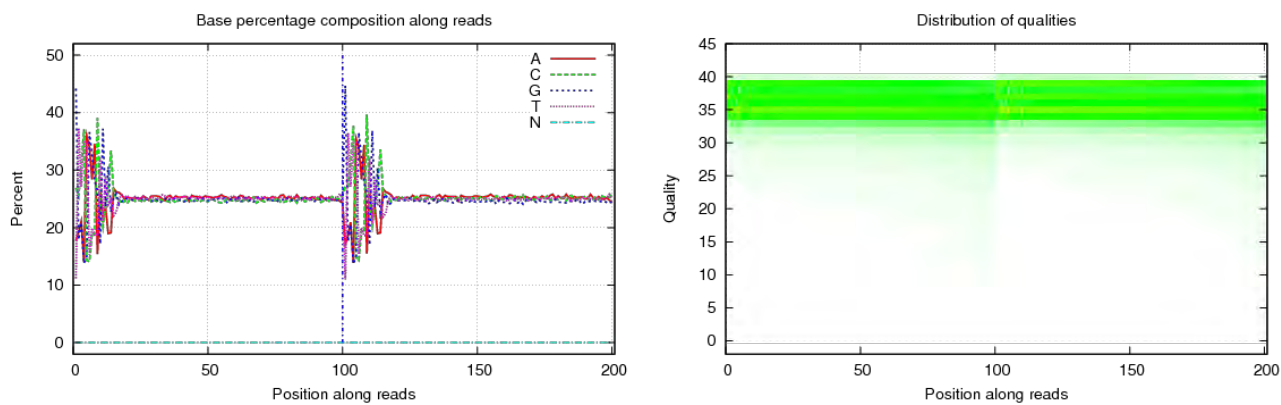


Figure 3 8SA

In the left figure, x-axis represents base position along reads, y-axis represents base percentage at the position; each color represents a type of nucleotide. Under normal conditions, the sample does not have AT/GC separation. It is normal to see fluctuations in the first several bp positions, which is caused by random



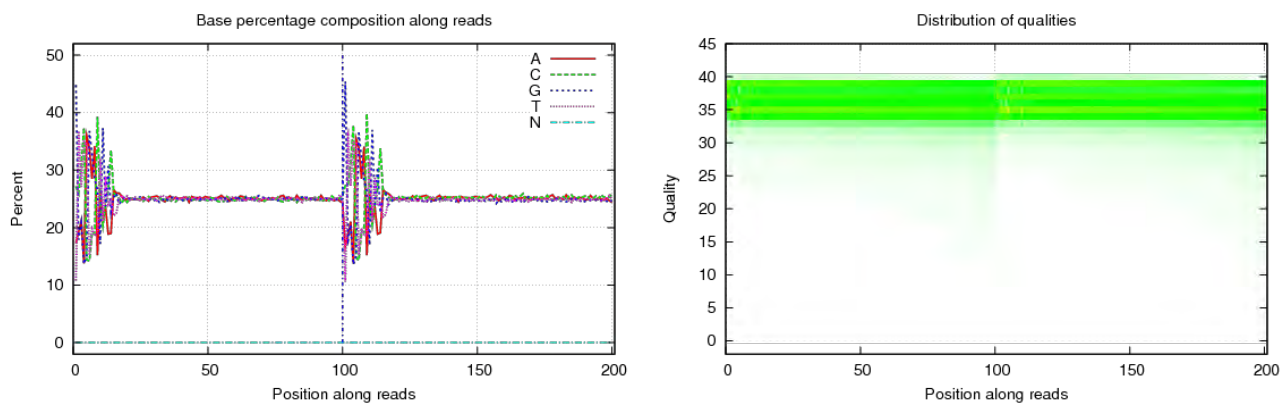


Figure 4 7SA

In the left figure, x-axis represents base position along reads, y-axis represents base percentage at the position; each color represents a type of nucleotide. Under normal conditions, the sample does not have AT/GC separation. It is normal to see fluctuations in the first several bp positions, which is caused by random primer and the instability of enzyme-substrate binding at the beginning of the sequencing reaction. In the right figure, x-axis represents base position along reads, y-axis represents base quality; each dot represents the base quality of the corresponding position along reads, color intensity reflects the number of nucleotides, a more intense color along a quality value indicates a higher proportion of this quality in the sequencing data.

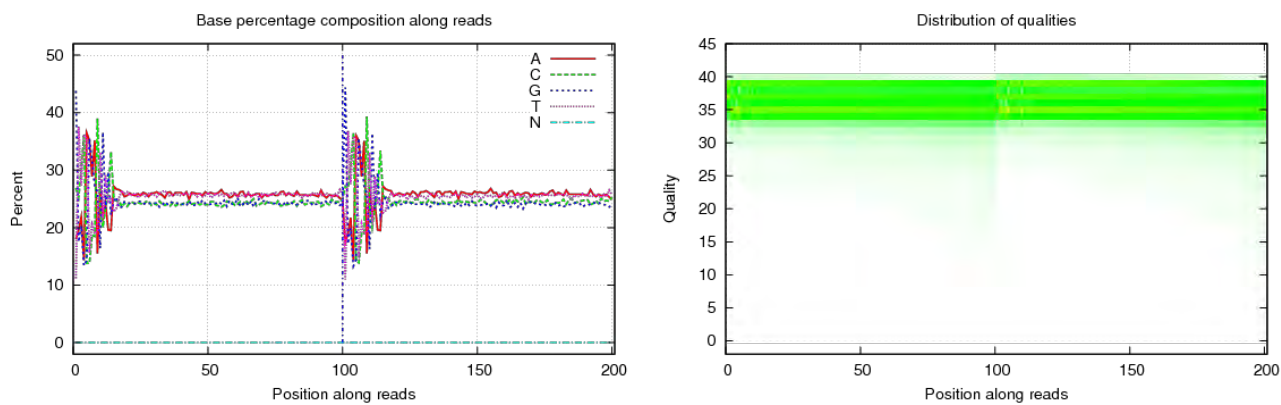


Figure 5 4EA

In the left figure, x-axis represents base position along reads, y-axis represents base percentage at the position; each color represents a type of nucleotide. Under normal conditions, the sample does not have AT/GC separation. It is normal to see fluctuations in the first several bp positions, which is caused by random

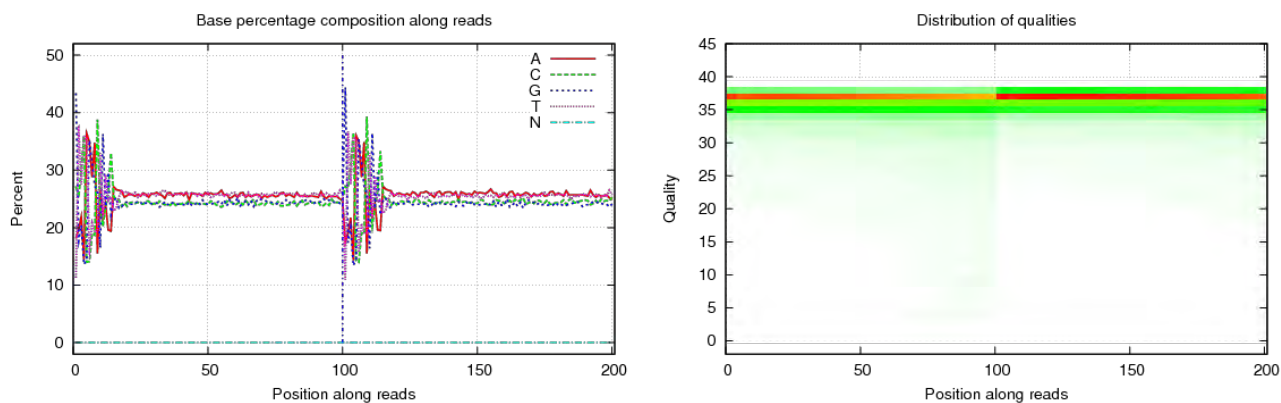


Figure 6 CEA

In the left figure, x-axis represents base position along reads, y-axis represents base percentage at the position; each color represents a type of nucleotide. Under normal conditions, the sample does not have AT/GC separation. It is normal to see fluctuations in the first several bp positions, which is caused by random primer and the instability of enzyme-substrate binding at the beginning of the sequencing reaction. In the right figure, x-axis represents base position along reads, y-axis represents base quality; each dot represents the base quality of the corresponding position along reads, color intensity reflects the number of nucleotides, a more intense color along a quality value indicates a higher proportion of this quality in the sequencing data.

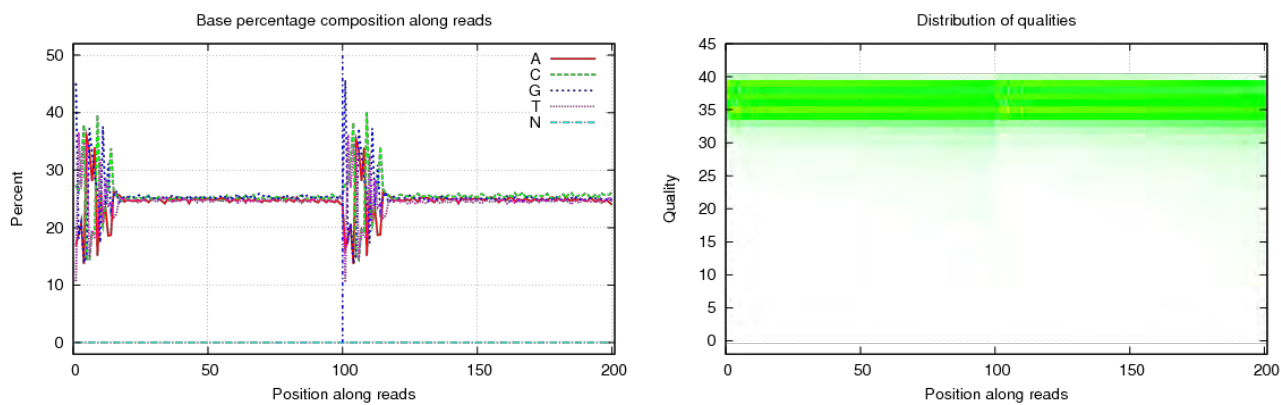


Figure 7 11SA

In the left figure, x-axis represents base position along reads, y-axis represents base percentage at the position; each color represents a type of nucleotide. Under normal conditions, the sample does not have AT/GC separation. It is normal to see fluctuations in the first several bp positions, which is caused by random

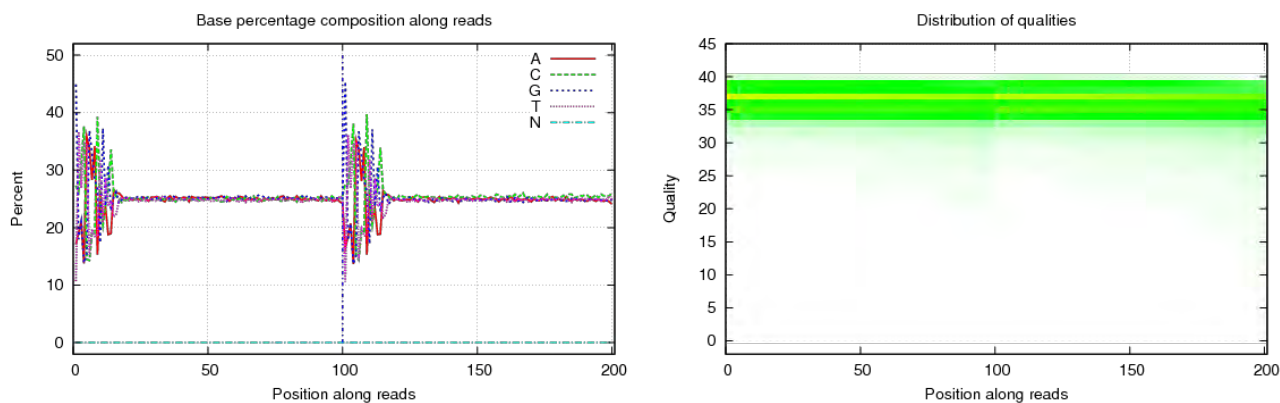


Figure 8 10SA

In the left figure, x-axis represents base position along reads, y-axis represents base percentage at the position; each color represents a type of nucleotide. Under normal conditions, the sample does not have AT/GC separation. It is normal to see fluctuations in the first several bp positions, which is caused by random primer and the instability of enzyme-substrate binding at the beginning of the sequencing reaction. In the right figure, x-axis represents base position along reads, y-axis represents base quality; each dot represents the base quality of the corresponding position along reads, color intensity reflects the number of nucleotides, a more intense color along a quality value indicates a higher proportion of this quality in the sequencing data.

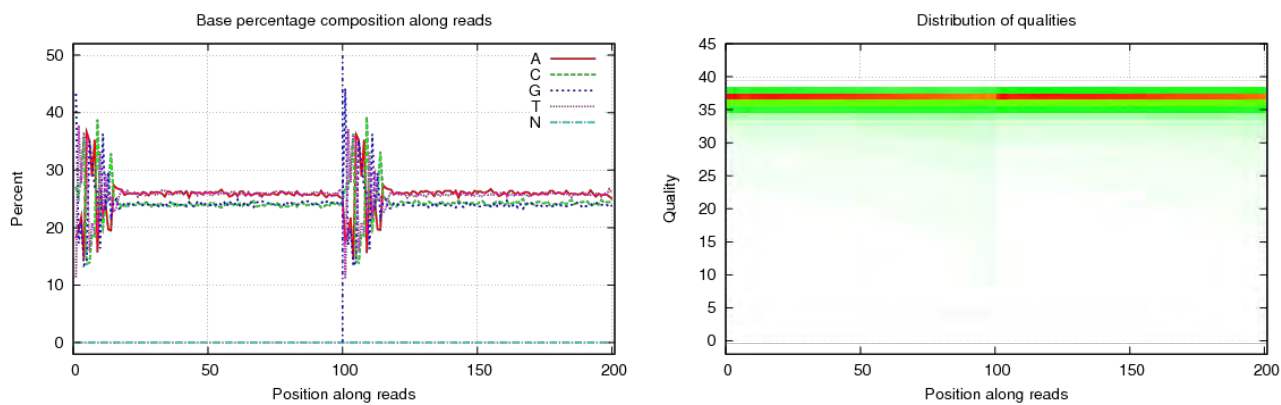


Figure 9 BEA

In the left figure, x-axis represents base position along reads, y-axis represents base percentage at the position; each color represents a type of nucleotide. Under normal conditions, the sample does not have AT/GC separation. It is normal to see fluctuations in the first several bp positions, which is caused by random

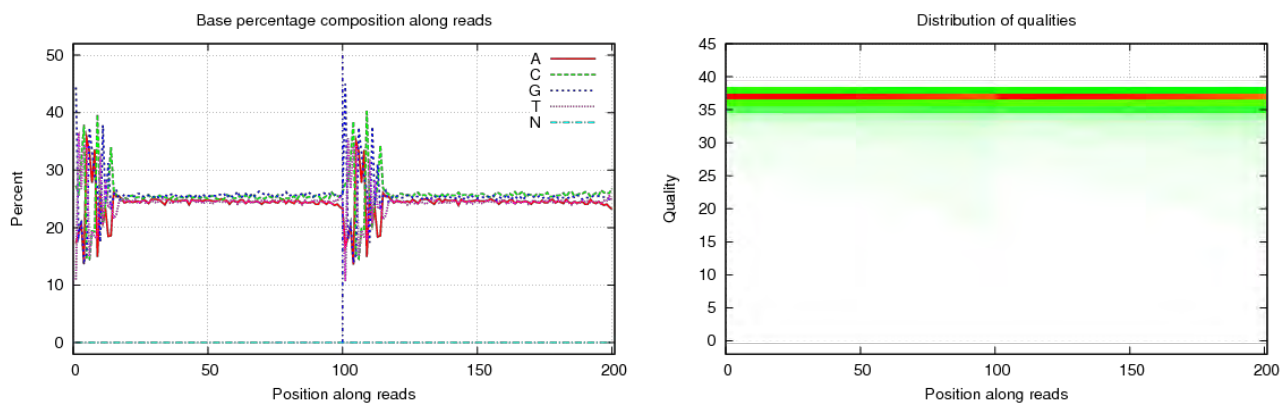


Figure 10 ASA

In the left figure, x-axis represents base position along reads, y-axis represents base percentage at the position; each color represents a type of nucleotide. Under normal conditions, the sample does not have AT/GC separation. It is normal to see fluctuations in the first several bp positions, which is caused by random primer and the instability of enzyme-substrate binding at the beginning of the sequencing reaction. In the right figure, x-axis represents base position along reads, y-axis represents base quality; each dot represents the base quality of the corresponding position along reads, color intensity reflects the number of nucleotides, a more intense color along a quality value indicates a higher proportion of this quality in the sequencing data.

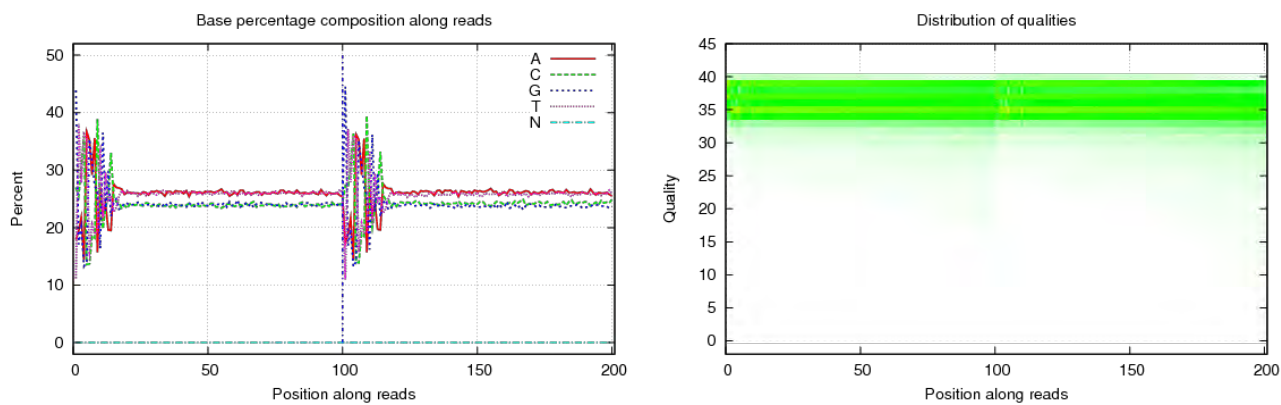


Figure 11 8EA

In the left figure, x-axis represents base position along reads, y-axis represents base percentage at the position; each color represents a type of nucleotide. Under normal conditions, the sample does not have AT/GC separation. It is normal to see fluctuations in the first several bp positions, which is caused by random



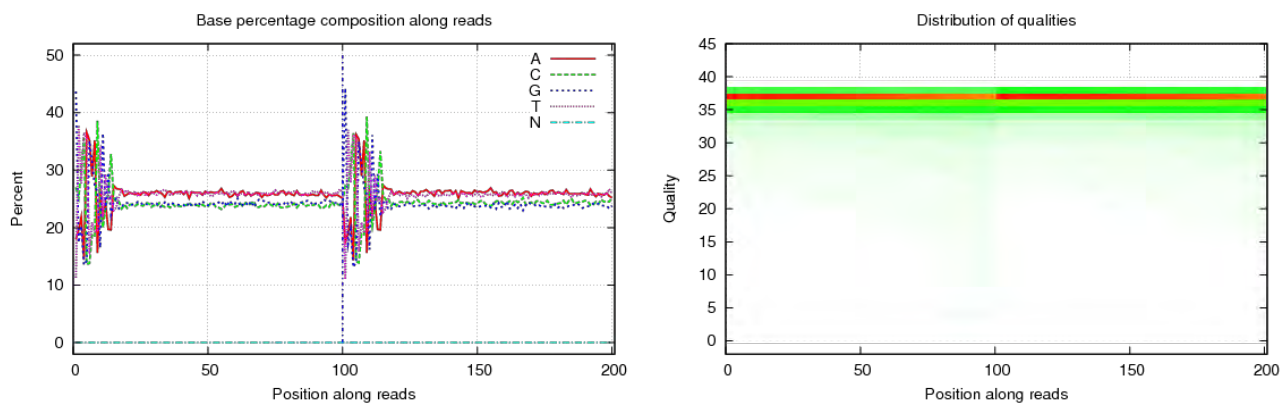


Figure 12 AEA

In the left figure, x-axis represents base position along reads, y-axis represents base percentage at the position; each color represents a type of nucleotide. Under normal conditions, the sample does not have AT/GC separation. It is normal to see fluctuations in the first several bp positions, which is caused by random primer and the instability of enzyme-substrate binding at the beginning of the sequencing reaction. In the right figure, x-axis represents base position along reads, y-axis represents base quality; each dot represents the base quality of the corresponding position along reads, color intensity reflects the number of nucleotides, a more intense color along a quality value indicates a higher proportion of this quality in the sequencing data.

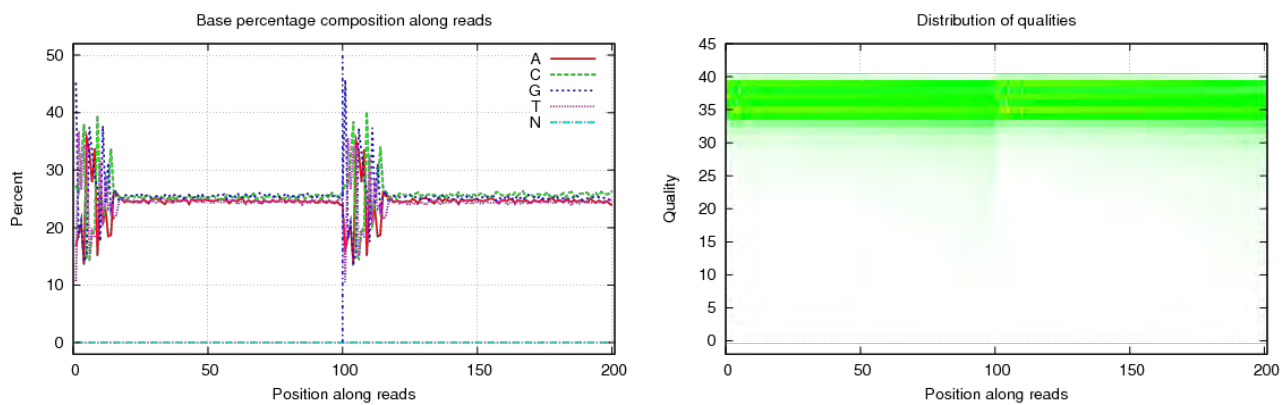


Figure 13 9SA

In the left figure, x-axis represents base position along reads, y-axis represents base percentage at the position; each color represents a type of nucleotide. Under normal conditions, the sample does not have AT/GC separation. It is normal to see fluctuations in the first several bp positions, which is caused by random

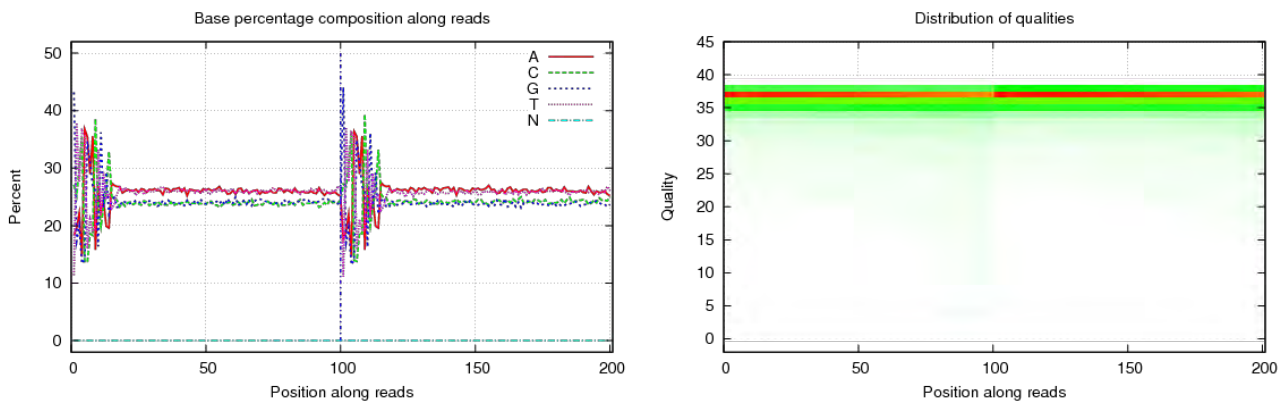


Figure 14 2EA

In the left figure, x-axis represents base position along reads, y-axis represents base percentage at the position; each color represents a type of nucleotide. Under normal conditions, the sample does not have AT/GC separation. It is normal to see fluctuations in the first several bp positions, which is caused by random primer and the instability of enzyme-substrate binding at the beginning of the sequencing reaction. In the right figure, x-axis represents base position along reads, y-axis represents base quality; each dot represents the base quality of the corresponding position along reads, color intensity reflects the number of nucleotides, a more intense color along a quality value indicates a higher proportion of this quality in the sequencing data.

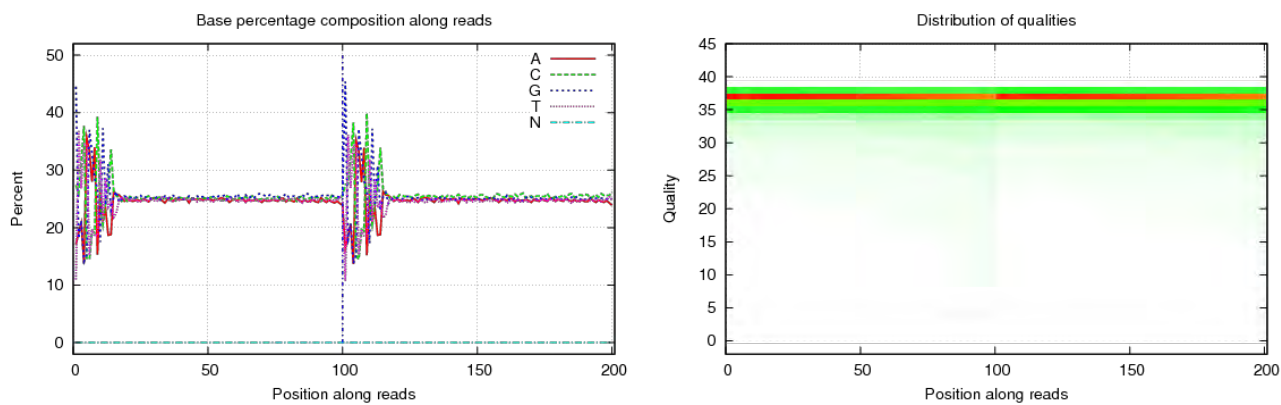


Figure 15 CSA

In the left figure, x-axis represents base position along reads, y-axis represents base percentage at the position; each color represents a type of nucleotide. Under normal conditions, the sample does not have AT/GC separation. It is normal to see fluctuations in the first several bp positions, which is caused by random

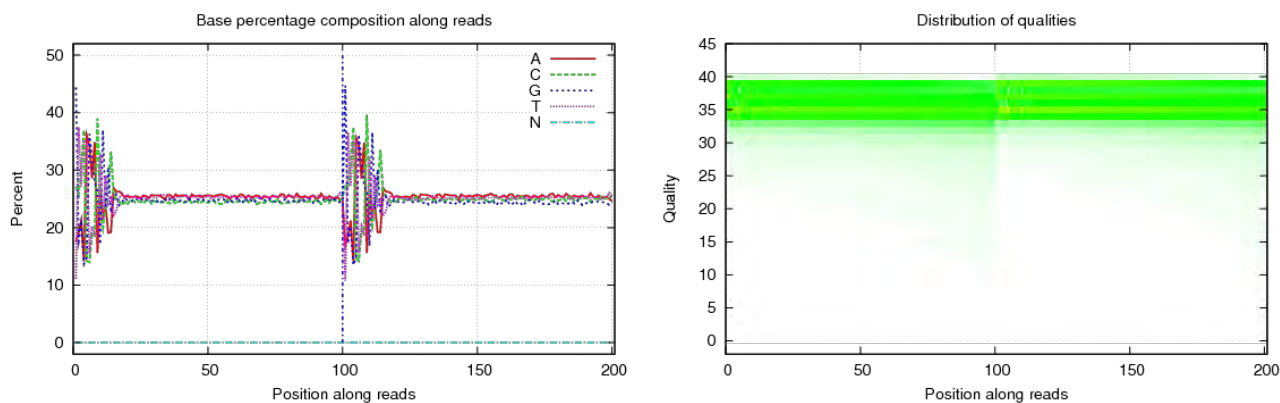


Figure 16 2SA

In the left figure, x-axis represents base position along reads, y-axis represents base percentage at the position; each color represents a type of nucleotide. Under normal conditions, the sample does not have AT/GC separation. It is normal to see fluctuations in the first several bp positions, which is caused by random primer and the instability of enzyme-substrate binding at the beginning of the sequencing reaction. In the right figure, x-axis represents base position along reads, y-axis represents base quality; each dot represents the base quality of the corresponding position along reads, color intensity reflects the number of nucleotides, a more intense color along a quality value indicates a higher proportion of this quality in the sequencing data.

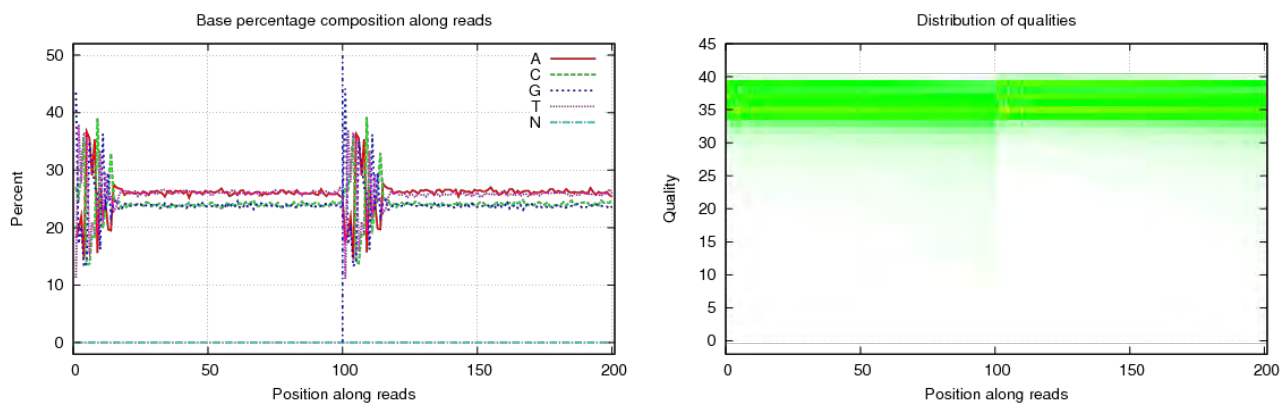


Figure 17 9EA

In the left figure, x-axis represents base position along reads, y-axis represents base percentage at the position; each color represents a type of nucleotide. Under normal conditions, the sample does not have AT/GC separation. It is normal to see fluctuations in the first several bp positions, which is caused by random

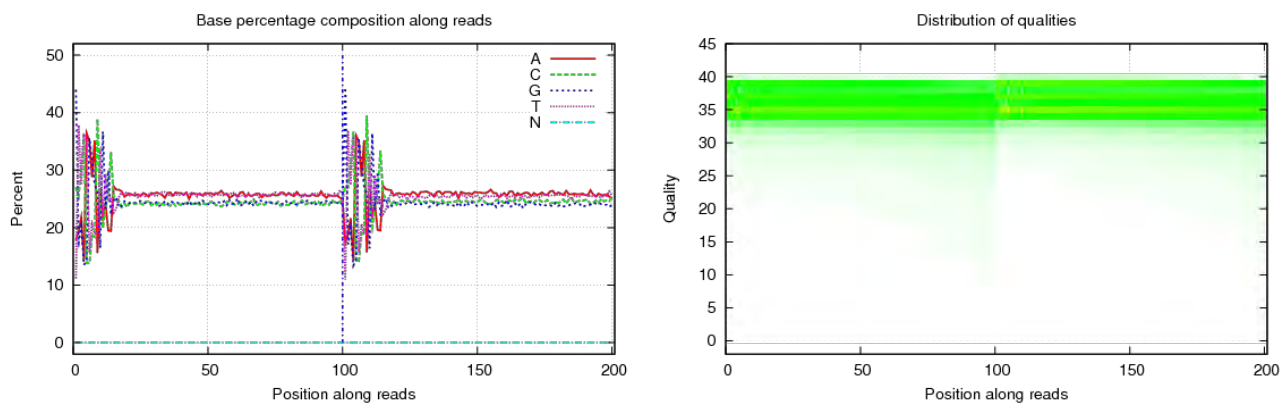


Figure 18 5EA

In the left figure, x-axis represents base position along reads, y-axis represents base percentage at the position; each color represents a type of nucleotide. Under normal conditions, the sample does not have AT/GC separation. It is normal to see fluctuations in the first several bp positions, which is caused by random primer and the instability of enzyme-substrate binding at the beginning of the sequencing reaction. In the right figure, x-axis represents base position along reads, y-axis represents base quality; each dot represents the base quality of the corresponding position along reads, color intensity reflects the number of nucleotides, a more intense color along a quality value indicates a higher proportion of this quality in the sequencing data.

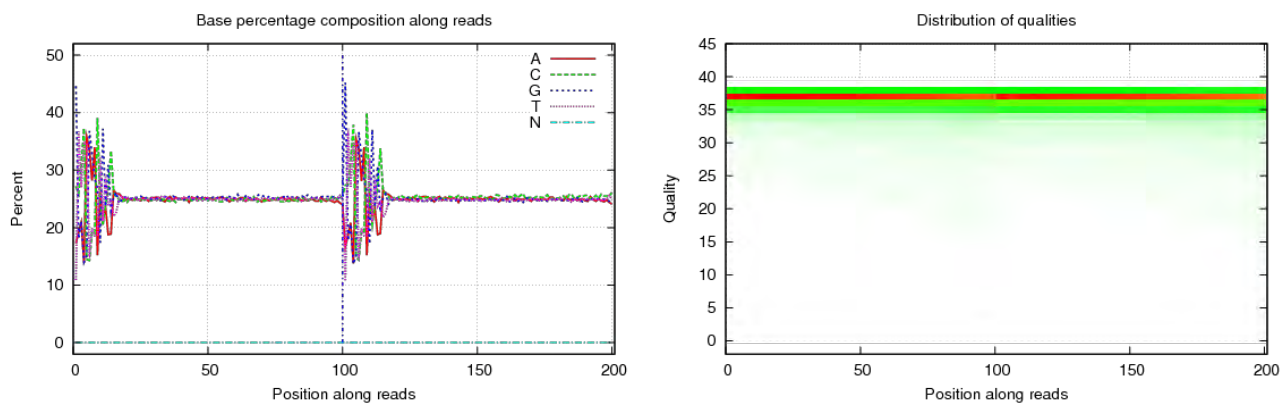


Figure 19 BSA

In the left figure, x-axis represents base position along reads, y-axis represents base percentage at the position; each color represents a type of nucleotide. Under normal conditions, the sample does not have AT/GC separation. It is normal to see fluctuations in the first several bp positions, which is caused by random



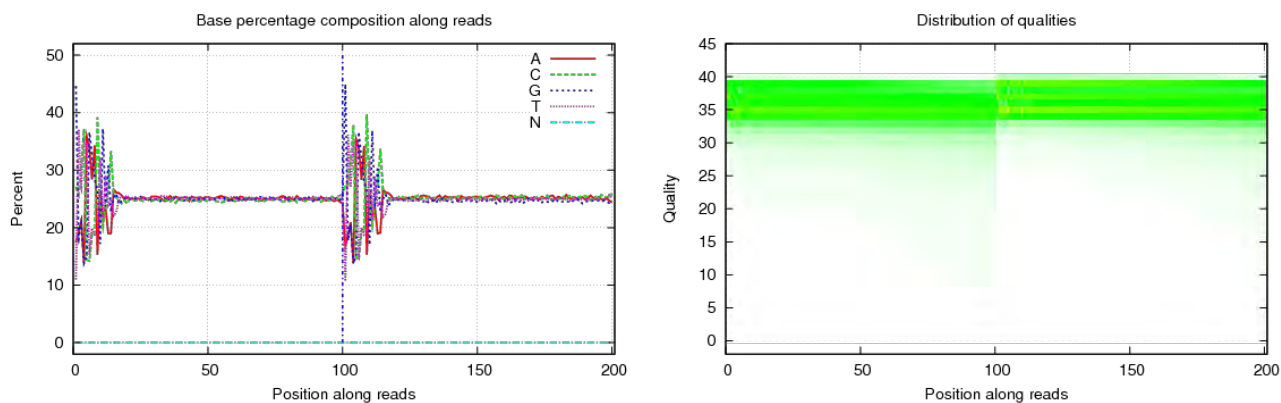


Figure 20 4SA

In the left figure, x-axis represents base position along reads, y-axis represents base percentage at the position; each color represents a type of nucleotide. Under normal conditions, the sample does not have AT/GC separation. It is normal to see fluctuations in the first several bp positions, which is caused by random primer and the instability of enzyme-substrate binding at the beginning of the sequencing reaction. In the right figure, x-axis represents base position along reads, y-axis represents base quality; each dot represents the base quality of the corresponding position along reads, color intensity reflects the number of nucleotides, a more intense color along a quality value indicates a higher proportion of this quality in the sequencing data.

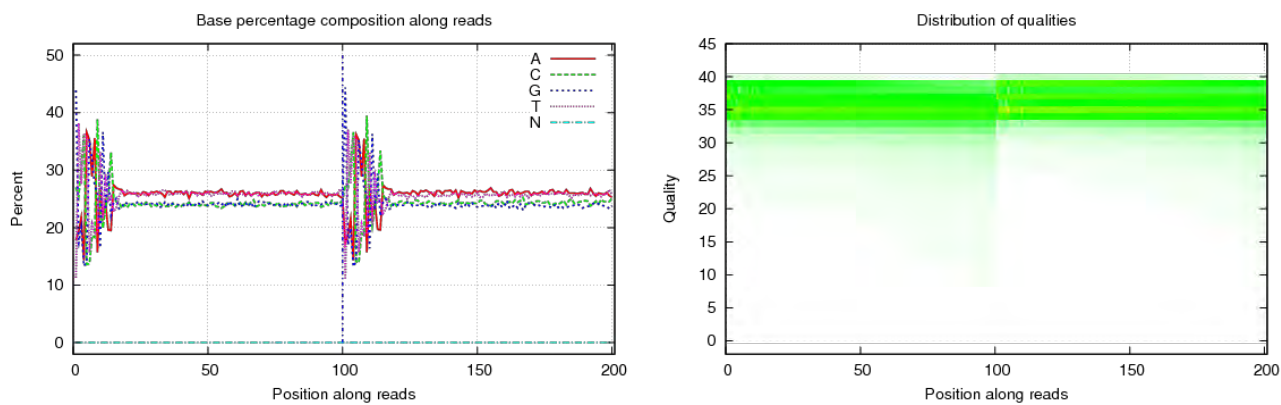


Figure 21 3EA

In the left figure, x-axis represents base position along reads, y-axis represents base percentage at the position; each color represents a type of nucleotide. Under normal conditions, the sample does not have AT/GC separation. It is normal to see fluctuations in the first several bp positions, which is caused by random

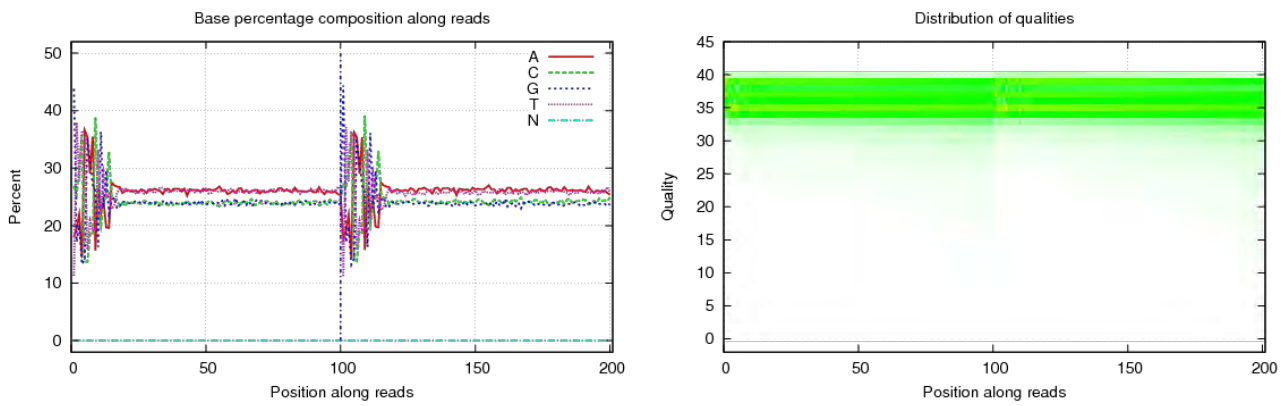


Figure 22 7EA

In the left figure, x-axis represents base position along reads, y-axis represents base percentage at the position; each color represents a type of nucleotide. Under normal conditions, the sample does not have AT/GC separation. It is normal to see fluctuations in the first several bp positions, which is caused by random primer and the instability of enzyme-substrate binding at the beginning of the sequencing reaction. In the right figure, x-axis represents base position along reads, y-axis represents base quality; each dot represents the base quality of the corresponding position along reads, color intensity reflects the number of nucleotides, a more intense color along a quality value indicates a higher proportion of this quality in the sequencing data.

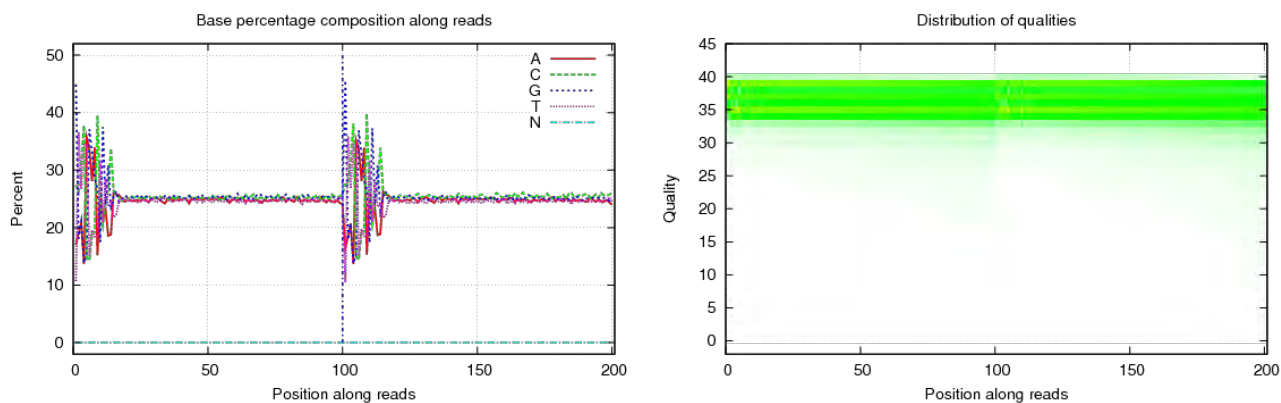


Figure 23 5SA

In the left figure, x-axis represents base position along reads, y-axis represents base percentage at the position; each color represents a type of nucleotide. Under normal conditions, the sample does not have AT/GC separation. It is normal to see fluctuations in the first several bp positions, which is caused by random

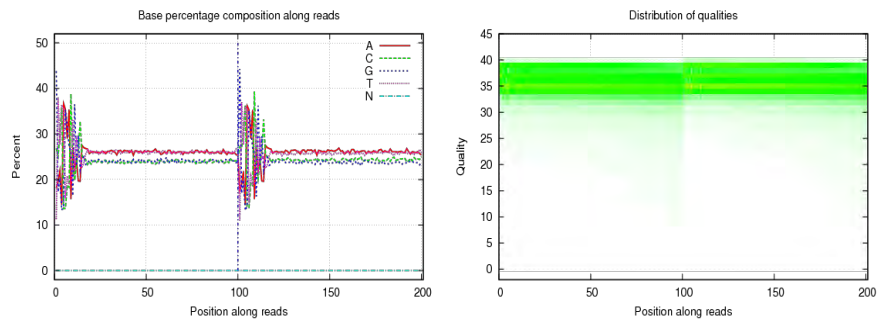


Figure 24

In the left figure, x-axis represents base position along reads, y-axis represents base position; each color represents a type of nucleotide. Under normal conditions, the sample AT/GC separation. It is normal to see fluctuations in the first several bp positions, which is primer and the instability of enzyme-substrate binding at the beginning of the sequencing reaction. figure, x-axis represents base position along reads, y-axis represents base quality; each dot base quality of the corresponding position along reads, color intensity reflects the number of more intense color along a quality value indicates a higher proportion of this quality in the

## 4 References

[1] [SOAPnuke: a MapReduce acceleration-supported software for integrated quality control and preprocessing of high-throughput sequencing data.](#)

Chen Y, Chen Y, Shi C, et al.

PMID: 29220494 PMCID: PMC5788068 DOI: 10.1093/gigascience/gix120

## Methods

### 1 Experimental procedure

The library construction method and sequencing process are carried out according to the following steps:

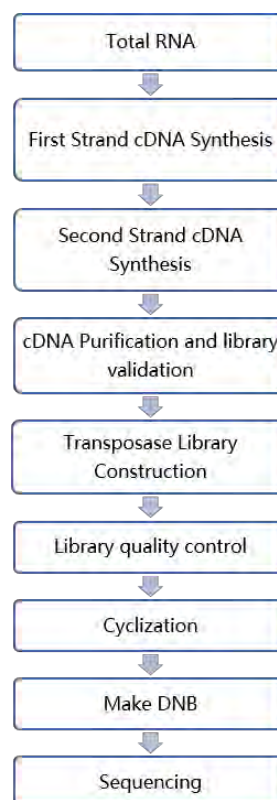


Figure 1 Workflow of experiment

8. Take appropriate amount of total RNA samples, and add oligo-dT reverse transcription primer and denature the total RNA sample by heat;
9. Add the reverse mix reagent, and reverse transcribed to first-strand cDNA by SMART amplification technology;
10. Synthesize the second-strand cDNA, and use magnetic beads to purify the cDNA, and validate the cDNA;
11. The qualified double stranded cDNA, were used to construct the library with transposase;

12. The library was qualified by the Agilent Technologies 2100 bioanalyzer;
13. The library was circularized;
14. Sequencing: The library was amplified to make DNA nanoball (DNB) and sequenced on DNBSEQ platform.

## 2 Bioinformatic analysis workflow

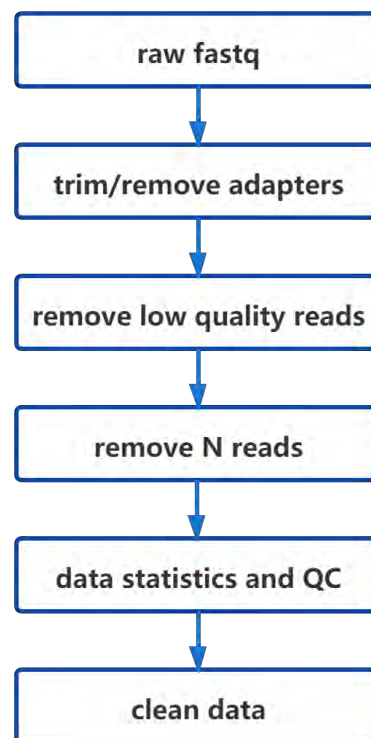


Figure 2 Bioinformatic analysis workflow

## 3 Parameters for data filtering

Raw data with adapter sequences or low-quality sequences was filtered. We first went through a series of data processing to remove contamination and obtain valid data. This step was completed by SOAPnuke software developed by BGI.

SOAPnuke software filter parameters: "-n 0.001 -l 20 -q 0.4 --adaMR 0.25 --ada\_trim --minReadLen 100", steps of filtering:

6. Filter adapter: if the sequencing read matches 25.0% or more of the adapter sequence (maximum 2 base mismatches are allowed), cut the adapter;
7. Filter read length: if the length of the sequencing read is less than 100 bp, discard the entire read;
8. Remove N: if the N content in the sequencing read accounts for 0.1% or more of the entire read, discard the entire read;
9. Filter low-quality data: if the bases with a quality value of less than 20 in the sequencing read account for 40.0% or more of the entire read, discard the entire read;
10. Obtain Clean reads: the output read quality value system is set to Phred+33.

## 4 References

[1] [SOAPnuke: a MapReduce acceleration-supported software for integrated quality control and preprocessing of high-throughput sequencing data.](#)

Chen Y, Chen Y, Shi C, et al.

PMID: 29220494 PMCID: PMC5788068 DOI: 10.1093/gigascience/gix120



## Help

### 1 FASTQ format description

Images generated by sequencers are converted by base calling into nucleotide sequences, which are called raw data or raw reads and are stored in FASTQ format. FASTQ files are text files that store both reads sequences and their corresponding quality scores. Each read is described in four lines as follows:

```
@V350016857L4C001R0010000078/1
TTTTTCTGCTCCTTTTGATGCTATTAACAATTGCTTCAAGTTCAAGGGCACCTGCCTCAAAGTCCC
TTTCTTCCAGACAAAATCTG +
=,DDE@EFFF=DFDEFCCFDEFEGFEEAFDFFE=FFCFFEEEDFDEEEFDF8FFEFFEFF:FFEDF
=EFDGE<1FDCEFFFFDFE
```

The first line is the sequence identifier and related description information, starting with '@'; the second line is the base sequence information; the third line starts with '+', followed by the sequence identifier, description information, or nothing; The four lines are quality information, which corresponds to the sequence in the second line. Each base has a quality score. Depending on the scoring system, each character represents a different quality value.

The figure below shows the concise correspondence between the sequencing error rate and the sequencing quality value. Specifically, if the sequencing error rate is denoted by E and the base quality value is denoted by SQ, there are the following relationships:

$$SQ = -10 \times (\log \frac{E}{1-E}) / (\log 10)$$

$$E = \frac{Y}{1+Y}$$

$$Y = \frac{SQ}{e^{-10 \times \log 10}}$$

- For the quality system data with a sequencing quality value of 33: the sequencing quality value of the base = the ASCII value corresponding to the quality information character -33, for example, the ASCII value corresponding to A is 65, then the corresponding base quality value is 65-33 = 32. The base quality value of the DNBSEQ sequencing platform ranges from 2 to 42.

2. For quality system data with a sequencing quality value of 64: the sequencing quality value of the base = the ASCII value corresponding to the quality information character -64, for example, the corresponding ASCII value of c is 99, then the corresponding base quality value is  $99-64=35$ .

The base quality value of the DNBSEQ sequencing platform ranges from 2 to 43.

Table 1 A summary table of the relationship between sequencing error rate and sequencing quality

Sequencing error rate	Sequencing quality value	Character(Phred64)	Character(Phred33)
5%	13	M	.
1%	20	T	5
0.1%	30	^	?

## Appendix 4

Letter Confirming Ethical Approval from MMU for project.

29/06/2022



**Project Title:** Investigating Implantation - developing clinical applications from in vitro models

**EthOS Reference Number:** 35999

### **Certification**

Dear Helen Hunter,

The above application was reviewed by the Research Ethics and Governance Team and on the 29/06/2022, was certified. The certification is in place until the end of your project and is based on the documentation submitted with your application.

### *Application Documents*

Document Type	File Name	Date	Version
Additional Documentation	research proposal for HSST Final Version	02/09/2021	1
External Approval Letter	REC approval 20.11.12	20/06/2022	1
External Approval Application Form	Final REC form for submission 26.10.12	20/06/2022	1
External Approval Supporting Information	Ethos letter PDF daniel docs	20/06/2022	1
External Approval Supporting Information	R03046 Approval Letter Signed_33	20/06/2022	1
Additional Documentation	IRAS 294303 Letter of HRA Approval 05.08.21 endo samples	20/06/2022	1

### **Conditions of certification**

The Research Ethics and Governance Team would like to highlight the following conditions

#### Adherence to Manchester Metropolitan University's Policies and procedures

This certification is conditional on adherence to Manchester Metropolitan University's Policies, Procedures, guidance and Standard Operating procedures. These can be found on the Manchester Metropolitan University Research Ethics and Governance webpages.

#### Amendments

If you wish to make a change to this approved application, you will be required to submit an amendment in accordance with Health Research Authority guidelines, and inform Manchester Metropolitan University of the change. Please contact the Research Ethics and Governance team for advice around how to do this.

We wish you every success with your project.

Research Ethics and Governance Team

## Appendix 5

Tables of differentially expressed genes (DEG) from conditioned media co-culture experiments.

List 1: List of DEG: Epithelial cells exposed to media from successful embryos versus unsuccessful embryos (125 genes)

	logFC	logCPM	PValue	FDR
SRPX	5.200710195	3.775390027	0.000135101	0.041089814
RHOJ	4.527949369	2.360242727	3.14E-05	0.027823322
CTD-3035K23.3	4.497163969	3.271077867	9.82E-05	0.039000942
Mar-04	4.262009904	2.43201661	0.000124113	0.041089814
VEGFC	4.208096683	3.266207774	0.000112736	0.041089814
TBC1D4	4.174512778	3.322194144	6.18E-05	0.03894374
HOXA-AS3	4.060537545	4.395685946	7.80E-05	0.03894374
MOXD1	4.035189968	2.589247023	1.33E-07	0.001905548
HAND2	4.03454477	4.043910863	0.000120784	0.041089814
RP11-1252I4.2	3.998483679	-1.93378111	0.000216333	0.049486499
RP11-459E5.1	3.993159601	-1.916582735	0.000150806	0.042497022
PDE4B	3.950358491	5.228883815	3.21E-05	0.027823322
FOXL2NB	3.894397228	4.701926101	9.46E-05	0.039000942
GLI3	3.865541494	4.43189391	7.11E-05	0.03894374
SOCS2-AS1	3.752975569	2.018401961	2.09E-05	0.027228543
CXCL12	3.717504607	5.640721089	1.83E-05	0.027228543
ADAMTS5	3.708496506	5.105142701	9.52E-05	0.039000942
HOXD9	3.706295551	4.678077302	4.35E-05	0.034522918
TWIST1	3.68245022	3.16761039	0.000151595	0.042497022
AC079776.2	3.653565626	4.882089784	2.48E-05	0.027823322
LDB2	3.619386063	3.449830383	0.000201024	0.047504733
ADAM23	3.619326793	3.102878625	0.000187524	0.046224666
VAT1L	3.561902641	4.632939471	0.000198225	0.047504733
TMEM119	3.414322661	7.142640244	1.10E-05	0.027228543
ZNF521	3.413989364	1.015095776	0.000137487	0.041089814
PDPN	3.394817296	4.563314049	0.00020102	0.047504733

COL5A1	3.381790717	9.12528053	9.83E-06	0.027228543
HOXD10	3.346324784	5.287614116	7.56E-05	0.03894374
SYNPO	3.328683414	5.153960204	3.48E-07	0.003320709
DCN	3.316892137	8.474944247	2.54E-05	0.027823322
SPARC	3.316436902	11.00087378	1.45E-05	0.027228543
PDGFRB	3.316074807	8.341886996	1.62E-05	0.027228543
RUNX1T1	3.300998879	4.780897599	0.000131299	0.041089814
CD248	3.261562596	9.702666911	2.98E-05	0.027823322
HAND2-AS1	3.248379972	4.103839876	0.00012804	0.041089814
PRELP	3.22529088	5.512048912	8.56E-05	0.03894374
MEG3	3.201541669	8.327954098	1.97E-05	0.027228543
AEBP1	3.180405963	8.276807979	1.88E-05	0.027228543
COL3A1	3.17823359	12.26561011	2.99E-05	0.027823322
ADPRH	3.175079281	-0.02617509	8.58E-05	0.03894374
MIR503HG	3.171152227	5.641299525	9.77E-05	0.039000942
COL6A2	3.15787697	10.82623239	3.01E-05	0.027823322
S1PR3	3.150558413	7.604129995	1.60E-05	0.027228543
BGN	3.143450812	7.533658686	1.70E-05	0.027228543
PAPPA-AS1	3.13931276	4.210338406	5.13E-05	0.03894374
RP11-334E6.12	3.135030184	8.233992255	1.75E-05	0.027228543
MIR143HG	3.133255459	6.17469173	1.76E-05	0.027228543
GYPC	3.126789657	6.82257848	8.41E-05	0.03894374
CCL2	3.124860429	8.603584499	7.43E-05	0.03894374
ADAMTS12	3.123653975	4.112293539	0.000113582	0.041089814
HOXA10	3.116227181	4.936471073	0.000134928	0.041089814
LUM	3.091298539	6.783267869	0.000186064	0.046224666
COL8A1	3.08493339	9.106266777	1.58E-05	0.027228543
SULF1	3.07046839	8.699405662	4.02E-05	0.033775103
MRC2	3.068224754	8.560409789	1.18E-05	0.027228543
TIMP3	3.053341018	10.10431508	2.28E-05	0.027228543
CHI3L1	3.052834919	10.77906103	1.34E-05	0.027228543
ISLR	3.040827579	9.327978182	9.36E-05	0.039000942
HLX	3.027373891	5.647826976	0.000166763	0.044985191
RP11-123M6.2	3.024696073	5.425480407	0.000181452	0.046224666

COL6A3	3.023043129	9.450367463	2.79E-05	0.027823322
PSG1	3.022035292	5.219813093	8.54E-05	0.03894374
RP11-554A11.5	3.018250351	5.44876038	0.000131393	0.041089814
GGT5	3.003126976	5.879704728	5.54E-05	0.03894374
THY1	2.994352826	9.339540512	2.19E-05	0.027228543
DPT	2.922844078	5.815987061	0.000193097	0.046791553
SHC3	2.874289573	4.768467492	2.29E-05	0.027228543
CTD-2033D15.3	2.847504112	7.215550572	9.04E-05	0.039000942
CEND1	2.832263373	1.586273757	0.000154247	0.042798668
THBS1	2.825458357	9.108401587	5.38E-05	0.03894374
CPXM1	2.82257891	6.855198344	0.000102659	0.039560081
MRGPRF	2.807003155	6.65599932	0.000111195	0.041089814
OSR2	2.799131644	6.559877073	0.00012383	0.041089814
CCND2	2.775745095	5.471169213	0.00014257	0.041089814
HOXD11	2.763379544	4.624234315	0.000175838	0.046127526
MSRB3	2.759650895	5.835315089	0.000130717	0.041089814
CLDN11	2.757255913	6.456857341	0.000131568	0.041089814
MFAP4	2.689301511	8.856355658	6.39E-05	0.03894374
GREM1	2.684057535	5.919928768	8.47E-05	0.03894374
C1QTNF1	2.683744448	5.05772708	0.000215513	0.049486499
ACTG2	2.676624794	7.945996556	5.46E-05	0.03894374
NLRP1	2.668919709	4.00950001	0.000127146	0.041089814
THBS2	2.655240066	6.628076469	5.92E-05	0.03894374
UCHL1	2.652737514	7.174800013	9.46E-05	0.039000942
FAP	2.636734604	5.896911229	0.000189759	0.04637577
FILIP1L	2.608514205	7.706892318	9.94E-06	0.027228543
MYL9	2.591696832	9.064261534	3.08E-05	0.027823322
COL5A2	2.551018414	8.081930558	0.000185803	0.046224666
CTD-2541J13.2	2.550177707	5.398112306	0.000163368	0.044489005
MMP2	2.504693312	8.502239433	0.000103087	0.039560081
COL1A1	2.495089769	12.69571163	1.93E-05	0.027228543
SEMA5A	2.488616302	7.412751733	8.04E-05	0.03894374
Xyac-YX65C7_A.2	2.387032163	6.369302396	0.000130135	0.041089814
ITGA11	2.379723044	7.803913695	7.00E-05	0.03894374

PAPPA	2.337171605	5.32213551	9.47E-05	0.039000942
PAMR1	2.330445144	7.818059087	0.000184146	0.046224666
UCN2	2.326798897	3.894556162	6.81E-05	0.03894374
PTGDS	2.311177583	7.204495943	0.000138061	0.041089814
MRAS	2.294753373	3.828270962	7.12E-05	0.03894374
EGR3	2.290759018	1.823637457	1.07E-05	0.027228543
SELM	2.260428499	8.478698675	0.000103763	0.039560081
SSC5D	2.242727352	5.946578822	8.38E-05	0.03894374
ZCCHC24	2.241642898	6.265352632	0.000209457	0.049091971
RP11-648L3.2	2.223610863	0.75603542	0.000213683	0.049486499
CARD16	2.088576689	5.930848506	9.76E-05	0.039000942
PDGFRA	1.993435721	6.847577268	0.000155664	0.042798668
SPON2	1.961280242	7.795440111	8.47E-05	0.03894374
TAGLN	1.944958877	10.64960903	7.12E-05	0.03894374
GNAO1	1.884023415	3.608040473	0.000137199	0.041089814
C1R	1.86193547	9.092537185	7.27E-05	0.03894374
ANPEP	1.854161011	6.075029596	0.000117434	0.041089814
CPZ	1.83556472	6.696174328	0.000118701	0.041089814
PCOLCE-AS1	1.77812441	8.300795585	0.000143701	0.041089814
GLI2	1.667544235	3.647139705	7.68E-08	0.001905548
GPR78	1.614152936	6.68365582	8.40E-05	0.03894374
BDKRB2	1.595645344	7.88934042	0.0001703	0.045371256
PRKCDBP	1.544805633	8.507340186	0.00018659	0.046224666
RCN3	1.170253355	7.836102825	0.000171368	0.045371256
FRMD6	1.134097922	5.126860266	0.000142728	0.041089814
LAMA2	1.128701031	3.706167354	4.15E-05	0.033884165
STAMBPL1	1.124293823	4.793303788	7.94E-05	0.03894374
TGFB1I1	1.085235005	7.464092676	0.000139627	0.041089814
DCLK2	0.980898259	2.7057981	0.000140465	0.041089814
NBEA	0.467683517	3.356640084	7.48E-05	0.03894374
ZNF442	-2.033246486	-1.403326514	0.000185344	0.046224666

List 2: List of DEG: Epithelial cells exposed to media from successful embryos versus untreated (control) media (117 genes)

	logFC	logCPM	PValue	FDR
AC079776.2	4.732221853	4.882089784	7.02E-05	0.030427106
ACTG2	4.823479409	7.945996556	4.36E-06	0.006923921
ADAMTS12	5.575232778	4.112293539	6.36E-05	0.029612587
ADAMTS2	5.358431279	5.273118041	5.29E-05	0.029128599
ADRA2C	8.147711691	4.700014586	9.89E-05	0.036271711
AEBP1	3.93355265	8.276807979	3.82E-05	0.022754943
ANGPTL2	3.370531497	4.662348827	4.28E-05	0.024984326
BGN	5.556055542	7.533658686	3.92E-06	0.006923921
C1QTNF1	4.060104131	5.05772708	0.000135482	0.042332469
CCL2	6.339235711	8.603584499	4.23E-06	0.006923921
CCND2	4.145509944	5.471169213	9.89E-05	0.036271711
CD248	5.840890481	9.702666911	2.21E-06	0.006392834
CDH11	5.904223771	4.451842065	9.34E-05	0.03560519
CDH13	3.874870577	7.029045457	0.000122031	0.040611676
CH17-13I23.3	5.571332642	1.691729228	6.01E-05	0.029612587
CHI3L1	4.754555578	10.77906103	1.92E-06	0.006392834
CLDN11	4.239465574	6.456857341	6.37E-05	0.029612587
CNN1	3.416718997	6.212056959	3.03E-05	0.020207097
COL1A1	3.255742688	12.69571163	1.21E-05	0.012345823
COL3A1	5.898700677	12.26561011	6.92E-07	0.006392834
COL5A1	5.305842175	9.12528053	2.84E-06	0.006392834
COL5A2	4.270979309	8.081930558	2.38E-05	0.01873331
COL6A2	5.481777525	10.82623239	1.75E-06	0.006392834
COL6A3	4.784022113	9.450367463	4.90E-06	0.007299608
COL8A1	5.712420167	9.106266777	9.07E-07	0.006392834
CPXM1	3.593406587	6.855198344	0.000158621	0.044977681
CTD-2033D15.3	4.39421118	7.215550572	3.74E-05	0.022754943
CTD-2541J13.2	4.049464109	5.398112306	6.70E-05	0.029931956
CXCL12	5.943687922	5.640721089	2.37E-05	0.01873331
DCN	6.512089216	8.474944247	2.43E-06	0.006392834
DKK3	2.951841974	7.738972291	0.000163793	0.045470826
DPT	5.487162818	5.815987061	6.07E-05	0.029612587



DPYSL3	4.330687465	6.539263876	1.76E-05	0.016190829
DSEL	3.773230614	6.289495665	0.000199698	0.04922557
FAP	3.556035501	5.896911229	0.000192051	0.048597287
FILIP1L	3.012905766	7.706892318	2.98E-05	0.020207097
FOXL2NB	6.090430737	4.701926101	0.000158871	0.044977681
FSIP1	2.707523568	6.584547765	0.000112796	0.038858782
GBP4	1.104317269	3.83970132	0.000181368	0.047578351
GGT5	4.99298295	5.879704728	2.79E-05	0.020207097
GREM1	3.526705462	5.919928768	0.000104671	0.037081209
GRK5	1.263817611	5.309169427	7.87E-05	0.032086875
GYPC	5.527853113	6.82257848	2.87E-05	0.020207097
HAND2-AS1	4.607640184	4.103839876	0.000179422	0.047503641
HLX	4.371407834	5.647826976	0.000175802	0.047423359
HOXA10	4.253887911	4.936471073	0.000197577	0.04922557
HOXA11-AS	7.94873129	4.638051667	0.000178699	0.047503641
HOXA5	6.462337932	3.147177954	6.49E-05	0.029612587
HOXD10	5.142012069	5.287614116	8.16E-05	0.032097566
HOXD11	4.201556787	4.624234315	0.000122145	0.040611676
HOXD9	5.476057415	4.678077302	7.54E-05	0.031235889
INHBA	4.684776749	5.023523008	0.000149612	0.044103172
ISLR	5.643888827	9.327978182	5.92E-06	0.008059392
ITGA11	3.253397218	7.803913695	3.81E-05	0.022754943
KIF3C	1.245455104	3.27641479	0.000162764	0.045470826
LINC01119	2.885461249	1.720064644	5.38E-05	0.029128599
LOXL4	2.395862435	6.146366376	0.000188131	0.048463107
LUM	4.637712167	6.783267869	0.000132805	0.042193711
MAGI2-AS3	7.281022606	3.657657755	0.000199456	0.04922557
MASP1	2.562808726	6.934817725	0.00015617	0.044977681
MEG3	5.756761444	8.327954098	2.91E-06	0.006392834
MEG8	6.582052058	5.269936731	0.000119249	0.040593013
MFAP4	4.026522031	8.856355658	1.63E-05	0.01560431
MIR143HG	4.300023796	6.17469173	2.42E-05	0.01873331
MIR503HG	4.82981123	5.641299525	9.29E-05	0.03560519
MMP2	3.482026965	8.502239433	4.78E-05	0.027327037
MMP3	3.258527513	7.638551698	0.000143179	0.043095512
MOXD1	4.962298591	2.589247023	8.47E-07	0.006392834
MRC2	3.660440906	8.560409789	3.06E-05	0.020207097
MRGPRF	4.249836817	6.65599932	6.18E-05	0.029612587
MSRB3	4.379159457	5.835315089	6.22E-05	0.029612587
MYL9	3.657987877	9.064261534	1.12E-05	0.011855103
NEXN	1.074804826	4.542302679	9.56E-06	0.011216212
OSR2	5.285462786	6.559877073	2.18E-05	0.01873331

PAMR1	5.3750909	7.818059087	1.86E-06	0.006392834
PAPPA-AS1	4.685359275	4.210338406	5.40E-05	0.029128599
PCBP3	4.242702792	2.19794184	7.01E-05	0.030427106
PDE4B	4.39338811	5.228883815	0.000186284	0.048423615
PDGFRB	4.872886971	8.341886996	1.01E-05	0.011216212
POSTN	5.605023767	7.218215433	3.43E-05	0.021817995
PRKCDBP	2.027072942	8.507340186	7.97E-05	0.032086875
PRRX1	6.431855941	5.731960961	7.20E-05	0.03071731
PSG1	4.029456101	5.219813093	0.000136203	0.042332469
PTN	5.345803328	4.731357392	2.68E-05	0.020149487
PTPRG-AS1	1.086840092	1.369483402	0.000101821	0.036854025
RHOJ	5.902042371	2.360242727	0.000106339	0.037081209
RP11-123M6.2	5.912689964	5.425480407	6.45E-05	0.029612587
RP11-334E6.12	4.76391198	8.233992255	7.14E-06	0.009285126
RP11-413E6.1	6.043157875	1.142123487	0.000130977	0.042193711
RP11-417E7.1	4.514537631	2.79778557	0.000143026	0.043095512
RP11-498P14.5	2.666479235	-0.616388509	0.000192022	0.048597287
RP11-521B24.3	-0.892237211	1.760302807	0.000142532	0.043095512
RP11-554A11.5	4.908630802	5.44876038	8.19E-05	0.032097566
S1PR3	5.181264652	7.604129995	5.11E-06	0.007299608
SELM	2.712522523	8.478698675	0.000156117	0.044977681
SEMA5A	4.972532603	7.412751733	3.44E-06	0.006750046
SGCD	5.951075733	0.995705051	0.000165583	0.045525902
SLC24A3	6.246284164	2.622102196	1.64E-05	0.01560431
SNHG23	4.851761377	4.671846915	0.000106243	0.037081209
SPARC	5.947479255	11.00087378	6.32E-07	0.006392834
SPOCD1	4.012447082	5.861706624	9.53E-05	0.035862863
SPON2	2.516247243	7.795440111	6.09E-05	0.029612587
SSC5D	3.50936922	5.946578822	2.08E-05	0.018542341
SULF1	5.927887654	8.699405662	2.73E-06	0.006392834
SYNPO	2.723861661	5.153960204	3.11E-05	0.020207097
TAGLN	2.402618595	10.64960903	6.52E-05	0.029612587
THBS1	4.414902528	9.108401587	1.02E-05	0.011216212
THBS2	3.063481379	6.628076469	0.000171631	0.046739259
THNSL2	5.88982516	4.287576925	0.000145255	0.043264808
THY1	4.771595726	9.339540512	3.54E-06	0.006750046
TIMP3	5.156315412	10.10431508	1.86E-06	0.006392834
TMEM119	5.306142522	7.142640244	8.01E-06	0.009956942
TNFSF18	6.337959833	4.86114184	0.000132029	0.042193711
UCHL1	4.276643931	7.174800013	2.41E-05	0.01873331
VEGFC	6.73492529	3.266207774	0.000201558	0.049259431
VGLL3	5.126859607	4.442919958	0.000127686	0.04196619

WASF3	3.915062031	2.64771948	7.38E-05	0.031034328
-------	-------------	------------	----------	-------------

List 3: List of DEG: Epithelial cells exposed to media from unsuccessful embryos versus untreated (control) media (1 gene)

gene	logFC	logCPM	PValue	FDR
GLI2	-1.876104612	3.647139705	2.38E-08	0.000681058

List 4: List of DEG: Stromal cells exposed to media from successful embryos versus unsuccessful embryos (6 genes)

gene	logFC	logCPM	PValue	FDR
RNF183	-3.136389562	6.217860327	1.02E-05	0.048494178
GCNT2	-3.020209132	4.292283409	3.31E-06	0.031560199
PLEKHA7	-2.493537642	3.885058268	7.14E-06	0.040858127
MECOM	-2.062412921	5.661801976	2.49E-06	0.031560199
RN7SL2	1.216373314	6.745175837	1.19E-06	0.031560199
RN7SL5P	2.624003763	4.426963751	6.81E-06	0.040858127

List 5: List of DEG: Stromal cells exposed to media from successful embryos versus untreated (control) media (1 gene)

gene	logFC	logCPM	PValue	FDR
S100A8	-4.943505388	1.942727642	1.69E-07	0.004830608

List 6: List of DEG: Stromal cells exposed to media from unsuccessful embryos versus untreated (control) media (207 genes)

	logFC	logCPM	PValue	FDR
PITX2	7.257408709	4.728086455	0.000205483	0.039433438
PSPHP1	7.100490534	4.279766656	0.000153719	0.033136182
HNF1A-AS1	6.75003128	4.166185351	0.000352333	0.049469455
ECEL1P1	6.332822343	5.352042286	0.000227813	0.041711749
CDC20B	5.902468002	6.407624817	2.62E-05	0.020228595
SCGB1D2	5.79143872	8.724340967	2.26E-06	0.009894229

SLC52A3	5.667466635	4.394170843	0.000352458	0.049469455
ALPPL2	5.665207006	7.926033084	1.35E-05	0.018019568
UNC93A	5.648639399	4.754115766	0.000109061	0.028657043
AGR3	5.549709071	5.99251549	3.80E-05	0.02088857
HLA-DQB1	5.541112262	4.482170244	0.000312072	0.047464773
SMOC2	5.521755187	4.756530228	1.70E-05	0.018019568
SCGB2A1	5.515208404	11.00421594	2.13E-06	0.009894229
RP11-627G23.1	5.505620352	4.720871135	0.000101839	0.02775015
LDLRAD1	5.44002396	4.753818353	0.00032601	0.048241597
RP11-532E4.2	5.309566314	7.577148419	8.99E-06	0.017871244
PLEKHS1	5.275968236	6.090263455	1.54E-05	0.018019568
SCGB2A2	5.250437283	6.088262656	1.79E-05	0.018019568
RP11-706C16.8	5.22336214	6.496321914	0.000291499	0.04698273
RNASE1	5.189080023	6.316492363	3.12E-05	0.020752334
LY6D	5.181836422	7.671868154	3.53E-05	0.02088857
TFF3	5.160139577	10.70690448	1.89E-06	0.009894229
SCARNA21~1	5.067631411	-2.081363046	0.000144012	0.032749148
MUC5B	5.065233509	11.68741359	5.55E-06	0.014433434
ALPP	5.031151292	8.06684433	4.22E-06	0.0120571
SCNN1G	5.016906204	5.032274911	0.00022098	0.04129875
C1orf168	4.965744175	4.013768371	5.69E-05	0.021374567
MUC5AC	4.9611544	9.153515926	1.10E-05	0.018019568
ERICH3	4.959768491	4.674754575	0.000297806	0.04698273
RP11-214C8.2	4.932532858	0.549094397	5.55E-05	0.021374567
RP11-319F12.2	4.879336004	4.888182863	5.41E-05	0.021374567
SPINK5	4.862604543	5.140219175	0.000171678	0.03506402
HLA-DMB	4.854730819	8.419755762	1.96E-06	0.009894229
RIMBP2	4.777148666	4.510835511	0.000107795	0.028657043
C6orf223	4.742755534	4.651780611	0.000211084	0.039971815
AC068134.8	4.692211954	6.115817493	1.70E-05	0.018019568
LINC01559	4.661168027	6.187396954	0.000121036	0.029835427
DNAH6	4.647356534	3.301607533	1.93E-05	0.018436871
TFF1	4.589583525	5.439354636	0.000352933	0.049469455
ADCYAP1R1	4.525015115	4.491809343	0.000328989	0.048241597
TRIM15	4.509316047	1.55025746	0.000352474	0.049469455
FHAD1	4.413295749	3.862934986	0.000327763	0.048241597
CCL20	4.290472917	7.392426342	3.44E-05	0.02088857
WDR72	4.255465115	2.873716379	0.000341037	0.049250583
CEACAM6	4.231595635	7.056320163	5.32E-05	0.021374567
S100P	4.164715639	5.856671062	0.000167636	0.034919178
MUC13	4.162140735	3.0520143	0.000194899	0.038434006
AC007255.8	4.130965906	2.073898878	1.67E-05	0.018019568

XXbac-BPG181M17.5	3.963653949	7.518914889	1.44E-05	0.018019568
GCNT2	3.949409616	4.292283409	2.50E-06	0.009894229
HLA-DRA	3.934304418	7.809345192	2.98E-05	0.020752334
CDS1	3.91995075	4.468882471	5.49E-05	0.021374567
FXYD3	3.857428366	6.562458249	5.20E-05	0.021374567
KLK11	3.72568864	6.949573738	8.47E-05	0.025754713
CALB1	3.613073345	8.625221573	9.37E-06	0.017871244
CTC-490G23.2	3.535701043	5.545754163	0.000255123	0.044149651
LINC00621	3.530090987	8.663943865	4.28E-05	0.0212164
AGR2	3.489333526	8.747972452	4.21E-05	0.0212164
RNF183	3.470492568	6.217860327	2.14E-05	0.01973342
ST6GALNAC1	3.45681381	6.037720054	5.53E-05	0.021374567
HLA-DRB1	3.446966075	7.67041762	5.18E-05	0.021374567
VWA3A	3.387632904	5.599640159	0.000136648	0.031583437
SERPINA1	3.256521473	9.924345686	1.83E-05	0.018019568
SLC44A4	3.244394025	7.698875005	6.41E-05	0.022357206
CDH1	3.230084386	5.776950146	0.000112422	0.02869387
LGR5	3.195162161	3.416528652	0.00028313	0.046527633
GRHL2	3.108619869	3.853140542	3.94E-05	0.02088857
EHF	3.013077632	6.535949768	9.56E-05	0.027572603
BASP1P1	2.983904237	7.884706537	8.85E-05	0.026358481
PLEKHA7	2.980419967	3.885058268	7.14E-06	0.017025248
C1orf186	2.947284246	8.39047352	2.77E-06	0.009894229
UCA1~1	2.886417987	8.206448554	7.98E-05	0.025149314
UCA1	2.854721499	10.35541462	4.17E-05	0.0212164
WFDC2	2.83837015	8.442164861	4.84E-05	0.021374567
FOLR1	2.766901126	5.135512876	2.56E-05	0.020228595
TMCS	2.719331559	6.746742587	3.31E-05	0.020870589
CTD-2531D15.5	2.703348833	6.842426641	1.14E-05	0.018019568
AC004510.3	2.676347523	8.507545139	0.000111394	0.02869387
HOOK1	2.670122001	3.75706151	0.000168526	0.034919178
SFTA2	2.646728108	6.22321495	0.000299044	0.04698273
CGN	2.589442712	5.03726115	0.000134835	0.031583437
EPCAM	2.582001622	7.944317193	3.17E-05	0.020752334
LRG1	2.576523717	5.208520788	9.49E-05	0.027572603
RP11-554D15.3	2.551838154	3.670080016	0.000323958	0.048241597
TGFA	2.54651823	5.320992674	4.38E-05	0.0212164
MPZL2	2.464868774	6.469585889	5.91E-05	0.021452046
CLDN10	2.406734726	7.780411125	1.48E-05	0.018019568
ASRGL1	2.317415981	8.30564706	1.41E-05	0.018019568
TC2N	2.287605198	3.954291533	2.50E-05	0.020228595
AC005077.14	2.237712419	4.404524752	8.12E-05	0.025149314

MUC16	2.237672224	10.54515655	0.000319965	0.048241597
NGEF	2.116005942	4.396367032	8.77E-06	0.017871244
RP11-703H8.7	2.10511219	5.751652214	0.00019028	0.03781906
VAV3	2.062960832	4.066349126	5.02E-07	0.009894229
MMP7	2.035996706	11.5227585	9.64E-05	0.027572603
SORL1	1.9651614	7.231157171	2.27E-05	0.019811768
KYNU	1.880695008	5.079359368	0.000136407	0.031583437
MECOM	1.868488723	5.661801976	3.05E-05	0.020752334
PROM1	1.866285933	6.439346811	6.79E-05	0.023388091
EGLN3	1.668006691	8.043913431	6.00E-05	0.021452046
TOB1-AS1	1.628811442	0.704598248	0.000231207	0.041711749
RP11-588K22.2	1.593822223	1.445113223	0.000231943	0.041711749
NLGN4X	1.469869532	4.212503179	0.000112964	0.02869387
CXADR	1.431663782	5.916265243	1.32E-05	0.018019568
CD24	1.414303486	8.294363462	3.84E-05	0.02088857
C2orf88	1.36744346	7.257060981	2.36E-05	0.019811768
RP11-10N23.4	1.18737522	1.098620652	0.000155286	0.033136182
CTC-498J12.3	1.120733576	1.908903375	4.65E-05	0.021374567
ZNF563	1.101539335	1.739213942	0.000282432	0.046527633
COMMD8	1.02866817	3.750702812	9.74E-05	0.027574832
CP	1.020682329	7.471666855	7.74E-05	0.025149314
TBC1D3P1-DHX40P1	0.955422002	2.392680647	0.000152692	0.033136182
CD58	0.949492441	4.452441732	3.57E-06	0.011354157
ABRACL	0.93010309	4.684331219	3.36E-05	0.020870589
MAP2K6	0.921831573	4.75679296	7.65E-05	0.025149314
POC1B	0.900020472	4.927106647	3.78E-05	0.02088857
PRPS2	0.888106862	4.732046373	0.000251593	0.044135232
RNFT1	0.866183588	3.569143345	7.67E-05	0.025149314
ALDH1A1	0.85464172	7.101279767	3.19E-05	0.020752334
DEPTOR	0.84140165	6.330292189	3.88E-05	0.02088857
SCRG1	0.839860864	1.924524866	0.000303743	0.047086914
TMEM126B	0.822775235	4.169739684	0.000173482	0.035181093
ZNF626	0.813080133	2.973078124	0.000354785	0.049486453
NPM1P27	0.80041196	3.493520743	9.45E-05	0.027572603
MEST	0.796270737	5.1619837	5.60E-05	0.021374567
LINC00998	0.768463905	4.536814602	4.60E-05	0.021374567
ACTR6	0.750993971	3.887233197	7.59E-05	0.025149314
STARD3NL	0.744252391	4.975661903	9.92E-05	0.02775015
MRPL50	0.737301002	4.839780148	3.02E-05	0.020752334
MICU2	0.732332926	4.712048755	0.00029718	0.04698273
RP11-761B3.1	0.718843332	6.389467896	6.00E-05	0.021452046
OSTC	0.709199765	7.472205242	0.000304647	0.047086914

TMEM128	0.707951962	4.356700118	0.000150693	0.033136182
MOB4	0.707747729	4.875347557	0.000259878	0.044231911
NME7	0.70667171	6.570151883	5.76E-05	0.021374567
VIL1	0.700794109	5.306219316	0.000212795	0.040030699
COPS4	0.69823647	4.150789052	8.03E-05	0.025149314
XRCC4	0.698196335	2.662742186	0.000162302	0.034123947
CTD-2410N18.5	0.686147901	6.931545498	0.000113395	0.02869387
NDUFA5	0.67474133	5.447022581	5.56E-05	0.021374567
CORO2A	0.674106353	5.576765103	0.000101901	0.02775015
HMGNI	0.671355679	6.755497139	6.41E-05	0.022357206
TMEM14A	0.667895488	5.319131823	0.000204212	0.039433438
BET1	0.652260063	4.764304989	5.71E-05	0.021374567
PEX13	0.652148073	4.464459188	4.35E-05	0.0212164
SLC30A5	0.64108551	4.415745724	0.000190458	0.03781906
FAM3C	0.631810503	4.600014065	4.53E-05	0.021374567
GULP1	0.608199797	4.272830304	0.0001707	0.03506402
MRPS14	0.604763683	5.086111754	5.09E-05	0.021374567
NDUFB6	0.604532952	5.673679787	0.000129403	0.031357235
ICA1	0.604414024	5.654398647	0.000279717	0.046507878
PPP2R3C	0.600564644	4.199728973	0.000243469	0.043030076
CD47	0.597325041	7.004133006	1.34E-05	0.018019568
PDHX	0.588296592	4.500997934	0.000356789	0.049524428
WARS2	0.585570777	3.547406626	0.00014431	0.032749148
RP11-363E6.3	0.583326797	4.510511253	0.000127623	0.031190084
SPTSSA	0.582010654	6.17734603	0.000198384	0.038853439
ANKMY2	0.575650902	4.094227543	8.71E-05	0.026202069
C8orf59	0.572494929	5.001729992	0.000136964	0.031583437
C6orf57	0.570552729	4.128550317	0.000274691	0.046391685
PPA2	0.570054512	6.089294353	0.000153464	0.033136182
LAPTM4A	0.562040929	8.78510753	0.000154566	0.033136182
FAM92A1	0.559510215	4.100247639	0.000226975	0.041711749
NHLRC3	0.559305844	4.515941302	0.000115932	0.029078481
CRIP1	0.557503868	4.35194268	0.000154359	0.033136182
TIMM9	0.556867775	3.960153352	0.000132332	0.031583437
TMEM59	0.549873392	8.438222196	0.000352071	0.049469455
TMEM70	0.542673881	4.208214127	0.000298174	0.04698273
FAM96A	0.54141672	5.552570127	7.92E-05	0.025149314
TBC1D7	0.538082722	4.56639517	0.000257851	0.044149651
EXOSC8	0.534398976	5.168485842	0.000153471	0.033136182
CALM2	0.515242243	9.685145026	0.000286668	0.046839833
PHYH	0.510864659	4.007889041	0.000291539	0.04698273
GGPS1	0.51044652	5.283178757	0.000310933	0.047464773

IER3IP1~1	0.509560328	5.886901696	2.86E-05	0.020752334
ATP6V1G1	0.502628138	7.322220603	0.000326855	0.048241597
ARHGEF38	0.490106486	4.17186387	0.000243788	0.043030076
HNMT	0.4857281	4.965921878	0.000120681	0.029835427
C18orf32	0.484767484	5.826074644	0.000231259	0.041711749
FBXL5	0.48185646	5.657280109	0.000351316	0.049469455
GABARAPL2	0.473348031	6.747706174	0.000358744	0.049555198
MANSC1	0.472289696	4.252825216	0.000161028	0.034106846
IER3IP1	0.462404237	5.233606531	0.000256848	0.044149651
C11orf58	0.462249796	7.133298967	3.70E-05	0.02088857
CCDC90B	0.456327232	5.111858617	8.18E-05	0.025149314
WLS	0.455200112	6.608215343	0.000297133	0.04698273
ZNF706	0.446394966	6.038454147	0.000275813	0.046391685
TMBIM4	0.436078146	6.931497104	0.000101542	0.02775015
HNRNPH1	0.427903673	8.121647903	0.000303006	0.047086914
ALCAM	0.426688757	6.190423866	0.000279756	0.046507878
RP11-745O10.4	0.415685543	6.88130452	0.000200056	0.038914294
HMGX3	0.415197719	7.029312268	0.000239774	0.04285064
MKL1	-0.478388876	5.301828246	0.000226691	0.041711749
ARHGAP35	-0.494042286	5.693845238	7.45E-05	0.025149314
MAFK	-0.519116935	4.602190705	0.000208957	0.039832812
ATF6B	-0.533998592	5.271561572	0.000335569	0.048706899
RGL3	-0.558759602	6.303197639	0.000333915	0.048706899
ADAMTS14	-0.736507054	3.944090709	0.000308904	0.047464773
C3	-0.744509042	9.0757334	5.01E-05	0.021374567
OLFM2	-0.842062353	4.3961733	0.000107099	0.028657043
RN7SL2	-0.851611403	6.745175837	0.000321477	0.048241597
GNA15	-0.881844741	4.554643101	0.000134656	0.031583437
NPIPA7	-1.119817982	2.662956134	0.000253456	0.044149651
RN7SL5P	-2.121970591	4.426963751	0.000177562	0.035755019
MT1G	-2.666399704	-2.048802682	0.00010924	0.028657043
S100A8	-3.2631558	1.942727642	1.17E-06	0.009894229
PLEK	-5.159245764	-2.349027325	2.31E-05	0.019811768